School of Engineering and Design

Brunel University

A Versatile Data Acquisition System for Capturing Electromagnetic Emissions in VHF Band

A thesis submitted for the degree of Doctor of Philosophy

By

Gregory Evangelos Koulouras

2007
LONDON, UK

Table of Contents

List of Figures

List of Tables

Abbreviations

Abbreviation	Description
ADC	Analogue-to-Digital Converter
AGC	Automatic Gain Control
AIU	Acquisition Interface Unit
ANSI	American National Standards Institute
API	Application Programming Interface
ASCII	American Standard Code for Information Interchange
ATA	Advanced Technology Attachment
BCD	Binary Coded Decimal
BEC	Backward Error Correction
BTL	Boot Loader
CAT	Cost Age Times
CF™	Compact Flash™
CHS	Cylinder Head Sector
CIU	Communication Interface Unit
CMOS	Complementary metal oxide semiconductor
CPU	Central Processing Unit
CRC	Cyclic Redundancy Check
CSV	Comma Separated Values
DAS	Data Acquisition System
DRAM	Dynamic Random Access Memory
DSS	Data Storage System
DSU	Data Storage Unit
EEPROM	Electrical Erasable Programmable Read Only Memory
ELF	Extra Low Frequency
EM	Electromagnetic
EMC	Electromagnetic Compatibility
EMV	Electromagnetic Variations
EQ	Earthquake
FAT	File Allocation Table
FDM	Frequency Division Multiplexing
FIFO	First-In First-Out
FTP	File Transfer Protocol
GOES	Geostationary Operational Environmental Satellite
GPRS	General Packet Radio Services
GPS	Global Positioning System
HF	High Frequency
I^2C	Inter-Integrated Circuit
IDE	Integrated Drive Electronics

Abbreviation	Description
IF	Intermediate Frequency
IP	Internet Protocol
ISP	In-System Programming
LBA	Logical Block Addressing
LCD	Liquid Crystal Display
LF	Low Frequency
LTA	Long Term Average
MIPS	Million Instructions Per Second
MTBF	Mean Time Between Failure
MW	Magnitude Wave
NASA	National Aeronautics and Space Administration
NGDC	National Geophysical Data Center
NMEA	National Marine Electronics Association
NOA	National Observatory of Athens
NOAIG	Institute of Geodynamics of the National Observatory of Athens
OOP	Object Oriented Programming
OSI	Open Systems Interconnection
OTP	One Time Programmable
PC	Personal Computer
PCB	Printed Circuit Board
PCI	Peripheral Component Interconnect
PLL	Phase Locked Loop
PPS	Pulse Per Second
PSU	Power Supply Unit
RF	Radio Frequency
RMS	Root Mean Square
RSSI	Received Signal Strength Indicator
RTC	Real Time Clock
RWW	Read – While – Write
SMTP	Simple Mail Transfer Protocol
SPI	Serial Peripheral Interface
SRAM	Static Random Access Memory
STA	Sort Term Average
STD	Standard Deviation
TCP	Transmission Control Protocol
TKU	Time Keeping Unit
UART	Universal Asynchronous Receiver-Transmitter
UHF	Ultra High Frequency
ULF	Ultra Low Frequency
UPS	Uninterrupted Power Supply
UTC	Universal Time Clock
VHF	Very High Frequency
VLF	Very Low Frequency
XML	eXtensible Mark-up Language

Acknowledgements

I owe a special debt of gratitude to those who contributed to the completion of this work. First of all, I would like to thank John Stonham, Professor of School of Engineering and Design of Brunel University, for his guidance through my PhD. His continuous support for this scientific work has proved determinant.

Prof. Constantinos Nomicos, from Electronics Department of Technological Educational Institution of Athens, whose great experience on field measurements has been extremely helpful. He supported this work continuously and guided me on the laboratory experiments. Furthermore, I would like to thank him for passing on to me his long year experience on electronics design and electromagnetic measurement techniques. Some of the earlier work in this thesis was carried out in collaboration with fellow researchers of the Institute of Geodynamics of the National Observatory of Athens. I would therefore like to offer my thanks to all members of the Institute of Geodynamics.

I would like to thank my collaboration team MSc. Evangelos Nannos, MSc. George Minadakis, MSc. Constantinos Euthimiatos for their assistance in setting up and running the experiment. I would have been unable to complete this project in such a short time, without the help and support of my collaborator Kyriakos Kontakos. He helped me in most stages of this work and especially on design, construction and installation of the devices of the field stations.

I would like to thank my friends Spiros Delgas, Jim Kosmadopoulos, Ilias Kiourktsidis and Vasilios Kostelidis for their unselfish encouragement and support. Additionally, I owe a special debt to my friend Vizandinos Repandis for his support on proofing this thesis.

I would like to thank the National Foundation of Scholarships (I.K.Y.) for the financial support during my studies. The Project is co-funded by the European Social Fund and National Resources - (EPEAEK II) ARXIMIDIS.

Last but not least my parents Evangelos and Helen and my brother Marios for their unending support and love that enabled me to fulfill this work.

Abstract

This research investigates the occurrence of EM emissions from compressed rock and assesses their value as precursors to earthquakes. It is understood that electromagnetic emissions are accompanied by crack generation in the Earth's crust, and effort has been targeted on the analysis of electromagnetic signals preceding seismic events.

There is a need for a robust Data Acquisition System for the reliable collection of such signals. The design and deployment of a novel system form part of this research. The EM data collected by the Data Acquisition System is subsequently analysed and correlations are made with natural phenomena.

The design of the Data Acquisition System is presented and meets a specification which includes accuracy, robustness, power consumption, remote configurability achieved by the development of a novel architecture for flash memories which significantly increases the live span of these devices.

The measuring of electromagnetic emissions should be performed by reliable systems, using devices that fully correspond to the specifications set by the needs of this research. This type of systems is not fully covered by existing commercial devices.

These prototype VHF field stations (ground base - electromagnetic variation monitors in VHF band) are located around the Hellenic Arc. This region is one of the most seismically active regions in western Eurasia due to subduction of the oceanic African lithosphere beneath the Eurasian plate. After approximately two years of electromagnetic VHF data collection, the final stage of this project took place. In this stage, possible correlation between naturally occurring electromagnetic emissions in VHF band and seismic events within a predefined radius around the observation location is investigated. Supplementary, effects of alternative electromagnetic sources, such as solar activity, is considered.

Whilst EM emissions from compressed rocks can be demonstrated in the laboratory, it was found from a two-year evaluation that no reliable correlation with

earthquake events could be established. However, significant patterns of activity were detected in EM spectrum and it was shown that these correlate strongly with other naturally occurring phenomena such as solar flares.

The Data Acquisition System as developed in this thesis has related applications in long term and remote sensing operations including meteorology, environmental analysis and surveillance.

1 Introduction

1.1 A Data Acquisition System for capturing electromagnetic emissions

This work focuses on the design and implementation of a versatile Data Acquisition System (DAS), for capturing reliable electromagnetic emissions in VHF band arising from rock compression and cracks. In this thesis, the entire implemented system is described analytically and its potential contribution to the earthquake research is discussed, as there is a potential connection between electromagnetic emissions and rock compression.

It is unfortunately impossible to follow the evolution of a preseismic process in the lithosphere by directly monitoring the stress variations. However, it seems possible to estimate the evolution of a seismic activity by monitoring the accompanying electromagnetic activity in various frequency bands. Many researchers are targeting their efforts towards the analysis of electromagnetic signals preceding seismic events. Some of them are examining the interaction between seismic activity and disturbances in radio broadcasts [e.g. Warwick J.W. et al. (1982), Hayakawa M. et al. (1996), Molchanov O.A. and Hayakawa M. (1998a), (1998b), Biagi P.F. et al. (2001)], while the rest are dealing with the occurrence of electromagnetic emissions in different bands [e.g. Merzer M. and Klemperer S.L. (1997), Nomicos K. et al. (1997), Vallianatos F. and Nomicos K (1998), Asada T. et al. (2001), Pham V.N. et al. (2002), Kapiris P. et al. (2002), Eftaxias K. et al. (2003), Kapiris P.G. et al. (2003)].

The work in this thesis concentrates on capturing continuous time series of electromagnetic emissions in the VHF band from an area with high seismicity, for quite a long period (at least two years), in order to examine any correlation between these emissions and seismic activity. The selected observation area is the Hellenic Arc. This region is one of the most seismically active regions in western Eurasia due to subduction of the oceanic African lithosphere beneath the Eurasian plate

[Makropoulos K. et al. (1985), Papazachos B. and Papazachou C. (1997), Clément C. et al. (2000), Laigle M. et al. (2002)].

Given the complexity of this research, the whole project was divided into three major sections, namely system hardware, software and data analysis. Regarding the system hardware, a requirements analysis was carried out. Unfortunately, neither commercial Data Acquisition Systems [e.g. CR10X datalogger manufactured by Campbell Scientific (2007)], nor PC-based machines with Analogue to Digital PCI cards [e.g. Embedded PC/104™ modules (2007)], were able to cover the needs of this project, given the fact that they don't incorporate special hardware necessary for capturing these emissions. Supplementary, PC-based machines add significant unwanted electromagnetic noise background to these measurements. So, by incorporating current technology, a versatile Data Acquisition System has been designed and constructed in order to research the relationship between EM emissions and seismicity.

Regarding the second section a new telemetry software has been designed and implemented, since all the evaluated existing software was either inadequate to incorporate with the implemented DAS or was limited in data collection procedure without offering auditing operations for the terminal devices.

Finally, after a long period (about two years) of data collection, analysis using several models and schemes will take place. Possible correlation between any abnormal VHF electromagnetic emissions and seismic events will be examined and effects of alternative sources, such as solar activity will be considered.

1.2 Seismic Prediction Strategies

Seismology (from the Greek seismos = earthquake and logos = word) is the scientific study of earthquakes and the movement of waves through the Earth. Earthquakes produce different types of seismic waves. These waves travel through rock, and provide an effective way to "see" events and structures deep in the Earth. Seismology is a recent science. Early work concentrated on determining the fundamental mechanisms for earthquakes and this eventually evolved into the theory of tectonic plates.

Most seismologists believe that a system to provide timely warnings for individual earthquakes has not yet been developed and some believe that such a system would be effectively impossible. Forecasting such a physical phenomenon is a general statement of future possibility of occurrence while its prediction specifies all its parameters like time, place, magnitude and probability of an anticipated event. Naturally, people desire to be able to predict the occurrence of an earthquake. Subsequently, many methods, scientific and not, have been proposed. Prediction of a physical phenomenon does not necessarily demand an understanding of the mechanisms related to it; however the ability to explain the phenomenon is desirable. In this case it will need a detailed description of the Earth's structure and how seismic energy is released. These can then be an explanation of accompanying physical phenomena that might be used as predictors. Unfortunately, the mechanisms responsible for earthquake events occur deep within the Earth's crust and are currently inaccessible for detailed study. Instead, models must be developed to explain these phenomena.

Many possible approaches for earthquake prediction have been proposed, including animal behaviour, statistical study of the seismic activity of areas with high seismicity, electric field variations, electromagnetic emissions, including seismic acceleration deformation, ionospheric variability, as well as acoustic emissions close to the earthquake epicentre. All the above approaches have seemed promising and have contributed knowledge to the study of earthquake prediction.

In particular, electromagnetic phenomena in the lithosphere, atmosphere and ionosphere, which are related to seismic events, have been observed, since 1982 [e.g. Gokhberg M. B. et al. (1982a), (1982b), Varotsos P. and Alexopoulos K. (1984a), (1984b), Hayakawa M. and Fujinawa Y. (1994), Hayakawa M. and Molchanov O. A. (2000), Tzanis A. et al. (2000), Kopytenko Y. et al. (2001)]. It is under consideration that seismo-electromagnetic phenomena are accompanied by crack generation in the Earth's crust [Molchanov O. A. and Hayakawa M. (1998a), (1998b), Surkov V. V. et al. (2003)].

Gokhberg M. B. et al. (1982a), (1982b), (1995), were the first to publish recordings of pre-seismic electromagnetic emissions at 81 KHz that had been detected by a receiver (loop antenna of narrow bandwidth) that was installed in a station in Japan. Probably, electromagnetic emissions exist over a wide range of frequencies and

thus several studies have been conducted in different bands. Qian et al. (1994) observed a wide range of frequencies. Their network was installed in 1993 and consisted of 200 stations at two earthquake experimental regions in China (Beijing and Western Yunnan). Specifically, eleven (11) types of experimental stations were used, variously tuned at fourteen (14) frequency bands (0.1-20Hz, DC-20Hz, 0.25-l0Hz, 0.1-2KHz, 5-1200Hz, 0.1-20KHz, 0.5-5KHz, 15KHz, 47KHz, 81KHz, 1.9KHz, 70KHz, 120-160KHz, l-65MHz). The results of this project are treated in the paper Qian et al. (1994).

This thesis focuses on capturing continuous time series of electromagnetic emissions in a wide range of frequencies in VHF band from a seismically active region, for quite a long period (about two years), in order to identify any correlation (or not) between these emissions and seismic activity. Frequencies from 70MHz to 130MHz have not been included in order to avoid conflicts from radio emissions of local radio stations and amateurs. The appropriate region selection is of great importance in order to achieve isolation from culture noise. In other words, field stations should be installed in the countryside isolated from man-made, artificial noise. In order to exclude these frequencies from being monitored, a commercial RF receiver with scanning capability was used for creating a site emission survey. The result of this task was the generation of a list with frequencies that will be excluded from monitoring. So, the selected monitoring frequencies were 142MHz, 178MHz, 230MHz, 320MHz, 390MHz and 415MHz.

Another usual problem that many research teams have to face during their research is the reliability of data. A suitable Data Acquisition System is one of the keys to any successful research. In this research field, such systems do not exist. If other commercial similar systems, which are not designed especially for this purpose, are to be used, a number of limitation or compatibility issues might be encountered. This is not desirable. Major companies in this field are capable of manufacturing reliable and fully customisable devices under contact but with excessive cost for most customers. As the budget drops the reliability and functionality drops as well, exceeding the permissible limit borders for a high end application. The perfect system should meet the criteria of both, cost and reliability.

In this thesis, such a system is being analysed, designed and implemented, giving great emphasis to above mentioned criteria.

1.3 Proposed Approach: Aims and Objectives

The proposed approach involves two phases that should be performed in chronological order. The first objective was to capture at least two years of reliable continuous time series of electromagnetic emissions in the VHF band. The second objective was to investigate possible correlations of these electromagnetic VHF emissions in relation to seismic activity.

In particular, this project aims to the execution of the following tasks:

a) Design and implementation of an embedded Compact Flash™ based Data Acquisition System (DAS), especially suitable for field operation, in order to acquire reliable environmental or other kind of measurements.

b) Design and implementation of a peripheral device for the above proposed Data Acquisition System, in order to record the variations of the electromagnetic field in a wide spectrum of frequencies up to UHF band (142MHz, 178MHz, 230MHz, 320MHz, 390MHz, and 415MHz).

c) Development and implementation of Telemetry Software. By using Object Oriented Analysis, the main tasks were identified and a list of required operations that the new telemetry software should incorporate was created. These operations are the following:

   - Remote data collection
   - Real time monitoring
   - Remote configuration and management

d) Design and deployment of a complete telemetric network, which includes:

   - Design and implementation of prototype EMV VHF field stations that will be responsible for measuring, logging and distributing electromagnetic measurements.
   - Design of a central station for connections establishment and data retrieval from all remote field stations.

The operation of this network should ensure reliable and error free communication between each prototype EMV VHF field stations and the central one.

e) Development and implementation of signal analysis methods in order to evaluate these measurements and investigate the relationship between VHF electromagnetic variations and seismic events. Influence derived from alternative sources, such as solar activity or artificial noise will be considered.

1.4 Research methods and practical issues

Preliminary studies prior to project initialization, gave the opportunity to select suitable research methods in order to approach the problem. The proposed approach involves four stages.

In the first stage of this project, the hardware design and implementation took place. Regarding the data acquisition device, new devices should be implemented to cover the needs of the new telemetry network, which will be described later in this thesis. The main operation of this device is to capture electromagnetic variations in a wide spectrum of frequencies up to UHF band. Furthermore, these devices should provide added value operations and hence deliver real-time monitoring, remote programming and administration, failure recovery mechanisms, easy expansion, lower power consumption and higher storage capacity than commercial similar acquisition devices.

Design and implementation of new telemetry software, have been included in the second stage of this project. This software stage covers the runtime data acquisition operations as it concerns remote administration, monitoring of the telemetry devices, data collection, manipulation, distribution and finally graphic data representation. The data collection method incorporates a polling technique as it is suitable for this scheme.

In the third stage of this project, a prototype VHF electromagnetic variation telemetric network has been designed and implemented. In order to study electromagnetic emissions in VHF band that could possibly occur prior to strong earthquakes, an area with a permanently high level of seismicity had to be selected. Earthquake occurrence reports demonstrate that the Ionian Islands belong to the highest shallow seismicity area in Europe. Consequently, the first goal of this stage is the study of the physical location of the new telemetry network, in order to identify the needs and the requirements of such systems. Analysis and investigation of

common telemetry problems in the fields of computer science and engineering are also required. Collaboration with the Institute of Geodynamics of the National Observatory of Athens provided the opportunity to use the existing network resources and structure for the purposes of this project. Using the existing infrastructure of the Institute of Geodynamics facilitated the communication between the central server and the field stations, reducing the total cost of the whole project, as well as the time needed for physical network design and implementation.

As far as the central station is concerned, the needs of a state of the art PC-based system should be met. These include: (a) uninterrupted communication with every remote field station, (b) appropriate processing power for any kind of operation, (c) a high capacity storage unit, (d) compatibility with other PC-based systems for data distribution and (e) easy maintenance.

The telemetric network system was launched on 06/2004 and is operational up to now (06/2006). The completion of this stage required strong seismic events to occur. So, the need of continuously monitoring the ongoing seismicity within a predefined radius around the observation location was obvious. This goal was achieved by considering the existing daily updated catalogue of seismic events in the region, from the Institute of Geodynamics of the National Observatory of Athens.

In the final stage of this project, analysis software developed for detection of electromagnetic events in VHF band that occurred concurrently from most field stations, adopting first order analysis methods. In this stage, possible correlation between VHF electromagnetic and seismic events will be investigated. Effects of alternative sources, such as solar activity will be considered.

1.5 Thesis Outline

This thesis is divided in six chapters which present different stages of this research project. Chapter 2 describes the hardware development and implementation of the new Embedded Compact Flash™ (CF™) based Data Acquisition System (DAS), considering previous research into existing, commercial DAS's. Considering the technical part, the implemented DAS consists of six (6) basic units that are described analytically later. These units deal with the microcontroller of the system (CPU), the Data Storage Unit (DSU), the Acquisition Interface Unit (AIU), the

Communication Interface Unit (CIU), the Time Keeping Unit (TKU) and finally the Power Supply Unit (PSU). The full detailed DAS specifications are described in APPENDIX B' (Specifications - Schematics - PCBs).

The innovation of this DAS is the Data Storage System (DSS) it incorporates. In the rest of chapter 2, the custom designed DSS is described analytically. The DSS is an efficient memory-management scheme that increases CF™ lifetime, while this scheme is suitable for large-capacity DAS's. Additionally, the AIU incorporates a custom designed sub-unit (VHF Scanner) for capturing electromagnetic emissions in VHF band, which is described analytically.

Chapter 3 deals with the software development and implementation. Considerations regarding the adopted programming methodology and the potential approaches which could be used, were made. In the software design stage of this thesis, many commercial telemetry computer programs were surveyed for suitability according to the specifications and the requirements of the proposed system. Using Object Oriented Analysis, the main tasks of the new telemetry software were identified and a list of required operations, that this software should support, was created. These operations are the following: (a) Remote data collection, (b) Real time monitoring and (c) Remote configuration and management

Chapter 4 deals with the design and implementation of a prototype EMV telemetric network in VHF band. Thus, in this chapter the principals of telemetry networks are reviewed. In order to study electromagnetic emissions in VHF band that could possibly occur prior to strong earthquakes, an area with a permanent high level of seismicity had to been selected. The appropriate geographic region selection is very important.

Chapter 5 deals with the application of DAS to EM emissions. This chapter focuses on EM data collection and on an initial analysis of EM recordings, as well as earthquake events. Additionally, possible correlation between VHF electromagnetic and seismic events will be investigated. Effects of alternative sources, such as solar activity will be considered.

Finally, chapter 6 draws together results and conclusions from the previous experiments. Suggestions are also made for further research in testing the model and applying it to other areas.

2 Design and Evaluation of the Data Acquisition System

2.1 Introduction

Several research teams have to face a major data acquisition problem, namely reliability versus cost. Major companies in this field are capable of manufacturing extremely reliable devices using cutting-edge technology, sometimes developed for the specific applications but with prohibitively high costs for most customers. The problem remains in the reliability and functionality of the certain device, while the product line sets budget limits. As the budget drops, the reliability and functionality drops as well, exceeding the permissible limit borders for a high end application.

An embedded Compact Flash™ based Data Acquisition System (DAS) especially suitable for field operation has been designed and implemented. In order to acquire reliable electromagnetic variation measurements, field stations should be installed in the countryside isolated from man-made, artificial noise. In such types of regions the usage of alternative energy sources, like solar cells, is almost always necessary. Hence, the system's overall power consumption is of significant importance. The common problem in data acquisition systems that are operating in the countryside is to combine the high capacity, non-volatile memory, with the lowest power system consumption [Chang L. P. and Kuo T. W. (2001)]. Some other problems were observed in the operation of the remote data collection, as well as the device configuration and the application firmware upgrade.

In this thesis, the embedded DAS is described analytically. The system ensures uninterrupted operation and low power consumption. Douglis F. et al. (1994) evaluated flash memory storage systems under realistic working circumstances for energy consumption considerations.

2.2 Embedded Compact Flash™ based Data Acquisition System

Considering the technical part (Figure 2.1) the implemented DAS consists of six (6) basic units including the core of the system (CPU) [Figure 2.1(a)] and the Power Supply Unit (PSU) [Figure 2.1(f)].

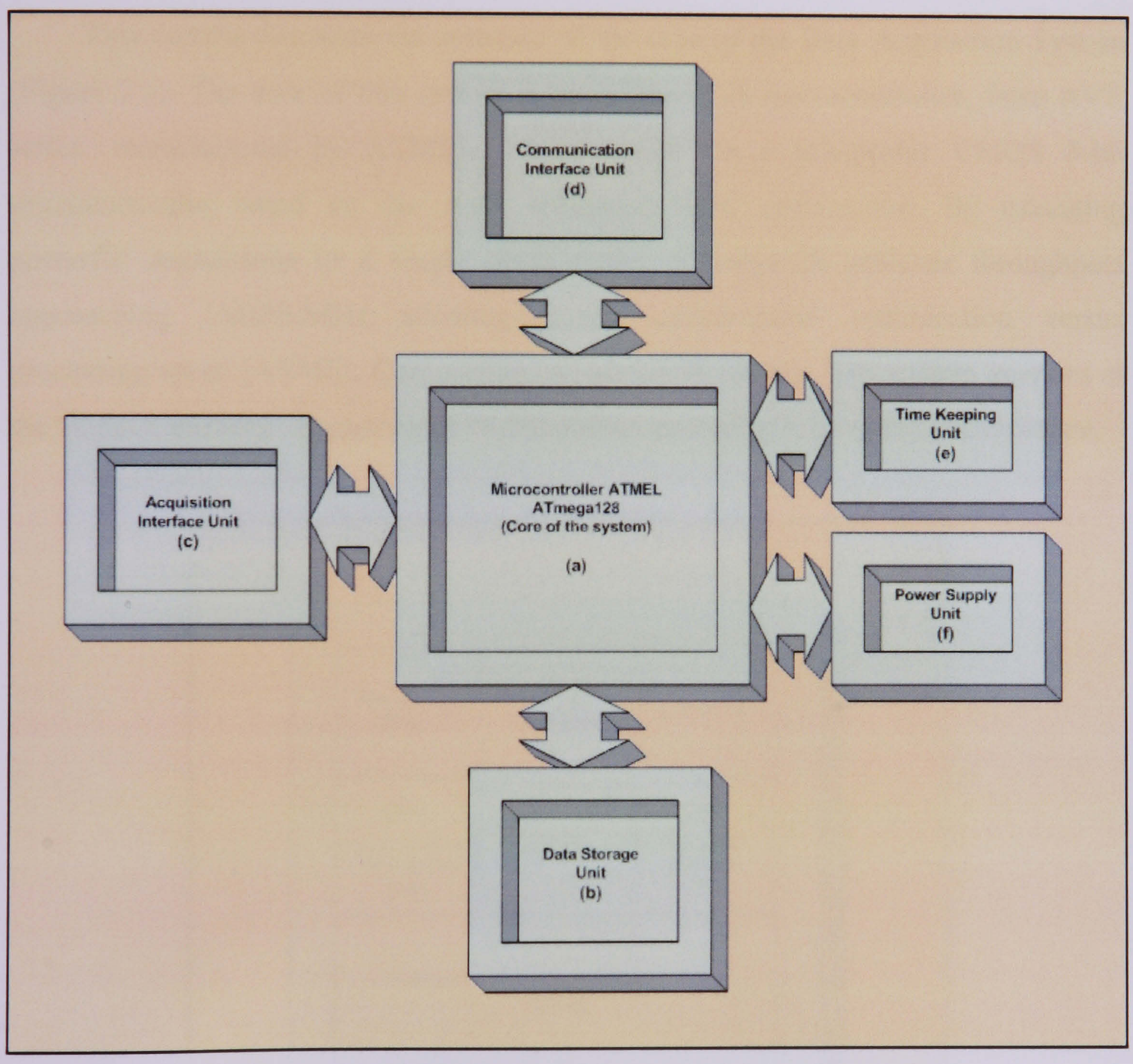

Figure 2.1 - Block diagram of the Data Acquisition System

The Data Storage Unit (DSU) uses Compact Flash™ card as high capacity (up to 8GB), non-volatile memory [Figure 2.1(b)]. The Acquisition Interface Unit (AIU) provides up to 32 channels [Figure 2.1(c)]. In order to acquire synchronized data, the device incorporates a Real Time Clock (RTC) synchronized by UTC-GPS reference,

broadcasted by the GPS satellite constellation all over the world [Figure 2.1(e)]. This synchronization ensures a reliable data analysis [Alfred Leick (2004)]. Finally, the built-in Communication Interface Unit (CIU) provides five different connection interfaces, namely EIA232E, EIA485, Ethernet 10Mbps, WiFi 802.11b 11Mbps and General Packet Radio Services (GPRS) class 10 [Figure 2.1(d)].

2.3 The microcontroller of the system

This section discusses the structure of the core of the Data Acquisition System (Figure 2.2). The core of this system is an ATmega128 microcontroller, from AVR series, manufactured by ATMEL. "ATmega128" is a low-power CMOS 8-bit microcontroller based on the AVR enhanced RISC architecture. By executing powerful instructions in a single clock cycle, ATmega128 achieves throughputs approaching 1MIPS/MHz allowing power consumption optimization versus processing speed [ATMEL Corporation, ATMega128 (2003)]. The system operates at the "UART friendly" frequency of 14.7456MHz, providing high speed performance.

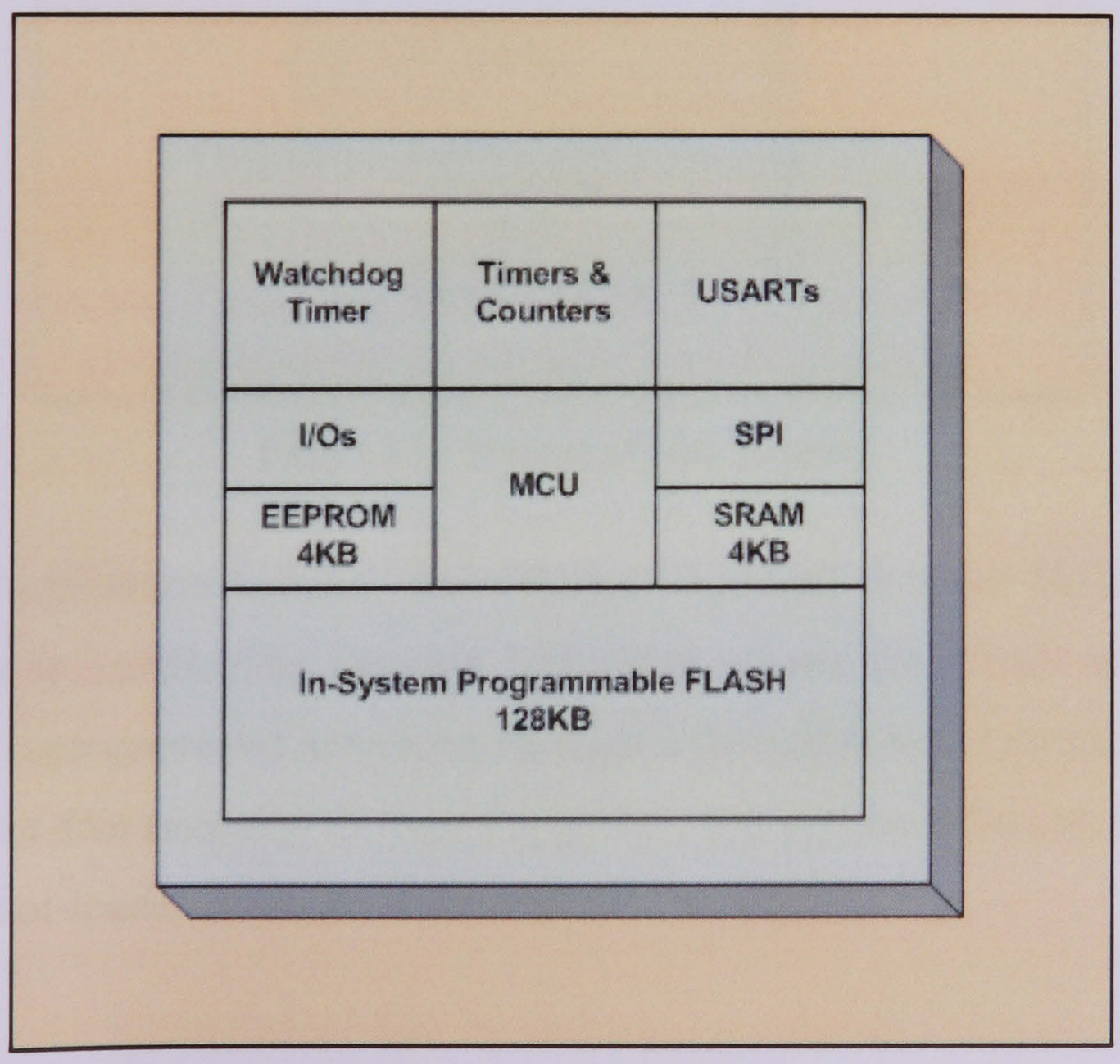

Figure 2.2 - Block diagram of the microcontroller of the system

ATmega128 provides the following memories: 128KB of Flash as code execution memory, 4KB EEPROM as settings memory and 4KB SRAM for temporary buffers and variables. The 128KB of Flash memory space is virtually separated into three main sections as shown in Figure 2.3. The first section is called "Boot Section" and contains the Boot-loader firmware, which is responsible for the proper boot operation of the system and for the remote Application firmware upgrades. The second section is the "Application Section" and contains the Application firmware, which includes all acquisitions and logging features. The third section is the "Backup Section", which is used for backup purposes, during firmware upgrades.

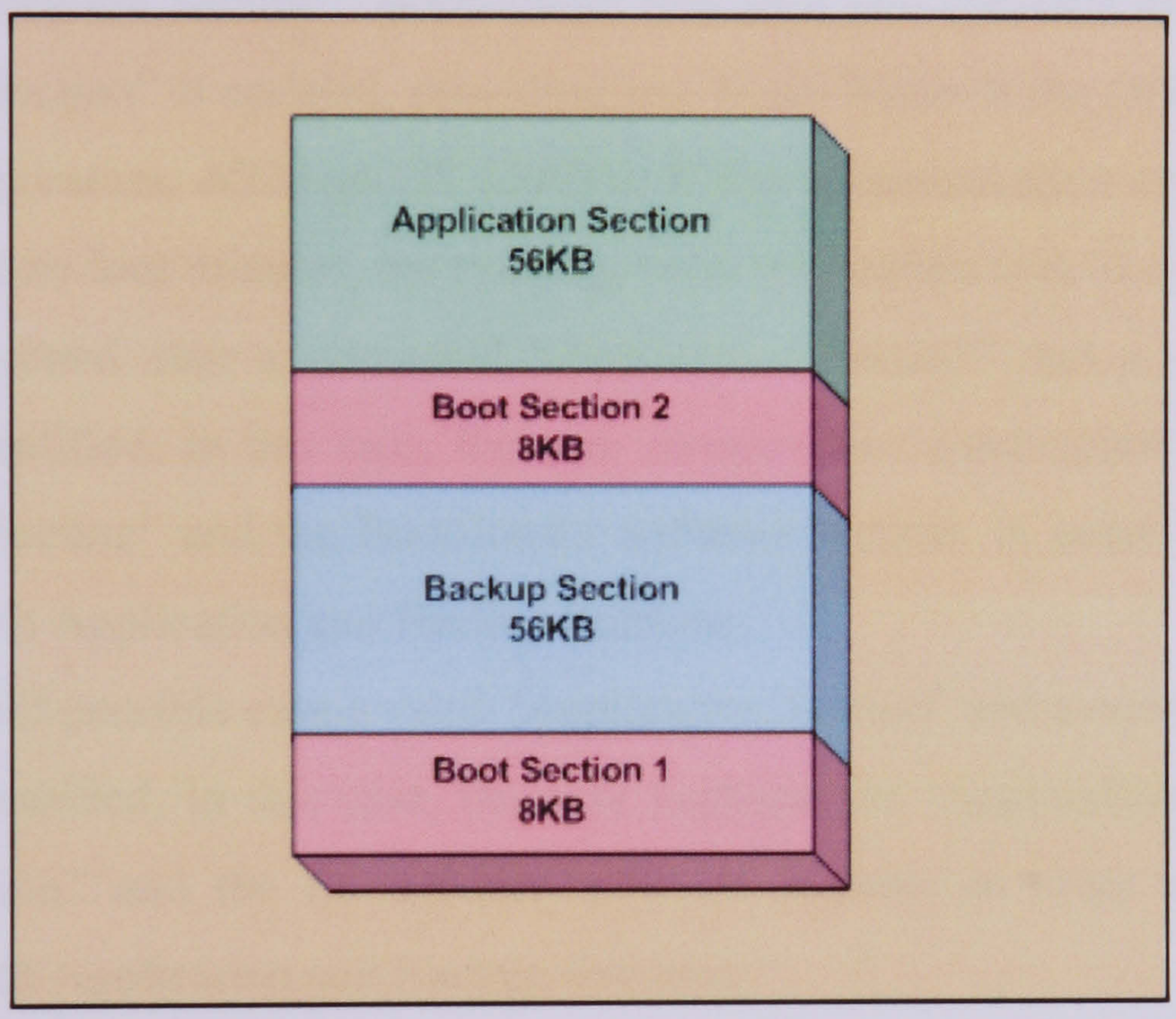

Figure 2.3 - Sections of code memory

Both "Application Section" and "Backup Section" size are 56KB. The "Boot Section" size is 16KB. The On-chip ISP Flash allows the "Boot Section" to be accessed and reprogrammed in-system, through a dedicated Serial Peripheral Interface (SPI). For error-free remotely firmware upgrades, this section is locked. The only way to upgrade Boot-loader firmware is through SPI, locally.

2.3.1 Boot Section

Code written in "Boot Section" is executed on every hardware reset. It is divided into two same sized sections, "Boot Section 1" and "Boot Section 2". On power-up, the Boot-loader software, using CRC-16 algorithm [Forsberg C. (1988)], checks the validity of both Application and Backup Sections. There are four different possible cases.

In the first case both Application and Backup Sections are identified as valid ones. The Boot-loader firmware handles any available communication interface (i.e. EIA232E, EIA485, Ethernet, WiFi or GPRS) in order to communicate with the remote or local host. In this case, the host is able to download the new application firmware into the "Application Section". Boot-loader firmware will continue to run while the "Application Section" is updated, providing true Read-While-Write (RWW) operation [ATMEL Corporation, ATMega128 (2003)]. If the communication channel remains idle for more than four minutes, the existing, valid application code is executed.

In the second case a corrupted "Application Section" and a valid "Backup Section" is identified. In this case, the core restores the "Application Section" from the "Backup Section" and the Boot-loader software restarts, in order to recheck the integrity of both Application and Backup Sections.

In the third possible case a valid "Application Section" and a corrupted "Backup Section" is identified. In this case, the core backups the "Application Section" into "Backup Section" and the Boot-loader software restarts, in order to recheck the integrity of both Application and Backup Sections.

The last and worst case is to identify both Application and Backup Sections corrupted. That means that there is no valid application firmware to execute. In this case the Boot-loader switches permanently into the remote update mode and waits for a host to be connected, in order to update the application firmware, remotely.

2.3.2 Application Section

The Boot-loader's complex integrity check guarantees a proper boot of the system. Code in "Application Section" is called application firmware. The application firmware is executed only if a valid firmware exists. Application firmware includes all communications, acquisitions, logging and data collection features.

2.4 Data Storage Unit

This section describes the Data Storage Unit of the designed Data Acquisition System (Figure 2.4). This Data Acquisition System supports an Integrated Drive Electronics (IDE) interface as data storage interface, mainly for backward compatibility. A Compact Flash™ (CF™) card also runs in True IDE Mode that is electrically compatible with an IDE interface. Backward compatibility means that we can use Hard Disk Drive (HDD) or Micro-Drive with IDE interface, instead of Compact Flash™. The greatest problem for such type of devices is the power consumption.

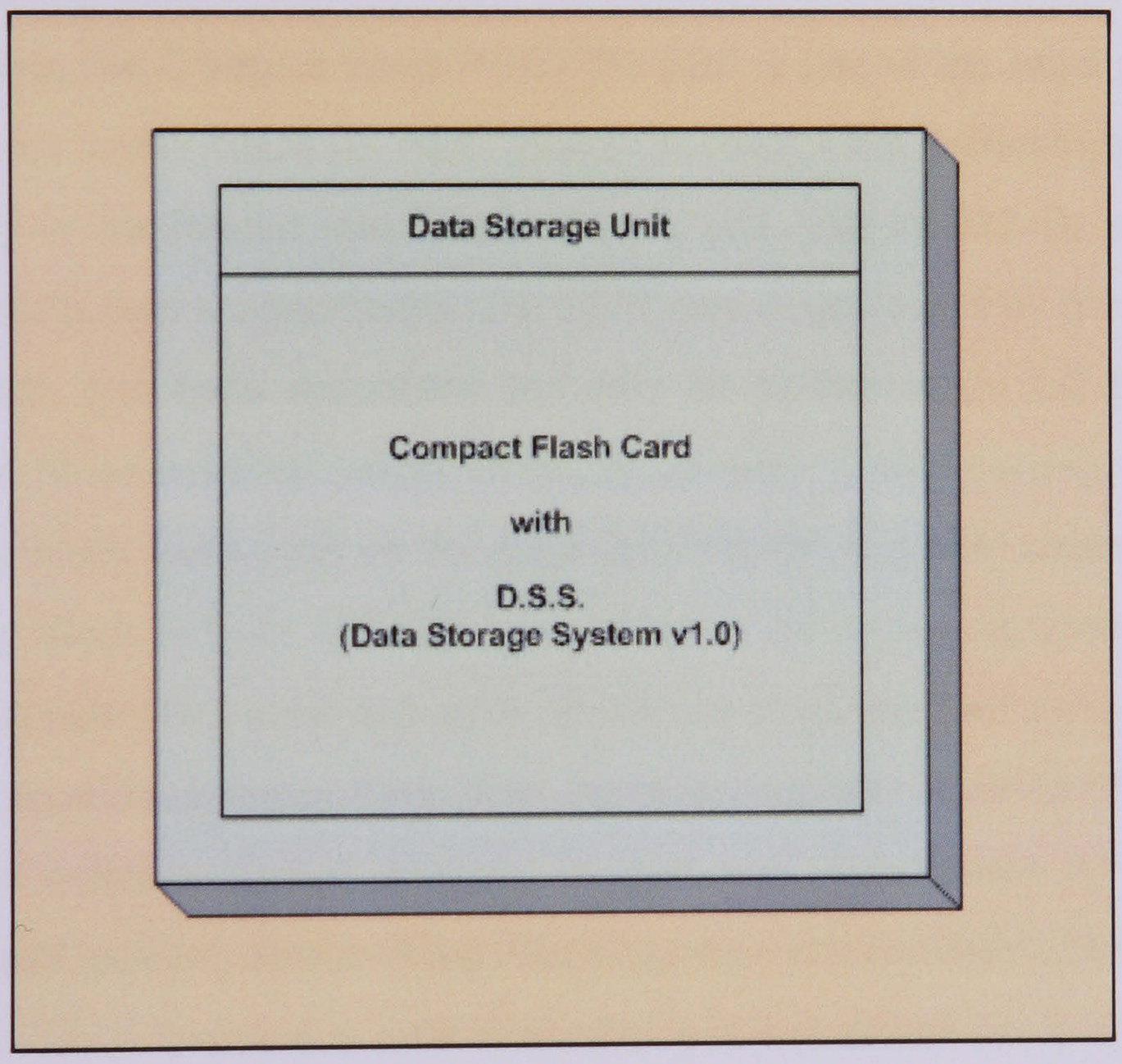

Figure 2.4 - Block diagram of Data Storage Unit

Compact Flash™ card is among the top choices for storage media in ubiquitous computing. It provides high capacity (up to 8GB), low latency and high throughput for read access. Additionally, it is non-volatile, small, lightweight, shock-resistant and power-economic. However the limited write cycles is a serious drawback for such type of memories.

Thus, we proposed a new Data Storage System (DSS) designed for embedded Compact Flash™ based Data Acquisition Systems (DAS's). The DSS, which is a large non-volatile memory storage system, is able to manage this drawback and finally, the system is capable to maximize CF endurance, while all data blocks wear out uniformly.

2.4.1 Introduction

Flash memory is non-volatile, tiny in physical size and power-economic solid-state memory. Therefore, flash memory is promising for use in storage devices for embedded systems, handheld computers, cellular phones, digital cameras, notebooks, and Data Acquisition Systems (DAS's). On the other hand, it has a number of drawbacks that we need to know in order to minimize the effects of them.

Nowadays, the Compact Flash™ (CF™) card is one of the most popular, non-volatile memory cards based on NOT AND (NAND) flash technology. In general, flash memory is partitioned into blocks of 64, 128, 256 or 512 B, predefined by hardware manufacturers. Specifically, the CF™ card is organized by blocks of 512 B. The read, write, and erase operations can only be performed on full blocks. These blocks cannot be overwritten unless erased in advance. Under current technology, a flash memory block has a limit on the erase cycle count. A typical range for a NAND flash memory block is from 100,000 to 1 million erase cycles. In contrast with read operation, supplementary erase and write operations consume more power.

Many researching teams have been investigating how to utilize flash memory technology in existing storage systems. In particular, Kawaguchi A. et al. (1995) proposed a flash memory device driver that supports a conventional UNIX file system transparently. They invented a new flash-memory translation layer that is able to provide a transparent way to access flash memory through the emulating of a block device. Douglis F. et al. (1994) evaluated flash memory storage systems under realistic working circumstances for energy consumption considerations. Wu M. and Zwaenepoel W. (1994) proposed the integration of a virtual memory mechanism with a non-volatile storage system based on flash memory. Chang L. P. and Kuo T. W. (2002), proposed an adaptive striping architecture for flash memory storage systems of embedded systems in order to increase their performance. Additionally, Chang L. P. and Kuo T. W. (2001) focused on a dynamic-voltage adjustment mechanism in

order to reduce the power consumption. The same researchers [Chang L. P. et al. (2004)] proposed a deterministic garbage-collection mechanism in order to increase the life of flash memory. Chiang M. L. and Chang R. C. (1999) proposed a new cleaning policy, the cost age times (CAT), in order to reduce the number of erase operations performed and to evenly wear flash memory. Wu C. H. et al. (2003) proposed an efficient R-tree implementation over flash-memory storage systems. Finally, Chang L. P. and Kuo T. W. (2004) proposed another flexible management scheme for large-scale flash-memory storage systems based on the behaviours of realistic access patterns. Beside research endeavours from the academics, many specifications and implementation designs were proposed from the industry, such as Compact Flash™ Association (2004), Intel Corporation (1995a), (1995b), (1995c), (1998a), (1998b), (1998c).

This chapter describes the architecture for a large non-volatile memory data storage system (DSS) mainly developed for CF™ memory. A DSS handles the available storage space of the medium as a circular buffer rather than as an emulated disk in order to provide an efficient and easy to use software interface. A circular buffer is simply another name for a first-in–first-out (FIFO) buffer. The name circular buffer helps to visualize the wraparound condition. CF™ memories provide a persistent storage medium using solid-state memory technology at a lower cost and lower power consumption than other solid-state technologies.

2.4.2 Flash Memory Technology

There are two available types of flash memory in the current market, namely NAND flash and NOR flash memories. NAND flash memories are specially designed for data storage, and NOR flash memories are used as electrically erasable programmable read-only memory (EEPROM) replacements. Due to the simple structure of the flash memories, high density at low cost is achieved. The CF™ card is one of the most popular non-volatile memory cards, based on NAND flash technology. Each card consists of one, two, or more flash-memory chips, depending on the manufacturer and the desired CF™ size. Each memory chip consists of many non-volatile memory cells, which are organized into independently erasable blocks of 512 B. Read operations can be performed with Dynamic Random Access Memory

(DRAM)-like access times [Lee H. G. and Chang N. (2003)]. Write operations are about ten times slower and blocks cannot be rewritten until the entire block is erased. Erase operation takes from 0.5 to 1ms per block. CF™ characteristics are shown in Table 2.1.

Current flash technology uses a block handing method that slightly degrades memory blocks each time write or erase operations are executed. Hence, each flash-memory block has a limitation on the maximum number of executed erase cycles until it is unusable. Each memory card has a minimum number of erase executions, ranging from 100,000 to 1 million, depending on the used flash-memory chips. A flash-memory block failure is defined as a given either write or erase operation that takes more time than described in the specifications [Wu M. and Zwaenepoel W. (1994)]. The operation might still succeed if more time is allowed. In any case, the most important fact is that the existing data will remain readable. On the other hand, a hard-disk failure denotes unrecoverable data loss. This feature makes flash-memory disks more reliable and fault tolerant, and as the technology matures, flash has the potential to become more durable.

CF™ Read cycle **Read Cycles Limit** **Sector Size**	**25 – 50 µs/sector** **Unlimited** **512 B**
CF™ Write cycle **Write Cycles Limit** **Sector Size**	**250 – 500 µs/sector** **100,000 – 1 million cycles** **512 B**
CF™ Erase cycle **Erase Cycles Limit** **Sector Size**	**0.5 – 1 ms/sector** **100,000 – 1 million cycles** **512 B**
Power consumption (Active state) **Power consumption (Standby state)**	**10 - 80mA @ 5V (for CF™ 128MB)** **20 - 100µA @ 5V (for CF™ 128MB)**
Price	**0.5 €/MB**

Table 2.1 - CF™ characteristics

Flash memory meets the specifications and requirements of the DAS, when used in read-only mode. When it is used to provide a general-purpose, non-volatile memory system, flash technology has three basic weaknesses. First, its bulk erase nature prevents the use of normal byte-oriented update. Second, write and erase operations take more time and consume more power than read. Finally, as mentioned before, each flash-memory block has a limitation on the erase cycle count. The next section describes a novel methodology developed during this research programme and how this Data Storage System (DSS) manages these weaknesses.

2.4.3 Compact Flash™ Card as a Storage Medium for a DAS

Today, the CF™ card is one of the most popular flash card media, which provides large capacities, high performance and low cost. The CF™ card supports three basic operation modes: 1) PC card advanced technology attachment (ATA) using I/O mode, 2) PC card ATA using memory mode, and 3) true integrated-drive electronics (IDE) mode, which is compatible with most hard-disk drives [American National Standards Institute (ANSI) (1996), (1997), (1998), (2000), (2002)]. In this project, a DSS is evaluated with a CF™ medium using the third operation mode, mainly for backward compatibility reasons.

CF™ supports the advance power management feature [Compact Flash™ Association (2004)].The host is capable to enable or to disable this feature. By setting up a specific register, the host is able to change the power management level. The power management level is a scale from the lowest power consumption to the maximum performance level. This feature is very important for DAS's and other portable devices that require minimum total power consumption.

Additionally, CF™ supports the translate sector feature [Compact Flash™ Association (2004)]. This feature provides to the host a means of determining the exact number of times that a sector has been erased and written. By using this feature in our DAS, it is feasible to check the wear level of a used CF™ medium.

CF™ is used in many commercial products like digital cameras, handheld computers, cellular phones and notebooks. Due to the massive production of CF™ cards, the cost of these cards is gradually decreased. For all the above reasons, the CF™ memory card was selected for implementing the proposed DSS against other storage media.

2.4.4 Memory Management Scheme

2.4.4.1 DSS Architecture

In the rest of this chapter, the DSS is described analytically. The DSS is an efficient memory-management scheme that increases CF™ lifetime, while it is suitable for large-capacity DAS's. The DSS uses the technique of circular buffer, but it is slightly different.

As mentioned before, the CF™ storage card is configured in true IDE mode of operation [Compact Flash™ Association (2004)]. We are using logical block address (LBA) mode, instead of cylinder/head/sector (CHS) mode. In LBA mode, CF™ presents its memory space, as a linear memory mapped array. The total amount of CF™ space is divided into equal blocks of 512 B, which are called sectors [American National Standards Institute (ANSI) (1996), (1997), (1998), (2000), (2002)]. In true IDE mode of operation, there is a limit of 28 b of LBA addressing. This limitation number is beyond the current project needs.

$$\text{Maximum Capacity} = 2^{28} * 512 \text{ B}$$
$$= 137,438,953,472 \text{ B}$$
$$= 128 \text{ GB}$$

Today, many manufacturers provide CF™ media up to 8 GB. In the current project, DSS is evaluated with a CF™ medium of 128 MB.

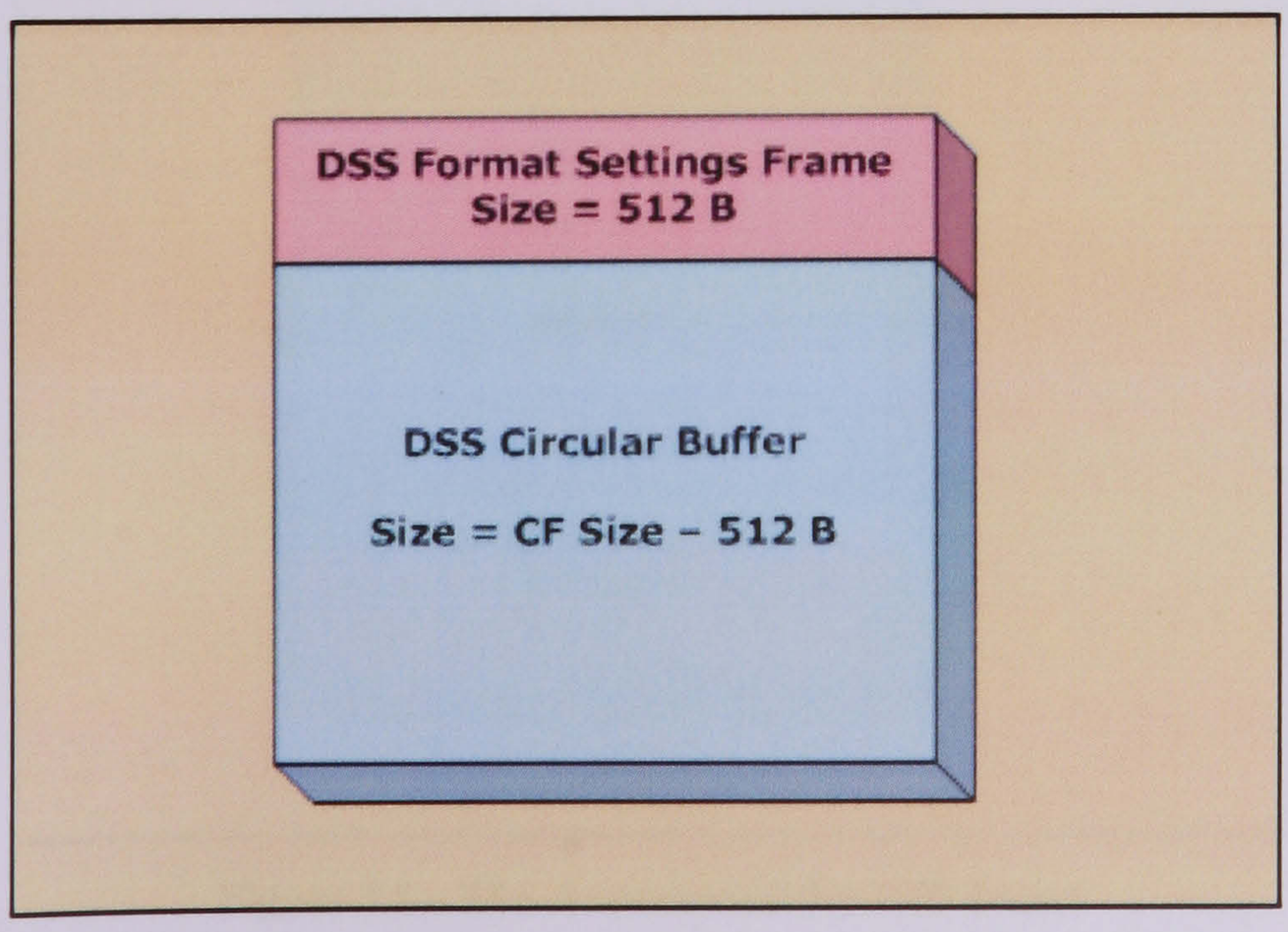

Figure 2.5 - The DSS Architecture

In the DSS, the CF™ space is divided into two virtual partitions, as shown in Figure 2.5. The first partition occupies 512 B and holds the settings of DAS, so it is called the DSS settings partition. The second virtual partition is the main data storage area. The DSS presents its storage space as a circular buffer in order to provide an efficient and easy-to-use software interface. The circular buffer is divided into DSS record frames of 512 B. The total number of DSS record frames depends on the CF™ size as evaluated in the following formula:

$$number\ of\ DSS\ record\ frames = number\ of\ CF\ \text{sec}tors - 1$$

2.4.4.2 DSS Frame Structure

The DSS represents every physical CF™ sector as a DSS frame using the structure shown in Figure 2.6.

The size of each DSS frame is equal to the size of the physical CF™ sector, namely 512 B. The DDS frame is divided into three virtual areas. The first block of 44 B is called the header area. The second block is called the data area and consists of 464 B, while the last four bytes are called the cyclic redundancy check (CRC) area.

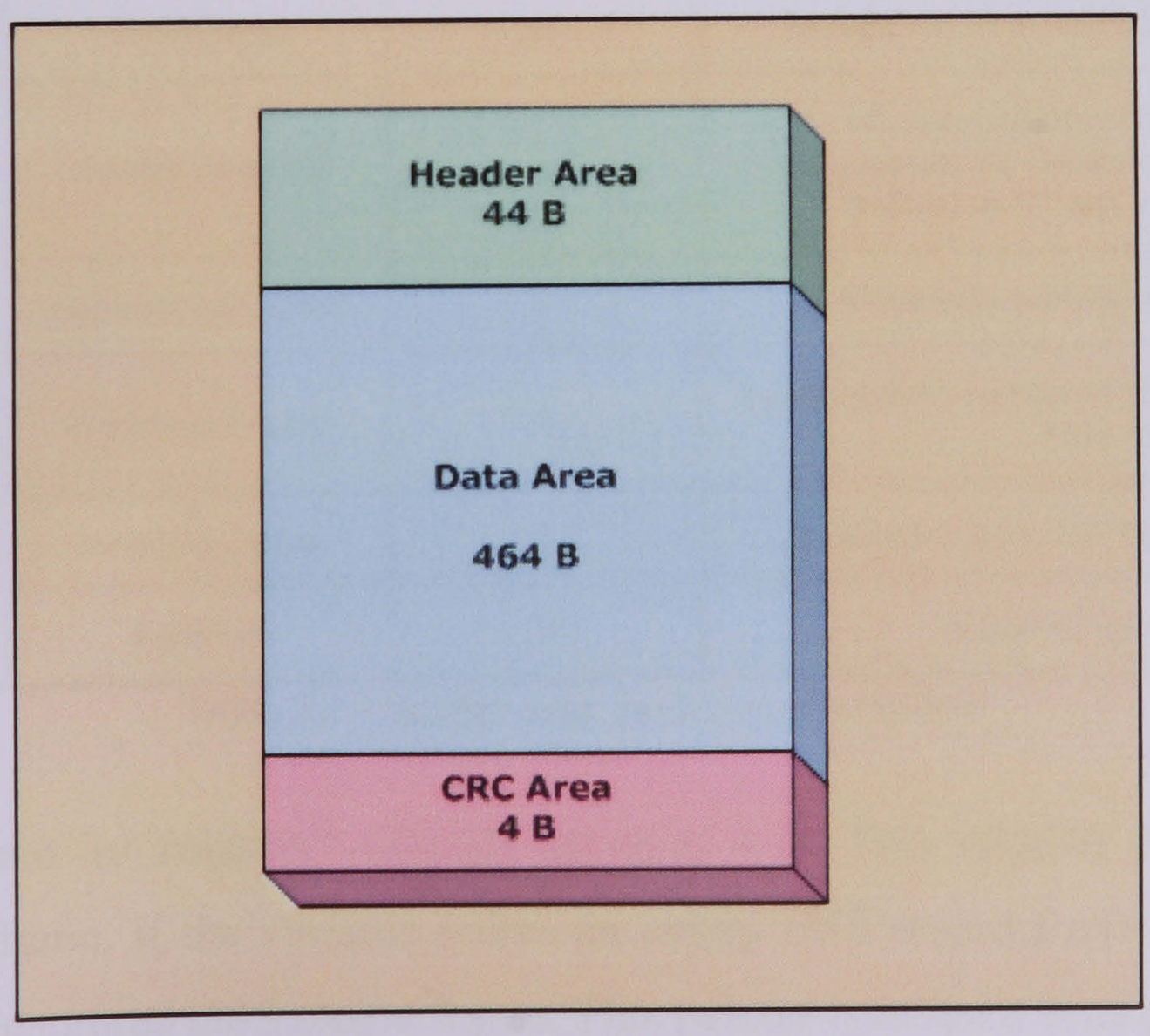

Figure 2.6 - The structure of the DSS frame

2.4.4.2.1 Header Area Structure

The header area contains a set of variables that represents the configuration of the DAS, as shown in Table 2.2. The variable named "packet index" occupies 4 B and represents the absolute DSS frame index number. It ranges circularly from 0×00000001 to 0×FFFFFFFE. There are two reserved packet index values: 0×00000000 and 0×FFFFFFFF. The DSS frame with a packet index value of 0×00000000 presents an empty DSS record frame. The DSS frame with packet index value of 0×FFFFFFFF is a DSS settings frame.

Byte Address	Field Name	Occupied Bytes	Description
0x00	packet index	4	Represents the absolute DSS Data Frame index number.
0x04	chain information	4	Points the next written DSS Data Frame.
0x08	read counter	1	Indicates the number of successful reads of the current DSS Data Frame.
0x09	frame timestamp	7	Represents in BCD format the timestamp (Year, Month, Date, Hour, Minute, Second) of the first sample of the current frame.
0x10	device serial number	2	Represents the device serial number in binary format.
0x12	device name	14	Represents the device name in ASCII format.
0x20	enabled channels	4	Each bit represents the status of a channel. So, 4 bytes represent 32 channels. An enabled channel is marked as "1" and a disabled as "0".
0x24	channels per record	1	Represents the total enabled channels.
0x25	records per frame	1	Represents the number of records contained into the Data Area.
0x26	sampling period	1	Represents the sampling interval in seconds.
0x27	Reserved	6	Reserved for future use.

Table 2.2 - Header area variables description

The "chain information" variable occupies 4 B. This variable points the next written DSS frame. If the variable points an empty DSS record frame, it means that this is the last captured DSS record frame. This pointer is called a head pointer.

The byte variable "read counter" informs us about the read status of that sector. If the read counter is greater than 0×00, it means that the host has accessed the context of this DSS record frame at least once.

The variable "frame timestamp" occupies 7 B. This variable represents the captured timestamp (year, month, date, hour, minute, second) in binary-coded decimal (BCD) format. The timestamp value into a DSS record frame represents the captured timestamp of the first samples record of the current frame.

The variable "device serial number" occupies 2 B. It represents the device serial number in binary format. The range is from 0×0001 to 0×FFFE. Values 0×0000 and 0×FFFF are reserved for multicast purposes.

The "device name" variable occupies 14 B. It represents the device name in ASCII format.

The variable "enabled channels" occupies 4 B. Each bit represents the status of a channel. So, 4 B represent 32 channels. An enabled channel is marked as "1" and a disabled as "0."

The byte variable "channels per record" represents the total number of enabled channels.

The byte variable "records per frame" represents the number of records contained into the data area.

The byte variable "sampling period" represents the sampling interval in seconds.

Finally, there are 6 B reserved for future use.

2.4.4.2.2 Data Area Structure

There are two types of information that can be stored into the data area of the frame. If this information contains settings, variables, or any other kind of configuration data, the frame is called a DSS settings frame, whereas DSS record frame is called the frame that contains records of samples.

The data area structure is different in DSS settings frames than in DSS record frames. The header area informs about the DSS frame type. A DSS frame with "packet index" value 0×FFFFFFFF is a DSS settings frame. Any other "packet index" value presents a DSS record frame. In the following paragraphs the structures of the data area of the DSS setting frame and DSS record frame will be stated.

2.4.4.2.2.1 Data Area Structure of DSS Settings Frame

The DSS settings frame holds information regarding the conventional name and the abbreviation of the measurement unit of each channel. In our project, due to the fact that there are 32 channels, the data area of the DSS settings frame holds 32 different sets of labels and measurement units in ASCII format, as shown in Figure 2.7.

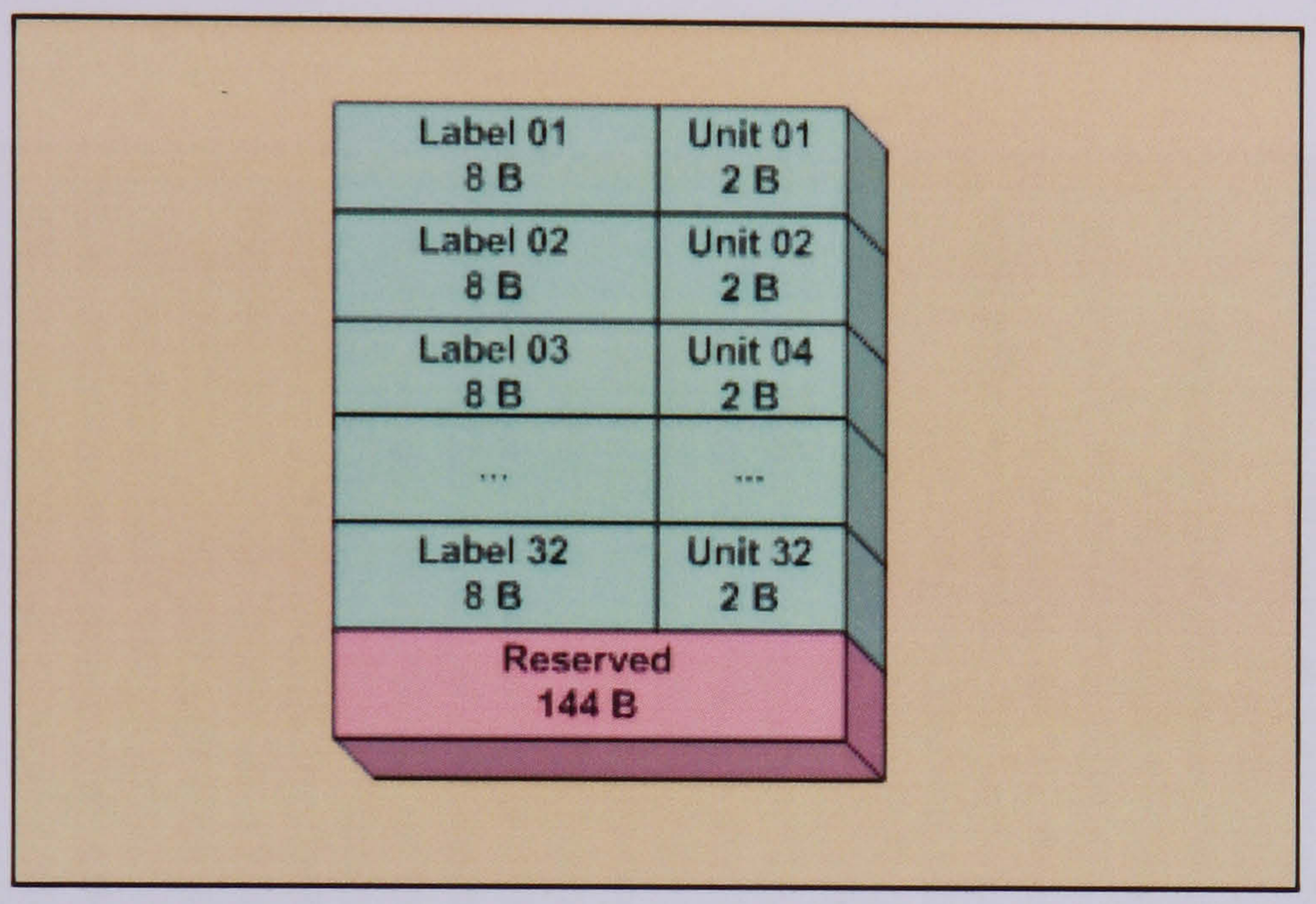

Figure 2.7 - The data area structure of the DSS setting frame

2.4.4.2.2.2 Data Area Structure of DSS Record Frame

In order to determine the utilization of the CF memory an analysis was carried out. The data area of a DSS record frame contains the stored data records, where each data record embodies all enabled channels samples. Since each data record contains one sample from each enabled channel, the actual length of the data record varies according to the number of enabled channels.

Inasmuch as each channel corresponds to a 16-b value, the total length of each data record ranges between 2 and 64 B in the case of 1 and 32 enabled channels, respectively.

The maximum number of records that can be stored in a single DSS record frame is determined by the number of the enabled channels since there is a fixed data area size of 464 B. The utilizable data area in conjunction with the number of records

per frame and the number of enabled channels per record can be evaluated using the following expression:

$$utilizable \quad data \quad area = 2 \cdot w \cdot n \leq 464B$$

Where,

w: The number of enabled channels per record,

n: The number of records per frame.

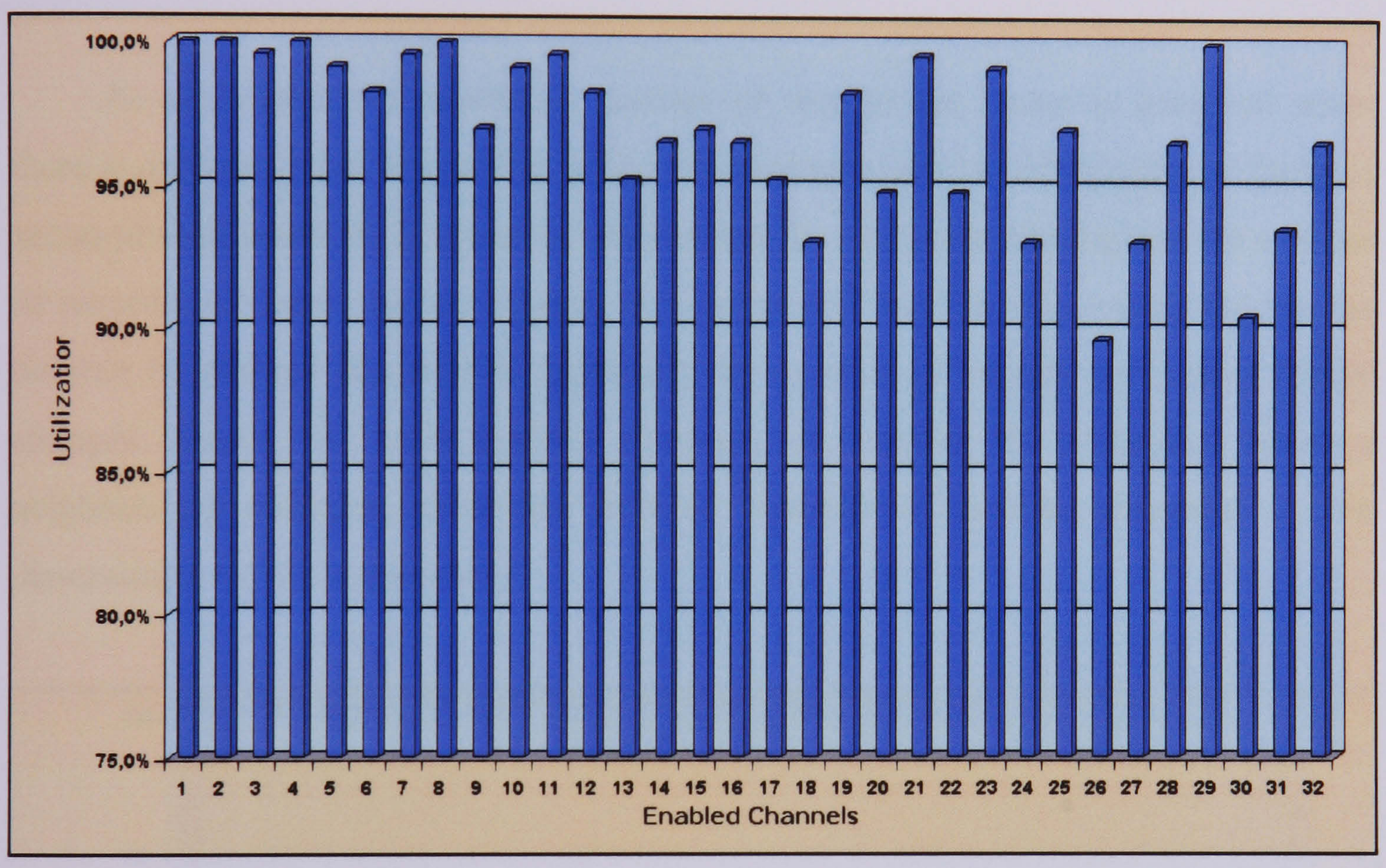

Figure 2.8 - Utilization versus enabled channels

Figure 2.8 is the visual representation of achieved data area utilization versus the number of enabled channels. As shown in this figure, the best memory utilization is achieved when the utilizable data area is equal to the data area size, which is 464 B. It occurs when the number of the enabled channels is equal to 1, 2, 4, 8 and 29.On the other hand, the minimum data area utilisation is observed when the number of the enabled channels is equal to 26 and 30 that correspond approximately to 90% of utilisation. Finally, the average memory efficiency of 32-channel DSS architecture is approximately 96.9%.

In addition to data area utilisation, interesting conclusions can be drawn by considering the number of records per frame in conjunction with the number of

enabled channels. As the number of enabled channels is increased, the number of records per frame is decreased. The expression used for this evaluation is the following:

$$RpF = floor\left(\frac{464}{2 \cdot n}\right)$$

Where,

RpF : The number of records per frame,

n : The number of enabled channels

As calculated, the maximum number of records per frame is achieved when there is only one channel enabled, while the minimum number of records per frame is accomplished when all 32 channels are enabled. Its worth mentioning that the number of records per frame are decreasing in a reciprocal way, demonstrating that as the number of enabled channels is increased, the number of records per frames hardly changes. Hence, the more enabled channels, the smaller the difference between neighbouring columns, since the variable "number of enabled channels" is the denominator of this expression.

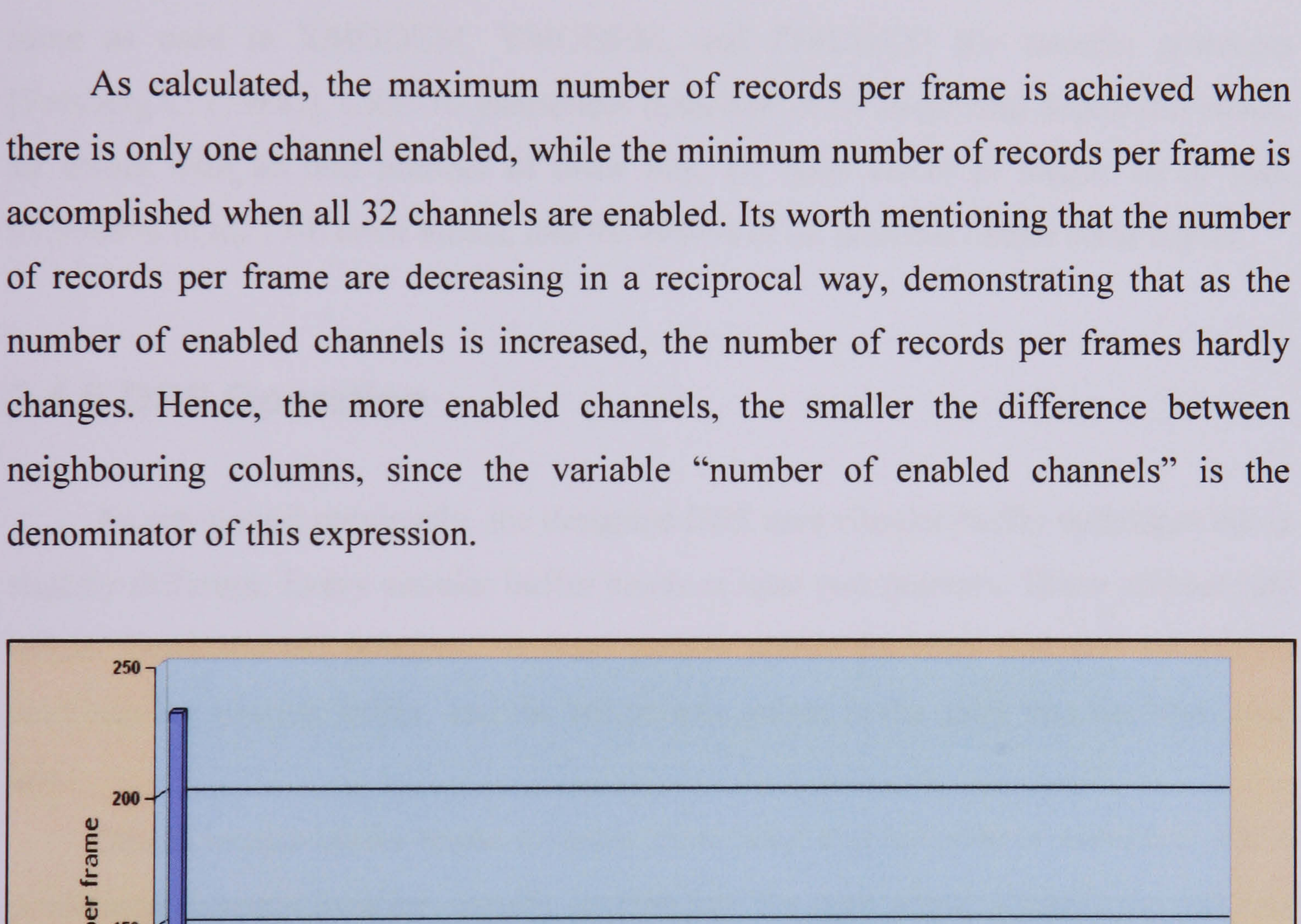

Figure 2.9 - Records per frame versus enabled channels

2.4.4.2.3 Cyclic Redundancy Check (CRC) Area Structure

A Cyclic Redundancy Check (CRC) is a type of hash function, which is used to produce a small, fixed-size checksum of a larger block of data, such as a packet of network traffic or a computer file. The CRC area consists of two CRC-16 values for the whole 508-B block (header and data area).The first 256-B block calculates the first CRC-16 word and the next 252-B block calculates the second CRC-16 word. Our CRC-16 function uses the polynomial formula ($x^{12} + x^5 + 1$). This 16-b CRC is the same as used in XMODEM, YMODEM, and ZMODEM file transfer protocols [Forsberg C. (1988)]. CRC-16 guarantees detection of all single and double-bit errors, all errors with an odd number of error bits, all burst errors of length 16 or less, 99.9969% of all 17-b error bursts, and 99.9984% of all possible longer error bursts.

2.4.5 DSS Operation

As mentioned previously, the designed DSS uses circular-buffer technique but is slightly different. Every circular buffer needs at least two pointers. These pointers are called "head and tail pointers." A head pointer points the entry that will be written next into the circular buffer, and the tail pointer points to the entry that has been read last.

Other circular-buffer-based systems, store head and tail pointer variables, into a predefined memory location, usually located into the boot sector. Despite the fact that this technique delivers easy implementation and quick pointer recovery, it is improper for CF™ card usage, due to limited write cycles of this medium. This means that, if this technique was adopted, the CF™ medium would be damaged in a couple of days. The reason is that this specific memory location "sector" needs to be updated each time a new record is written.

Another circular-buffer-based system stores head and tail pointer variables in an external battery back-up SRAM module in order to avoid write-cycle limitation problems. The major disadvantage of this technique is that, since the pointers are stored in a different medium than the data, whenever either the CF™ card is changed

or the SRAM module's data are corrupted, in most cases there is no way to reconstruct the pointers. Another disadvantage that is revealed by using this technique is that the complexity of the external circuitry and the total device cost increases.

The innovation of the DSS circular buffer is that the head and tail pointers are able to be recovered anytime by simply running a seeking procedure into the circular buffer. The circular buffer is divided into DSS data frames of 512 B. The circular buffer occupies almost the total CF™ memory size, with the exception of a small memory block that holds the DSS settings frame.

The overview of the DAS's operation will be presented using a two-fold operation-oriented procedure that corresponds to the initialization and main data-logging operation. First, the initialization procedure is responsible for recovering the head and tail pointers. Once seeking the entire flash memory, the DAS recovers and stores header and tail pointers into the microcontroller's internal SRAM. Seeking time depends on pointer's position and the total CF™ size. CF™ delivers low latency and high throughput for read accesses; hence, seeking time is acceptable. Each DSS sector header encapsulates "chain-link info", a circularly incremental "packet index" and a "read counter" among others. Each chain-link info field points at the next DSS data frame. The read-counter field gives the read status information of the current frame. Figure 2.10 represents unread frames as turquoise, and already read frames as rose colour. The header pointer is allocated by seeking the entire buffer. This procedure stops when a packet index discontinuity is detected, and the "chain-link info" field points at an erased DSS data frame. An erased DSS data frame is defined as a 512-B zero-filled frame. The tail pointer allocation procedure stops at the last already read frame after the head pointer. After successfully completing the pointers' allocation procedure, the DAS configures the enabled channels and the current sampling rate.

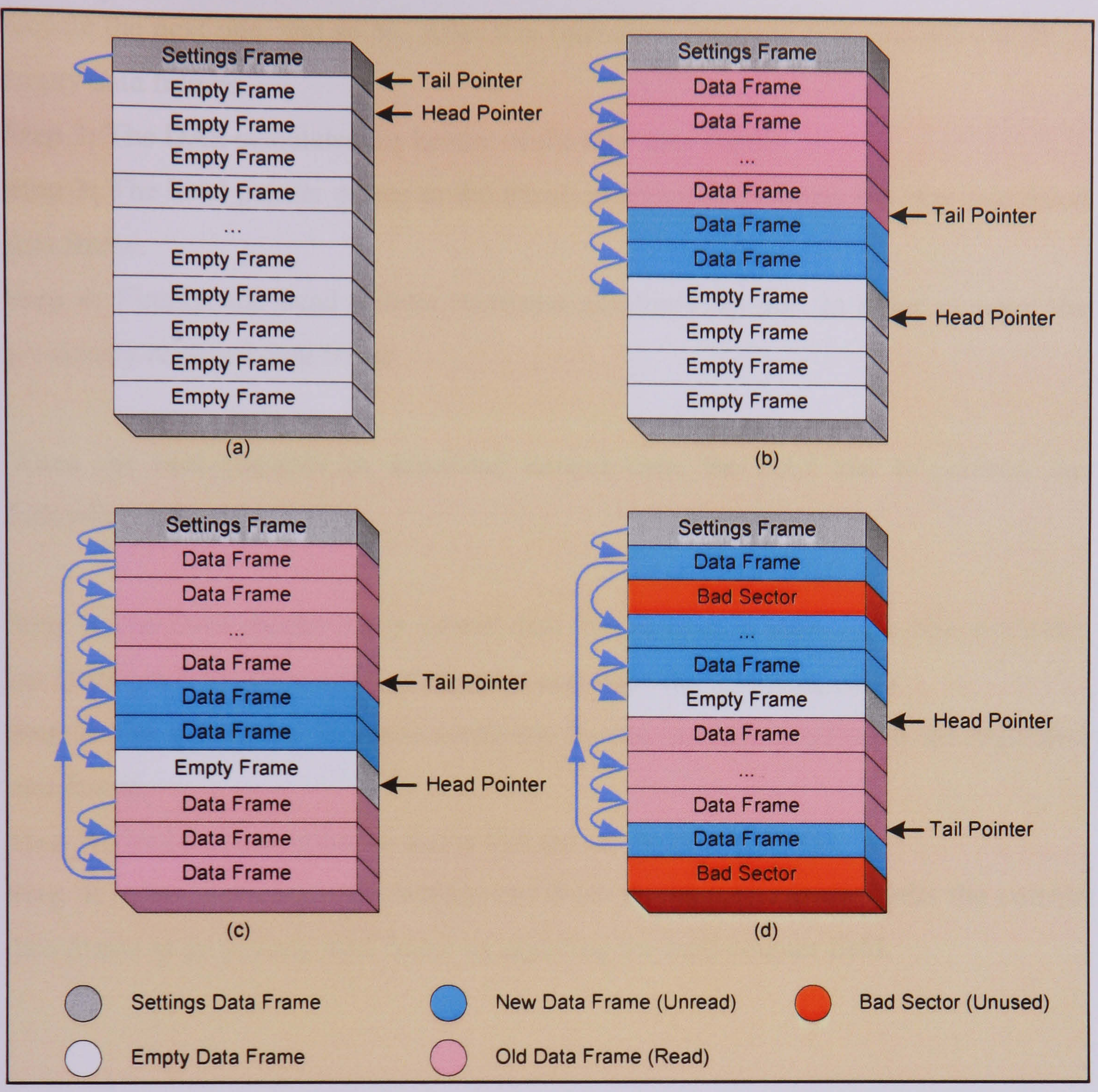

Figure 2.10 - Chain-link information

After completing the initialization procedure, the main data-logging procedure is ready to start. Figure 2.10(a) shows the structure of a DSS-formatted CF™ card. In this phase, there are no data stored except DSS settings frame. After a couple of measurements, the semblance of the CF™ card looks like Figure 2.10(b), (c) and (d). When new data is ready for storing, the DAS has to perform the following steps:

Step 1: As shown in Figure 2.10(a), (b), (c) and (d), the head pointer always points to the first empty data frame. As it is well-known, each flash block cannot be overwritten unless erased in advance. So, the DAS recycles one more data frame, the oldest one. If a bad sector is detected, as shown in Figure 2.10(d), the DAS tries to

recycle the next one, and so on. After that operation, there are two, one after another, empty data frames.

Step 2: The DAS calculates the header of the new data frame.

Step 3: The head pointer points to the frame in which DAS stores the new calculated data frame.

Step 4: Finally, the head pointer increases circularly by one, in order to point the previously recycled data frame.

When the host requests to download unread data, the DAS has to perform the following steps:

Step 1: The DAS checks if any unread data frames exist. If there is no data available, the DAS sends negative acknowledgment and skips the following steps.

Step 2: The tail pointer increases circularly by one in order to point out the requested data frame.

Step 3: The DAS transmits the frame that the tail pointer indicates.

Step 4: After receiving acknowledgment from the host, the DAS marks the current data frame as an already read frame by updating the read-counter field.

2.4.6 Theoretical Evaluation of DSS

The DAS was designed based on the principals DSS. An ATmega128 microcontroller is the core for this prototype system. In addition, special application firmware was designed for this microcontroller in order to support all the required operations, including all acquisitions, logging and data-collection features.

In order to perform the theoretical evaluation of the system, some basic assumptions and theoretical selection were hypothesized in terms of storage medium, sampling rate and number of enabled input channels. The purpose of this theoretical evaluation is to calculate and define the key characteristics of the system, namely storage capability versus enabled channels and Mean Time Between Failure. These two estimations will be the proof of reliability and sufficiency of the system.

The first theoretical selection was the capacity of the storage medium. Specifically, during this evaluation, the system was virtually equipped with a 128-MB CF™. Regarding the sampling rate as well as the number of enabled input channels, the system was considered to support a fixed sampling rate of 1 Hz while the number of the analogue input channels will vary from 1 to 32 using 1 channel step.

Hence, by gradually changing the number of the enabled channels from 1 to 32, the maximum number of days that CF™ can store without overwriting older samples was calculated by using the following formula:

$$CFduration = \frac{\left(\frac{CFsize}{512} - 1\right) \cdot floor\left(\frac{464}{2 \cdot n}\right)}{SR \cdot 86400}$$

Where,

CFduration : Maximum number of days that CF™ can store new data without overwriting older samples,

CFsize : CF™ size in Bytes

n : The number of enabled input channels

SR : Sampling Rate in Hz.

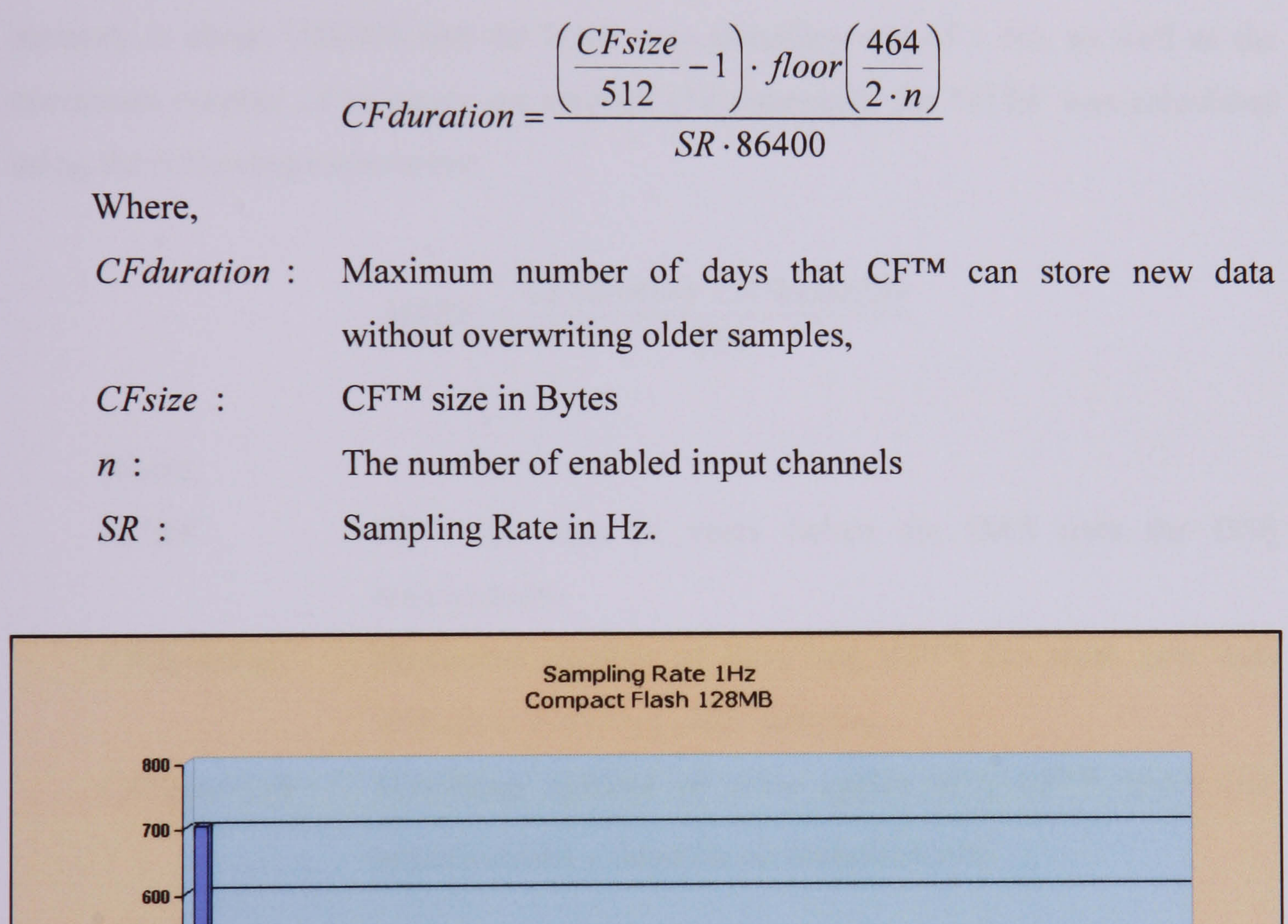

Figure 2.11 - A cycle period versus enabled channels

The graphical representation of the calculated theoretical results is shown in Figure 2.11. In this figure, it is shown that by using the above configuration in the system (SR=1Hz and CFsize=128MB), the maximum number of days without overwriting older samples that corresponds to the minimum number of enabled channels is about 704 days, whereas the minimum number of days which corresponds to the maximum number of enables channels is approximately 21 days.

Additionally, the Mean Time Between Failures (MTBF) was evaluated. Assuming that the maximum number of write cycles of the 128MB in size CF™ memory is about 100,000 and the DAS uses sampling rate of 1 Hz, as well as the maximum number of channels are enabled (32 channels), the MTBF was calculated using the following expression:

$$MTBF = \frac{CFduration \cdot CFSectorLife}{365}$$

Where,

MTBF : CF™ life time in years (when the DAS uses the DSS architecture).

CFduration : Maximum number of days that CF™ can store new data without overwriting older samples,

CFSectorLife : Maximum number of write cycles of a CF™ sector (CF specifications – depends on manufacturer)

The result of this calculation is approximately 5,818.75 years. On the other hand, if instead of using the DSS architecture, the File Allocation Table (FAT) file system was used, the corresponding MTBF would then be limited in a couple of days, due to the continuous write operations on the same blocks of the storage medium.

The result of this theoretical evaluation is obviously the theoretical validation that the proposed DSS architecture covers the needs of our experiment.

2.5 Acquisition Interface Unit

The Data Acquisition System is versatile and can be configured to monitor a variety of parameters at both outdoor and indoor sites. The unit of the DAS, which is responsible for acquiring digital and analogue measurements, is called Acquisition Interface Unit (AIU). This unit consists of 3 different sub-units (Figure 2.12). The new Data Acquisition System is able to record up to 32 channels. The Acquisition Interface Unit provides up to 15 analogue inputs, up to 6 monitoring frequencies in VHF band, up to 8 temperature sensors and a single relative humidity sensor, at a sampling rate up to 1Hz. The depth of the buffer varies from a few months to many years depending on the number of stored channels, the sampling rate and finally the total capacity of the storage medium.

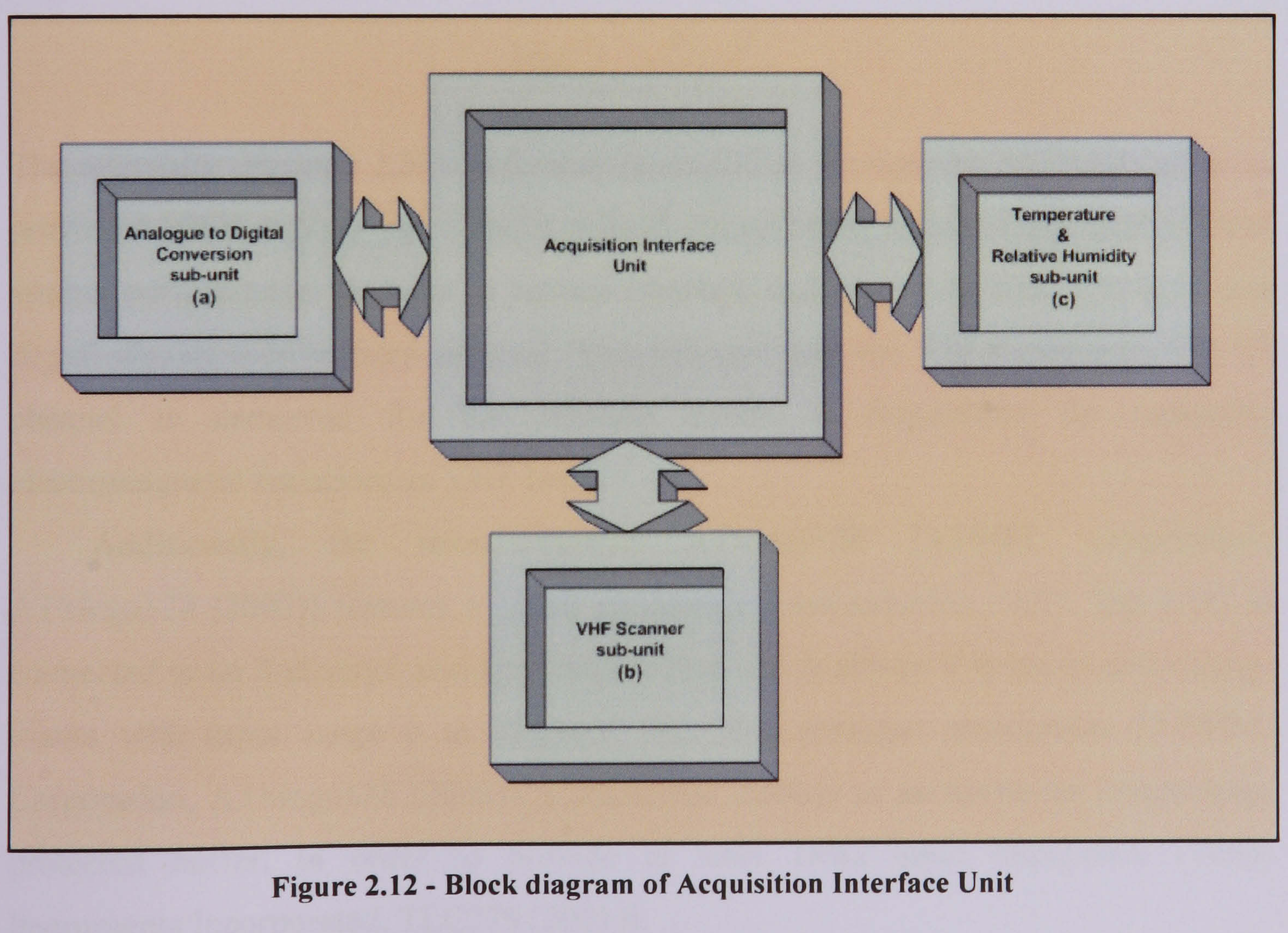

Figure 2.12 - Block diagram of Acquisition Interface Unit

2.5.1 Analogue to Digital Conversion sub-unit

This section defines the sixteen (16) analogue inputs of the Acquisition Interface Unit (AIU) of the Data Acquisition System [Figure 2.12(a)]. The DAS features a 12-bit successive approximation ADC. The ADC chip MAX1270 is a MAXIM product. The MAX1270 multi-range, fault-tolerant ADC [MAXIM Corporation, MAX1270 (1999)] uses successive approximation and internal track/hold (T/H) circuitry to convert an analogue signal to a 12-bit digital representation. The ADC is connected to an 8-channel Analogue Multiplexer, which allows 8 single-ended voltage inputs with input range 0 to 5000mV DC. The Analogue Multiplexer is connected directly to an 8-channel buffer. Each analogue input provides 1MΩ input impedance and overvoltage protection [Texas Instruments Incorporated, TLC279 (2001)]. So, for single ended conversion, the acquisition result is:

$$ADC_{12bit} = \frac{V_{IN} \cdot 2^{12}}{V_{REF}}$$

The internally trimmed 2.50V reference is amplified through the REFADJ buffer to provide 4.096V at V_{REF} pin. Careful printed circuit board layout is essential for best system performance. In order to reduce crosstalk and noise injection, analogue and digital signals tried to keep separate. This sub-unit uses the 7 of 8 channels. The 8^{th} channel is dedicated for the sub-unit which is responsible for capturing electromagnetic emissions in VHF band.

Additionally, the microcontroller ATmega128 [ATMEL Corporation, ATMega128 (2003)] features a 10-bit successive approximation ADC. The ADC is connected to an 8-channel analogue multiplexer which allows 8 single-ended voltage inputs with input range 0 to 2500mV DC. The analogue multiplexer [ATMEL Corporation, ATMega128 (2003)] is connected directly to an 8-channel overvoltage protected buffer, in order to provide at least 1MΩ input impedance [Texas Instruments Incorporated, TLC279 (2001)].

2.5.2 Sub-unit for capturing EM emissions in VHF band

Given that the purpose of this project is to capture EM emissions in VHF band and possible correlations of these emissions with strong earthquakes exist. It is necessary to record the variations of the electromagnetic field in a wide spectrum of frequencies up to UHF band. A new peripheral device for the above Data Acquisition System, "VHF Scanner" [Figure 2.12(b)], has been designed and implemented. The in-built VHF TV tuner (ALPS TEDE9) [PHILIPS Semiconductors, TSA5520 (1996)] in combination with an omni-directional Discone antenna, is responsible for that task. The circuitry of the tuner has been specially designed to cover project needs. In particular the internal Auto Gain Control (AGC) of the tuner is bypassed and a fixed maximum gain is established. This ensures that VHF recordings will be analogous to signal input and independent from any internal variable amplification of the tuner.

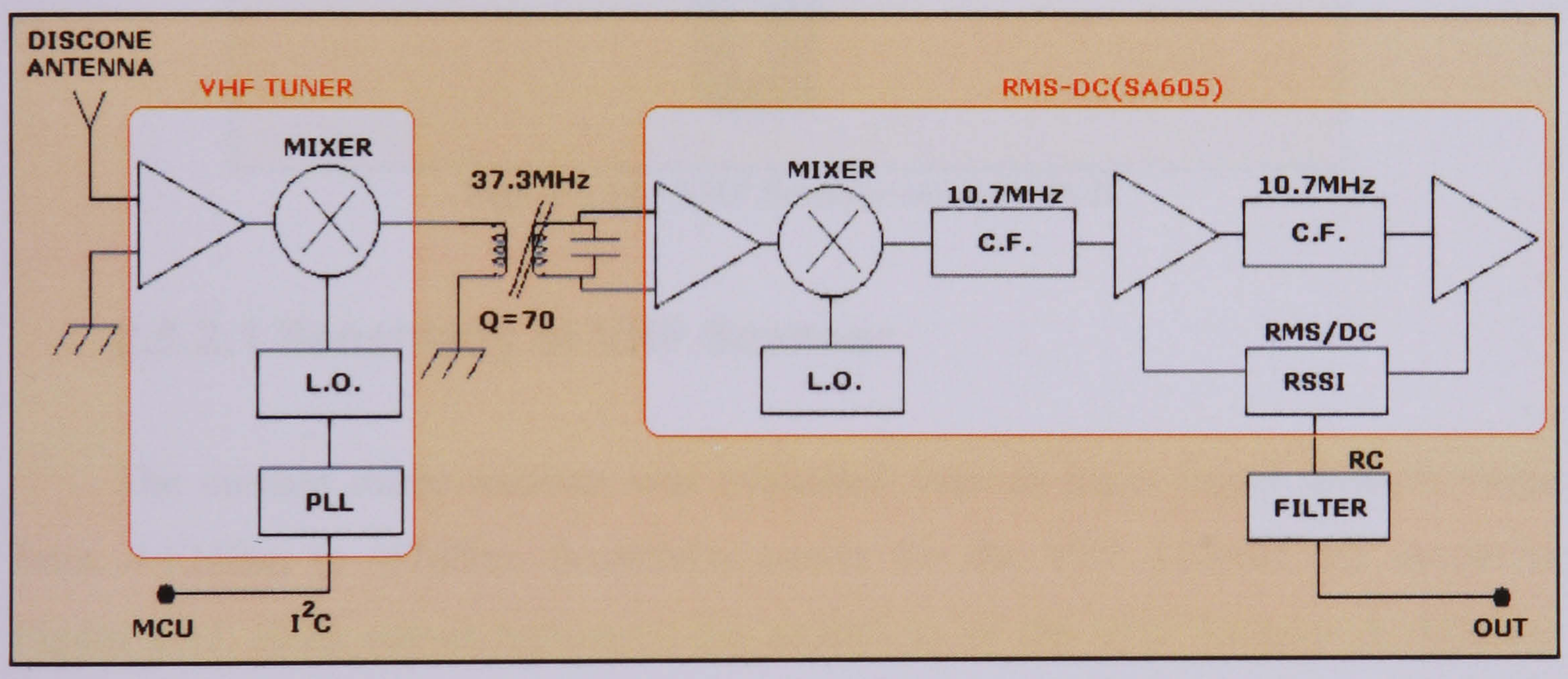

Figure 2.13 - Block diagram of VHF Scaner sub-unit

Figure 2.13 displays the block diagram of sub-units, while Figure 2.14 its Printed Circuit Board (PCB). The Intermediate Frequency (IF) output of 37.3MHz of the tuner is connected directly to a RMS to DC converter circuitry, based on a Philips integrated circuit, the SA605 [PHILIPS Semiconductors, SA605 (1997)]. The logarithmic Received Signal Strength Indicator (RSSI) output of SA605 is connected to a 12-bit input ADC channel through a high input impedance buffer. The tuner communicates with the Data Acquisition System via the I^2C bus interface [PHILIPS Semiconductors, I^2C (2000)]. The spectrum of the tuner ranges from 70MHz to 470MHz. In a sampling rate of 1Hz, up to 6 monitoring frequencies in this range can

be selected dynamically from us. The Phase Locked Loop (PLL) of the tuner is tuned-up circularly every 120msec to the monitoring frequencies. Frequencies from 70MHz to 170MHz have not been included in order to avoid conflicts from radio emissions of local radio stations and amateurs.

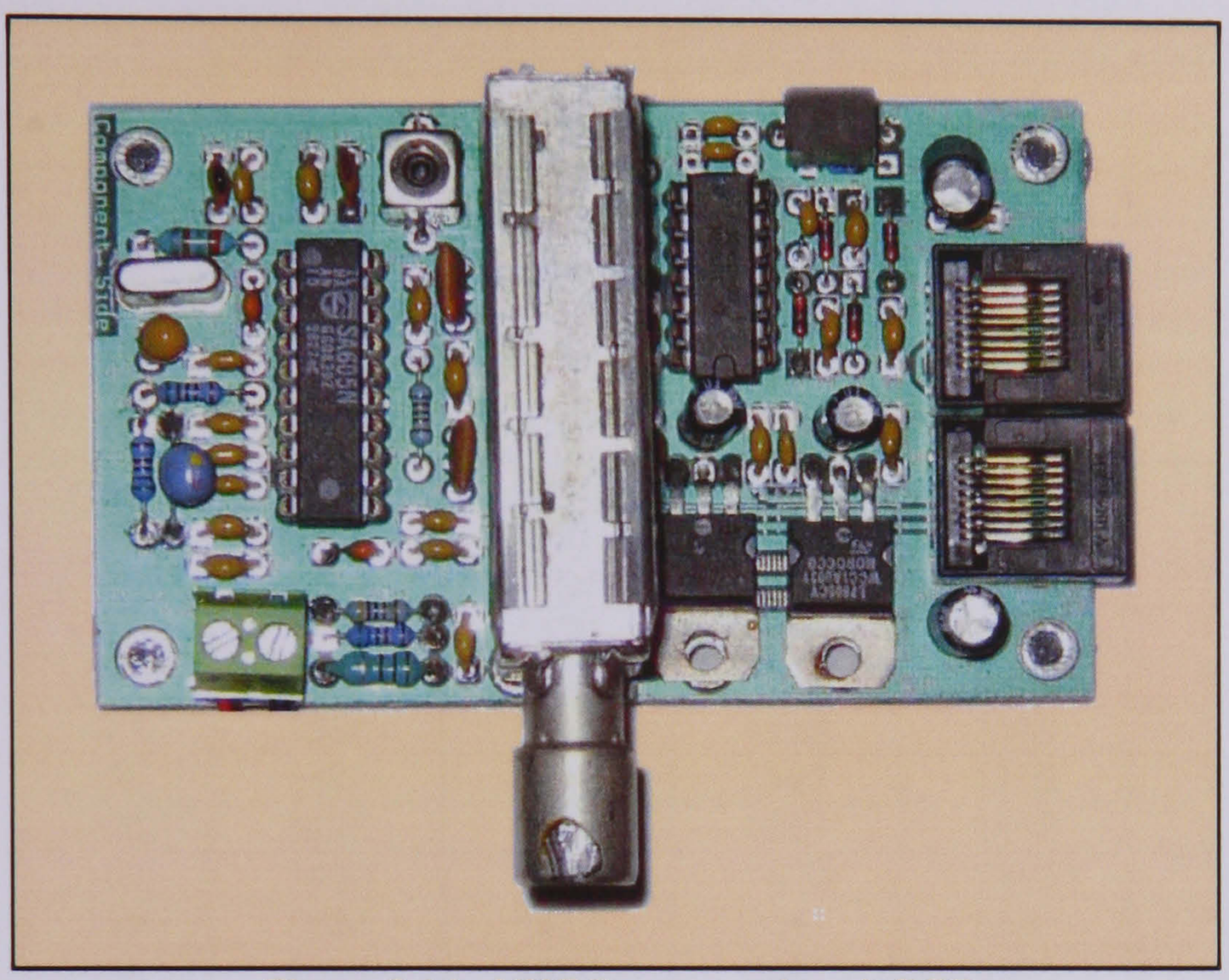

Figure 2.14 - VHF Scanner sub-unit PCB

2.5.2.1 Sensitivity of VHF Scanner

The custom made receiver was evaluated over an input signal strength range from -112dBm to -47dBm. Sensitivity curves for the VHF Scanner are shown in Figure 2.15. Each colour represents the sensitivity of the VHF Scanner in different frequencies. The VHF receiver has good linearity over most of the range and there is little inter-receiver variability, eliminating the need for individual calibration once gain levels were set up. Performance at levels below -110dBm is likely to be dominated by noise and cease to be linear. Sensitivity is about 23.2mV/dBm and is linear up to -50dBm. Maximum input is -44dBm before saturation, but linearity is not maintained between -50dBm and -44dBm.

$$P_{dBm} = 20 \cdot \log \frac{V_{IN}}{\sqrt{R \cdot P_0}}$$

$$R = 50\Omega$$

$$P_0 = 1mW$$

$$P_{dB\mu V} = 20 \cdot \log \frac{V_{IN}}{V_0}$$

$$V_0 = 1\mu V$$

RF IN			DC V_{OUT}					
V_{IN}	P_{IN}		142MHz	178MHz	230MHz	320MHz	390MHz	415MHz
(µV)	(dBµV)	(dBm)	(mV)	(mV)	(mV)	(mV)	(mV)	(mV)
0.562	-5	-112	675	512	422	735	517	341
1	0	-107	689	520	444	736	522	422
1.41	3	-104	706	530	483	737	541	470
1.99	6	-101	752	555	534	738	577	563
2.82	9	-98	808	591	593	739	636	632
3.98	12	-95	871	640	667	740	702	698
5.62	15	-92	958	711	747	806	783	790
7.94	18	-89	1043	801	846	914	881	899
11.22	21	-86	1109	889	940	998	967	987
15.85	24	-83	1180	986	1029	1079	1052	1070
22.39	27	-80	1244	1066	1110	1157	1128	1156
31.62	30	-77	1299	1136	1175	1222	1192	1219
44.67	33	-74	1347	1201	1239	1280	1252	1278
63.09	36	-71	1388	1263	1298	1333	1309	1331
89.12	39	-68	1425	1316	1347	1378	1356	1376
125.9	42	-65	1454	1359	1387	1417	1397	1416
177.8	45	-62	1480	1400	1425	1453	1436	1452
251.2	48	-59	1504	1437	1457	1480	1466	1481
354.8	51	-56	1529	1464	1481	1503	1490	1504
501.2	54	-53	1558	1491	1507	1530	1517	1532
707.9	57	-50	1614	1515	1531	1558	1545	1557
1000	60	-47	1362	1545	1561	1597	1575	1590

Table 2.3 - VHF Scanner Sensitivity

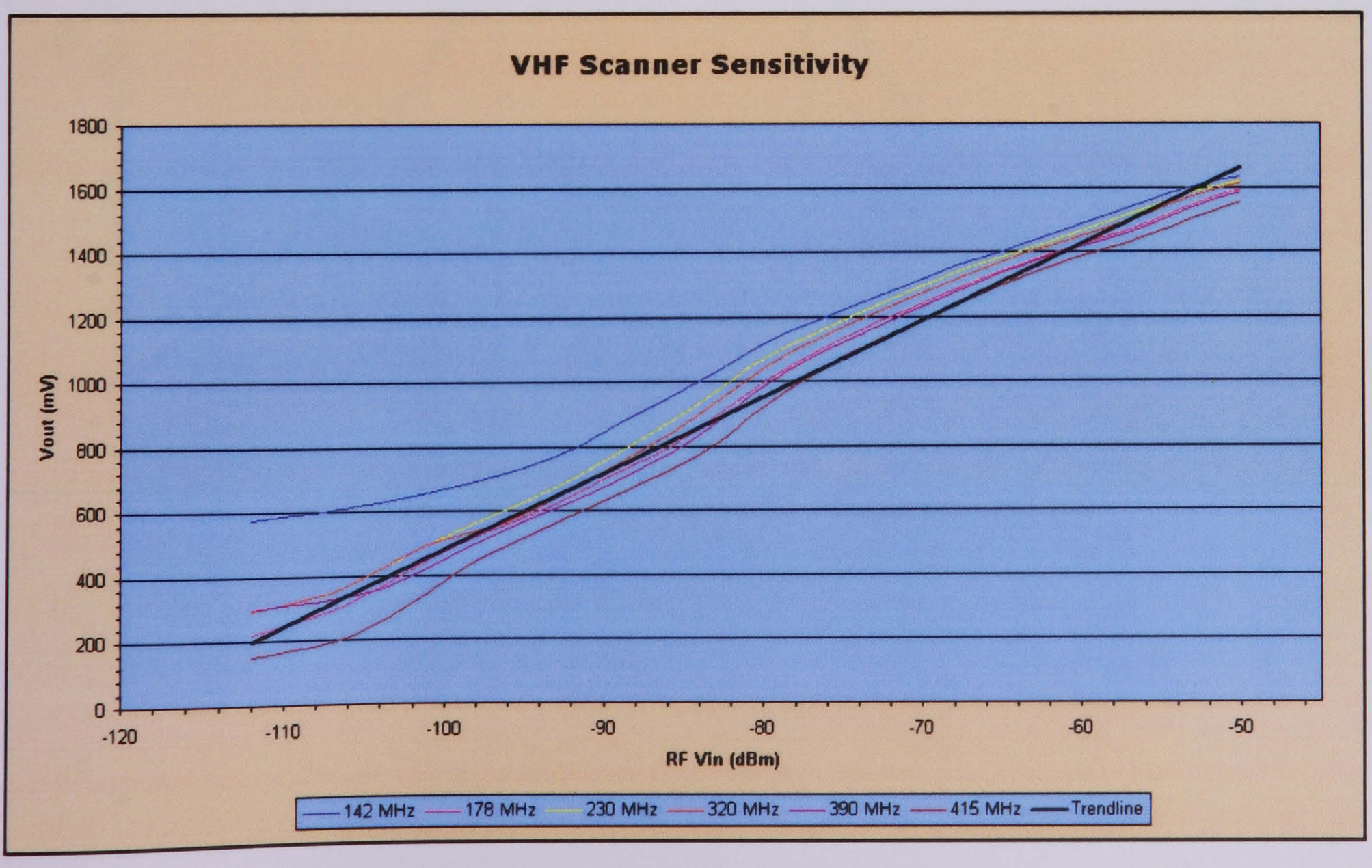

Figure 2.15 - VHF Scanner Sensitivity

Normalised frequency response for VHF scanner tuned at 142MHz, 178MHz, 230MHz, 320MHz, 390MHz and 415MHz is shown in Figure 2.16. The Intermediate Frequency (IF) of the tuner is 37.3MHz, while the bandwidth of the receiver is about 180 KHz. This is wide enough to detect EM emissions and narrow enough to reduce the possibility of co-channel interference. The quality factor for the VHF receiver is given from the following formula:

$$Q = \frac{f_C}{\Delta f} = \frac{37.3MHz}{180KHz} \cong 200$$

Where,

Q = Quality Factor,

f_C = Resonant Frequency

Δf = Bandwidth

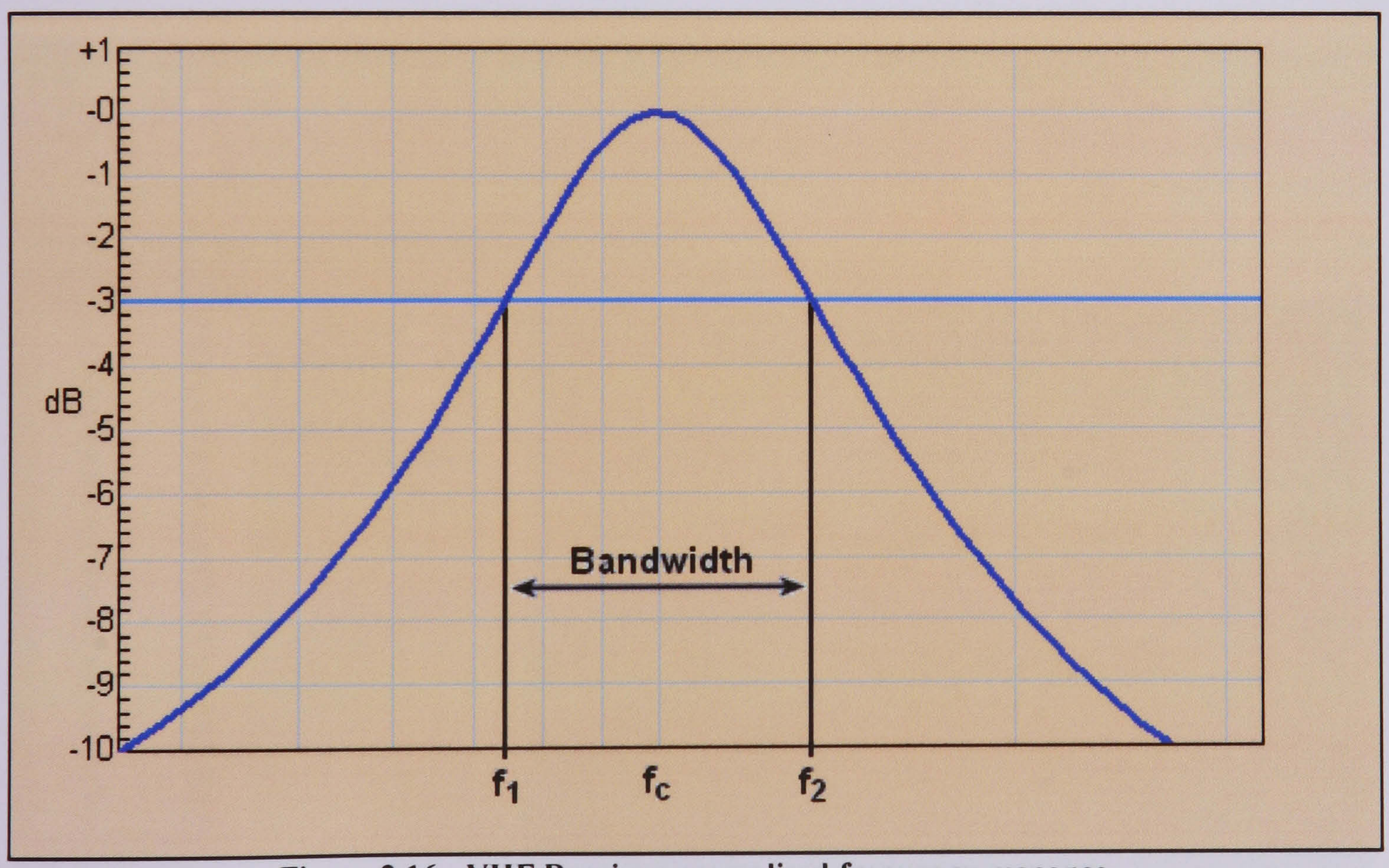

Figure 2.16 - VHF Receiver normalised frequency response

2.5.2.2 VHF Scanner testing device and software

In order to plot sensitivity curves and frequency response for the VHF receiver, dedicated software and hardware developed. The hardware was a microcontroller with UART and a single channel, 12-bit ADC. Dedicated software developed in order to interface simultaneously the RF programmable synthesizer (HAMEG HM-8134-2) and the previously mentioned custom made ADC device. This software plots in real time the sensitivity of the RF receiver, which is going to be tested. The following figure represents the sensitivity of the VHF tuner in resonant frequency of 415MHz (Figure 2.17).

There is also compatibility with other commercial analysis software, in order to use this data for further analysis.

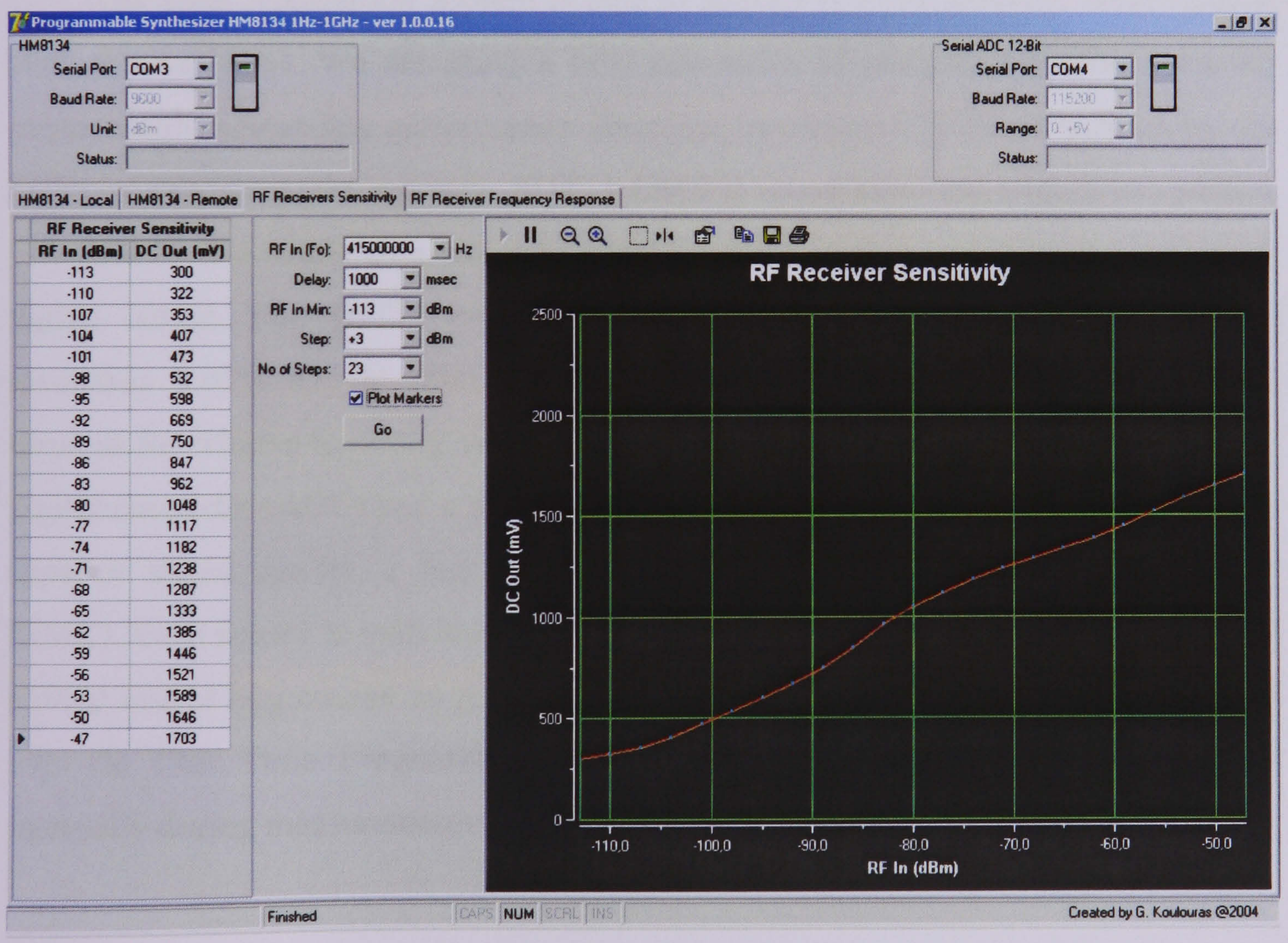

Figure 2.17 - Software for testing custom made RF Receivers Sensitivity

2.5.3 Digital temperature and relative humidity sensors

The Data Acquisition System is able to record up to 8 temperatures. For that purpose the digital thermometers DS1631 is used [DALLAS Semiconductors - MAXIM, DS1631 (2002)]. The DS1631 uses a bandgap temperature sensing architecture in conjunction with a sigma-delta analogue-to-digital converter (ADC) to provide digital temperature measurements. The bandgap circuit produces a voltage that varies linearly with temperature. This voltage is converted to a digital value by the analogue-to-digital converter (ADC). DS1631 digital thermometers provide 12-bit temperature readings over a -55°C to +125°C range. The accuracy of DS1631 thermometer is ±0.5°C from 0°C to +70°C. Communication with the DS1631 is achieved through a 2-wire serial interface, while three address pins allow up to eight devices to be multidropped on the same 2-wire I^2C bus [PHILIPS Semiconductors, I^2C (2000)].

The Data Acquisition System is able to acquire relative humidity level ranging from 0% to 100%. We are using a new generation of integrated relative humidity sensors with outstanding performance. Based on intelligent CMOSens technology, the SHT11 [SENSIRION Company, SHT11 (2003)] offers excellent long-term stability. The SHT11 is a single chip relative humidity sensor module comprising a calibrated digital output. The SHT11 provides Relative Humidity accuracy ±3.5% RH and resolution 0.03% RH @ 12bit. The SHT11 includes a capacitive polymer sensing element for relative humidity sensor. It is seamlessly coupled to a 12-bit analogue-to-digital converter (ADC) and a serial interface circuit on the same chip. This results in superior signal quality, a fast response time and tolerant to external disturbances (EMC). Each sensor is individually calibrated in a precision humidity chamber with a chilled mirror hygrometer as reference. The calibration coefficients are programmed into the One Time Programmable (OTP) memory. These coefficients are used internally during measurements to calibrate the signal from the sensor.

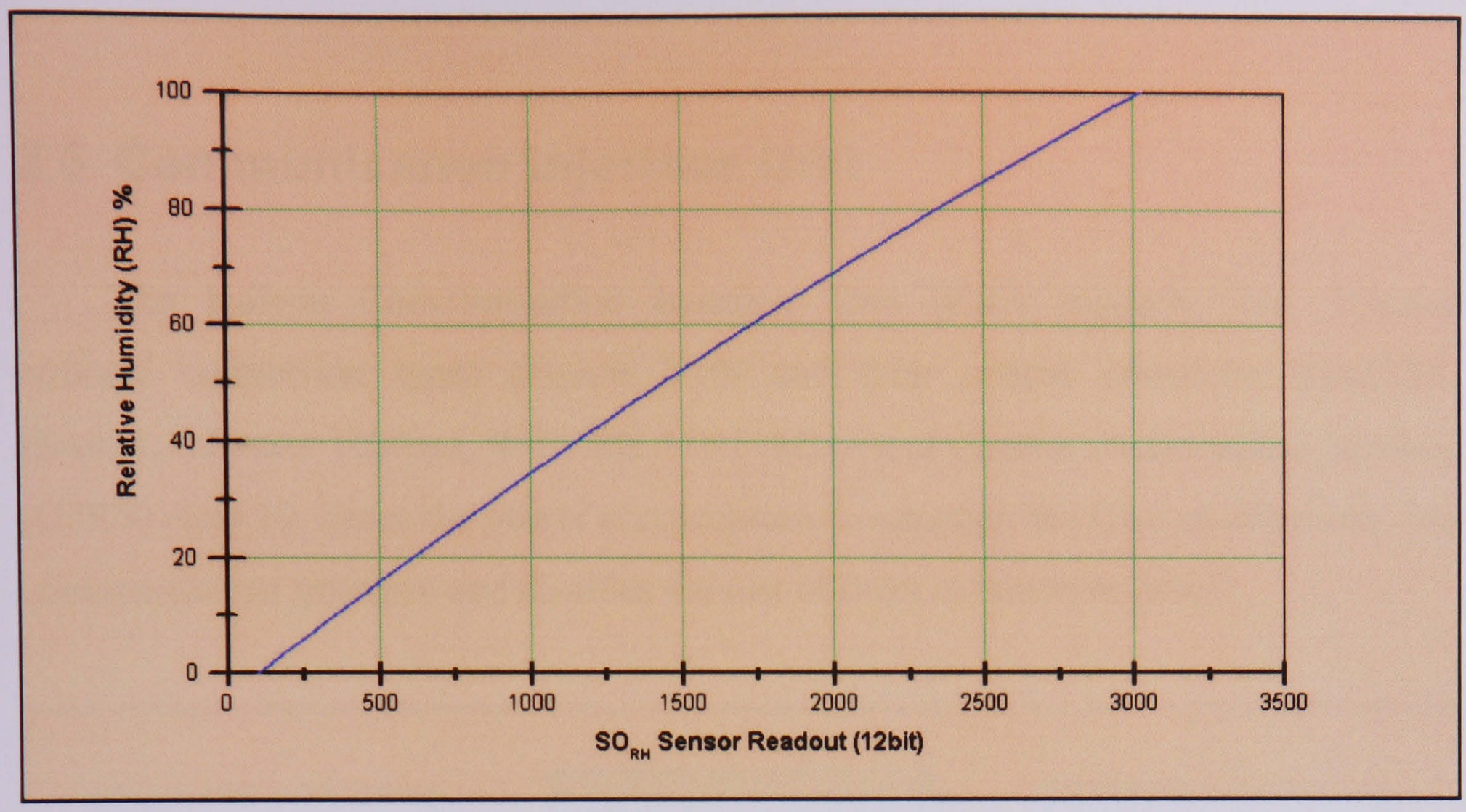

Figure 2.18 - Relative Humidity sensor (SHT11) sensitivity

In order to compensate for the "non-linearity" of the humidity sensor and to obtain the full accuracy, the manufacturer recommends converting of the readout value with the following formula:

$$RH_{Linear} = c_1 + c_2 \cdot SO_{RH} + c_3 \cdot SO_{RH}{}^2$$

Where,

$c_1 = -4$

$c_2 = 0.0405$

$c_3 = -2.8 \cdot 10^{-6}$

2.6 Communication Interface Unit

The built-in Communication Interface Unit (CIU) supports five different optional connection types (Figure 2.19) and their related protocols: EIA232E, EIA485, Ethernet 10Mbps, WiFi 802.11b 11Mbps and General Packet Radio Services (GPRS) class 10. Since the power consumption is essential, the DAS enables only one communication interface and disables the rest of them to conserve power.

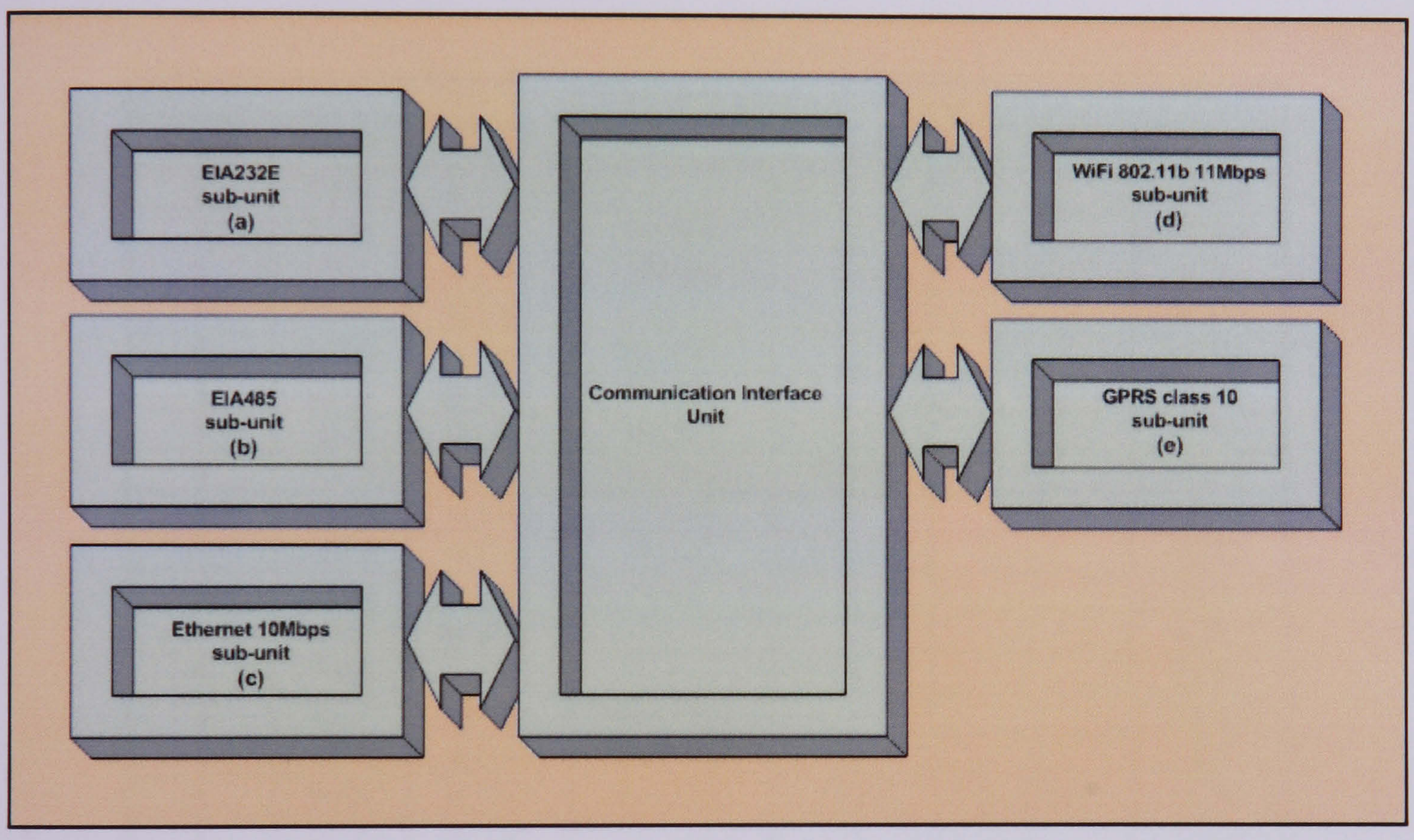

Figure 2.19 - Block diagram of Communication Interface Unit

2.6.1 Custom designed communication protocol

Concerning the application layer of the OSI reference model, a custom designed communication protocol has been implemented in order to retrieve data trustworthily from each field station. If any communication error is detected, Backward Error Correction (BEC) is used, where the corrupted blocks of data are rejected and the central station commands the data acquisition system to retransmit them. The following tables summarize this custom designed communication protocol.

Host Writes						
Start	**CMD**	**Serial**	**Parameters**	**Data**	**CRC**	**End**
$	DEV	w (/w)	-	-	-	<CR>
$	EPM	w (/w)	dw(/dw)	-	-	<CR>
$	INF	w (/w)	B (/B)	-	-	<CR>
$	RTD	w (/w)	-	-	-	<CR>
$	WTD	w (/w)	9B (/9B)	-	-	<CR>
$	CHK	w (/w)	B (/B)	-	-	<CR>
$	REB	w (/w)	w (/w)	-	-	<CR>
$	WEB	w (/w)	w (/w)	B (/B)	-	<CR>
$	RRB	w (/w)	w (/w)	-	-	<CR>
$	WRB	w (/w)	w (/w)	B (/B)	-	<CR>
$	RUN	w (/w)	-	-	-	<CR>
$	SRS	w (/w)	-	-	-	<CR>
$	HRS	w (/w)	-	-	-	<CR>
$	RCF	w (/w)	dw (/dw)	-	-	<CR>
$	ECF	w (/w)	dw (/dw)	-	-	<CR>
$	WCF	w (/w)	dw (/dw)	512B	dw (/dw)	<CR>
$	SCF	w (/w)	-	-	-	<CR>
$	ICF	w (/w)	-	-	-	<CR>
$	PCF	w (/w)	-	-	-	<CR>
$	LCF	w (/w)	dw (/dw)	-	-	<CR>
$	VER	w (/w)	-	-	-	<CR>

Table 2.4 - Communication Protocol (Host writes)

Table 2.4 and Table 2.5 show the twenty one (21) instruction set of the new Data Acquisition System (DAS). The first table shows the command and the syntax of what host transmits, while the second one shows the response from the DAS.

For example, the command "$SCF" followed by the serial number of the device, has as result the specified device to return eighteen bytes that comprise the Status of Compact Flash™ medium it uses. The full detailed DAS communication protocol described in APPENDIX C' (Data Acquisition System - API interface).

Host Reads							
Start	**CMD**	**Serial**	**Ack/Nak**	**Parameters**	**Data**	**CRC**	**End**
$	DEV	w (/w)	Y	-	-	-	<CR>
$	EPM	w (/w)	Y/N/?	-	-	-	<CR>
$	INF	w (/w)	Y/N/?	B(/B)	Length*B	-	<CR>
$	RTD	w (/w)	Y/N/?	-	9B (/9B)	-	<CR>
$	WTD	w (/w)	Y/N/?	-	-	-	<CR>
$	CHK	w (/w)	Y/N/?	B(/B)	B (/B)	-	<CR>
$	REB	w (/w)	Y/N/?	w (/w)	B (/B)	-	<CR>
$	WEB	w (/w)	Y/N/?	w (/w)	-	-	<CR>
$	RRB	w (/w)	Y/N/?	w (/w)	B (/B)	-	<CR>
$	WRB	w (/w)	Y/N/?	w (/w)	-	-	<CR>
$	RUN	w (/w)	Y/N/?	-	-	-	<CR>
$	SRS	w (/w)	Y/N/?	-	-	-	<CR>
$	HRS	w (/w)	Y/N/?	-	-	-	<CR>
$	RCF	w (/w)	Y/N/?	dw (/dw)	512B	dw (/dw)	<CR>
$	EFP	w (/w)	Y/N/?	dw (/dw)	-	-	<CR>
$	WFP	w (/w)	Y/N/?	dw (/dw)	-	-	<CR>
$	SCF	w (/w)	Y/N/?	-	18B (/18B)	-	<CR>
$	ICF	w (/w)	Y/N/?	-	512B	dw (/dw)	<CR>
$	PCF	w (/w)	Y/N/?	-	9B (/9B)	-	<CR>
$	LCF	w (/w)	Y/N/?	-	-	-	<CR>
$	VER	w (/w)	Y/N/?	-	512B	dw (/dw)	<CR>

Table 2.5 - Communication Protocol (Host reads)

2.6.2 Wired connection sub-units

The built-in Communication Interface Unit (CIU) supports three different wired connection types and their related protocols: EIA232E, EIA485 and 10Base-T/100Base-TX Ethernet connection.

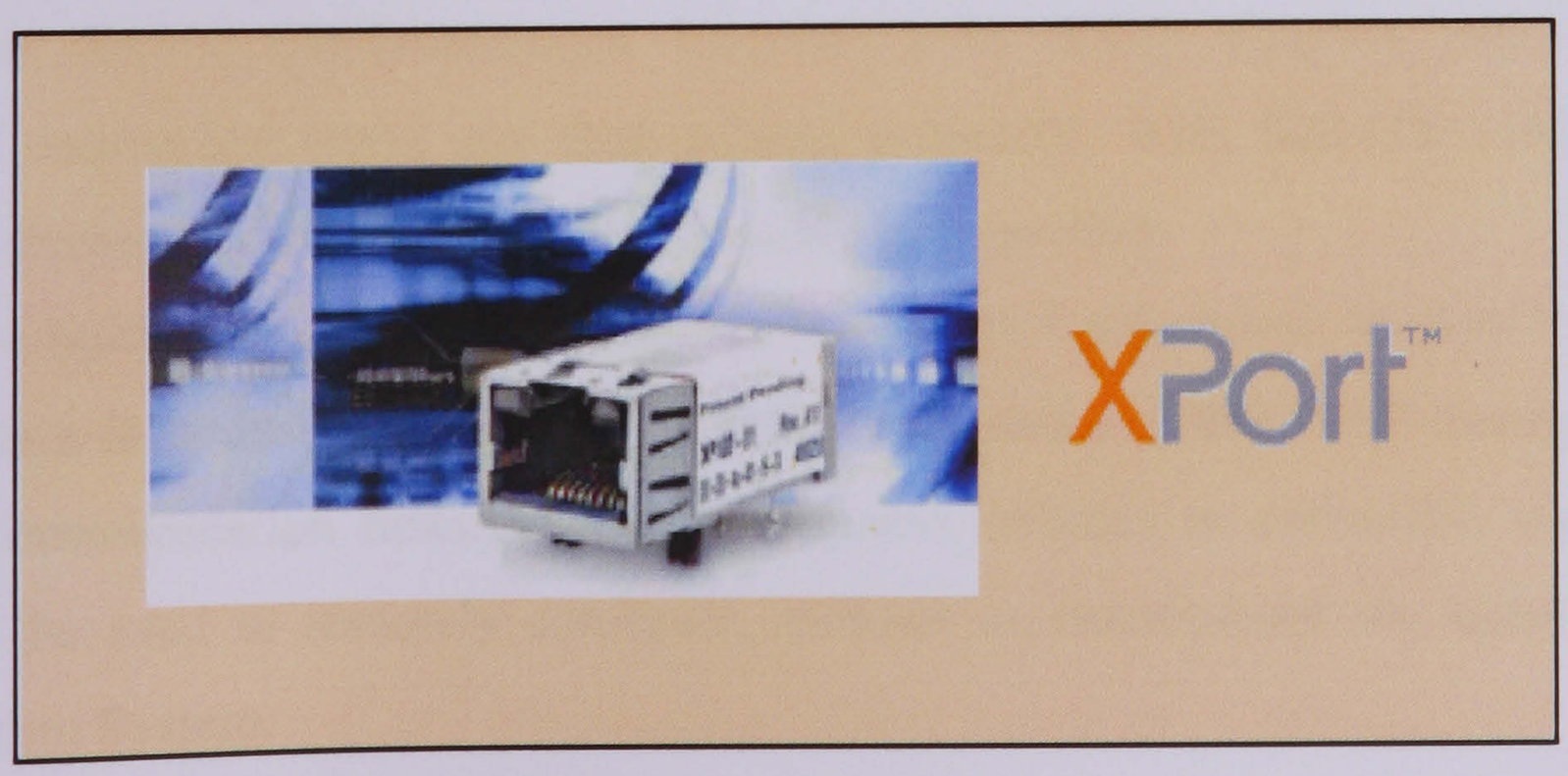

Figure 2.20 - XPort™ device server

EIA485 over EIA232 communication protocol has the advantage of being able to support single master, multiple-slave devices all running on the same line and requires four wires for a full-duplex connection. This means that up to 32 data acquisition systems can be connected on the same line. An EIA485 repeater hub can be used to expand EIA485 serial communication network by increasing the maximum distance and the number of slave devices.

The built-in XPort™ server device [Lantronix Corporation, XPort™ (2005)], uses the Internet Protocol (IP) for network communications. It uses the Transmission Control Protocol (TCP) to assure that no data is lost or duplicated, and that everything sent to the connection arrives correctly at the target. The XPort™ module incorporates all essential networking features, including a 10Base-T/100Base-TX Ethernet connection, a full TCP/IP protocol stack and a 256-bit AES encryption for secure communications. XPort™ also offers a built-in Web server using Java applets for interactive data communications to and from the Data Acquisition System through a standard Internet browser. Web capability can be used for configuration, remote monitoring, or troubleshooting. Additionally, the XPort™ acts as a dedicated co-processor to optimize network activities, permitting the host microprocessor to function at maximum efficiency.

2.6.3 Wireless connection sub-units

The built-in Communication Interface Unit (CIU) supports two different wireless connection types and their related protocols: WiFi 802.11b 11Mbps and General Packet Radio Services (GPRS) class 10 connection.

The built-in WiPort™ server device [Lantronix Corporation, WiPort™ (2006)], integrates a fully developed TCP/IP network stack and a 128bit WEP Encryption for secure communication links. The WiPort™ also includes an embedded web server that can be used to remotely configure, monitor or troubleshoot the attached Data Acquisition System.

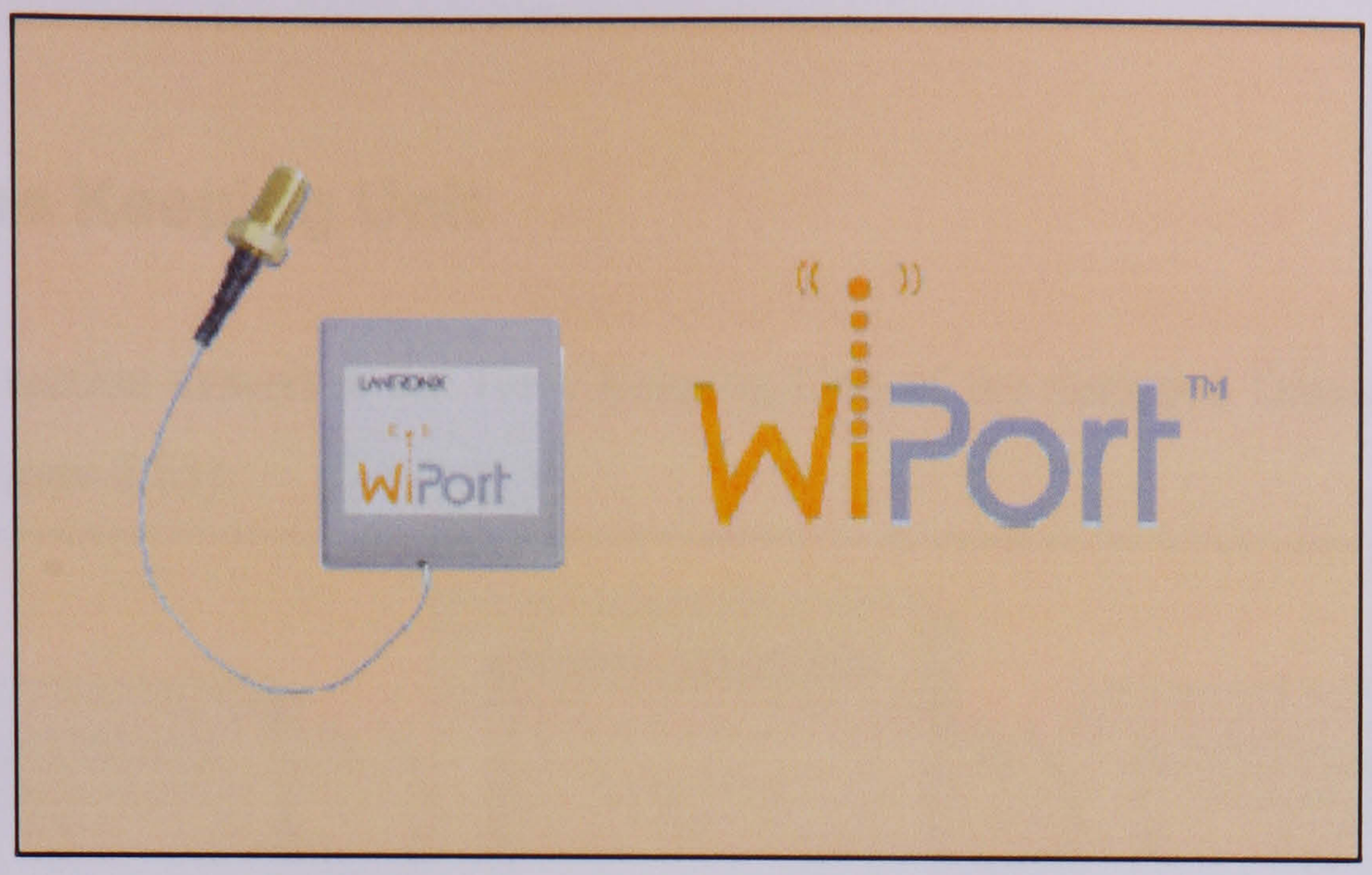

Figure 2.21 - WiPort™ device server

The built-in GM862-GPRS module [Telit Communications, GM862-GPRS (2004)], integrates a cellular phone with GPRS support. That module provides an easy way to establish a socket connection thru internet and communicate with the remote host from anywhere, using wireless technology.

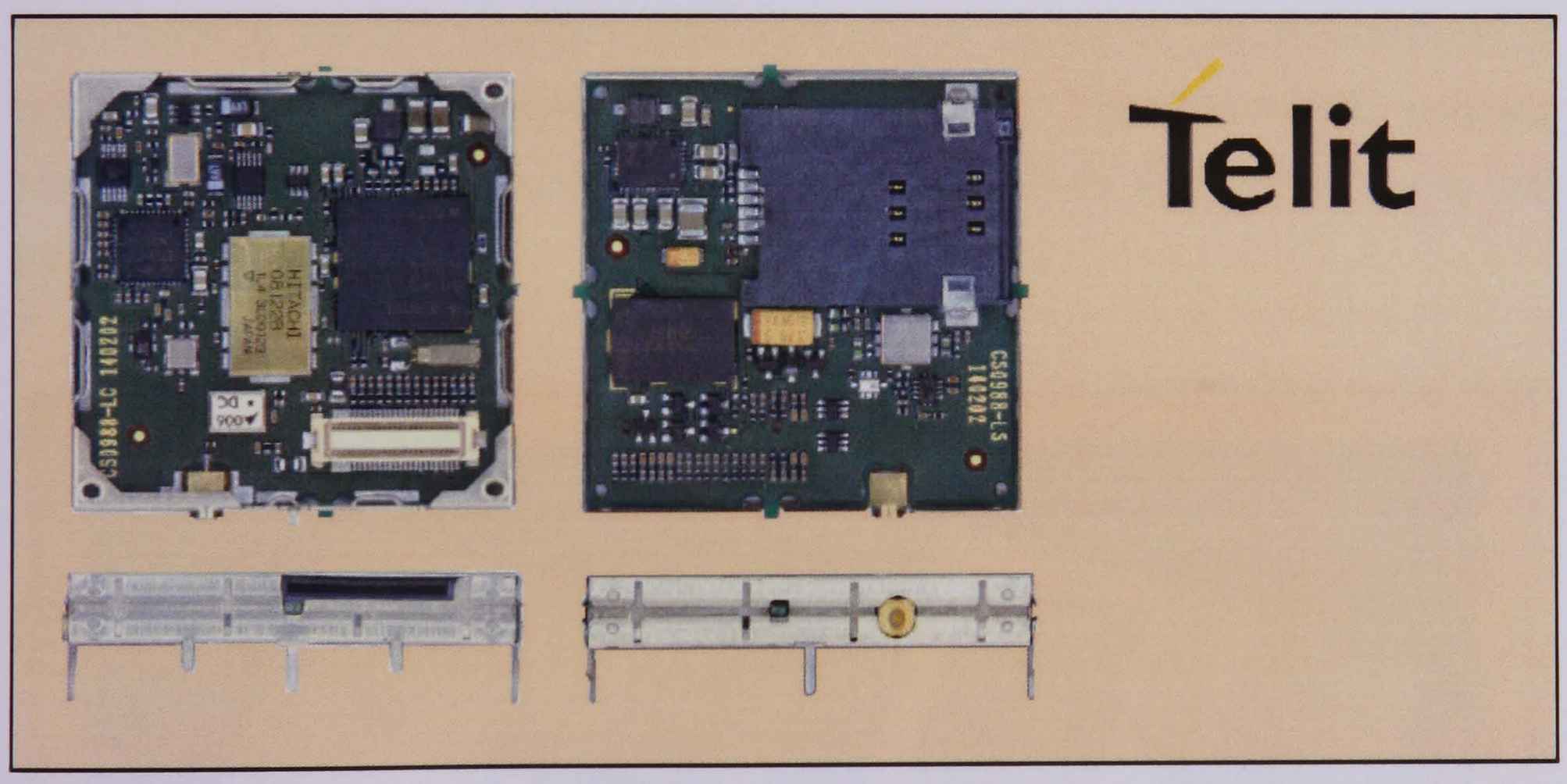

Figure 2.22 - Telit GPRS module

2.7 Time Keeping Unit

This section describes the Time Keeping Unit of the designed Data Acquisition System (Figure 2.23).

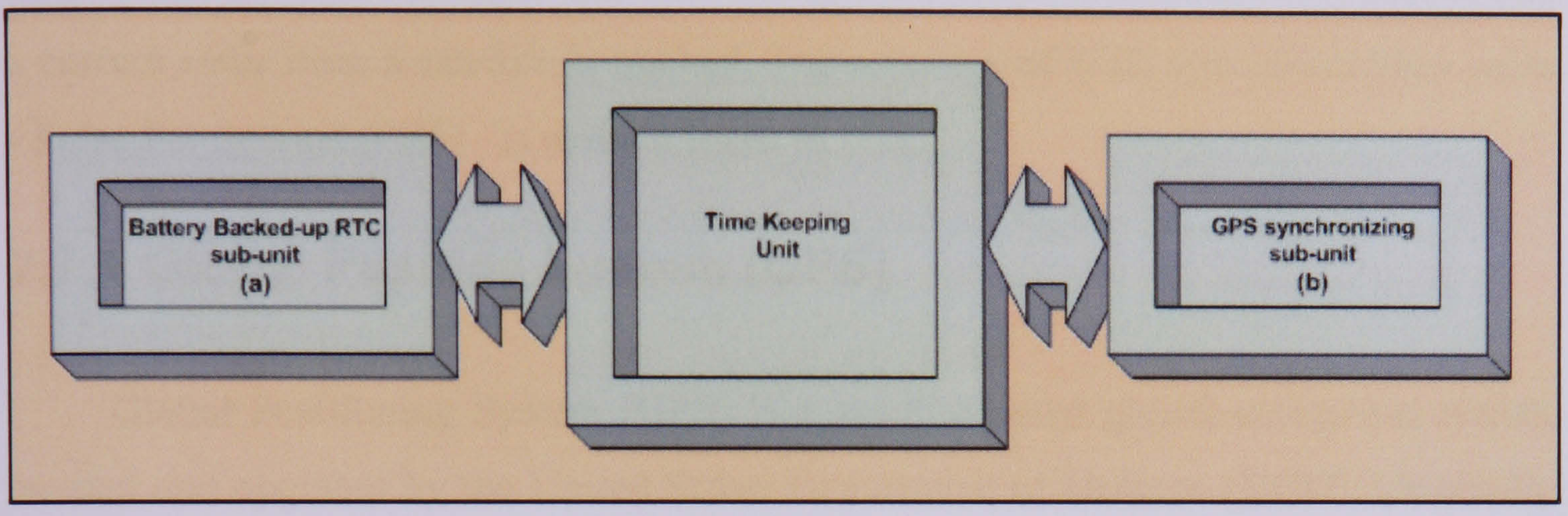

Figure 2.23 - Block diagram of Time Keeping Unit

In order to acquire synchronized data measurements, the Data Acquisition System incorporates a Real Time Clock (RTC) synchronized by UTC-GPS reference, broadcasted by the GPS satellite constellation all over the world. This synchronization ensures a reliable data analysis [Alfred Leick (2004)]. The NMEA-0183 standard explains in detail the communication protocol between Data Acquisition System and FV-18B GPS module.

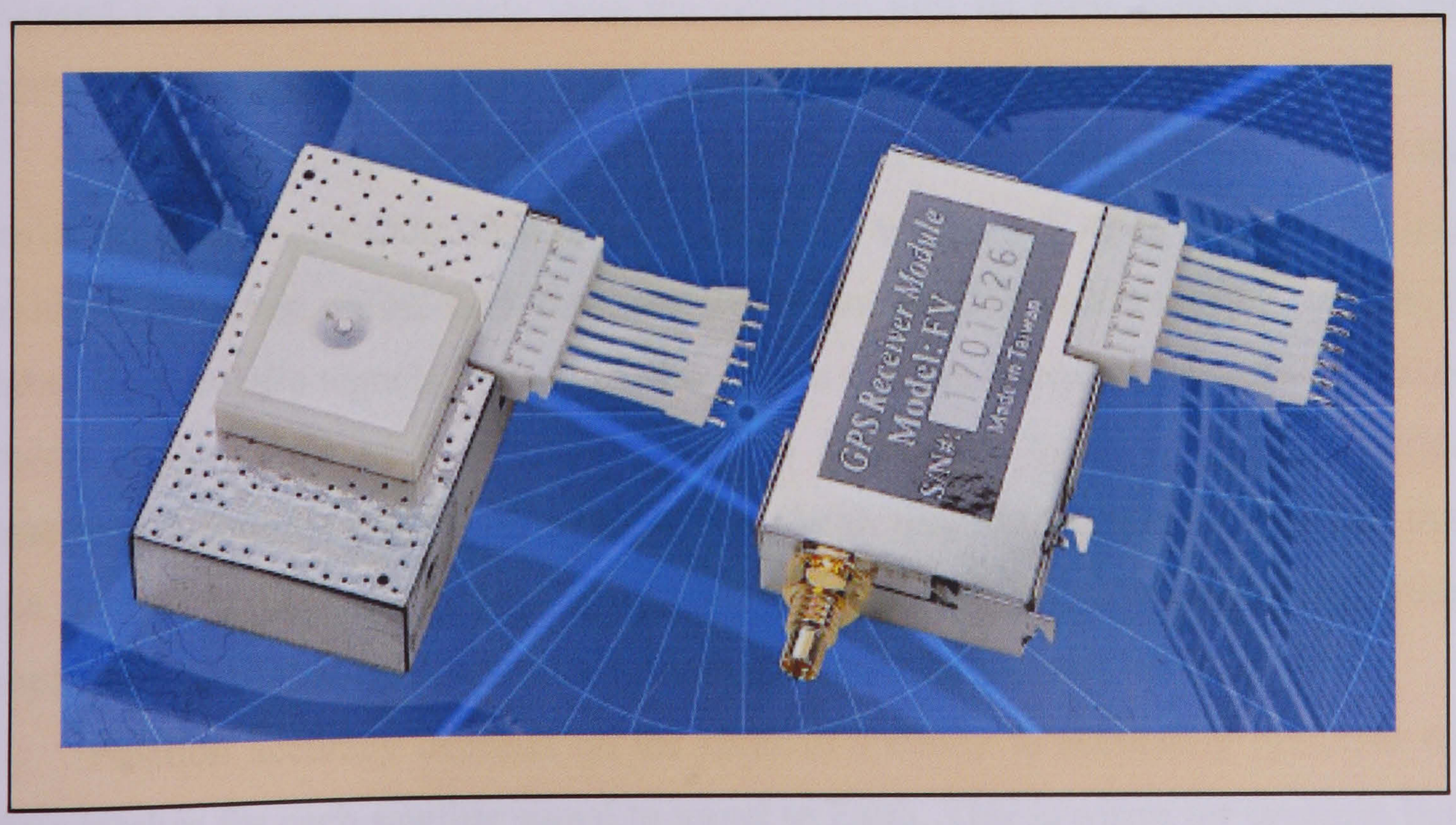

Figure 2.24 - GPS receiver module (FV-18)

UTC time is the acronym of Coordinated Universal Time. Depending on the Earth's rotating speed, leap time of one second or so may be inserted per year. The UTC output by the unit is based on both almanac data and satellite tracking. Therefore, the UTC output directly after power-on may not be accurate. Data Acquisition System's internal real-time clock, UTC-RTC, is automatically adjusted to a correct value once a satellite is tracked. The accuracy of UTC synchronization pulse - Pulse Per Second (PPS) - is about ±1μsec to UTC.

2.7.1 Global Position System (GPS)

Global Positioning System (GPS) is a satellite-based global navigation system created and operated by the United States Department of Defence (DOD). Originally intended solely to enhance military defence capabilities, GPS capabilities have expanded to provide highly accurate position and timing information for many civilian applications.

An in-depth study of GPS is required to fully understand how it works, but simply stated: Twenty four satellites in six orbital paths circle the Earth twice each day at an inclination angle of approximately 55 degrees to the equator. This constellation of satellites continuously transmits coded positional and timing information at high frequencies in the 1.5 GHz range. GPS receivers, with antennas located in a position to clearly view the satellites, pick up these signals and use the coded information to calculate a position in an Earth coordinate system.

GPS is the navigation system of choice for nowadays. While GPS is clearly the most accurate worldwide all-weather navigation system yet developed, it still can exhibit significant errors. GPS receivers determine position by calculating the time it takes for the radio signals transmitted from each satellite to reach Earth. Radio waves travel at the speed of light (Rate). Time is determined using an ingenious code matching technique within the GPS receiver. With time determined and the fact that the satellite's position is reported in each coded navigation message by using sophisticated trigonometry the receiver can determine its location on Earth.

Position accuracy depends on the receiver's ability to accurately calculate the time it takes for each satellite signal to travel to Earth. This is where the problem lies. There are primarily five sources of errors which can affect the receiver's calculation.

These errors consist of (1) ionospheric and tropospheric delays on the radio signal, (2) signal multi-path, (3) receiver clock biases, (4) orbital errors, also known as ephemeris errors of the satellite's exact location, and (5) the intentional degradation of the satellite signal by the DOD. This intentional degradation of the signal is known as "Selective Availability (SA)" and is intended to prevent adversaries from exploiting highly accurate GPS signals and using them against the United States or its allies. Today, GPS units are accurate to within 20 meters (approximately 60 feet); although in good conditions, units should display an error of less than 10 meters. The combination of these errors in conjunction with poor satellite geometry can limit GPS accuracy to 100 meters 95% of the time and up to 300 meters 5% of the time. Fortunately, many of these errors can be reduced or eliminated through a technique known as “Differential”.

The European Galileo system, which is set to supplant GPS when it hopefully gets going properly, is all set to meet its operational deadline of 2010. An international effort through and through (the European Union will be sharing some of the technological benefits with China); the system will have the potential to be accurate to within one metre. GPS is only accurate to within about 20 metres for civilian applications. Plus, unlike standard GPS, Galileo is deliberately designed to work inside buildings and built-up areas.

2.8 Power Supply Unit

In order to acquire reliable measurements, data acquisition systems should be installed in the countryside isolated from man-made, artificial noise. In such types of regions the use of alternative energy sources, like solar cells, is almost always necessary. Hence, the total power consumption of the system is of great importance. The system ensures the uninterrupted operation and low power consumption.

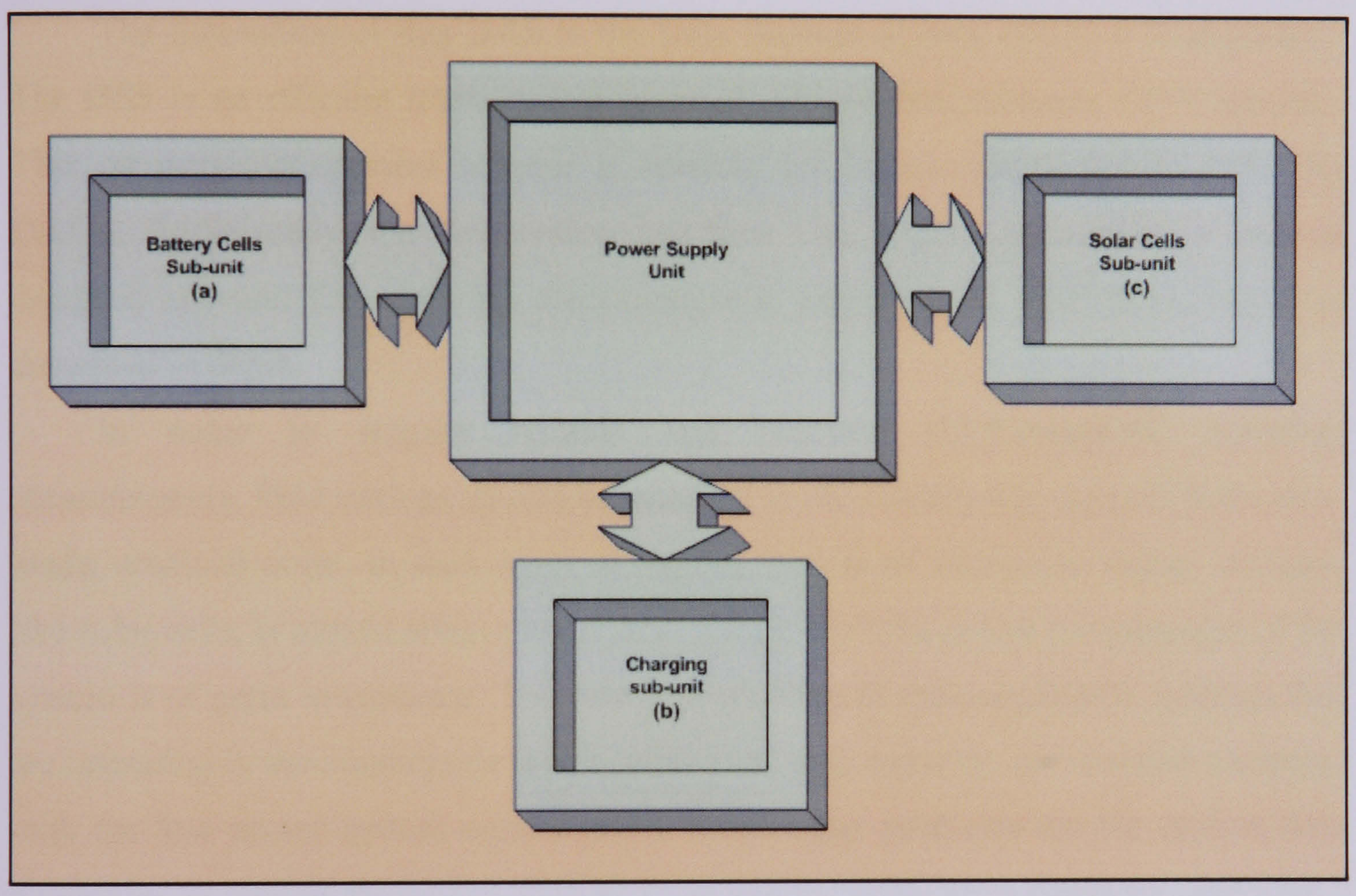

Figure 2.25 - Block diagram of Power Supply Unit

The reliability of the system ensures collection of time-stamped data, even under adverse circumstances. Due to the fact that they have their own power supply (rechargeable batteries), the data acquisition systems continue to measure and record existing conditions during power outages. Time-stamped data provides valuable information for identifying and verifying past events.

2.9 Conclusions

In this chapter the technical specifications as well as the key features of the embedded Compact Flash™ based Data Acquisition System (DAS) were described analytically. Since this device was mainly designed for outdoor experimental purposes, it had to face all the problems derived from rugged environments and also ensuring long term availability, high reliability, high robustness, rich set of certifications life cycle management and longevity.

The innovation of this DAS is the Data Storage System (DSS) it incorporates. The DSS is an efficient memory-management scheme that increases CF™ lifetime. This memory-management scheme is suitable for large-capacity (up to 128 GB) DAS's. Additionally, the Acquisition Interface Unit (AIU) incorporates a custom designed sub-unit for capturing electromagnetic emissions in VHF band, which is described in depth.

In order to acquire reliable and accurate electromagnetic variation measurements, field stations should be installed in the countryside isolated from man-made, artificial noise. In such types of regions the use of alternative energy sources, like solar cells, is almost always necessary. Hence, the total power consumption of the system is of great importance. The common problem in data acquisition systems that are operating in the countryside is to combine the high capacity, non-volatile memory, with the low power system consumption. Some other problems are the remote data collection, as well as the device configuration and the application firmware upgrades.

In this thesis, the embedded DAS ensures reliable electromagnetic variation measurements, efficient memory-management scheme that increases CF™ lifetime, uninterrupted operation and low power consumption.

3 The Development and Implementation of Telemetry, Data conversion and Data monitoring software

3.1 Introduction

In the software design stage of this thesis, many commercial telemetry computer programs were surveyed for suitability according to the specifications and the requirements of the existing system [Lekas S. (1996)].

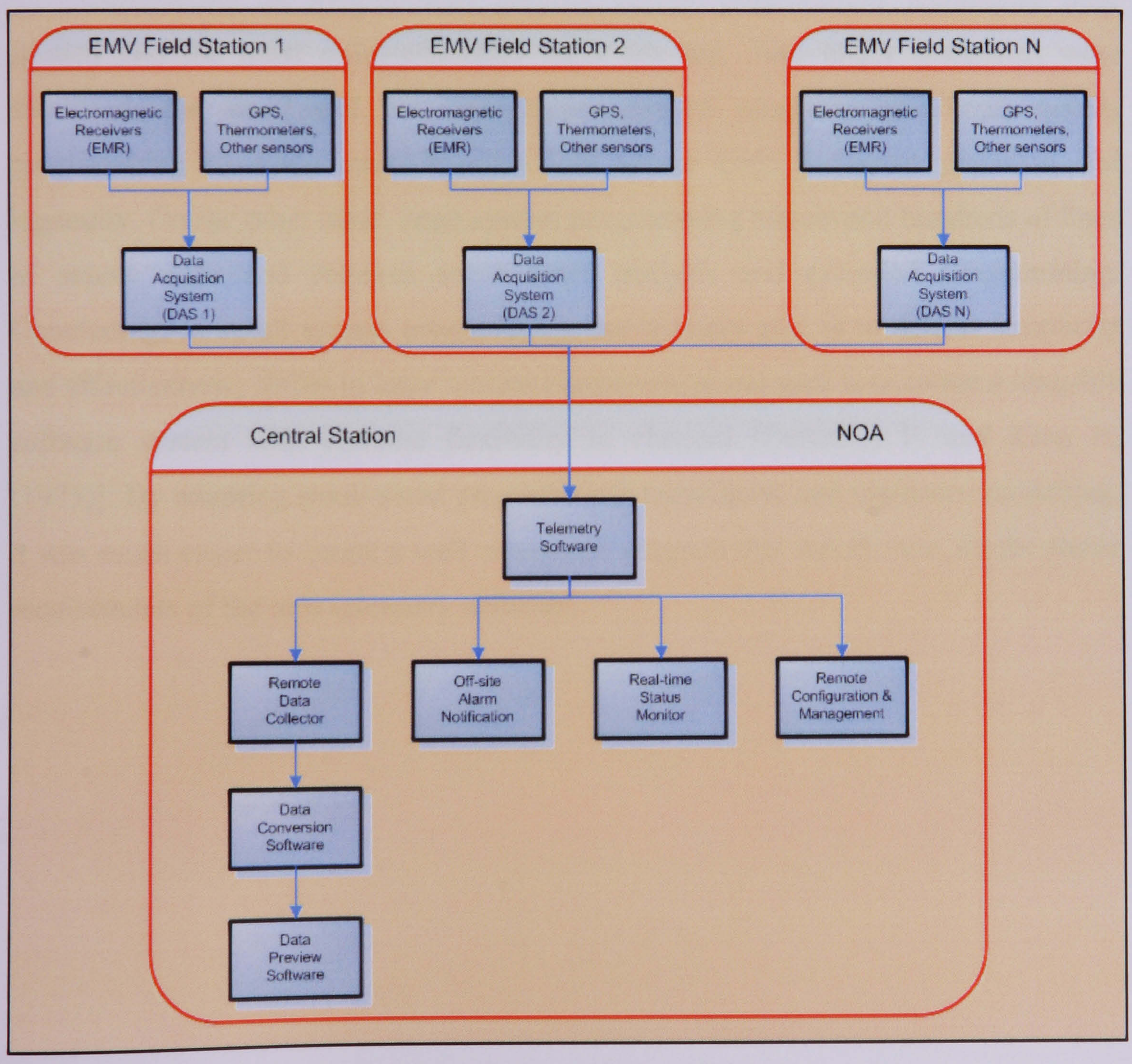

Figure 3.1 - System Software Diagram

The survey found that the functions of the commercial telemetry software were either limited to only the remote data retrieval operation or not at all compatible with the embedded Compact Flash™ Data Acquisition System hardware. The required parameters were also not available from those programs, resulting to several hardware incompatibilities on the proposed DAS. Under these demands, a new software interface was developed to meet the requirements of the DAS project. This includes three stages of implementation: the telemetry software, the data conversion software and the data monitoring software. In this chapter the software development and implementation processes will be described.

3.2 Methodology

Considering the methodology process, several programming techniques were studied and the most reliable/suitable were adopted. Two major categories were identified; the small and the large scaled system programming. Small system programming in many cases requires less source code but great precision and ingenuity. On the other hand, large system programming has several hundreds of lines of source code and requires much more analysis and extended programming. Concluding, in small system programming our primary goal is to deliver simplicity and effectiveness, whilst in large system programming our goal is to create a long-life software system with extreme flexibility in changes [DeRemer F. and Kron H. (1975)]. By adopting small-sized programming techniques, and top-down modelling, it was much easier to create a well structured program that would meet all the above requirements of the new telemetry software.

3.3 Operation Analysis and Software Design

By analyzing the needs of the system, the main tasks were identified and a list of required operations, the new telemetry software should execute, was created. These operations are the following:

a) Remote data collection management,

b) Off-site alarm notification,

c) DAS real-time status monitoring and

d) DAS remote configuration and management.

Both Remote data collection management (a) and off-site alarm notification (b) are automated operations that require no human interference. These operations should be executed continuously and include recovery mechanisms.

On the other hand, DAS real time status monitoring (c) and DAS remote configuration and management (d) are manual operations that are used either for provisioning and diagnostic reasons or for remote control and administration.

3.3.1 Data Collection Management Software

The notion of remote data collection signifies the transfer of the data stored into the Data Acquisition System to the central station. This is an automated operation and it is executed for every field station sequentially. This operation is divided into two sub-operations. The first one is the remote data collection and the second one is the alarm notification, which notifies predefined recipients for system events. These events are generated by the remote data collection operation whenever an error or change occurs.

The Remote data collection can be achieved through a four-step procedure.

1) Connection to the DAS:

In the first step the central station tries to establish a communication session with the DAS. If the execution of this step fails for more than 5 times, the operation

will abort and an alarm will be triggered, hence a notification will be sent to the system administrator.

2) Enquiry for new data

In the second step, the central station asks the DAS if newly stored data or new system events are available. This operation is achieved through Memory Pointer comparison. The DAS transmits the current Data Storage Pointer and the central station compares it with the Local Pointer. If the remote Pointer is greater than the local one, the central station commands the DAS to send the new data. Additionally, if new system events are recorded, the DAS informs the central station of their existence.

3) Remote data collection

In the third step, the central station commands the DAS to send the desirable stored data using Data Start and Data Stop Pointers. When the DAS receives the command, it checks the availability of the requested data and, transmits blocks of data to the central station using packets of 512 Bytes. It is worth mentioning that each data packet contains 4 bytes generated from the calculation of the checksum using the CRC-16 error detection algorithm. When the remote data collection is successfully completed, the central station commands the DAS to shift its Data Storage Pointer to the Local Pointer.

4) Data validation and storage

In the fourth step, the central station checks the data integrity using the CRC-16 algorithm [Forsberg C. (1988)] and finally stores the data to the local hard disk. If any data error is detected in this step, Backward Error Correction (BEC) is used, where the bad blocks of data are rejected and the central station commands the DAS to retransmit the data. The output of this operation is a binary file that contains exactly the same data as the Compact Flash™ memory of the DAS do.

As mentioned earlier, besides the remote data collection operation, another supplemental operation is the continuous monitoring of each DAS and the alarm notification when errors or changes occur and called alert notification.

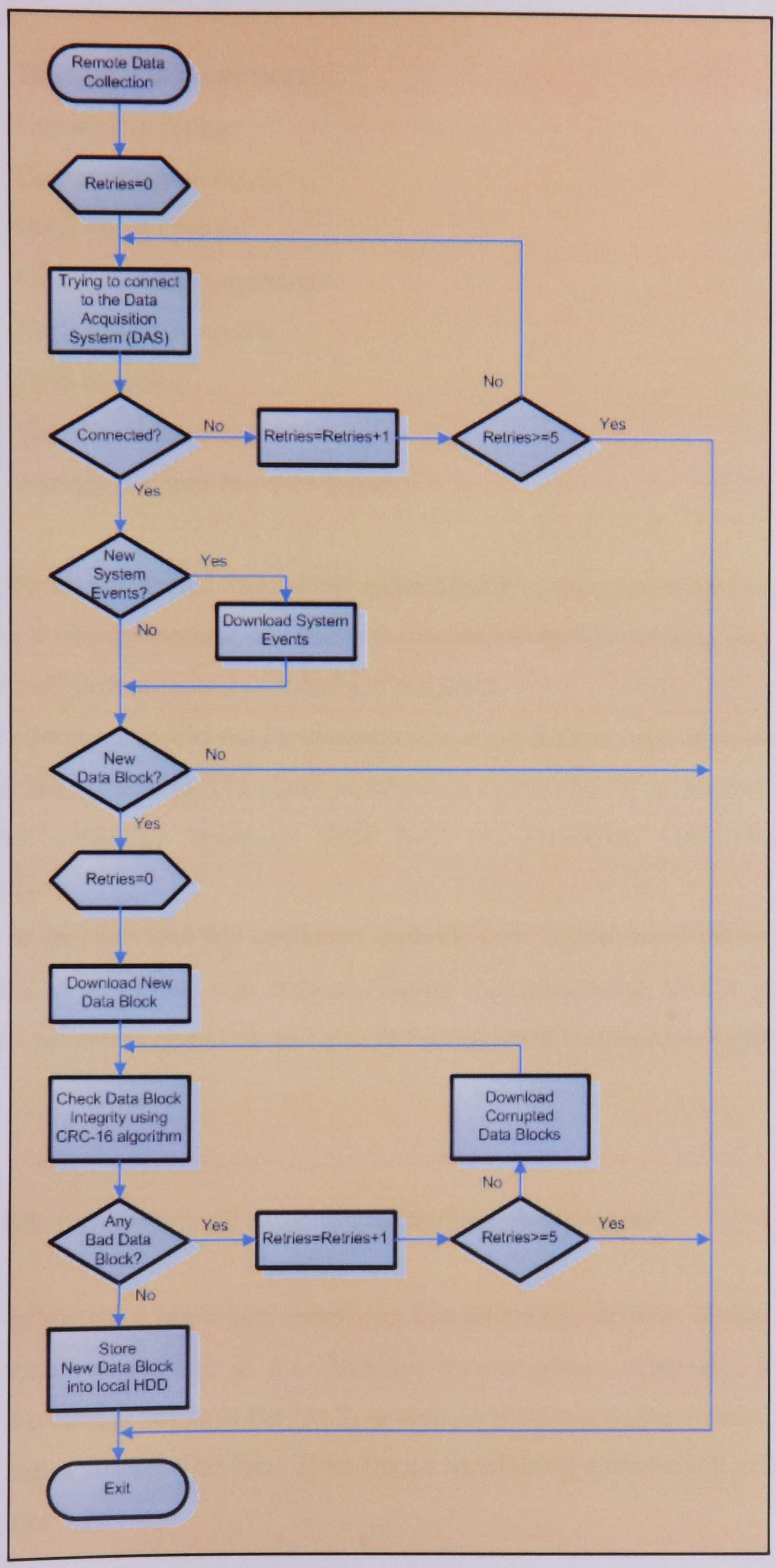

Figure 3.2 - Remote data collection & alarm notification Flowchart

This operation includes notifications generated from the following events:

a) Telemetry software launch
b) Connection failure
c) Communication errors
d) DAS status change
e) DAS configuration change
f) DAS firmware update
g) DAS overheat
h) Storage medium change
i) Storage medium low free space

All the above events should be automatically generated when a problem is detected or a change occurs, resulting in the central station sending any generated alarm in e-mail format to every predefined recipient.

This operation should not be distinguished from the run time operation which is the remote data collection. The alarm notification events should be generated from the remote data collection operation since both are automated operations and run continuously.

Due to the fact that this operation depends upon coordinated software running on the DAS, a flowchart was created (Figure 3.2) containing all the steps of the remote data collection operation and also including alarm notification features.

3.3.2 DAS real-time Status Monitoring Software

One of the most important operations that telemetry software should support is real-time status monitoring of the DAS for remote system diagnosis. Information regarding the current status of the DAS, as well as previous system events is gathered from the central station. The Real Time Status Monitoring operation flowchart can be seen in Figure 3.3.

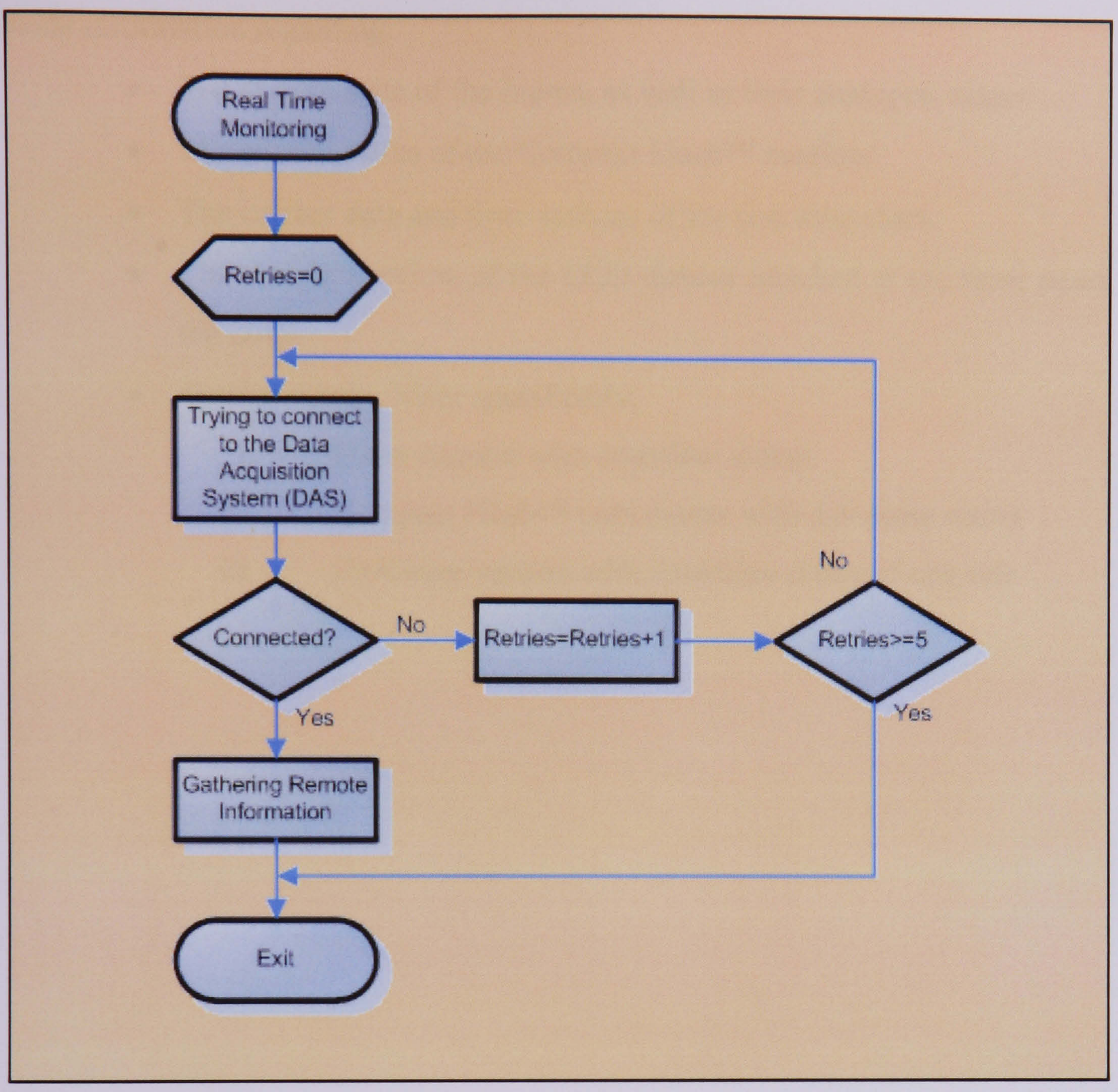

Figure 3.3 - Real Time Status Monitoring Flowchart

In order to execute this operation the following steps should be performed:

1) Connection to the DAS:

During this first step, the central station tries to establish a communication session with the DAS. If the execution of this step fails for more than 5 times, the operation will be aborted.

2) Gathering remote information:

In this step, the type of the required information can be selected. The DAS can provide information regarding:

- The current state of the inputs, as well as their analogue values
- The current status of the Compact Flash™ medium
- The current date and time settings of the real time clock
- The current preview of the LCD display attached at the front panel of the DAS
- System events. More specifically:
  - i. Reset counter with date/time stamp
  - ii. Compact Flash™ card events with date/time stamp
  - iii. Firmware version with date/time stamp of upgrade

3.3.3 DAS Configuration and Management Software

Despite the fact that Data Acquisition Systems are standalone systems and their configuration rarely changes, remote configuration and management is very important due to the large distances between the remote devices and the central station.

This operation relies on measurement settings and system wide settings.

Measurement settings configuration consists of:

- Name modification of the DAS.
- Global sampling period configuration; for setting the sampling interval from 1 to 255 seconds and applies to the analogue inputs and temperature measurements.
- Analogue inputs configuration; for activating/deactivating, changing the label, the multiplier and the measurement unit of each analogue channel. Due to the fact that the stored measurement is the average value of many samples, the number of these samples can also be changed.
- Thermometers configuration; for activating/deactivating, changing the label and the measurement unit of temperature sensor.
- External VHF measuring device configuration; for activating/deactivating and changing tuned up frequency of each one of the input channels. Furthermore the sampling per channel interval can be changed.

System-wide settings consist of:

- RTC date/time configuration; for synchronizing the RTC to the Universal Time (UTC) from the host, if there is no GPS module attached to the DAS.

Due to the nature and the characteristics of each one of the above settings, there is a difference in the adopted technique regarding the configuration and the update operation.

While the system's wide settings configuration must be updated on the spot (some microseconds), the update of the measurements settings can be completed without any time considerations.

In order to execute the update operation for the system wide settings, the following steps should be performed:

1) Connection to the DAS:

In the first step, the central station tries to establish a communication session with the DAS. If the execution of this step fails for more than 5 times, the operation will be aborted.

2) Gathering Remote Configuration:

In this step, the central station asks the DAS to transmit the current configuration settings, including RTC information and synchronization method (GPS or host). When the DAS receives the information, it retrieves all the local settings including the RTC information and sends them to the central station. If the selected synchronization method is "GPS-UTC sync" the next step is skipped.

3) Updating the RTC:

This step requires the central station to compare the received remote date/time settings of the DAS to the local ones, which are synchronized to the Universal Time (UTC). If the difference between these two date/time values is greater than 10 seconds, the central station sends a synchronization command to the DAS containing the right date and time values.

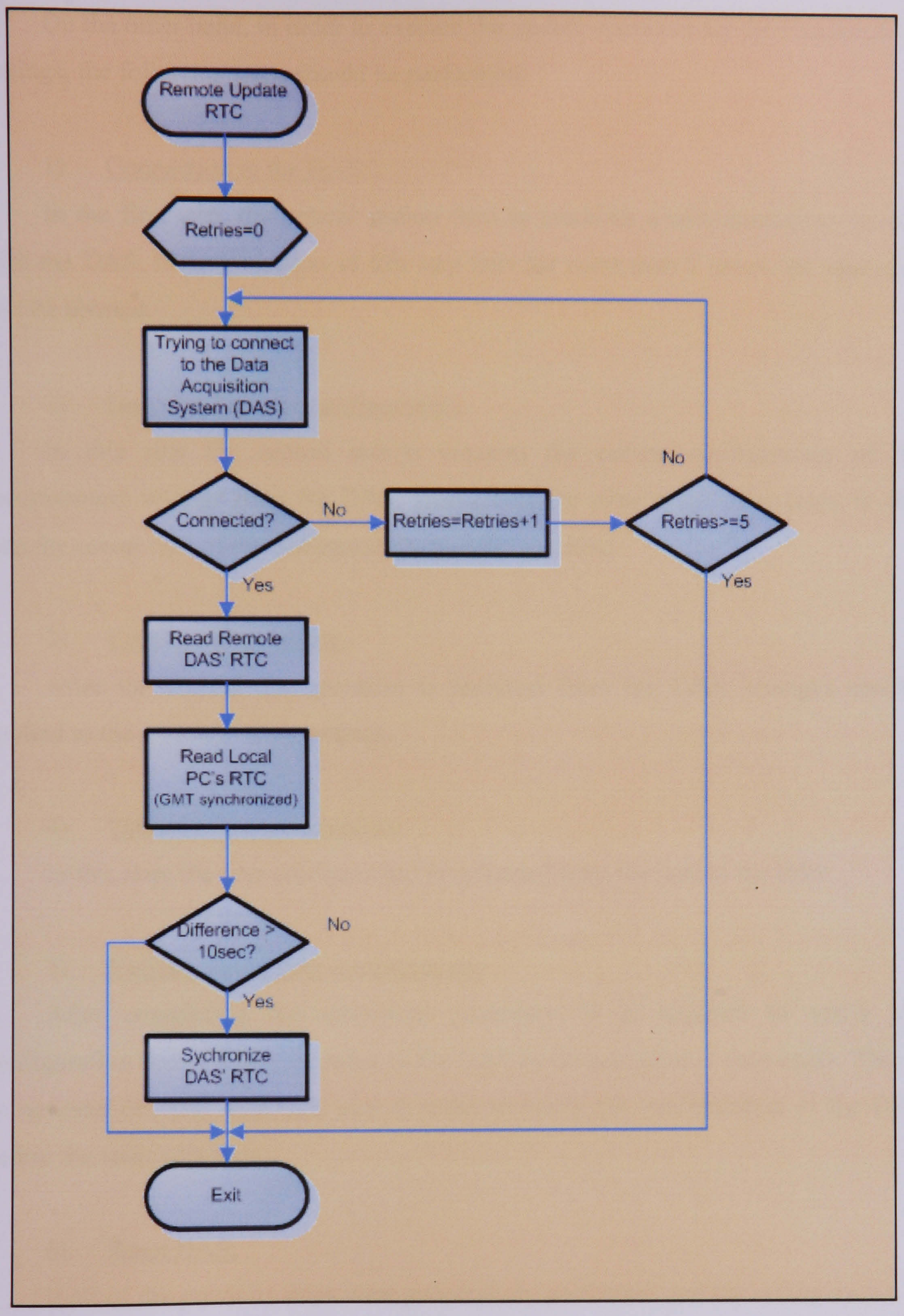

Figure 3.4 - Flowchart of Remote RTC update

On the other hand, in order to execute the update operation for the measurement settings, the following steps should be performed:

1) Connection to the DAS:

In the first step, the central station tries to establish a communication session with the DAS. If the execution of this step fails for more than 5 times, the operation will be aborted.

2) Download remote configuration:

In this step the central station requests the current configuration of the measurement settings from the DAS. Because of the wide range of settings, in this step the actual type of the configuration must be specified.

3) Configuration update:

After the current configuration is received from the DAS, changes can be applied to the measurements settings.

4) Upload new configuration:

In this step, the new configuration is uploaded from the host to the DAS.

5) Verification of new configuration:

After completing the uploading procedure, it is required to verify the configuration that was just uploaded to the DAS by downloading it once again. This is an optional but also important step in order to verify the configuration of the DAS before the reset operation.

6) Reset DAS:

If all of the previous steps were successfully performed and the configuration is verified, a DAS reset must be performed in order for the changes to be applied.

The flowchart of the steps of the Remote configuration and management is displayed in Figure 3.5.

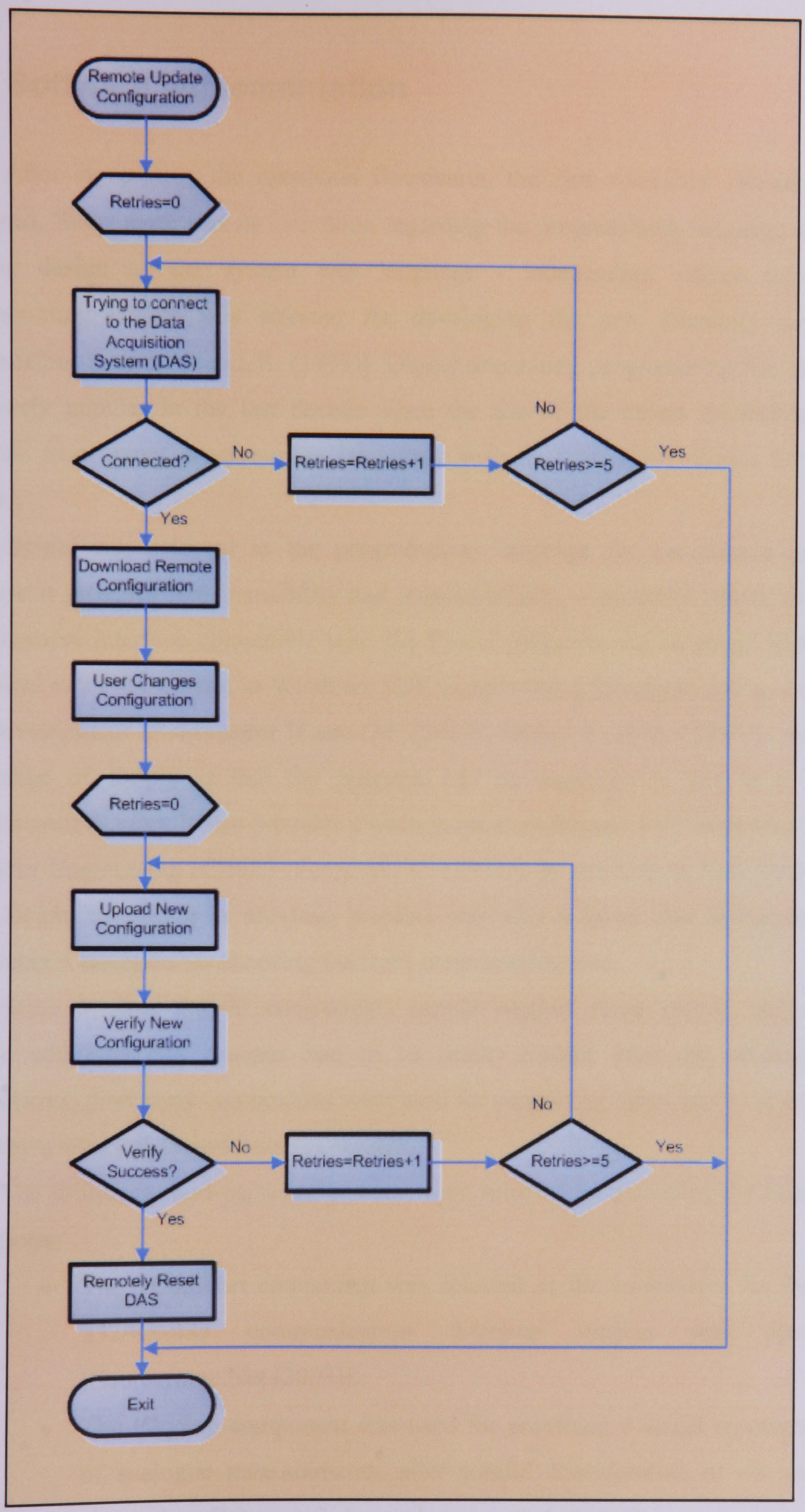

Figure 3.5 - Flowchart of Remote update configuration

3.4 Software Implementation

After completing the operation flowcharts, the new telemetry software was designed. Since there was no limitation regarding the programming language as well as the design of the system was language - independent, object orientated programming (OOP) was selected for developing the new telemetry software [Khoshafian S. and Abnous R. (1995)]. Object orientating programming has become extremely popular in the last decade since the use of the object orientation was adopted from many programming languages such as Java, C++, Visual C++ and Delphi.

Delphi was selected as the programming language for the current project, because it provides high reusability and maintainability, a powerful object oriented development interface compatible with the Pascal programming language (but with graphical extensions based in Windows SDK programming Interface) and an easy-to-use development environment [Cantu M. (2003), Weber E. et al. (1995)]. Another advantage of Delphi is that the program can be compiled to run in a Linux environment (Kylix). It also provides a wide range tools through its Component Based Software Engineering (CBSE) [Szyperski C. (2002)]. In addition to that, familiarity with Delphi according to previous projects was also a factor that influenced the researcher's selection for choosing the right programming tool.

Since original Delphi components cannot support some special operations, certain additions and changes had to be made. Except from the accompanied components, third party components were used for supporting these special operations and others were developed from the scratch.

The following third-party components were selected for providing the following operations:

- The TComPort component was selected as the component for the RS-232/RS-485 communication interface support and operation [Sourceforge.Net (2003)].
- The IOcomp component was used for providing a visual representation of analogue measurements, after careful consideration of all possible alternatives [IOcomp Software Incorporated (2003)].

The visual representation of the operations that the new telemetry software provides was developed in a hierarchical way by means of operation type and human interaction. As mentioned in section 3.3, the new telemetry application should support:

a) Remote data collection management,

b) Off-site alarm notification,

c) DAS real-time status monitoring and

d) DAS remote configuration and management.

Many considerations were made regarding the visual interface design and implementation. The result of them was that the above operations were divided into two major groups according to the start-up type of the operation. The first group of operations was named "Collector" and the second one "Manager". The "Collector" contains all the automatic operations of the application including the configuration interface. On the other hand, the "Manager" contains the real-time status monitoring, DAS configuration and management operations.

Before starting the implementation of the new telemetry software, an extended study of the accompanied Application Programming Interface (API) of the DAS was carried out. The documentation of the system's API is shown in APPENDIX C' (Data Acquisition System - API interface). After completing the acquaintance with the DAS' API, the new acquisition software was developed using these functions.

The new telemetry software has to support all above tasks. Concerning the application layer of the OSI reference model, a custom designed communication protocol has been implemented in order to retrieve data trustworthily from each field station. These commands must be recognised by both host and terminal devices using a common and dedicated library that will translate all the received commands and service all the requested operations. For this reason an Application Programming Interface was implemented for supporting requests for the above mentioned services as shown in APPENDIX C' (Data Acquisition System - API interface). After completing the implementation of this interface, new PC based telemetry software was developed, which is presented in the next chapter.

3.5 Telemetry Software Overview

The development of the software resulted in an application, which was compiled and finally the telemetry software, namely MEGADLG was created. The output of the compilation was named MEGADLG.EXE.

After executing the application the main window appears (Figure 3.6). The main window of the telemetry application is divided into four different frames. The first frame contains the main menu of the application. Specifically, the first frame contains two buttons for the selection of either the "Manager" or the "Collector" to be executed. The second frame contains a list of the attached Data Acquisition Systems while the third one, which is a dynamic frame, contains the operations of either the "Manager" or the "Collector" when selected. The last frame is static and contains the control buttons.

The overview of the application will be presented using a two-fold operation oriented procedure that corresponds to the "Collector" and the "Manager" groups of operations. Taking into consideration that a DAS should firstly be configured and then start its normal acquisition operation, the "Manager" will be explained prior to the "Collector".

Before explaining the operations that the application provides, it must be made clear that automated operations must be executed in turn with manual operations; hence simultaneous execution is impossible and therefore prohibited.

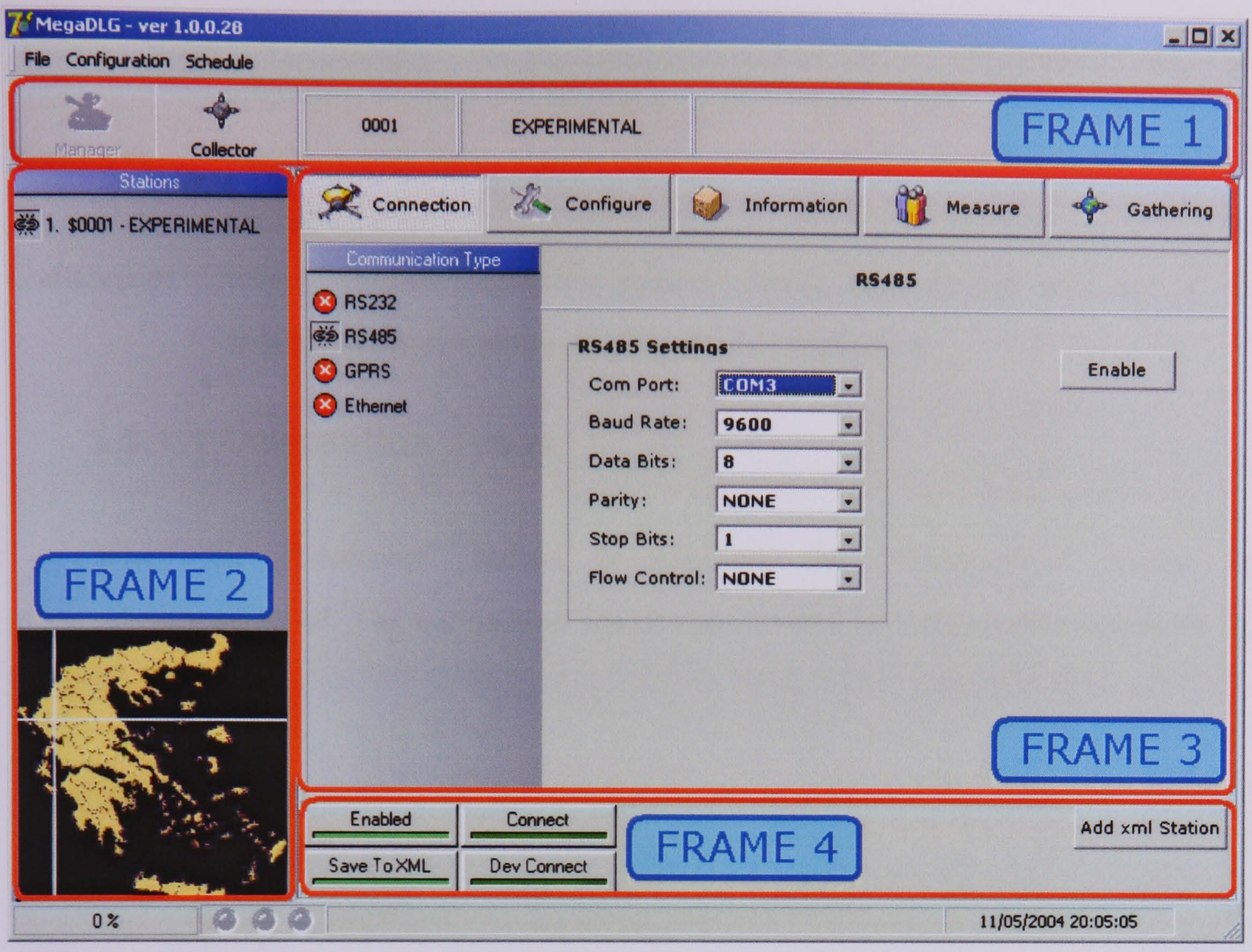

Figure 3.6 - MegaDLG - Main window

3.5.1 Manager Overview

As mentioned in the implementation phase, the "Manager" contains the real time monitoring, remote configuration and management operations. Because of the fact that the main operation of the application, which is the remote data collection, is stopped whenever the "Manager" is executed, the user should re-enable the "Collector" when the configuration of the system finishes.

Regarding the visual representation of the real time monitoring and remote configuration and management operations, the "Manager" is divided into five different frames that correspond to five different operations. These operations are the following:

Connections: where the communication type and settings are defined.

Configure: where the main configuration including analogue inputs, thermometers, VHF device frequencies, DAS's name, date and time settings are defined

Information: where the main configurations, as well as, LCD display, reset, version, upgrades, storage and setting information are displayed.

Measure: where a real time visual representation of the inputs of the DAS is displayed

Gathering: where settings regarding system check, data packet size and RTC synchronization can be displayed and configured

3.5.1.1 Connection Types

When the "Manager" button is selected, the "Connection" button is automatically selected. The connection frame appears and becomes active as shown in Figure 3.7.

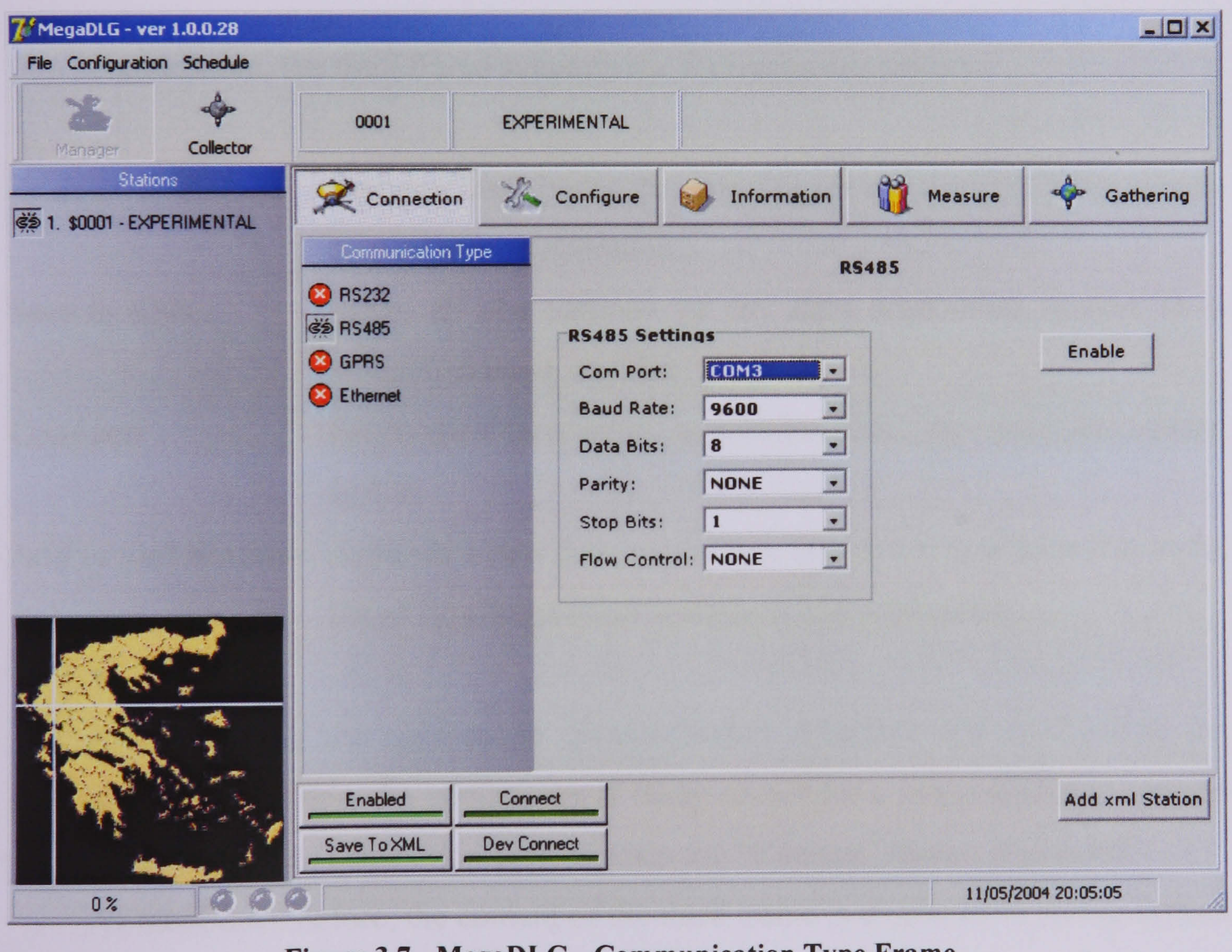

Figure 3.7 - MegaDLG - Communication Type Frame

The "Connection" frame consists of three separate frames. The first one indicates the connection type while the second one refers to the settings of the selected connection type. The third frame is visible in all the frames of the "Manager"

and offers additional functions for the configuration file of the data acquisition system.

The application was designed and implemented in order to support the RS-232 and RS-485 communications interfaces. The communications configuration of both supported interfaces is the same and consists of the following settings:

Com Port: Contains the port name of the serial interface [COM1..COMx]
Baud Rate: Contains the data speed in baud per second [110...921600]
Data Bits: Contains the number of the data bits [5...8]
Parity: Contains the parity check type used [none, even, odd, mask, space]
Stop Bits: Contains the number of the stop bits [1, 1.5, 2]
Flow control: Contains the flow control type used [none, Hardware, Xon/Xoff]

Furthermore, the third frame supports the following operations:

Enable: Activate/Deactivates the data acquisition system for the remote data collection operation
Save to XML: Saves all the settings of the data acquisition system to a uniquely named xml file.
Connect: Establishes/Terminates a session with the data acquisition system
Add to xml Station: Appends a new data acquisition system configuration file to the list of data acquisition systems of the application.

After selecting the appropriate communication interface and configuring the communication settings, the application is ready to initiate a communication session with the attached data acquisition system when the "Connect" button is pressed.

As mentioned before, the content of the third frame is displayed in all the frames of the "Manager" in order to provide easy and fast access to the above functions.

3.5.1.2 Configure DAS

When the "Configure" button is selected, the "Configure" frame becomes active as shown in Figure 3.8. The "Configuration" frame consists of two separate frames. The first one contains a list of the available configuration settings while the second one contains the settings of the selected option. The list of the configurations setting is the following:

Main configuration: Contains system wide settings

ADC 10-Bit: Contains the settings of the eight analogue inputs using 10-bit resolution

ADC 12-Bit: Contains the settings of the eight analogue inputs using 12-bit resolution

VHF Tuner: Contains the settings of the eight VHF inputs

Thermometers: Contains the setting of the eight temperature sensors

When a button that corresponds to one of the above operations is pressed, the second frame displays the respective configuration.

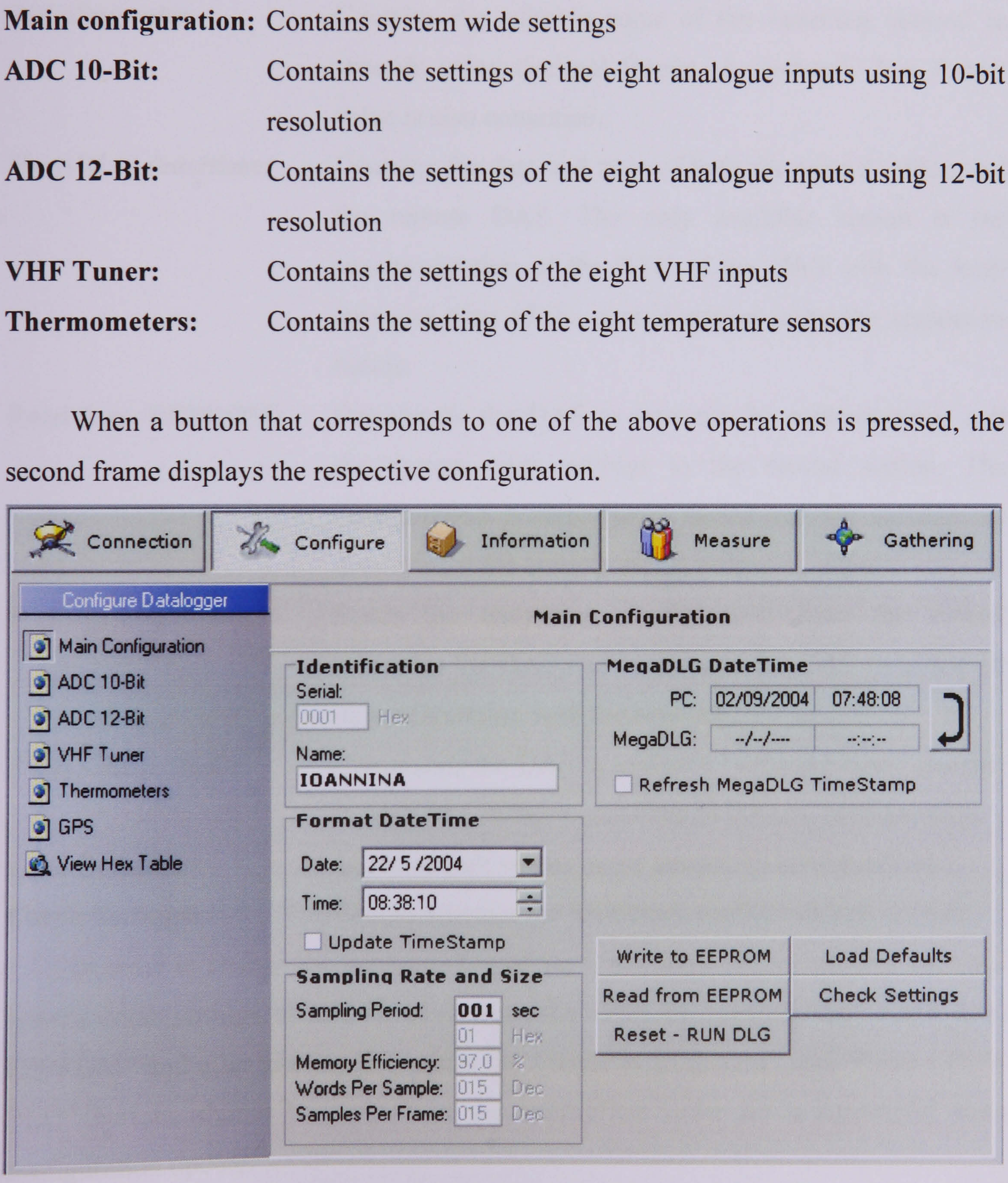

Figure 3.8 - MegaDLG - Configuration Frame

3.5.1.2.1 DAS Main configuration

As shown in Figure 3.8, the "Main Configuration" contains the following options:

Serial: Contains the read-only value of the serial number of the attached Data Acquisition System.

Name: Contains the editable value of the name of the DAS.

Sampling rate: Contains the editable value of the sampling interval in seconds using decimal format. A read-only hex format value is also contained.

MegaDLG date/time: Contains the date and time of both the central station and the remote DAS. The only available option is the synchronization of the RTC of the DAS with the local date and time of the central station using the respective button

Read from EEPROM: Commands the DAS to transmit the measurements and the system wide settings to the central station. The configuration is temporarily stored and the settings are displayed in the corresponding fields.

Write to EEPROM: Sends the temporary configuration from the central station to the DAS and commands the DAS to overwrite its configuration with the new one.

Reset - RUN DLG: Commands the DAS to initiate a "software reset" in order to apply the changes contained in the new configuration.

Load Defaults: Loads default values in the temporary configuration.

Check Settings: Checks whether the temporary configuration is correct.

In order to change the configuration of the DAS, the current measurements and system wide settings should be read from the DAS by pressing the "Read from EEPROM" and after altering the values the "Write to EEPROM" and "Reset - RUN DLG" buttons should be pressed in the appropriate order for a successful main configuration update.

3.5.1.2.2 DAS ADC 10-bit configuration

When the "ADC 10-Bit" button is pressed, the "ADC 10-Bit Configuration" frame appears as shown in Figure 3.9. This frame consists of a table that contains configuration options regarding the eight 10-bit resolution analogue inputs of the DAS. This table provides direct access to the following settings of each channel:

Status: Activates/Deactivates the selected channel

Channel: Contains the system name of the channel

Caption: Contains the editable name of the channel

Unit: Contains the editable measurement unit of the channel

Multiplier: Contains the editable multiplier value of this channel in decimal format

Mult Hex: Contains the read-only multiplier value in HEX format

Average: Contains the editable number of the samples used for calculating an average value that is eventually stored.

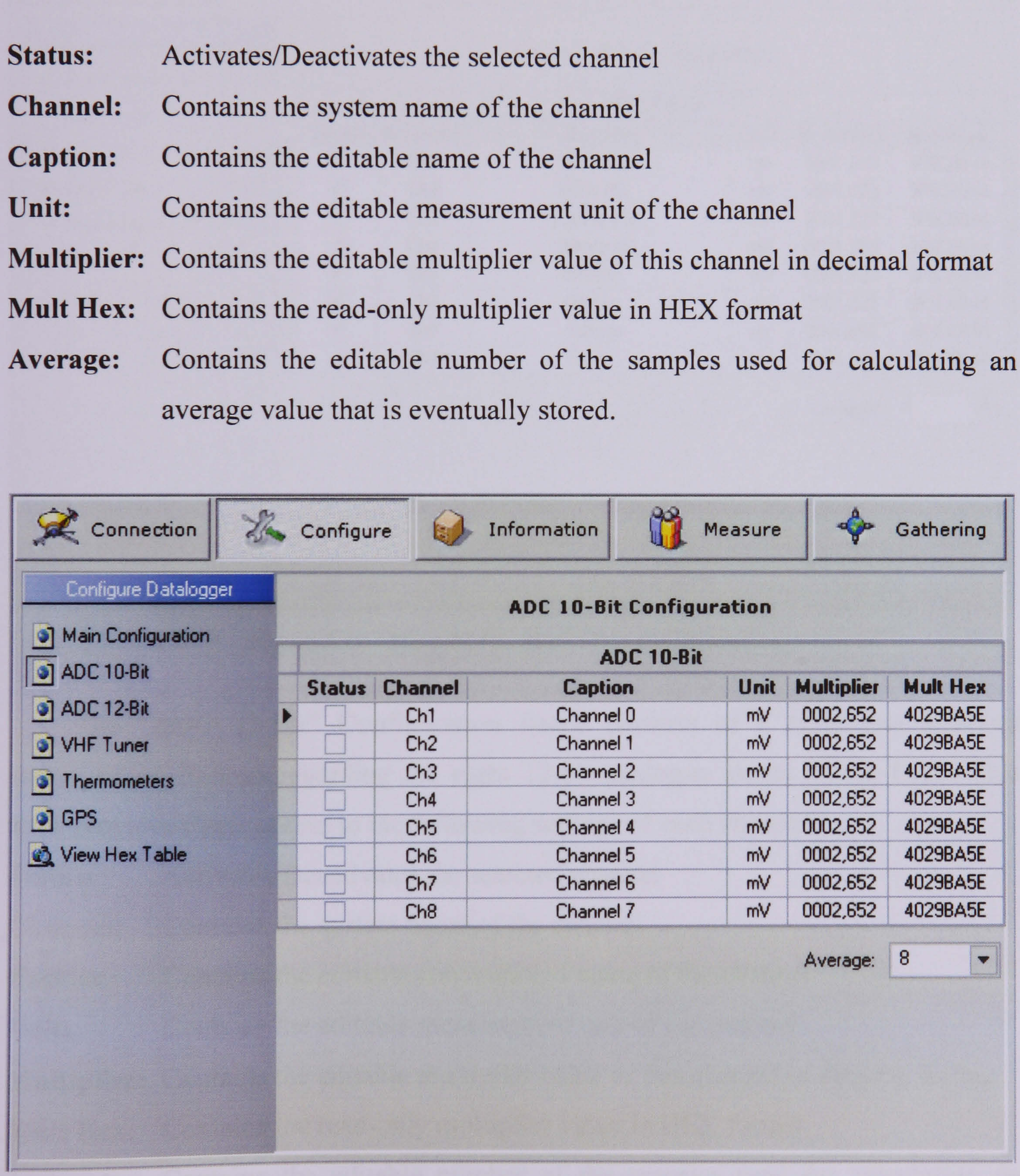

Figure 3.9 - MegaDLG - ADC 10bit Configuration

3.5.1.2.3 DAS ADC 12-bit configuration

When the "ADC 12-Bit" button is pressed, the "ADC 12-Bit Configuration" frame appears as shown in Figure 3.10.

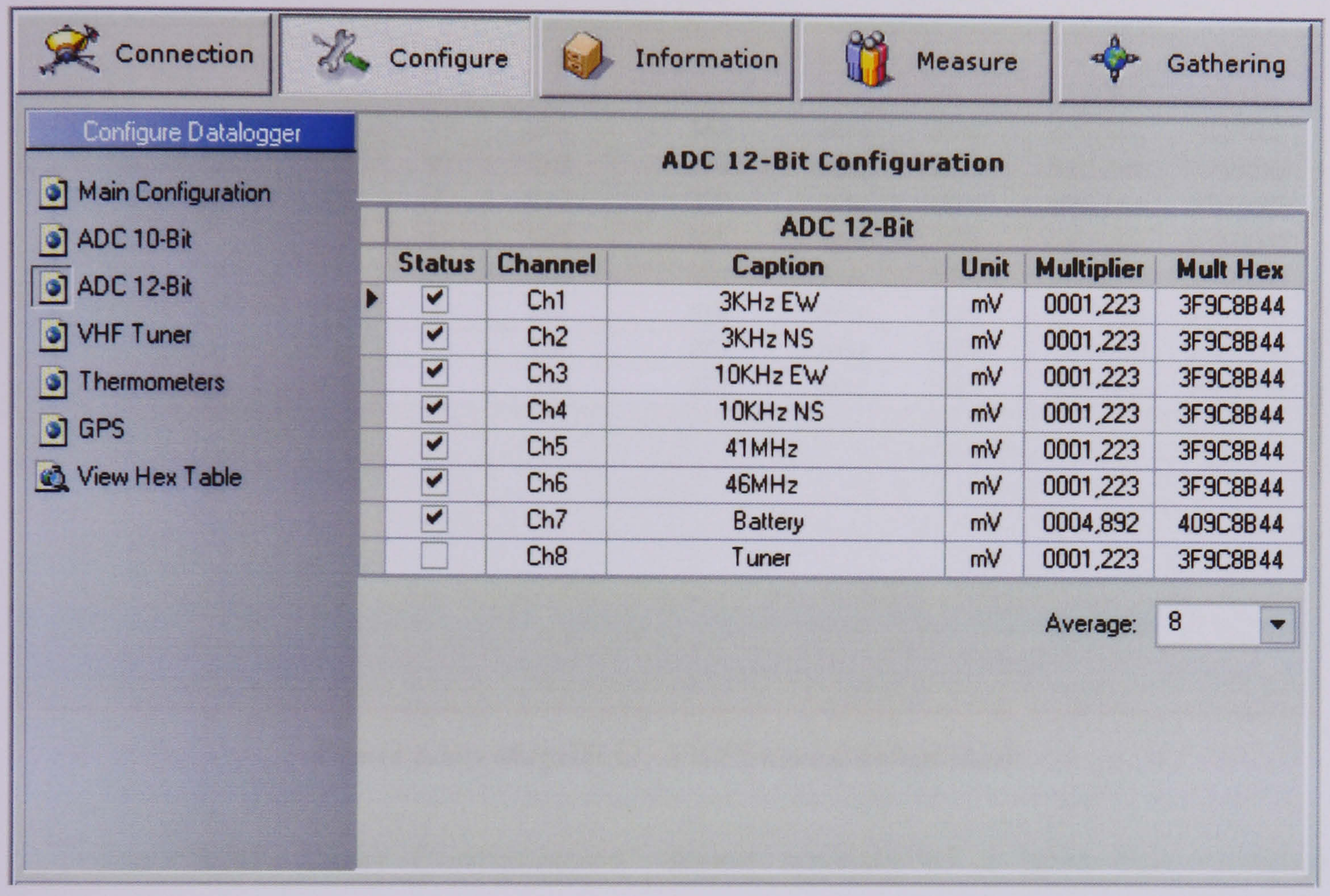

Figure 3.10 - MegaDLG - ADC 12bit Configuration

The "ADC 12-Bit" Configuration frame consists of a table that contains configuration options regarding the eight 12-bit analogue inputs of the DAS. This table provides direct access to the following settings of each channel:

Status: Activates/Deactivates the selected channel

Channel: Contains the system name of the channel

Caption: Contains the editable conventional name of the channel

Unit: Contains the editable measurement unit of the channel

Multiplier: Contains the editable multiplier value of this channel in decimal format

Mult Hex: Contains the read-only multiplier value in HEX format

Average: Contains the editable number of the samples used for calculating an average value that is eventually stored.

3.5.1.2.4 DAS VHF Tuner configuration

When the "VHF Tuner" button is pressed, the "VHF Tuner Configuration" frame appears as shown in Figure 3.11.

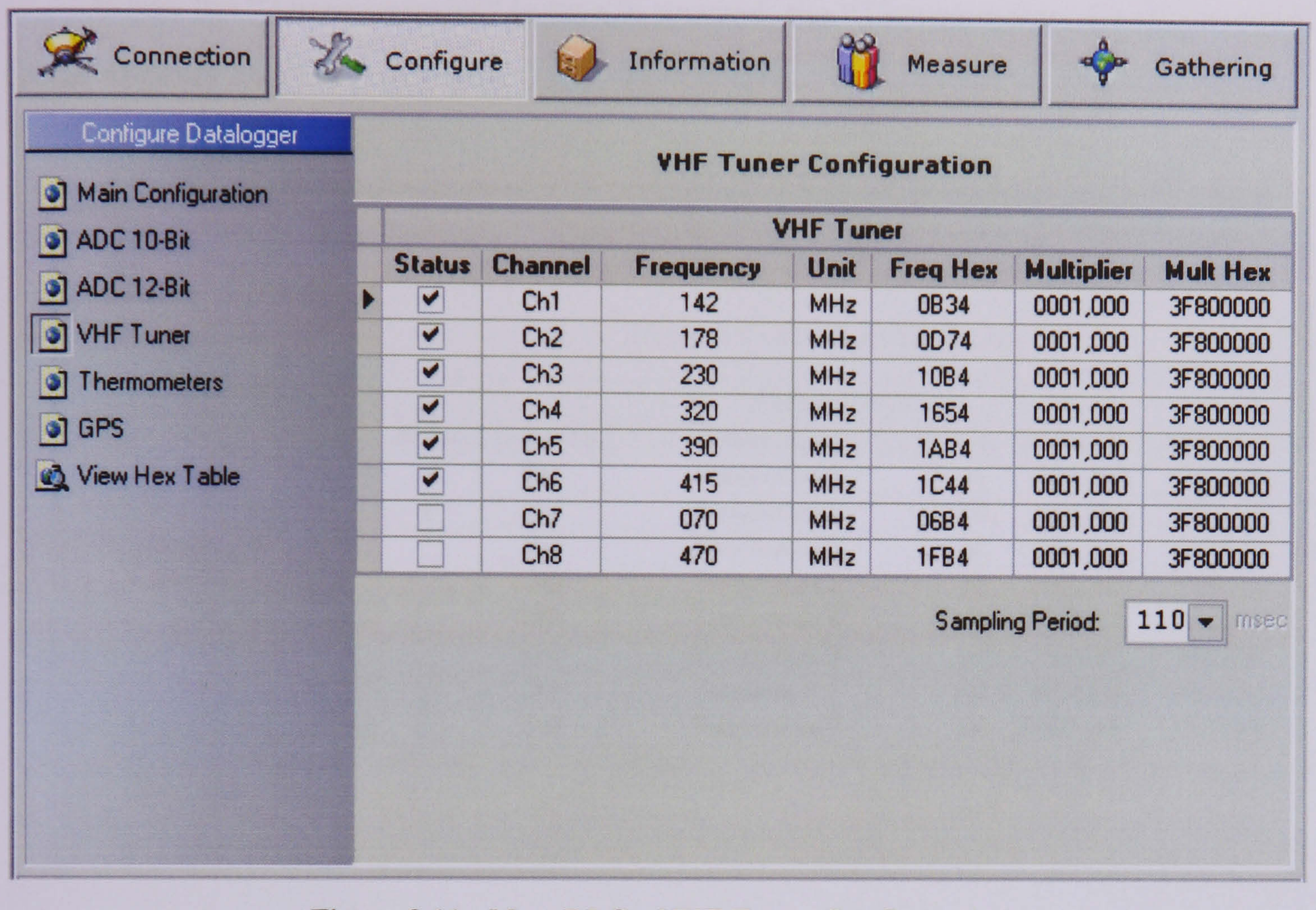

Figure 3.11 - MegaDLG - VHF Tuner Configuration

The "VHF Tuner Configuration" frame consists of a table that contains configuration options regarding the attached VHF tuner device. This table provides direct access to the following settings of the VHF measuring device:

Status: Activates/Deactivates the selected channel

Channel: Contains the system name of the channel

Frequency: Contains the editable value of the measured frequency of this channel in decimal format

Unit: Contains the editable measurement unit of the channel

Freq. Hex: Contains the read-only frequency value in HEX format

Multiplier: Contains the editable multiplier value of this channel in decimal format

Mult Hex: Contains the read-only multiplier value in HEX format

Sampling Period: Contains the editable sampling interval for each channel.

3.5.1.2.5 DAS Thermometers configuration

When the "Thermometers" button is pressed, the "Thermometers Configuration" frame appears as shown in Figure 3.12.

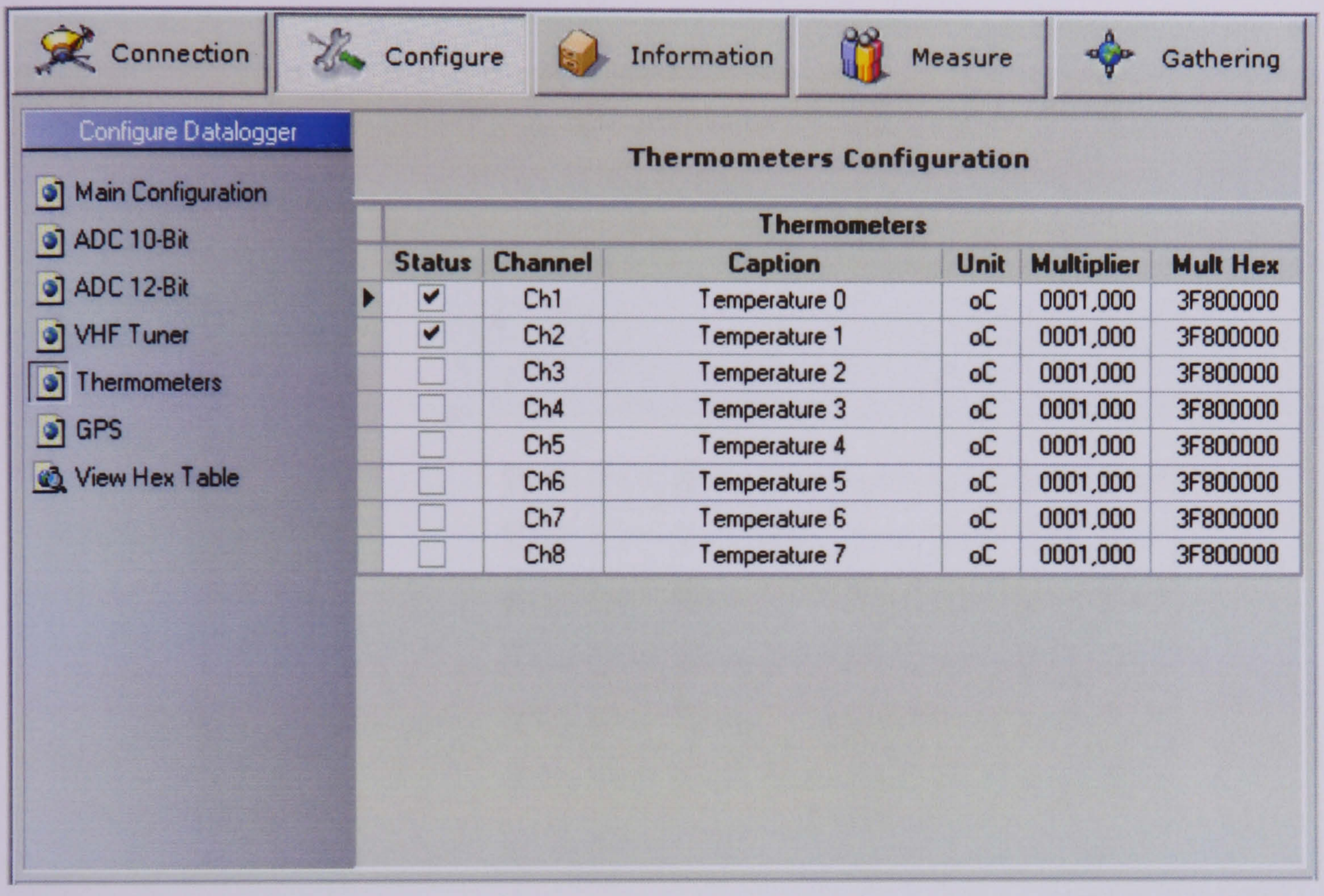

Figure 3.12 - MegaDLG - Thermometers Configuration

The "Thermometers Configuration" frame consists of a table that contains configuration options regarding the attached thermometers. This table provides direct access to the following settings of the temperature sensor:

Status: Activates/Deactivates the selected sensor

Channel: Contains the system name of this sensor

Caption: Contains the editable name of this sensor

Unit: Contains the editable measurement unit of this sensor

Multiplier: Contains the editable multiplier value of this sensor in decimal format

Mult Hex: Contains the read-only multiplier value in HEX format

3.5.1.3 DAS Real-time Status Information

The "Real-time Status Information" frame displays the configuration, as well as information data of the attached DAS in read only format. When the "Information" button is pressed, the "Information" frame is displayed (Figure 3.13).

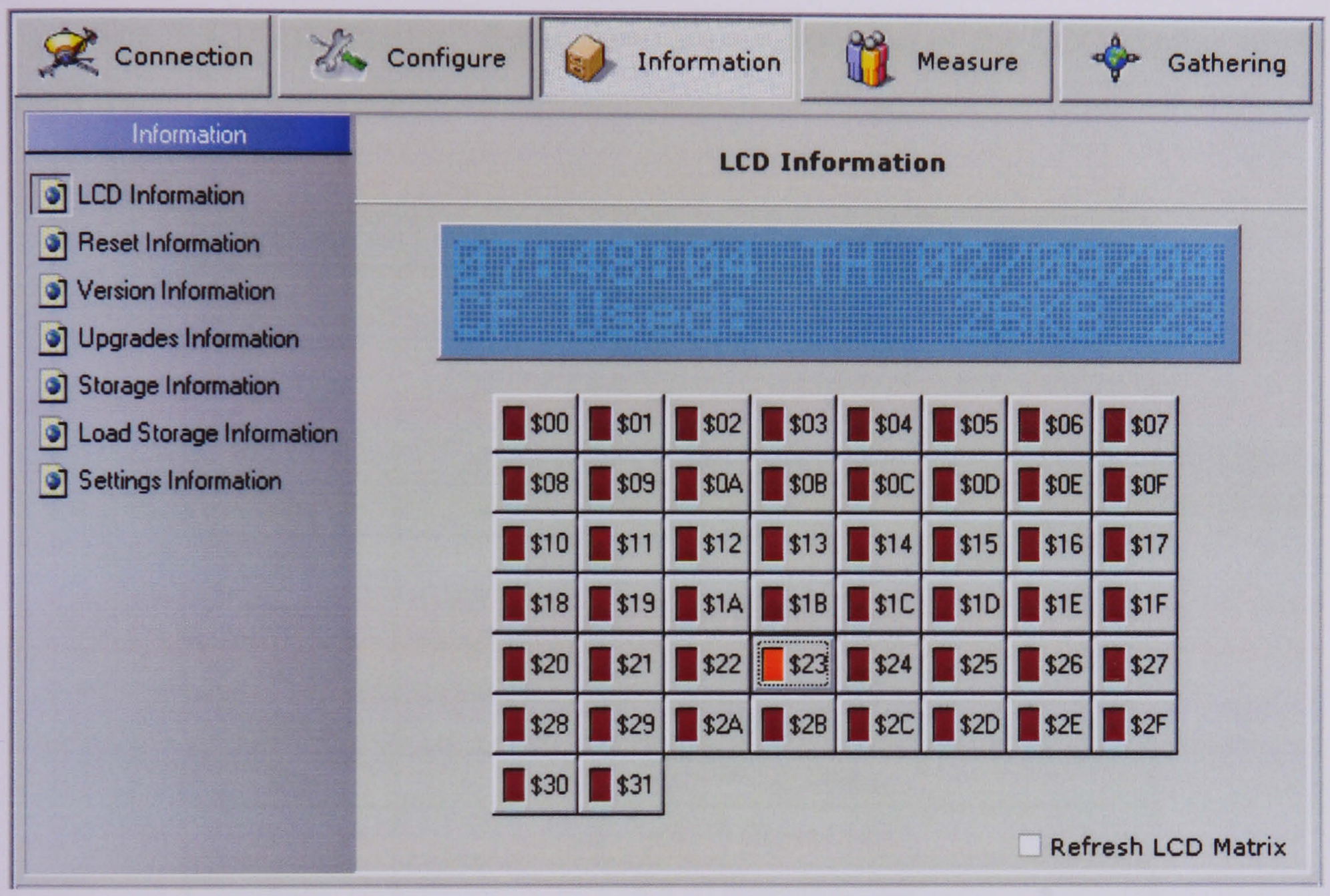

Figure 3.13 - MegaDLG - Real-time LCD Information

The "Information" frame consists of two separate frames. The first one contains a list of the available categories of information while the second one is a dynamic frame that displays the corresponding information when one of the categories is selected.

The information data are divided into the following seven categories:

LCD information:	Displays the information of the LCD mounted on the front panel
Reset Information:	Displays the history of the reset operations of the DAS
Version Information:	Displays the version information of the DAS
Upgrades Information:	Displays the history of the upgrades of the DAS

Storage Information: Displays the information of attached CF™ card of the DAS

Load Storage information: Displays the history of the used CF™ cards

Settings Information: Contains system wide settings and intervals

3.5.1.3.1 DAS Real-time LCD information

The "LCD information" frame provides a simulation of the LCD display of the DAS shown in Figure 3.13.

MODE	DISPLAY OUTPUT
$00 - $07	ADC 10bit Channels (0-7)
$08 - $0F	ADC 12bit Channels (0-7)
$10 - $17	VHF Tuner 12bit Channels (0-7)
$18 - $1F	Thermometers 12bit Channels (0-7)
$20	Print all channels sequentially
$21	Print all enabled channels sequentially
$22	CF™ size
$23	CF™ used space
$24	CF™ free space
$25	CF™ total time
$26	CF™ elapsed time
$27	CF™ remaining time
$28	CF status
$29	GPS UTC Time
$2A	GPS UTC Date
$2B	GPS Speed Over Ground
$2C	GPS Course Over Ground
$2D	GPS Latitude
$2E	GPS Longitude
$2F	GPS Error
$30	Change Sequentially GPS Latitude and GPS Longitude
$31	CPU Usage

Table 3.1 - MegaDLG - Real-time LCD Information Modes

The "LCD Information" frame consists of a virtual LCD display that corresponds to the LCD display attached on the DAS as well as 50 buttons that correspond to the 50 different display modes that can be accessed through the mode button of the DAS. In each mode the previously mentioned information is displayed (Table 3.1). Furthermore, the "Refresh LCD Matrix" checkbox enables/disables automatic refresh of the display every 5 seconds.

3.5.1.3.2 DAS Reset information

When the "Reset Information" button is pressed, the "Reset Information" frame appears as shown in Figure 3.14.

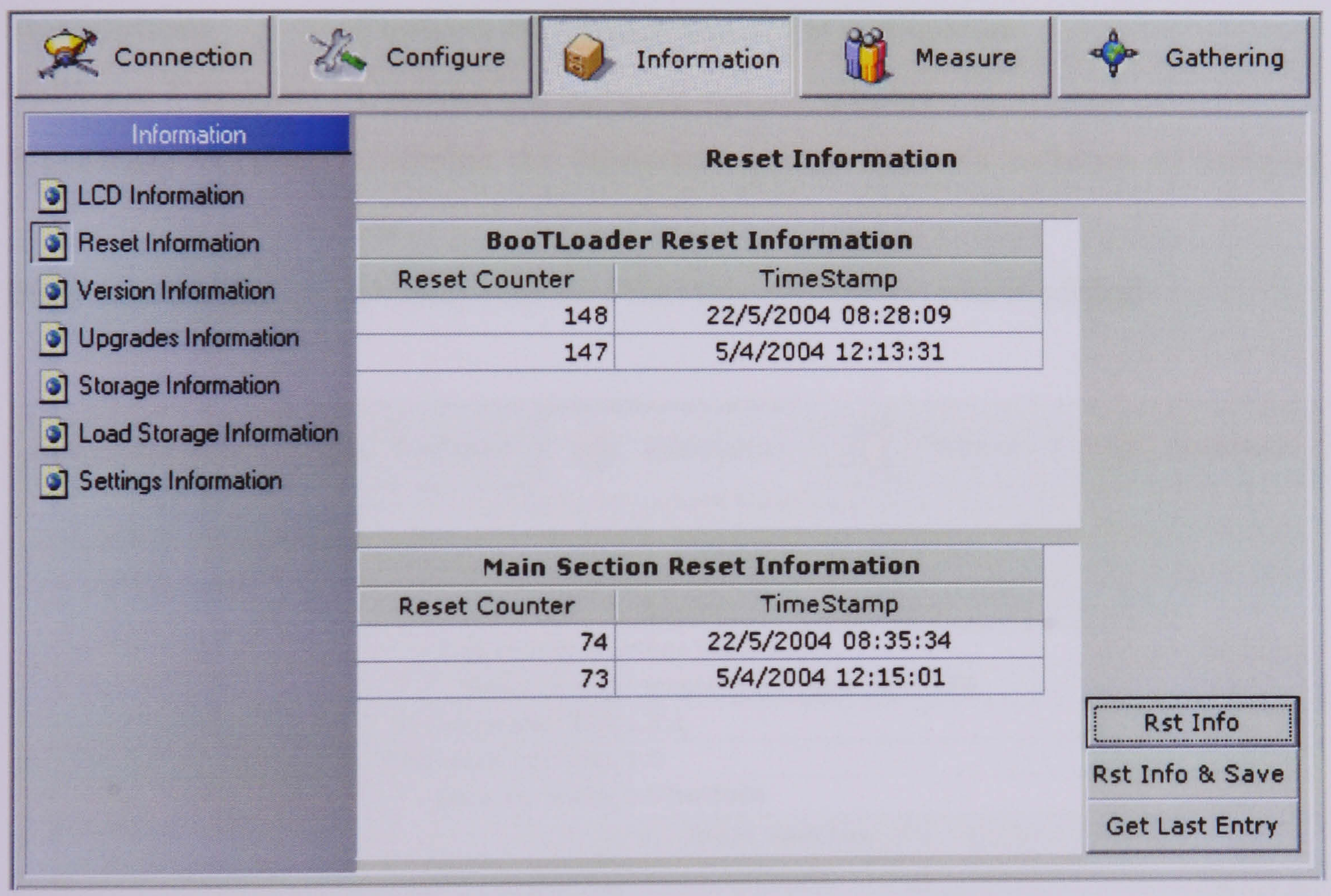

Figure 3.14 - MegaDLG - Reset Information

Due to the architecture of the DAS there are two types of reset information that can be gathered. The first one corresponds to the Boot-Loader and the second one corresponds to the Main Application of the system. Both pieces of information are valuable for troubleshooting and error detection.

The "Reset Information" frame consists of two tables that contain the last two reset events as well as the total number of resets executed.

3.5.1.3.3 DAS Version information

When the "Version Information" button is pressed, the "Version Information" frame appears as shown in Figure 3.15.

The "Version Information" frame consists of three different tables that contain information regarding the "Boot-Loader Version", the "Main Version" and the "Backup Version".

For each type of application the following information is displayed:

Device Name: Contains the name of the application

Description: Contains the Description of the application

Software Version: Contains the software version number

Hardware Version: Contains the hardware version that this software is designed for.

Date modified: Displays the date that this application was modified

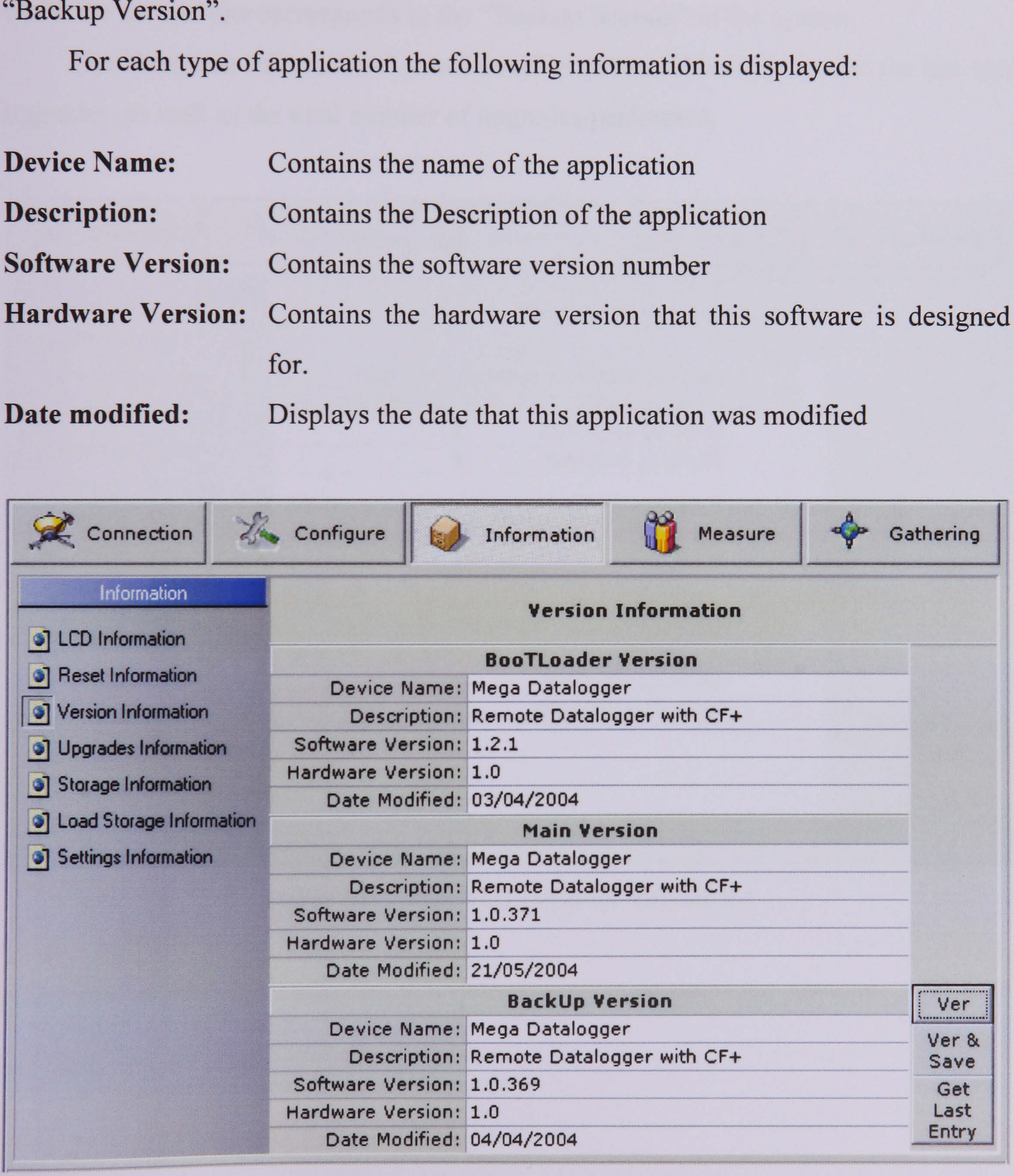

Figure 3.15 - MegaDLG - Version Information

3.5.1.3.4 DAS Upgrade information

When the "Upgrade Information" button is selected, the "Upgrade Information" frame appears as shown in Figure 3.16.

Due to the architecture of DAS there are two types of firmware upgrade information that can be gathered. The first one corresponds to the "Main Section", while the second one corresponds to the "Backup Section" of the system.

The "Upgrade Information" frame consists of two tables that contain the last two upgrades, as well as the total number of upgrades performed.

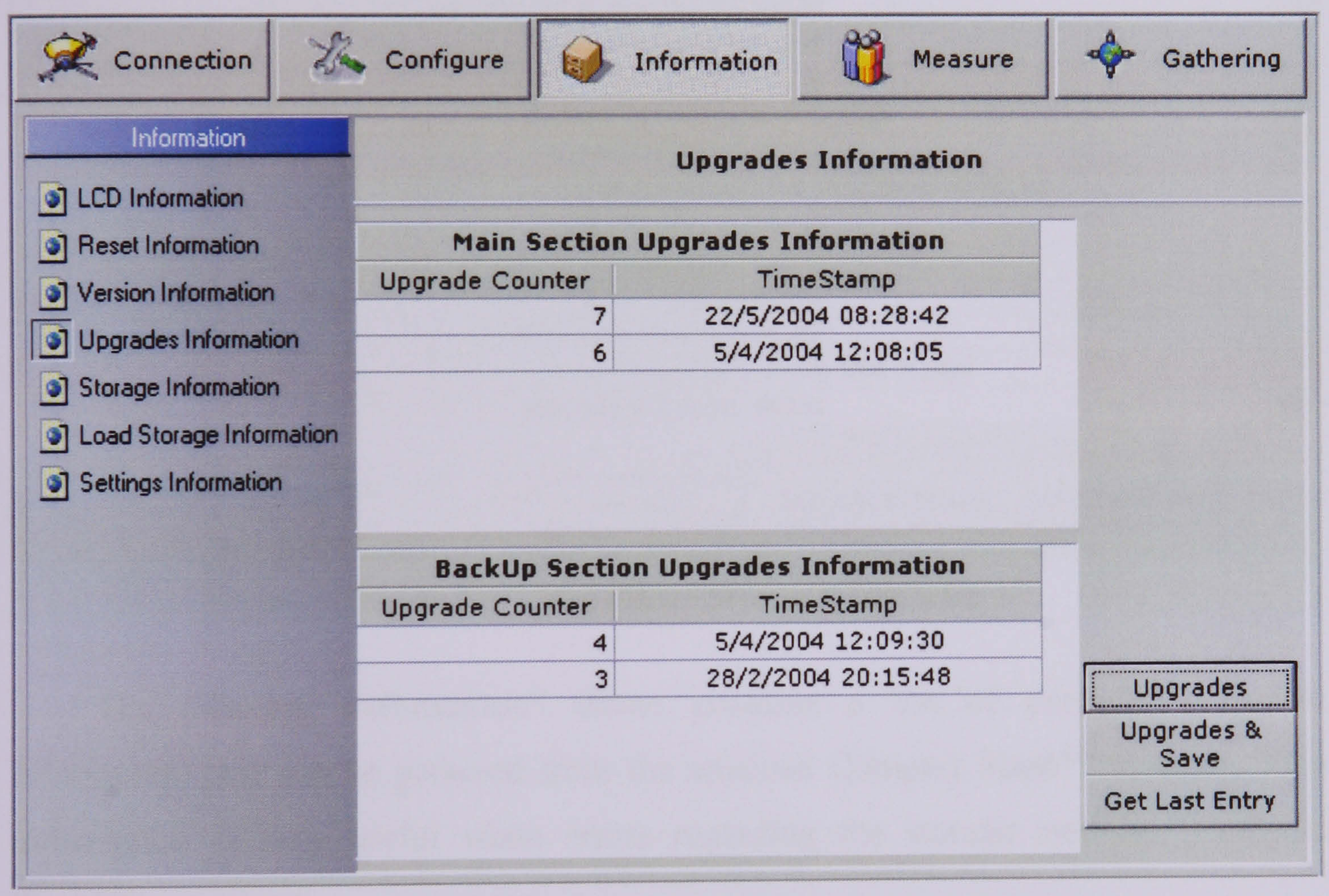

Figure 3.16 - MegaDLG - Upgrade Information

3.5.1.3.5 DAS Storage information

When the "Storage Information" button is pressed, the "Storage Information" frame appears as shown in Figure 3.17.

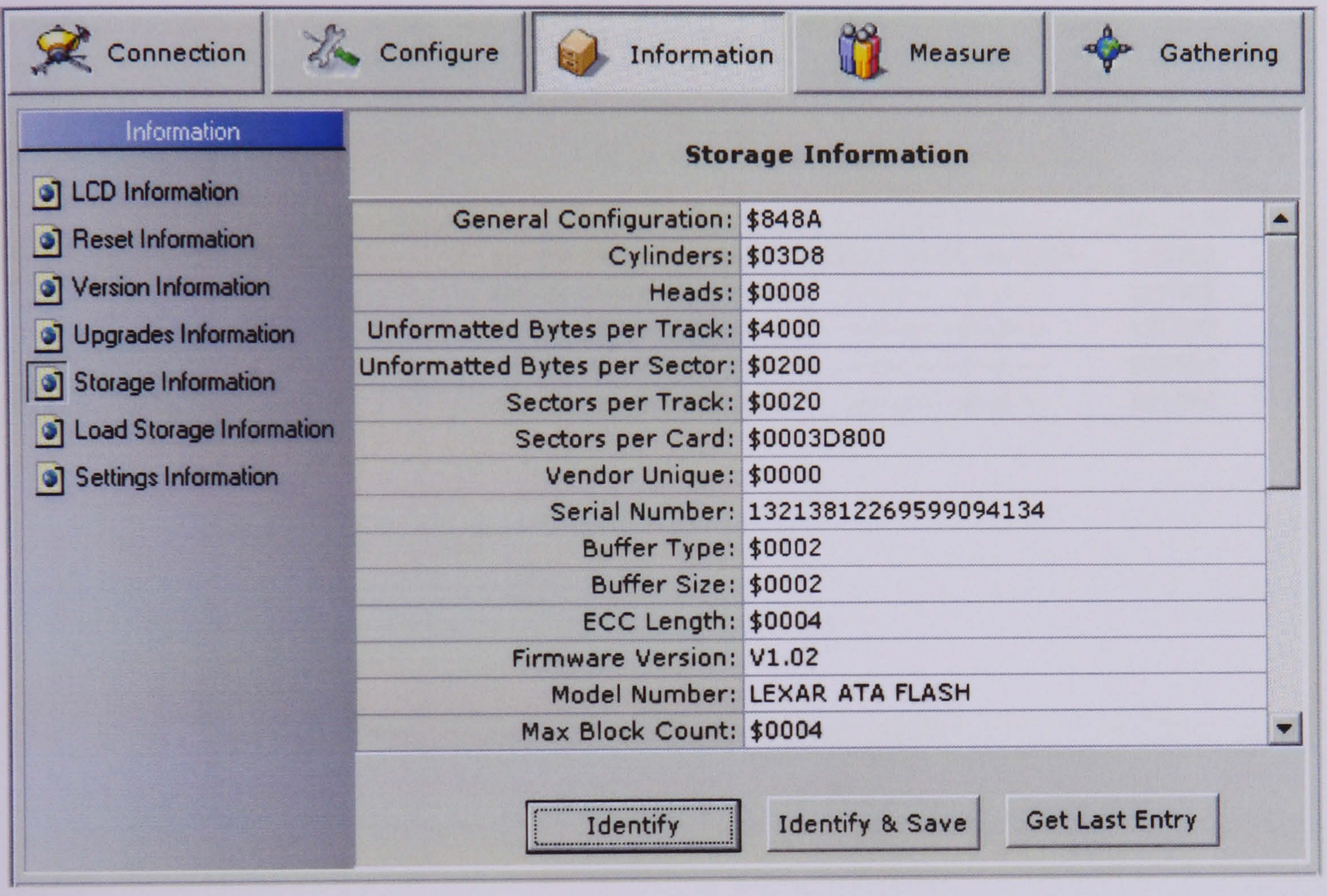

Figure 3.17 - MegaDLG - Storage Information

The "Storage Information" frame contains a list of extended technical information that can be gathered from the attached Compact Flash™ memory. This information is very useful when errors regarding the storage medium (Compact Flash™) are raised.

3.5.1.3.6 DAS Load Storage information

When the "Load Storage Information" button is pressed, the "Load Storage Information" frame appears as shown in Figure 3.18.

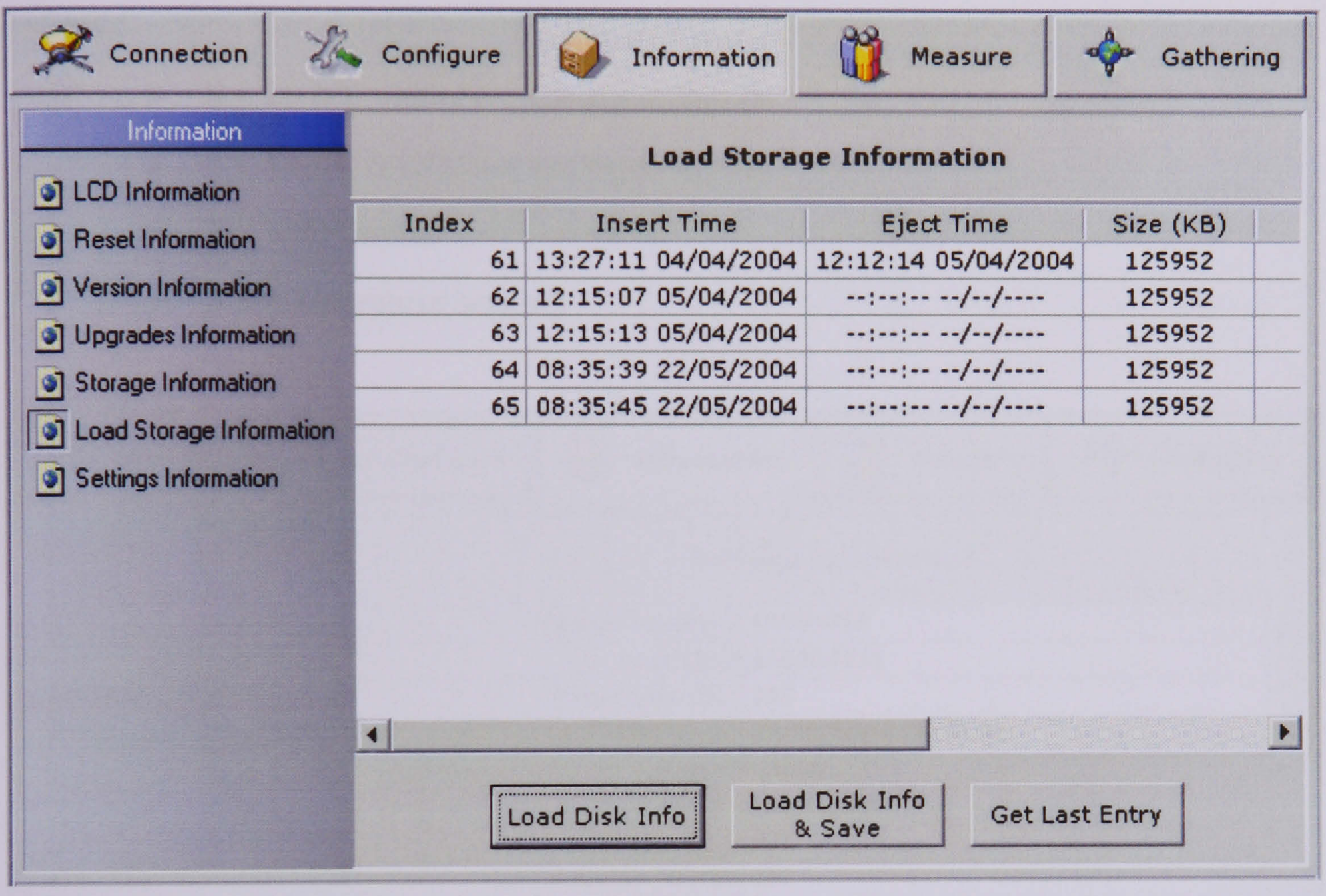

Figure 3.18 - MegaDLG - Load Storage Information

This frame contains a history list of the insert/eject events of the removable Compact Flash™ medium. This list displays the date and time of the event, the number of the event and the size of the specific Compact Flash™ medium in Kbytes.

3.5.1.3.7 DAS Settings information

When the "Settings Information" button is pressed, the "Settings Information" frame appears as shown in Figure 3.19.

The "Settings Information" frame contains the list of the following measurement options:

- 8 x 10-bit resolution analogue inputs
- 8 x 12-bit resolution analogue inputs
- 8 x VHF inputs
- 8 x temperature sensors

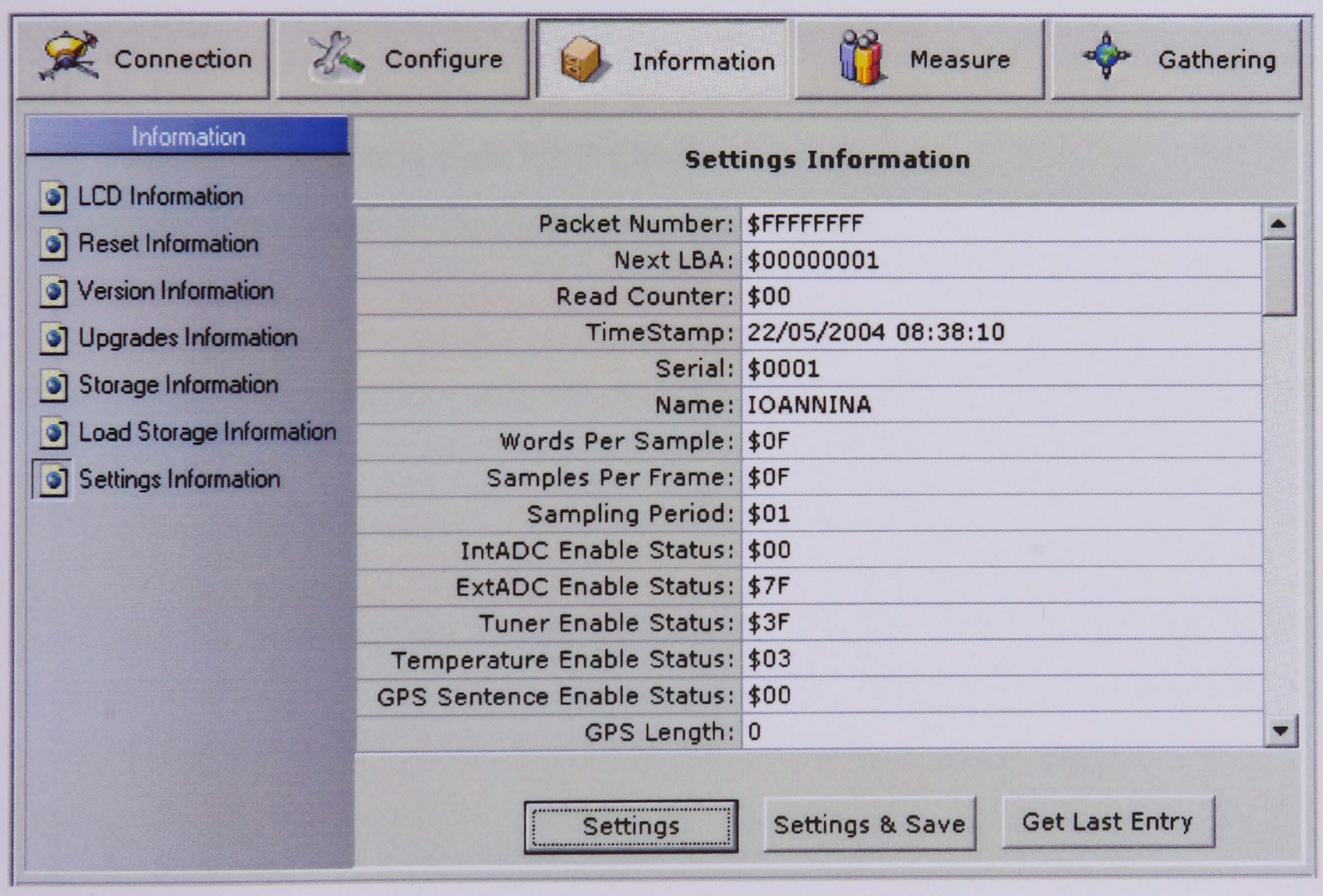

Figure 3.19 - MegaDLG - Settings Information

Using this frame, an extensive comparison of the configuration of the DAS with the temporary configuration from the "Configure" frame can be performed.

3.5.1.4 DAS Real-time Measurements

The "Measure" frame provides a visual real-time monitoring of the inputs. When the "Measure" button is pressed, the information frame is displayed (Figure 3.20).

The "Measure" frame consists of two separate frames. The first one contains a list of the available measurement inputs while the second one is a dynamic frame that displays the corresponding information when one of the categories is selected.

The information data are divided into seven categories which are the following:

ADC 10-Bit: Displays the eight 10-bit resolution inputs

ADC 12-Bit: Displays the eight 12-bit resolution inputs

VHF Tuner: Displays eight VHF signals

Thermometers: Displays the eight temperature signals

3.5.1.4.1 DAS ADC 10-bit measurements

When the "ADC 10-Bit" button is selected, the "ADC 10-Bit" frame becomes active as shown in Figure 3.20.

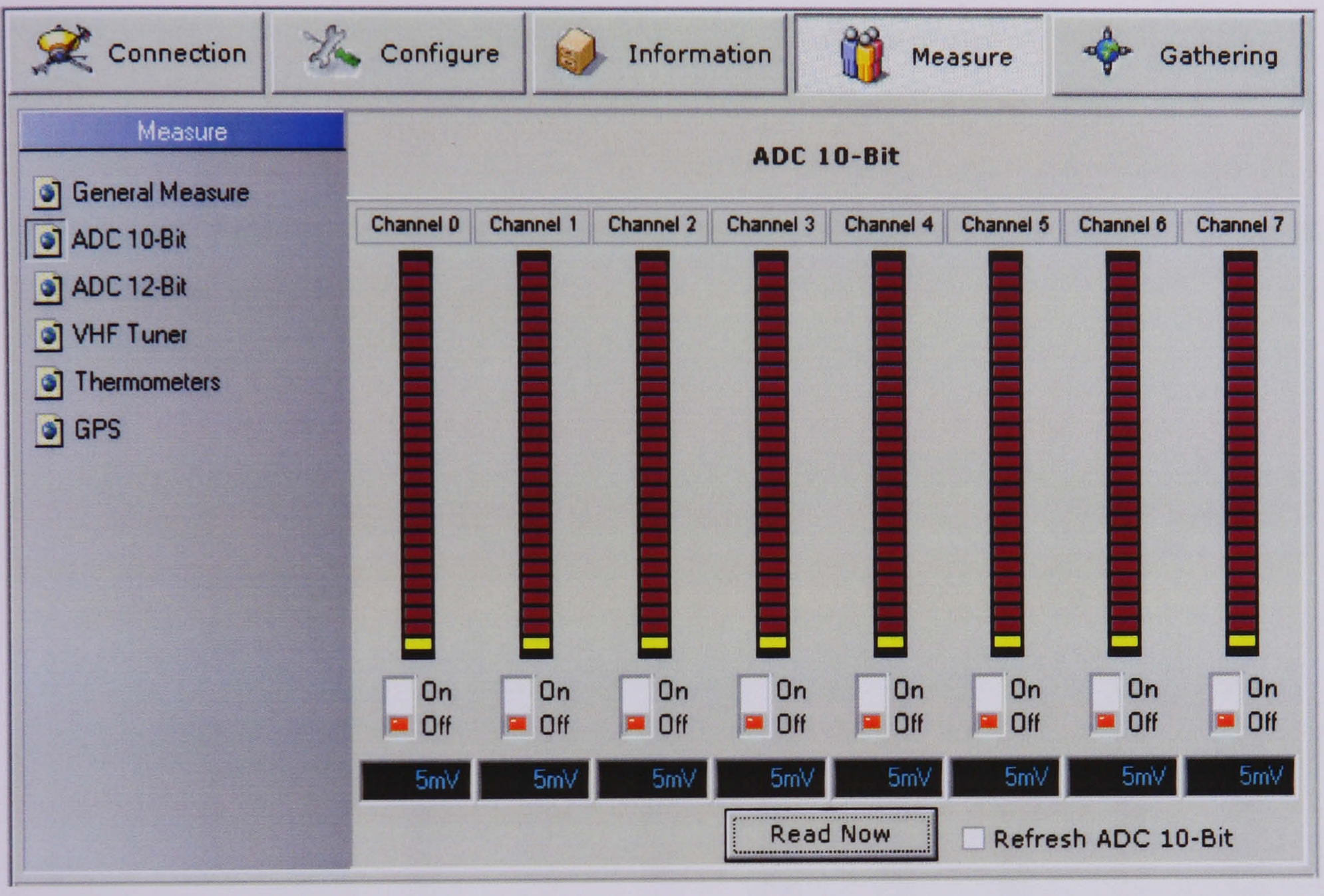

Figure 3.20 - MegaDLG - ADC 10-bit measurements

The "ADC 10-Bit" frame consists of eight separate groups of controls that represent the corresponding analogue input channel. Each group of control includes one visual progress bar, one virtual switch and one virtual digital meter.

When one of the switches is turned either on or off, the progress bar and the virtual digital meter, display the signal applied to the input of that channel. When the specific switch is activated, the measurement of the corresponding channel is stored into the Compact Flash™ medium.

The "Read Now" button executes an on-demand refresh of the displayed measurements while the "Refresh ADC 10-Bit" checkbox executes an automated, continuous refresh.

3.5.1.4.2 DAS ADC 12-bit measurements

When the "ADC 12-Bit" button is selected, the "ADC 12-Bit" frame becomes active as shown in Figure 3.21.

The "ADC 12-Bit" frame consists of eight separate groups of controls that represent the corresponding analogue input channel. Each group of control includes a visual progress bar, a virtual switch and a virtual digital meter. When one of the switches is turned on (green colour), the selected channel is enabled, otherwise (red colour) it is disabled. The progress bar and the virtual digital meter display the signal applied to the input of that channel.

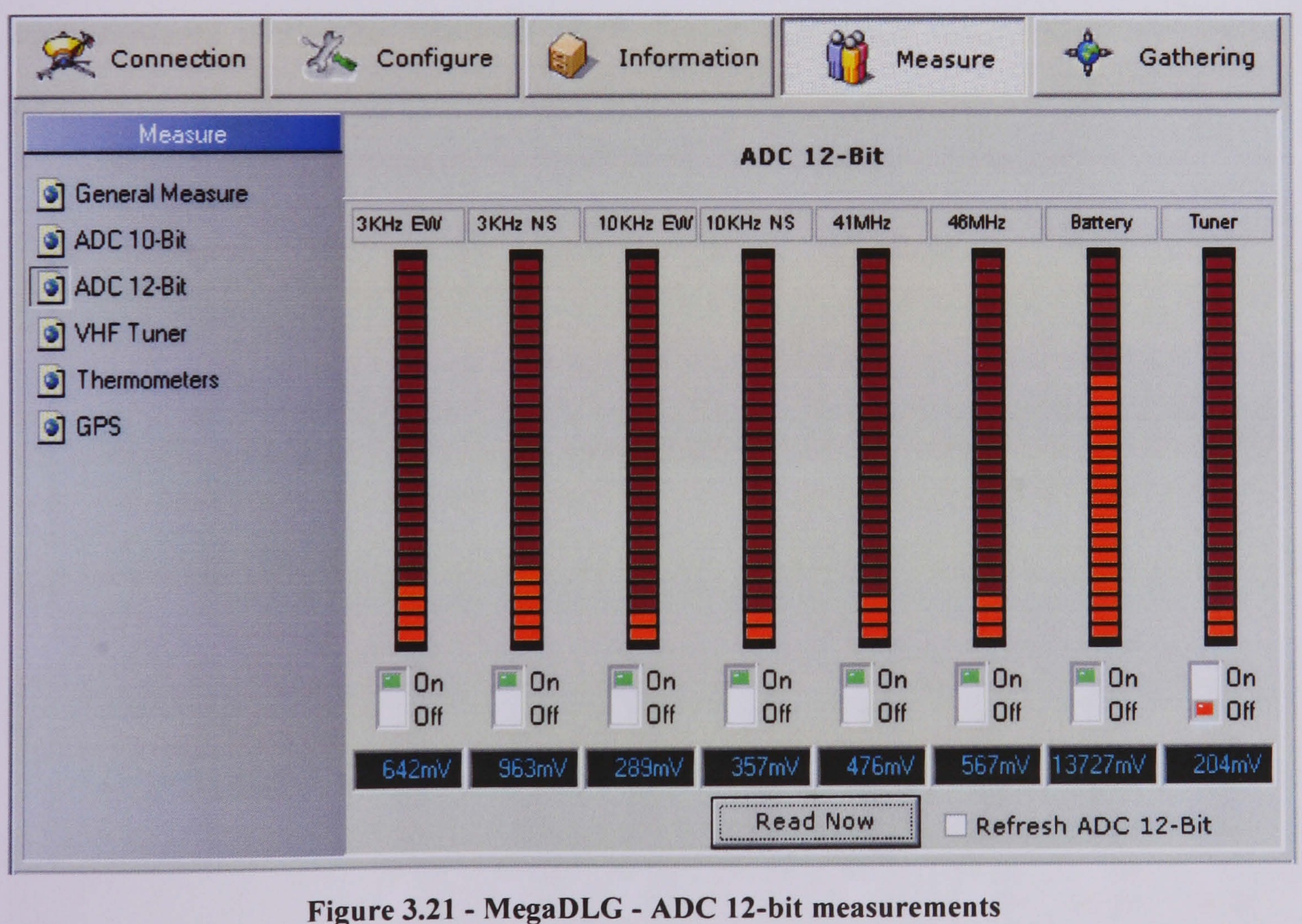

Figure 3.21 - MegaDLG - ADC 12-bit measurements

The "Read Now" button executes an on-demand refresh of the displayed measurements while the "Refresh ADC-12-Bit" checkbox executes an automated, continuous refresh.

3.5.1.4.3 DAS VHF Tuner measurements

When the "VHF Tuner" button is selected, the "VHF Tuner" frame becomes active as shown in Figure 3.22.

The "VHF Tuner" frame consists of eight separate groups of controls that represent the corresponding VHF input. Each group of control is labelled after the predefined frequency of the channel and includes a visual progress bar, a virtual switch and a virtual digital meter. When one of the switches is turned on (green colour), the selected channel is enabled, otherwise (red colour) it is disabled. The progress bar and the virtual digital meter display the level of the signal applied to the input of that channel.

The "Read Now" button executes an on-demand refresh of the displayed measurements while the "Refresh VHF Tuner" checkbox executes an automated, continuous refresh.

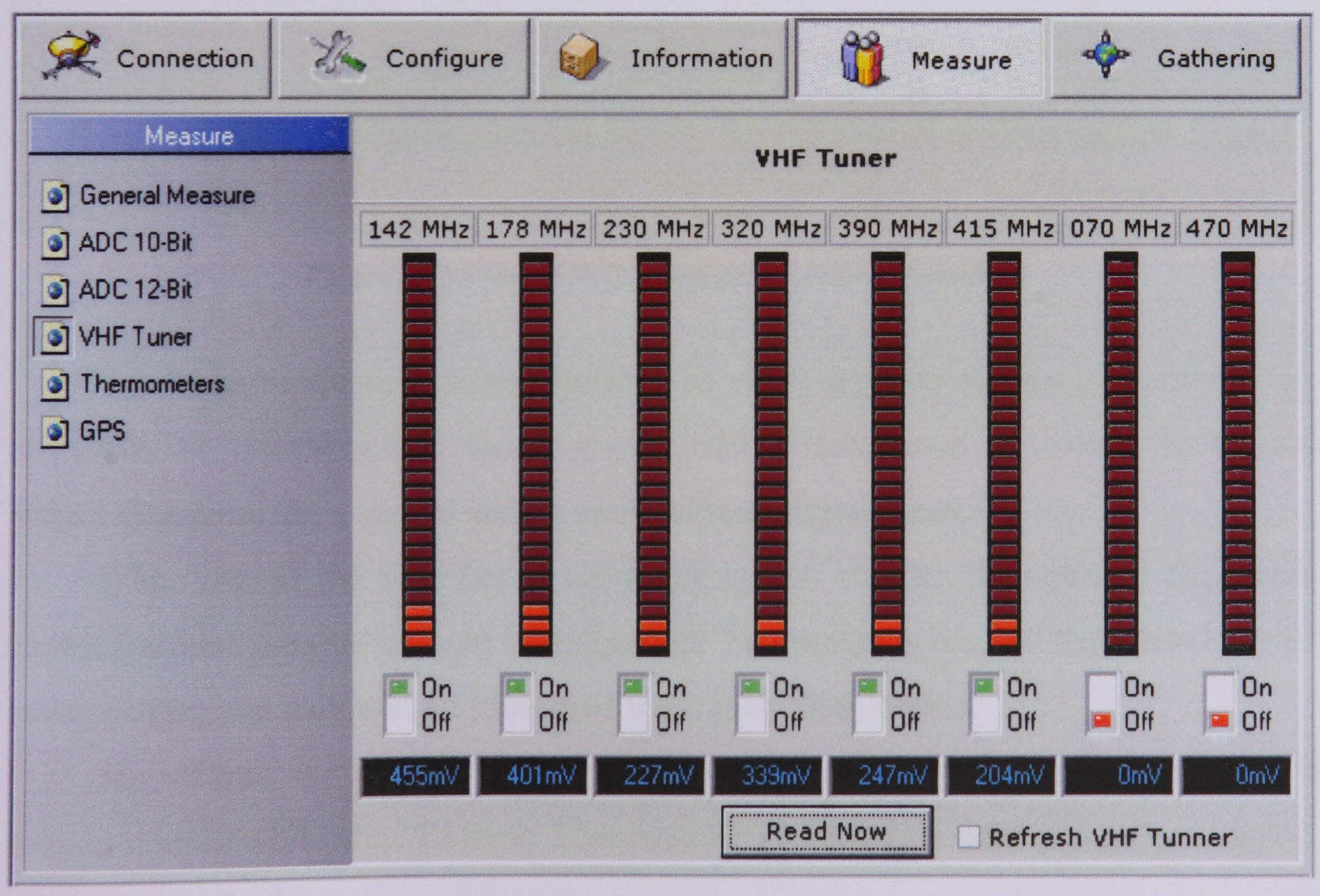

Figure 3.22 - MegaDLG - VHF Tuner measurements

3.5.1.4.4 DAS Temperature measurements

When the "Thermometers" button is selected, the "Thermometers" frame becomes active as shown in Figure 3.23.

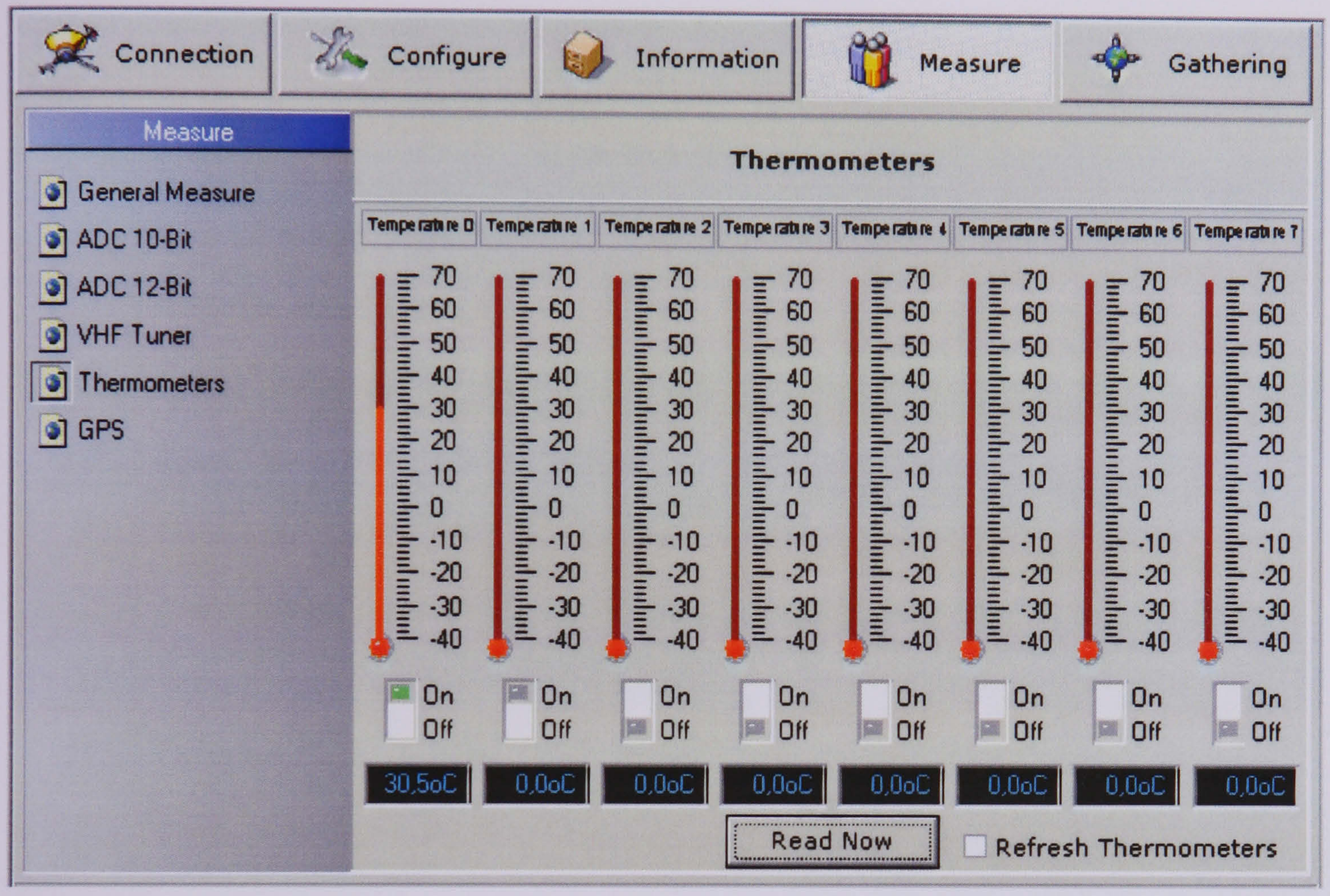

Figure 3.23 - MegaDLG - Temperature measurements

The "Thermometers" frame consists of eight separate groups of controls that represent the corresponding temperature sensor. Each group of control includes a virtual thermometer, a virtual switch and a virtual digital meter.

When one of the switches is turned on (green colour), the selected channel is enabled, otherwise (red colour) it is disabled. The progress bar and the virtual digital meter display the temperature measured from each thermometer.

The "Read Now" button executes an on-demand refresh of the displayed measurements while the "Refresh Thermometers" checkbox executes an automated, continuous refresh.

3.5.1.5 Gathering Settings

When the "Gathering" button is selected, the "Gathering" frame becomes active as shown in Figure 3.24.

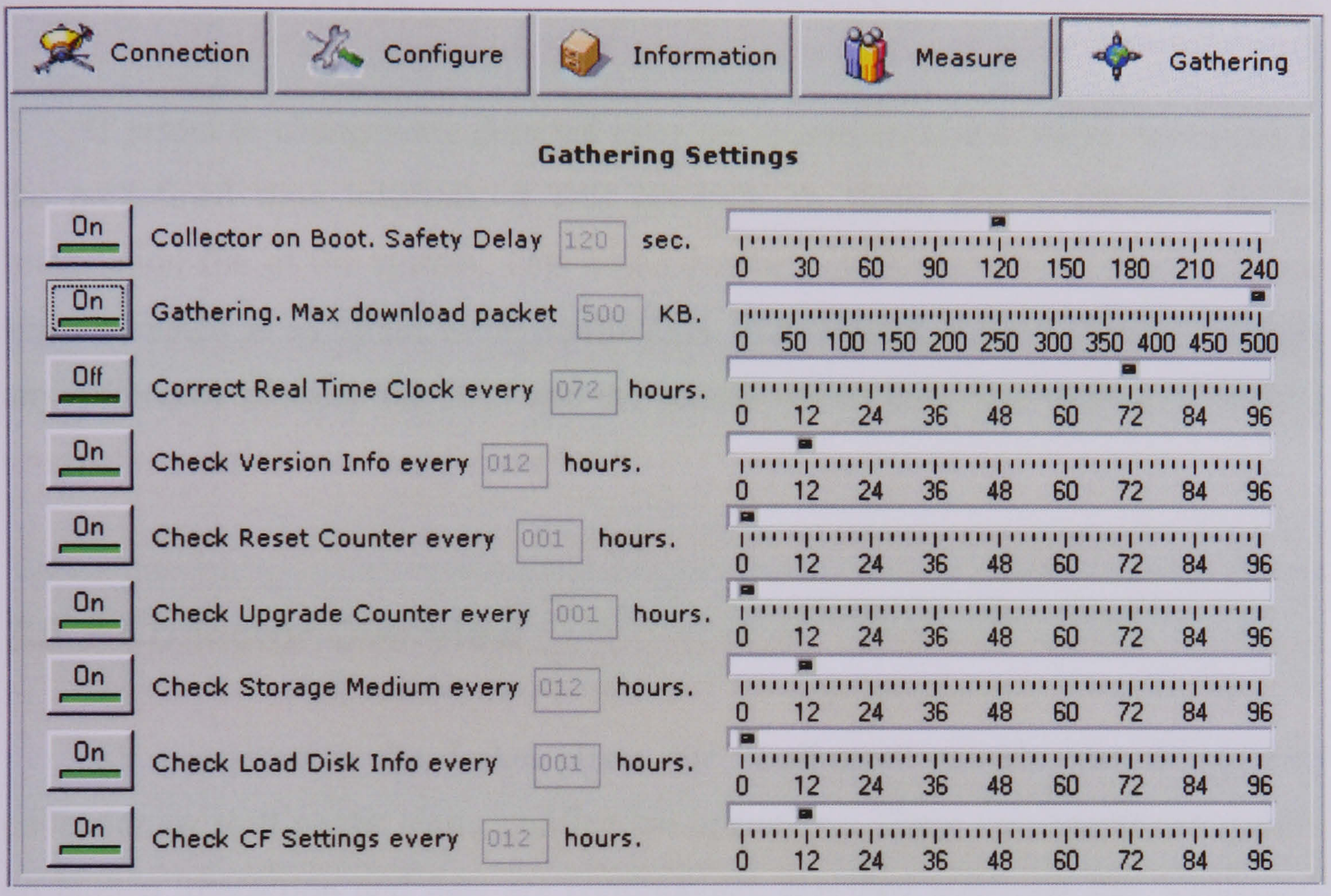

Figure 3.24 - MegaDLG - Gathering Settings

The "Gathering" frame contains operational settings for telemetry software. Each setting consists of a button, an edit box as well as a slider component. If the button of one control is enabled, the value selected from the slider is applied to either the telemetry application. It is worth mentioning that these settings are not global but private ones and they are unique for every DAS.

These settings are the following:

Collector on Boot. Safety Delay: Delay interval between sequential connections in seconds.

Gathering. Max download packet: Maximum packet size in Kbytes.

Correct Real Time Clock every: Interval between RTC settings check in hours

Check Version Every: Interval between Version info check in hours

Check Reset Counter Every: Interval between Reset Counter check in hours

Check Upgrade Counter Every:	Interval between Upgrade Counter check in hours
Check Reset Counter Every:	Interval between Reset Counter check in hours
Check Storage Medium Every:	Interval between Flash card check in hours
Check Load Disk Every:	Interval between insert/eject CF™ card check in hours
Check CF settings every:	Interval between CF™ settings check in hours

If errors or changes are detected after the execution of the above operations at the predefined time intervals, it will generate an alarm that is recorded in the Information file of the system. This alarm can be sent to every predefined recipient since it treated as an offsite event notification. Furthermore, if the RTC check detects any difference between the DAS and the central station date/time settings, it sends a re-synchronization command to the DAS.

3.5.2 Collector Overview

As mentioned in the design phase, the "Collector" provides the remote data collection as well as the alarm notification operations. These two operations require no human interaction and they are continuously executed whenever the "Collector" button is selected.

The key operation of the "Collector" is shown in the "Remote Data Collection" flowchart (Figure 3.2). When the "Collector" service is executed, the central station retrieves the list of the available data acquisition devices, as well as the settings of them, and a loop operation of remote data collection is initiated. This list is created by the Manager and is contained in an XML file that is stored in the directory of the application.

This XML file is named «MegaDLG.xml» (Figure 3.25) and contains the list of the Data acquisition devices, the communication interface and settings of each DAS as well as the gathering setting of it.

```
<?xml version="1.0" encoding="UTF-8" ?>
- <STATIONS COLLECTOR="0" SAFETYDELAY="090">
  - <STATION SERIAL="$0001">
      <ENABLED>1</ENABLED>
    - <GATHERINGSETTINGS>
        <MAXDOWNLOADPACKET ACTIVE="1">200</MAXDOWNLOADPACKET>
        <REALTIMECLOCK ACTIVE="0">072</REALTIMECLOCK>
        <VERSIONINFO ACTIVE="1">012</VERSIONINFO>
        <RESETCOUNTER ACTIVE="1">001</RESETCOUNTER>
        <UPGRADECOUNTER ACTIVE="1">001</UPGRADECOUNTER>
        <STORAGEMEDIUM ACTIVE="1">012</STORAGEMEDIUM>
        <LOADDISKINFO ACTIVE="1">001</LOADDISKINFO>
        <CFSETTINGS ACTIVE="1">012</CFSETTINGS>
      </GATHERINGSETTINGS>
    - <CONNECTIONS ACTIVE="1">
      - <CONNECTION TYPE="0">
          <NAME>RS232</NAME>
          <COMPORT>COM1</COMPORT>
          <BAUDRATE>9600</BAUDRATE>
          <DATABITS>8</DATABITS>
          <PARITY>NONE</PARITY>
          <STOPBITS>1</STOPBITS>
          <FLOWCONTROL>NONE</FLOWCONTROL>
        </CONNECTION>
      - <CONNECTION TYPE="1">
          <NAME>RS485</NAME>
          <COMPORT>COM1</COMPORT>
          <BAUDRATE>9600</BAUDRATE>
          <DATABITS>8</DATABITS>
          <PARITY>NONE</PARITY>
          <STOPBITS>1</STOPBITS>
          <FLOWCONTROL>NONE</FLOWCONTROL>
        </CONNECTION>
      - <CONNECTION TYPE="2">
          <NAME>GPRS</NAME>
          <PROVIDER>COSMOTE</PROVIDER>
          <APN>INTERNET</APN>
          <SERVERIP>195.130.107.90</SERVERIP>
          <PORT>1234</PORT>
          <DATAPACKET>512</DATAPACKET>
          <TIMEOUT>10</TIMEOUT>
        </CONNECTION>
      - <CONNECTION TYPE="3">
          <NAME>ETHERNET</NAME>
          <PROVIDER>OTENET</PROVIDER>
          <APN>INTERNET</APN>
          <SERVERIP>195.130.107.90</SERVERIP>
          <PORT>1234</PORT>
          <DATAPACKET>512</DATAPACKET>
          <TIMEOUT>10</TIMEOUT>
        </CONNECTION>
      - <CONNECTION TYPE="4">
          <NAME>WiFi</NAME>
          <PROVIDER>OTENET</PROVIDER>
          <APN>INTERNET</APN>
          <SERVERIP>195.130.107.90</SERVERIP>
          <PORT>1234</PORT>
          <DATAPACKET>512</DATAPACKET>
          <TIMEOUT>10</TIMEOUT>
        </CONNECTION>
      </CONNECTIONS>
    </STATION>
</STATIONS>
```

Figure 3.25 - Configuration file - MegaDLG.xml

This loop operation contains the following operations for each station:

a) Connection to the DAS

b) Remote Data Collection and events retrieval

c) Local Data Storage

d) Operation Logging

When the loop operation starts, the central station asks the first DAS if new data are available using Memory Pointers Comparison. If there is new data available, the DAS transmits them to the central station. It then receives the data and the following scenarios are available regarding the local storage of these data:

1) If the DAS is operated for the first time, a new zero-filled binary file is created with the size of the attached Compact Flash™ card. The name of this file is comprised of the four-digit Serial Number of the device followed by the extension .dat.

2) Whenever a new CF™ card is inserted in the DAS, the current file located in the central station is updated, backed up after being renamed by adding a number that associates it with the previously inserted CF™ Card. After that, a zero-byte binary file is created in the central station using the serial number of the DAS, which in turn corresponds to the newly inserted CF™ card.

3) Under normal operation, the Data storage Pointer is Greater than the Local pointer of the central station and the remote data is stored in the binary file.

4) If the Local Pointer of the central station is greater than the Data Storage Pointer of the DAS, the central station assumes that the DAS recorded data till the end of the Compact Flash™ card and started recording from the beginning of the card. Hence, the DAS stores the data from the LOCAL Pointer till the end of the CF™ card to the current binary file, closes and renames the binary file and then creates a new one. At that point, the Data Storage Pointer is greater than the Local Pointer.

In either scenario, these binary files are stored in the directory "D:\DATATELE\" which is a shared directory via FTP service.

After execution of remote data collection from every remote DAS, the central station sends to the predefined recipients any pending offsite alarm notifications that were logged during the previous collection and continuous the loop operation.

When the "Collector" button is selected, the third frame displays the "Monitoring" frame and the whole window has the following appearance (Figure 3.26).

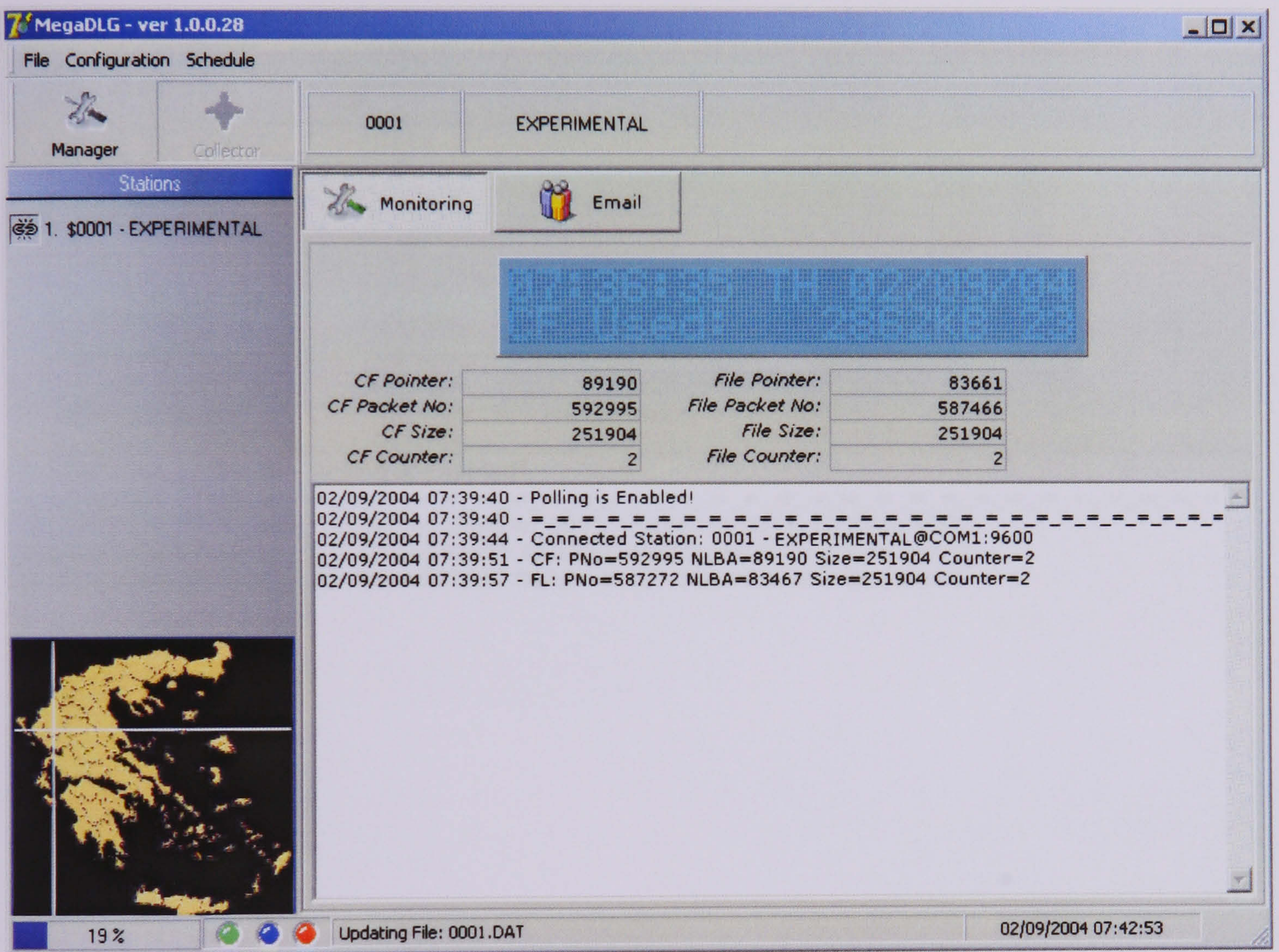

Figure 3.26 - Collector Frame

The "Collector" frame consists of two frames. The first one contains the list of the available stations while the second one contains the main operations of the "Collector", namely the "Monitoring" and the "Email" frames.

When the central station is connected to the remote DAS, the corresponding button of the station is activated.

3.5.2.1 Monitoring Status

The “Monitoring” frame is displayed when the “Collector” or the “Monitoring” button are selected. The “Monitoring” frame is divided into three sections as shown in Figure 3.27.

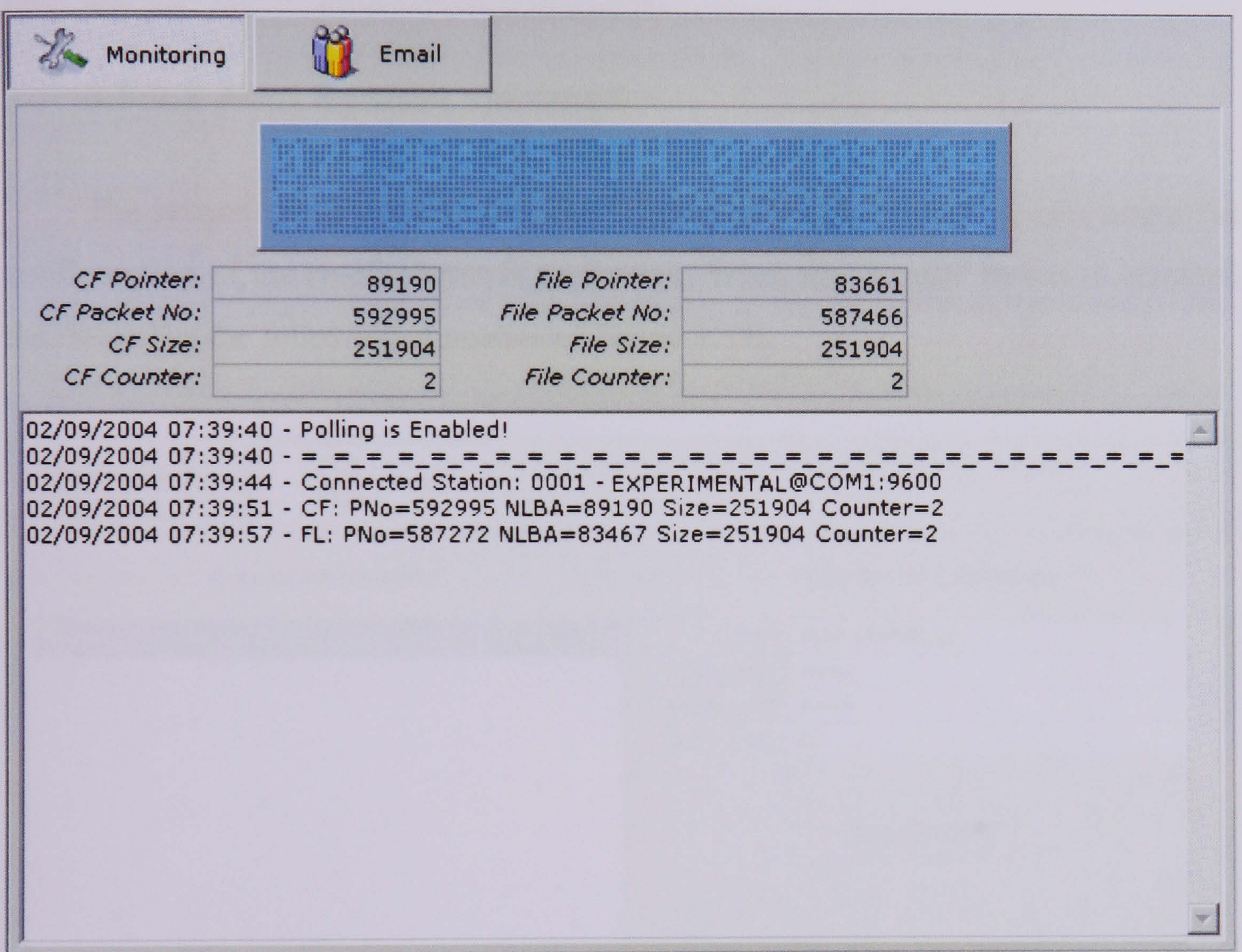

Figure 3.27 - MegaDLG - Monitoring Frame

The first section is the Virtual display of the DAS. It simulates the LCD display of the connected device. The Second section provides information regarding the “Compact Flash™” and the “Local File” pointers. The following specific pieces of information are displayed:

CF™ & File Pointer: Contains the memory pointers of the “Local File” and the “CF™ Card”

CF™ & File Packet No: Contains the Packet number of the “Local File” and the “CF™ Card”

CF™ & File Size: Contains the size of the "Local File" and the "CF™ card" in Kbytes.

CF™ & File Counter: Contains the number of the "Local Files" and the "CF™ cards" used.

The third Section of the "Monitoring" frame is the logger output section. In this section, information regarding the established communication sessions, the "Local File" and the "CF™" information is displayed.

3.5.2.2 Alert System via email

The second frame contained in the "Collector" is the "Email" frame where the configuration of the email clients is performed. When the "Email" button is selected, the frame has the following appearance (Figure 3.28).

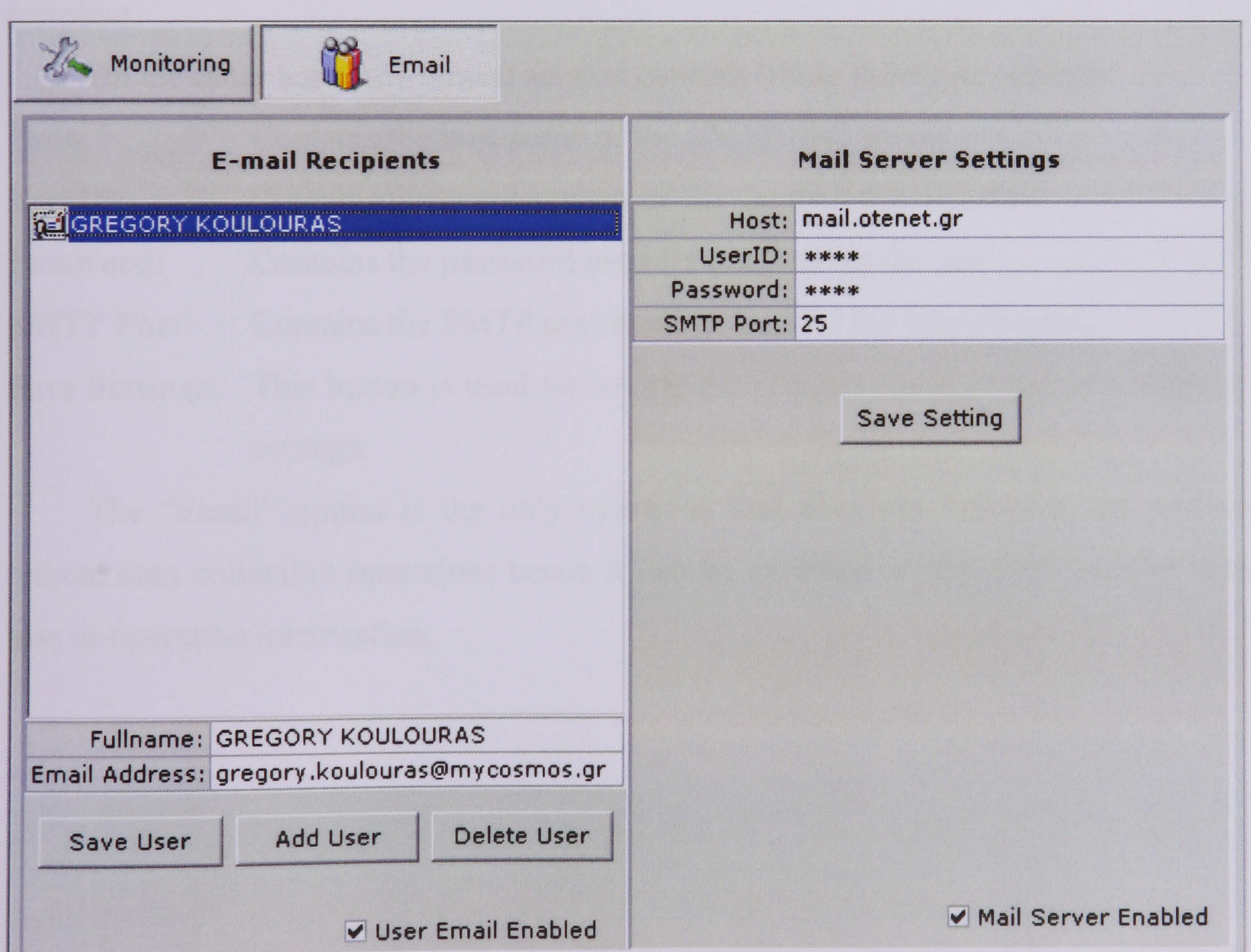

Figure 3.28 - MegaDLG - Email Frame

The "Email" frame contains information and settings of the predefined email accounts of the recipients. In more detail, the frame consists of two sections. The first section contains information regarding email address of the recipients, while the second one contains the mail server settings that will be used for email transmission.

The first section consists of a list of the full name of the recipients as well as the data entry interface. The operation supported by the data entry interface is the following:

Save User: That saves the changed of the Full name and the email address of the selected recipient.

Add Users: Inserts a new empty record that corresponds to a new email account

Delete User: Deletes the information of the selected User

In this interface an email account-oriented checkbox is also contained. If this checkbox is checked, the generated offsite notifications are transmitted to the selected recipient.

On the other hand, the second section consists of the following settings:

Host: Contains the host name of the SMTP mail server

UserID: Contains the user names used for the mail transmission

Password: Contains the password used for authorizing the user

SMTP Port: Contains the SMTP port number used for the transmission.

Save Settings: This button is used for saving the changes made in any of the above settings.

The "Email" option is the only operation that does not influence the normal remote data collection operation; hence it can be executed at any time without data loss or operation interruption.

3.6 Data Conversion Software Overview

After the telemetry software implementation, it was necessary to implement software for the data conversion. Telemetry software continuously updates the binary data files that are being saved in the host. The number of these files is equal to the number of the remote monitoring DAS devices and each one is an exact copy of the corresponding remote flash storage medium until the last update. Data conversion software has been developed in order to extract daily measurements in ASCII CSV (Comma Separated Values) format, which is a universal format and promises compatibility with most data analysis software. This software is scheduled to be executed daily on 04:00 UTC. The main form of EMV Data Conversion software, as shown in Figure 3.29 has the following appearance. Figure 3.30 shows the settings form of the same software.

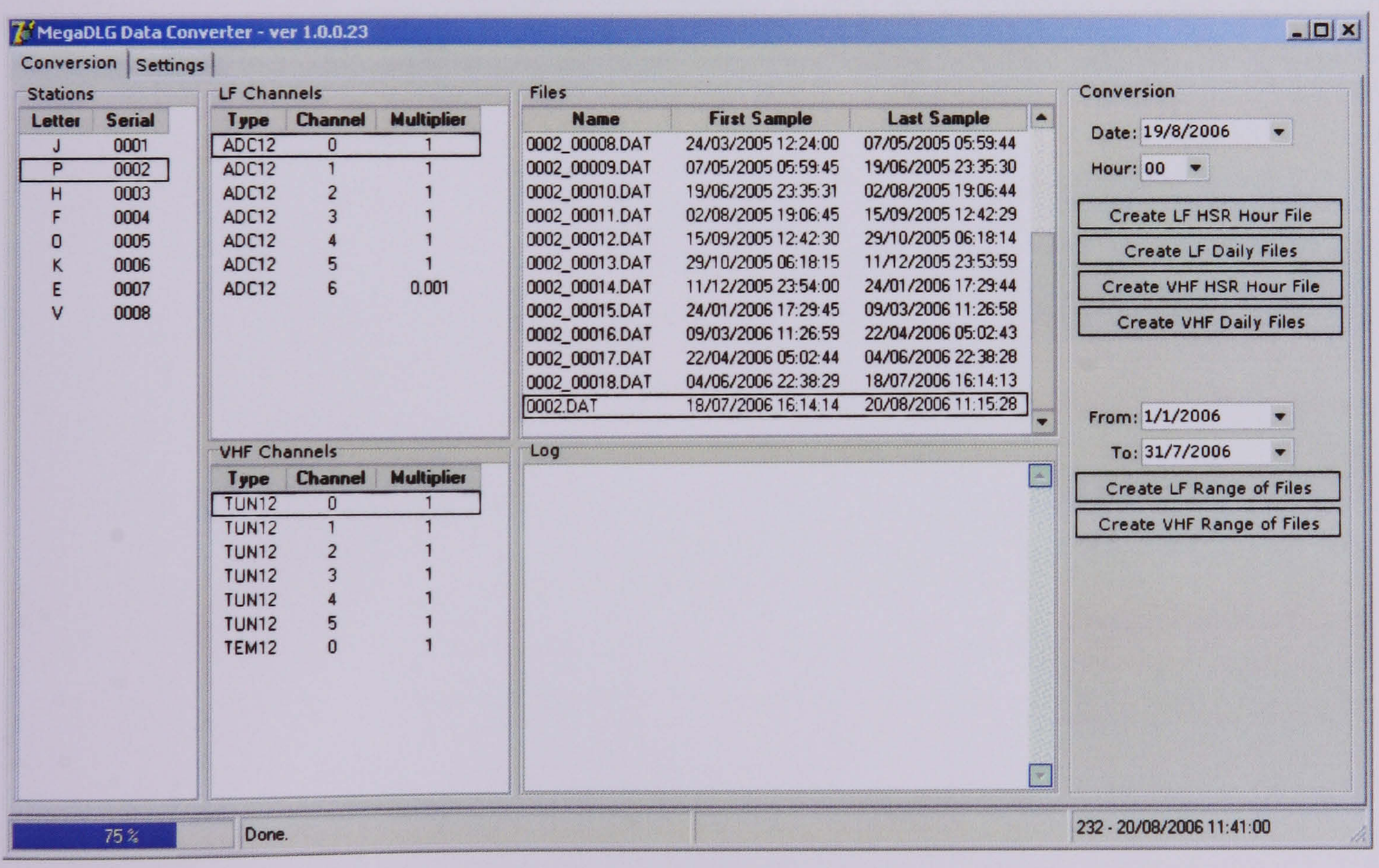

Figure 3.29 - EMV Data Conversion Software

The name of these files is comprised of the first letter of each station, followed by the four-digit number (i.e. 2005) representing the year of sampling and the three-digit number (i.e. 065) the Julian day of year. Finally the file extension is «.dat».

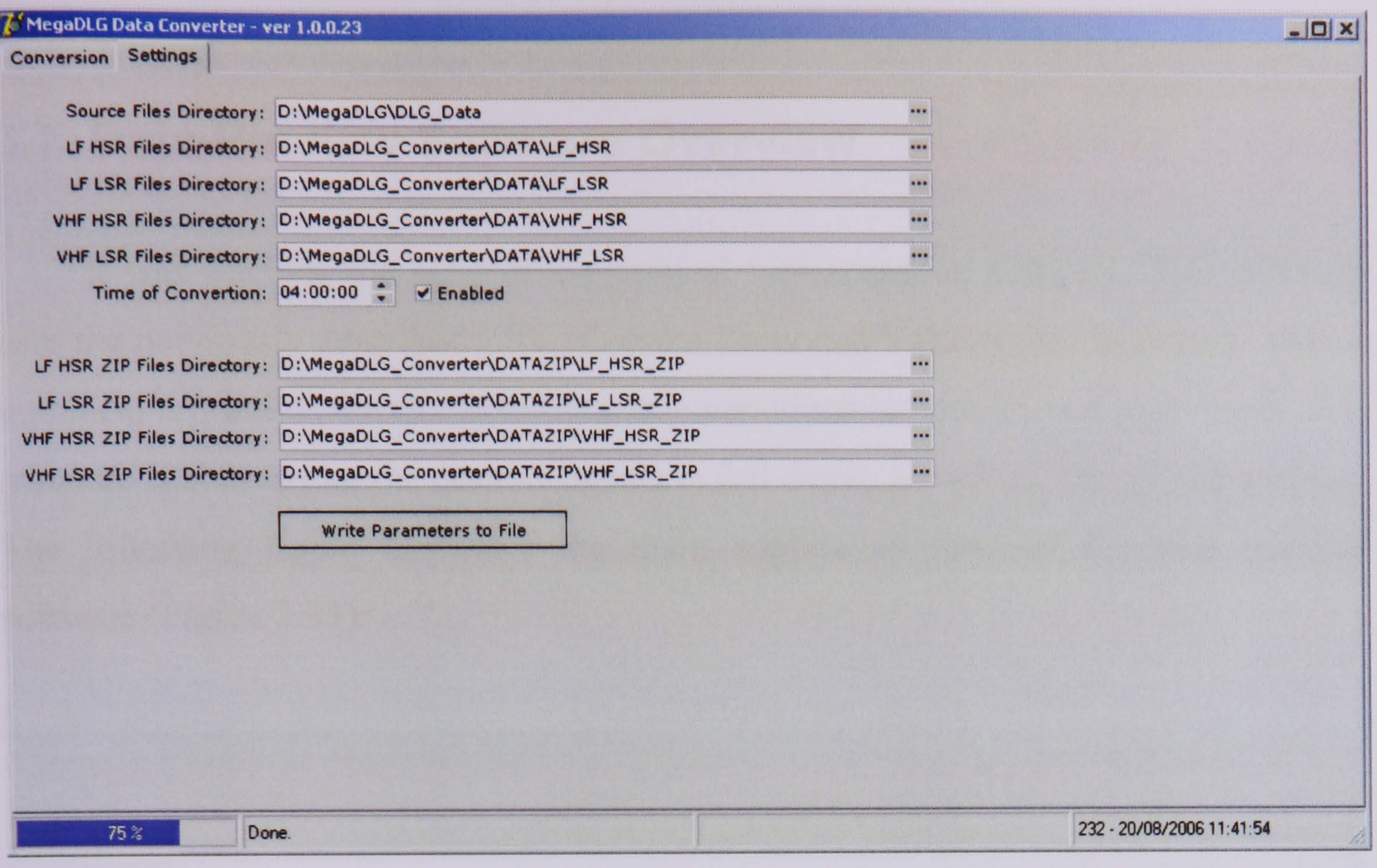

Figure 3.30 - Settings of EMV Data Converter Software

3.7 Data Preview Software Overview

It was obvious the need of a graphical representation software. This software uses the previously described CSV (Comma Separated Values) files in order to have a graphical representation of electromagnetic variations in both LF and VHF band. This software is able to plot the desired signals in full detail, as well as, the minute average. The following figure illustrates the main application form of the data preview software (Figure 3.31).

Figure 3.31 - EMV Data preview software

3.8 Signal detections processing and algorithms

The selected monitoring frequencies in VHF band are known to be free from artificial interference. Levels of EM activity were recorded and later correlated to seismological data from the selected geographic region of Greece.

For strong EM events a simple threshold of the signal level proved reliable enough. Although for minor events more powerful algorithms were developed in order to be identified. Among these Standard Deviation level and STA/LTA algorithm proved more accurate.

Four field stations collect the electromagnetic variations in VHF band. These data are used as input to the signal detection system. Data from possibly defective stations is removed in the first step. The data originating from all field stations is then synchronized. Feature generation step, which is described in section 3.8.1, is significant for the signal detection processing algorithm, in order to prevent system from false triggers.

An alarm at a single station is searched by using the calculated Standard Deviation (STD) and the STA/LTA criterion described in detail in sections 3.8.2 and 3.8.3 correspondingly. When the amplitudes of the observation frequencies of a field station exceed the threshold limit (above mean value), other concurrent activations originating from any station of the network are sought. In case no other anomaly is detected in the network, then the signal recorded from the first station is considered to be local noise (false alarm). As an important rule for any alarm trigger, is the concurrent activation from most field stations.

3.8.1 Feature generation

The data preview software focused on daily signals plot. At the same time this software generates the features of the current preview signal that will help in further data analysis and event detection.

The processing was focused on the calculation of a number of features for each isolated signals. The following features were automatically calculated for every selected daily signal.

1) Signal Duration Window (DUR, d):

$$d = t_{end} - t_{start} \tag{1}$$

2) Maximum signal value (MAX, s_{max}):

$$s_{\max} = \max_{t=t_{start}}^{t=t_{end}}\{s(t)\} \tag{2}$$

3) Minimum signal value (MIN, s_{min}):

$$s_{\min} = \min_{t=t_{start}}^{t=t_{end}}\{s(t)\} \tag{3}$$

4) Peak to peak:

$$pp = s_{\max} - s_{\min} \tag{4}$$

5) Area (ARE, a):

$$a = \sum_{t=t_{start}}^{t=t_{end}} s(t) \tag{5}$$

6) Mean value (MNV, μ):

$$\mu = \frac{a}{d} \tag{6}$$

7) Standard deviation (STD, σ):

$$\sigma = \sqrt{\frac{\sum_{t_{start}}^{t_{end}}[s(t) - \mu]^2}{d}} \tag{7}$$

8) Maximum to mean value (MAM, $s_{\max \mu}$):

$$s_{\max \mu} = s_{\max} - \mu \tag{8}$$

9) Minimum to mean value (MIM, $s_{\min \mu}$):

$$s_{\min \mu} = \mu - s_{\min} \tag{9}$$

10) Area from mean value (AFM, a_{mean}):

$$a_{mean} = \sum_{t_{start}}^{t_{end}} |s(t) - \mu| \tag{10}$$

3.8.2 Calculation of Standard Deviation

The standard deviation is the root mean square (RMS) deviation of the values from their arithmetic mean. Standard deviation is the most common measure of statistical dispersion, measuring how spread out the values in a data set is. If the data points are all close to the mean, then the standard deviation is close to zero. If many data points are far from the mean, then the standard deviation is far from zero. If all the data values are equal, then the standard deviation is zero.

The following figure shows a graphical representation of daily calculated STD of a single EM VHF station.

Figure 3.32 - Standard Deviation window

3.8.3 The need for STA/LTA algorithm

The STA/LTA algorithm continuously keeps track of the changes in recording noise amplitude at the station site and automatically adjusts the sensitivity to the actual EMV noise level. Calculations are repeatedly performed in real-time. The STA/LTA algorithm processes filtered EM signal in two moving time windows - a Short Time Average (STA) window and a Long Time Average (LTA) window. The STA measures the "instant" amplitude of the EM signal and is watching for EM emission. The LTA takes care of average EM noise. First, absolute amplitude of incoming signal is calculated. Next, average amplitudes in both windows are calculated. In the next step a ratio of both values - STA/LTA ratio - is a calculated.

This ratio is continuously compared to a user selected threshold value - STA/LTA trigger threshold level. If the ratio exceeds this threshold, a channel trigger is declared.

After the EM emission gradually terminates, the channel de-triggers. This happens when the STA/LTA ratio falls below another user selectable parameter - STA/LTA de-trigger threshold level. Obviously, the STA/LTA de-trigger threshold level must be lower (or rarely equal) than the STA/LTA trigger threshold level.

3.8.3.1 Duration for Short Term Average window (STA)

Analysis shows that a typical EM VHF event has duration of 1 hour with the shortest being 30 minutes. Noise burst duration varies but most of them persists a couple of minutes. In order to reduce the effect of the noise bursts and enhance the frequencies of the EM events, a window length of 10 minutes was chosen.

3.8.3.2 Duration for Long Term Average window (LTA)

By studying EM VHF recordings, it was observed that the background noise, rather than spikes in several cases, had the form of a slow fluctuation that could last for several hours. Such noise can be attributed to several sources such as man-made activity. In order to reject these kinds of disturbances, the LTA was selected to be 2 hours. The STA/LTA can be seen as a band-pass filter, having the LTA as low-pass and the STA as high-pass.

3.8.3.3 Selection of STA/LTA trigger threshold level

The STA/LTA threshold level will affect the detection of EM VHF events. Too low threshold will likely be susceptible to detecting periods of high levels of noise, and thus produce many false alarms. Conversely, too high a threshold will reduce the effects of noise but it will also fail to detect EM VHF events having low levels. An optimum value for threshold should be sought for each station independently.

3.9 Conclusions

Software and hardware go together. Everybody knows that one cannot exist without the other so a mutual respect is required. Without software, hardware would be lifeless silicon. Without hardware, software cannot exist. Software ultimately controls the Data Acquisition System, but under the hood, it's the hardware that implements the software code.

Since this is a large and complex project to maintain, the need of special software exists. This software should be responsible for real time monitoring, configuration, management, data collection, alarm notification operations, data conversion in a universal format e.g. CSV, and a graphical tool to make the results visible to the eye. The survey verified that most of the requirements were not available in those programs, thus incompatibilities with the proposed DAS and problems with the control of the whole telemetry system could occur. After that

consideration, the decision was made to create a dedicated and fully functional software packet for the system that would meet the requirements set.

This software packet contains:

a) The telemetry software – this is responsible for real-time monitoring, configuration, management, data-collection and alarm notification operations. It continuously updates the binary data files of monitoring DAS devices.

b) The data conversion software – that is used to extract daily measurements in ASCII CSV (Comma Separated Values) format, which is a universal format and promises compatibility with most data analysis software (e.g. Matlab).

c) The data preview software – this is a graphical tool for the data CSV files. It is able to plot the desired signals in full detail, as well as other useful computations like standard deviation (STD) and the STA/LTA ratio.

After a long software/hardware evaluating period, the system has proved its stability and functionality to the above mentioned steps and it is clearly stated that the whole application can be used as a fully functional product.

4 Design and implementation of a VHF EMV telemetric network

4.1 Introduction

This chapter deals with the design and implementation of a prototype EMV telemetric network in VHF band. Initially, the reader will be introduced to the principals of telemetry networks and the most common problems that exist on a typical field station. Considering the advantages and disadvantages of the available telemetry techniques, the reasons of data-logging telemetry selection will become clear.

Figure 4.1 - Map of prototype EMV telemetric network in VHF band

In order to study electromagnetic emissions in VHF band that could possibly occur prior to strong earthquakes, an area with a permanent high level of seismicity had to been selected. So, the next subsection involves with the appropriate geographic region selection, which is very important. The rest of this chapter describes the structure of a prototype EMV field station in VHF band, as well as the central one. Supplementary, for the completion of this chapter it was necessary an overall system evaluation subsection to be included, in order the system to be estimated.

4.2 Telemetry Networks

In order to methodically investigate such EM phenomena, it was necessary to study the design of a complete telemetric network, which will be responsible to capture reliable electromagnetic emissions in VHF band. Therefore, the practical nature of this research dictates that the reader should be introduced to the principles of telemetry networks.

Telemetry is the science that is involved with the transfer of either environmental or other kind of data measurements from remote measurement devices, mainly installed at the countryside, to a central station. Telemetry systems have been developed for a wide number of researches and experiments. Amongst the potential constraints, inaccuracy of measurements and lack of sufficient time-lead in the information delivery are probably the major scientific constraints [Nomicos C. (1995)]. According to the format of the signal used, in the transfer procedure, the available telemetry techniques are categorised into analogue and digital.

Recent progress in information technologies provides a great opportunity to improve the accuracy and functionality of telemetry information and to increase time-lead in the information delivery.

4.2.1 Analogue Telemetry Networks

Analogue telemetry is the simplest one, regarding the electronic design and implementation of both the telemetry devices and the central station. In this type of telemetry, the remote devices are directly connected to the central station and directly transmitting the modulated analogue signal to the central station. The most popular modulation method is FDM (Frequency Division Multiplexing) [Nomicos C. and Giakoumakis G. (1985)]. The central station, in turn, receives and demodulates the signal stream from every telemetry device and either displays the signals directly or converts and stores them for future displaying, processing or analysis [Morris A. (2001)].

All the above characteristics and features of this simple to implement and maintain telemetry technique motivate the researchers to adopt it pretty quickly, in most of their experiments, in order to cover their communication needs. Due to the nature of the transmitted signal, this technique is not reliable considering the susceptibility of analogue signals to any kind of natural noises that in many cases is catastrophically. Furthermore, there must always be an active communication link for real time signal transfer, otherwise unrecoverable data loss will occur.

The above disadvantages were solved by the technological revolution in terms of digital data communication systems that minimize noise effects.

4.2.2 Digital Telemetry Networks

The second generation technique is digital telemetry. In this technique the original analogue signals are converted to their corresponding digital representation, which are afterwards transmitted to the central station. Recent technological advances in the area of digital recording and telemetry make it possible to design and implement remote instrumentation that can receive, convert and record a great variety of analogue physical signals in the appropriate sampling rate and transmit them via wired or wireless communication links [Nomicos C. (1995)]. The major advantage of digital telemetry is that maximum reliability is achieved, since the possibility of signal

distortion from natural noise is evanesced by adopting modern communication, flow control and error correction techniques. Considering the data distribution techniques, digital telemetry can be divided in two major techniques; i) pseudo real-time and ii) data-logging telemetry.

In pseudo real-time digital telemetry, the received signals are being recorded in both the remote instrumentation and the central station almost simultaneously. Hence, the major advantage of this technique is immediate data receipt and pseudo real-time remote monitoring, assuming minimum communication transfer delay.

In data-logging telemetry, the received analogue signals are sampled, digitized and temporarily stored in a local memory of the remote device. Thereafter, the central station, using either temporary or permanent communication links, communicates with and commands each remote device to start sending the temporarily stored data to the central station [Austerlitz H. (2002)]. The major advantages of data-logging telemetry are:

a) The use of connection oriented communication links.
b) The ability for partial data transmission.
c) The ability for data retransmission in case of long-term communication link failure.
d) The ability for stand-alone operation for a long time depending on the available storage medium capability of the remote device.

4.3 Geographic region selection

In order to study electromagnetic emissions in VHF band that could possibly occurred prior to strong earthquake, an area with a permanent high level of seismicity had to been selected. The highest seismic activity in Europe occurs currently in that region of the Western Hellenic subduction zone which includes the Ionian Islands. It is documented by instrumental seismicity and by a historical record over several centuries [Papazachos B. and Papazachou C. (1997)]. Recent earthquake events catalogue show that the Ionian Islands belong to the highest shallow seismicity area in Greece. The Hellenic Arc is the seismically most active region in western Eurasia due to subduction of the oceanic African lithosphere beneath the Eurasian plate [Clément C. et al. (2000), Laigle M. et al. (2002)].

In particular, the island of Kefallonia has a permanent high level of seismicity and has experienced earthquakes of magnitude equal or greater to 6.0 Richter approximately every 20 years [Makropoulos K. and Burton P.W. (1985)]. The occurrence frequency of large earthquakes is at least one with magnitude in the range of 5.5 - 6.0 Richter every 10 years. The macroseismic information from the 20th century earthquakes shows that the shallow foci in the area (average depths around 10 km) indicate its capability for intensities of high degree and elliptical to strongly elliptical shapes of isoseismals, with major axes mainly in the NW-SE direction, parallel to the coastline and the Hellenic trench.

Figure 4.2 - The Hellenic Arc

Name	Location	Installation Date
Ioannina	39.66N – 20.85E	22/05/2004
Kerkyra	39.71N – 19.80E	22/05/2004
Ithomi	37.18N – 21.93E	27/05/2004
Kefallonia	38.18N – 20.59E	10/06/2004

Table 4.1 - Prototype VHF EMV field stations information

These criteria led our team to study this geographic region. So, four (4) prototype electromagnetic variation (EMV) field stations are already installed in Western Greece. Table 4.1 gives the location and the installation date of each prototype EMV field station, while Figure 4.2 illustrates the map of these locations.

4.4 Prototype EMV field station in VHF band

A prototype electromagnetic variation (EMV) field station has been designed, in order to measure time dependent changes of the electromagnetic field at both low and high frequencies. Each field station consists of an improved Data Acquisition System, a number of EMV receivers and an uninterrupted power supply unit (UPS). Figure 4.3 illustrates the installation of such a field station.

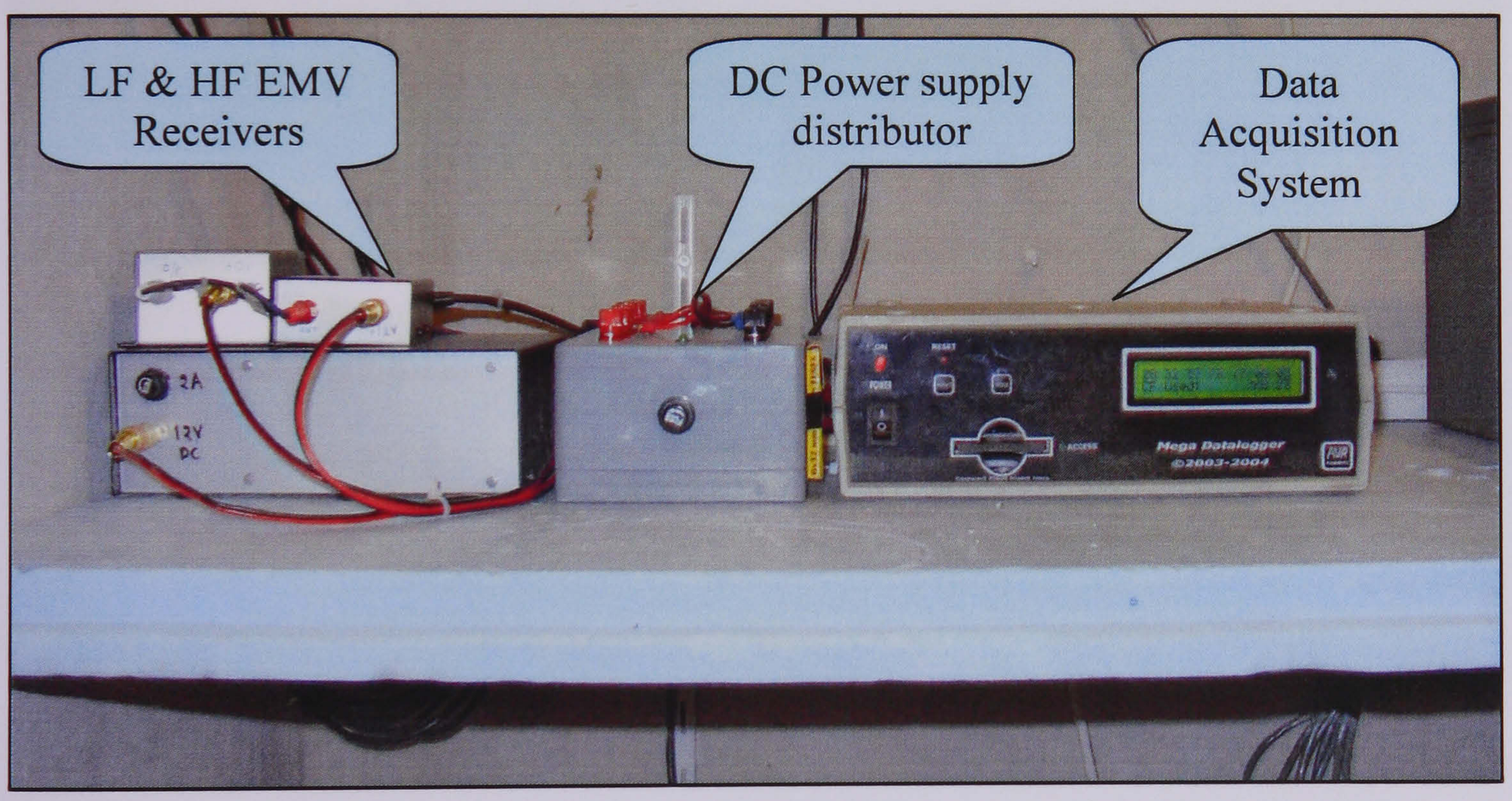

Figure 4.3 - Prototype EMV Field Station (Inside view)

Figure 4.4 shows the outside view of a prototype EMV field station. It is easy to identify the red and black loop antennas. These four (4) loop antennas detect the two components, East-West and North-South, of the electromagnetic field variations at 3KHz (red colour) and 10KHz (black colour), correspondingly. The dipole antennas, detects the HF components in 46MHz (upper - short dipole) and 41MHz (lower – long dipole), correspondingly. The Discone antenna is responsible for the reception of the electromagnetic field at Very High Frequencies (VHF) (70MHz to 470MHz).

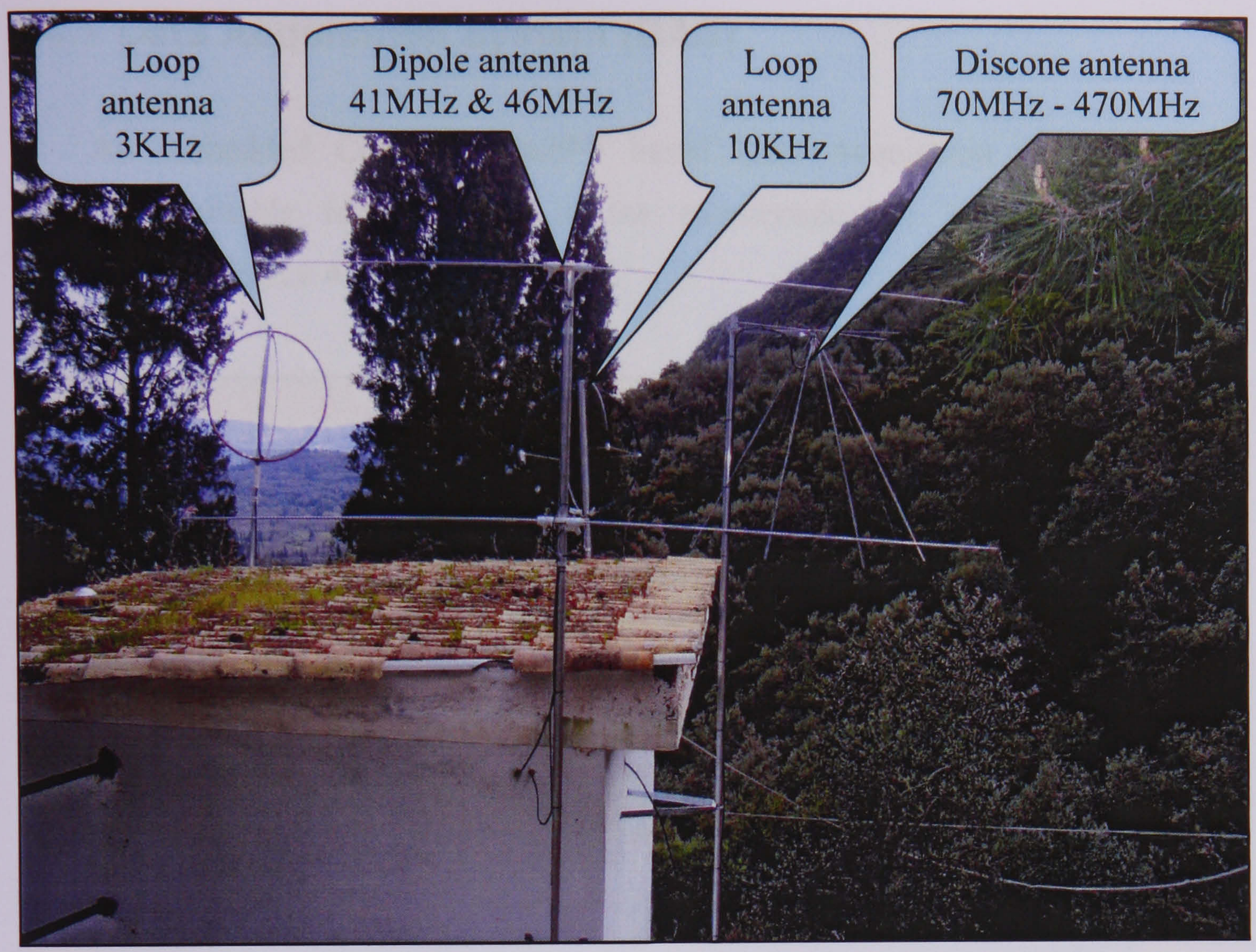

Figure 4.4 - Prototype EMV Field Station (Outside view)

4.4.1 Data Acquisition System (DAS)

An embedded Compact Flash™ based Data Acquisition System (DAS) especially suitable for operating in the countryside has been designed and implemented (Figure 4.5).

Figure 4.5 - Compact Flash™ based Data Acquisition System (DAS)

Chapter 2 describes the hardware development and implementation of the new embedded Compact Flash™ based Data Acquisition System, considering previous research into commercial DAS's. The innovation of this DAS is the Data Storage System (DSS) it incorporates. In the rest of Chapter 2, the custom designed DSS is described in detail. The DSS is an efficient memory-management scheme that increases CF™ lifetime. This memory-management scheme is suitable for large-capacity DAS's.

In this project the Data Acquisition System, is programmed to store 14 channels at a sampling rate of 1Hz. Thus the depth of the buffer with a Compact Flash™ of 128MB is approximately 43 days. By using this technique, temporary data-link failures can be overcome, as well as, Backward Error Correction (BEC) can be achieved.

4.4.2 EMV Receivers

The DAS is able to record up to 14 channels. We can divide the experimental data measurements into three major categories:

1) LF (Low Frequencies),

2) HF (High Frequencies) and

3) VHF (Very High Frequencies).

The first four (4) Data Acquisition System's channels record the variations of the electromagnetic field at Low Frequencies (LF). Four (4) Loop antennas detect the two components, East-West and North-South, of the electromagnetic field variations at 3 KHz and 10 KHz, correspondingly. These EMV signals are received, by equal in number LF receivers.

Next two (2) channels record the variations of the electromagnetic field at High Frequencies (HF). Two (2) vertical $\lambda/2$ electric dipoles detect the strength of the electromagnetic field at 41 MHz and 46 MHz. These EMV signals are received by corresponding HF receivers.

The next six (6) channels record the variations of the electromagnetic field at Very High Frequencies (VHF). The dedicated VHF Tuner in conjunction with a Discone antenna, which is described in section 4.4.3, is responsible for that task. The VHF Tuner has a scanning capability, in order to measure a wide spectrum of frequencies up to UHF band (70MHz to 470MHz). These six (6) frequencies can be dynamically altered, in order to minimize the effects of the sources of cultural noise. These frequencies are 142MHz, 178MHz, 230MHz, 320MHz, 390MHz and 415MHz. The 13th channel records the battery voltage that supplies the system. Finally the 14^{th} channel records the temperature of the station in the countryside.

4.4.3 Discone Antenna

A discone antenna is a version of a biconical antenna where one of the cones is replaced by a disc. It is usually mounted in vertical orientation, with the disc at the top and the cone under it. It may be made of solid metal sheets, which is practical for small indoor high-frequency antennas, such as for WiFi, or of discrete metal elements assembled to a "star" at the top and a cone of beams going down from the star's centre, which makes it less vulnerable to wind. The cone and the disc are separated by an insulator.

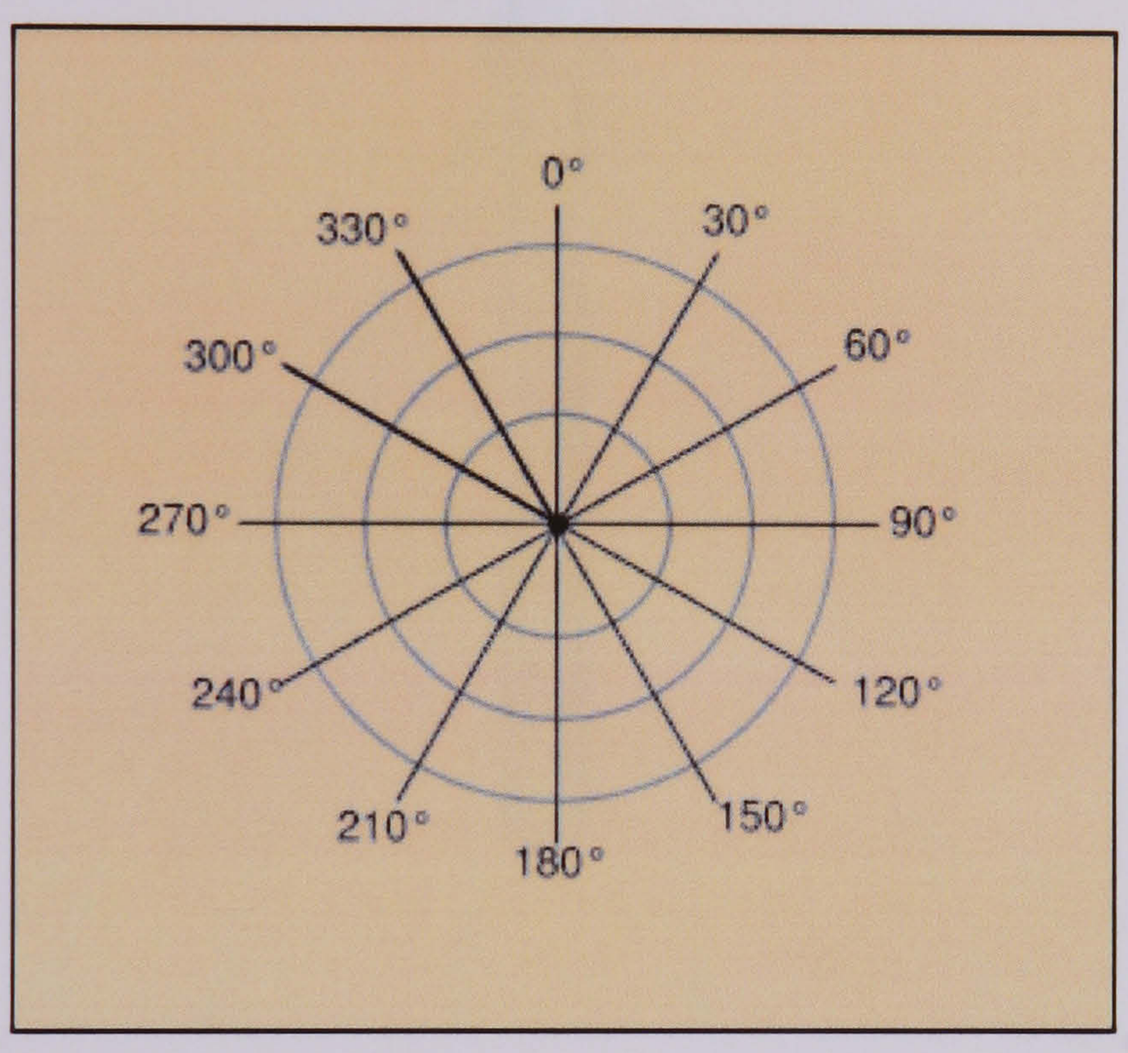

Figure 4.6 - Discone Antenna's Polar Diagram

A discone antenna is omni-directional (Figure 4.6), vertically polarized and wideband, allowing frequency ranges of up to 10:1, and its radiation pattern in the horizontal plane is quite narrow, making its sensitivity highest in the plane parallel to Earth. It is suitable for a wide range of applications, from amateur radio to various commercial and military uses. While it can be used for transmitting, its wideband characteristics make it more likely to transmit undesired spurious frequencies, and it is less efficient than some other designs.

Every discone antenna, as shown in Figure 4.7, has three components: the disc, the cone, and the insulator. Each of them determines the antenna's parameters. The length of the cone elements should be a quarter wavelength of the antenna's minimum operating frequency. The diameter of the top of the cone depends on the diameter of

the feed coaxial cable, and determines the upper frequency limit of the antenna (the smaller diameter, the higher frequency). The disc elements should have an overall length of 0.7 times a quarter wavelength of the antenna's minimum frequency. The insulator keeps the disk and the cone a fixed distance apart. This distance determines part of the antenna's properties. It should be about a quarter of the diameter of the top of the cone, which is usually about 3 mm.

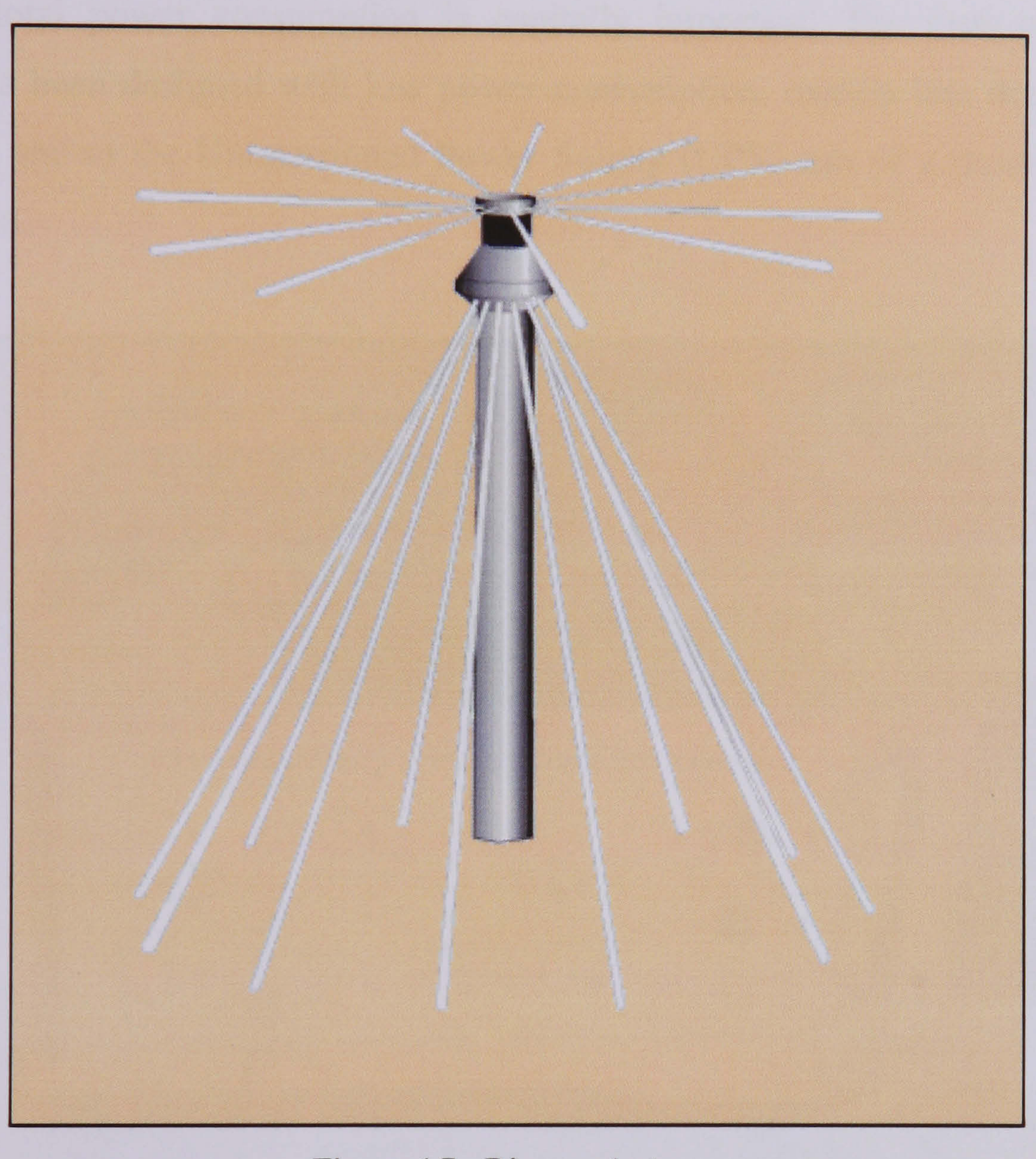

Figure 4.7 - Discone Antenna

The antenna's feed point is in the center of the disc. Under the antenna's minimum frequency, it has a poor match. However, once the frequency rises over this limit, a reasonable match is maintained over its entire band. The number of the elements is usually not critical. Often as few as six are used, though the simulation of the electrically complete disk and cone becomes more accurate by increasing the number of elements. The result is usually a compromise between cost, performance, and resistance to wind.

4.4.4 Uninterrupted Power Supply (UPS)

The electromagnetic variation (EMV) field station should be installed in the countryside, isolated from man made, artificial noise. In such types of regions the use of alternative energy sources, like solar cells, is almost always necessary. Hence, the system's total power consumption is capitally important. The Data Acquisition System has been designed with low power consumption, namely less than 700mW. Figure 4.8 shows the Uninterrupted Power Supply (UPS) unit of a prototype EMV field station.

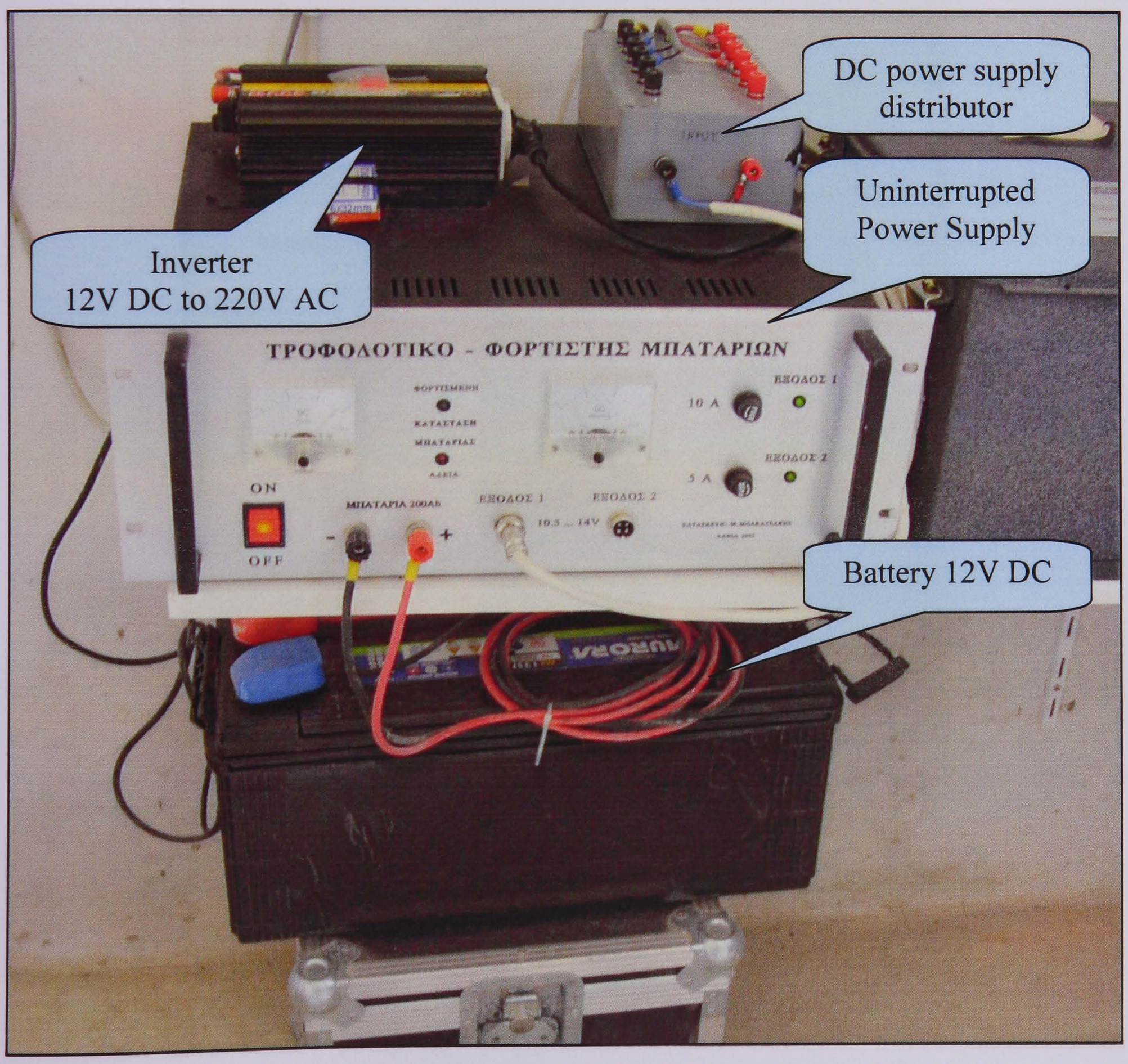

Figure 4.8 - Prototype EMV Field Station - UPS (Inside view)

4.5 Central station

The central station is located at the Institute of Geodynamics of the National Observatory of Athens [NOAIG (2007)] (Figure 4.9). Table 4.2 displays some information about the location and the installation date of the central station. This telemetric network system was launched on 06/2004 and is operational up to now (06/2006).

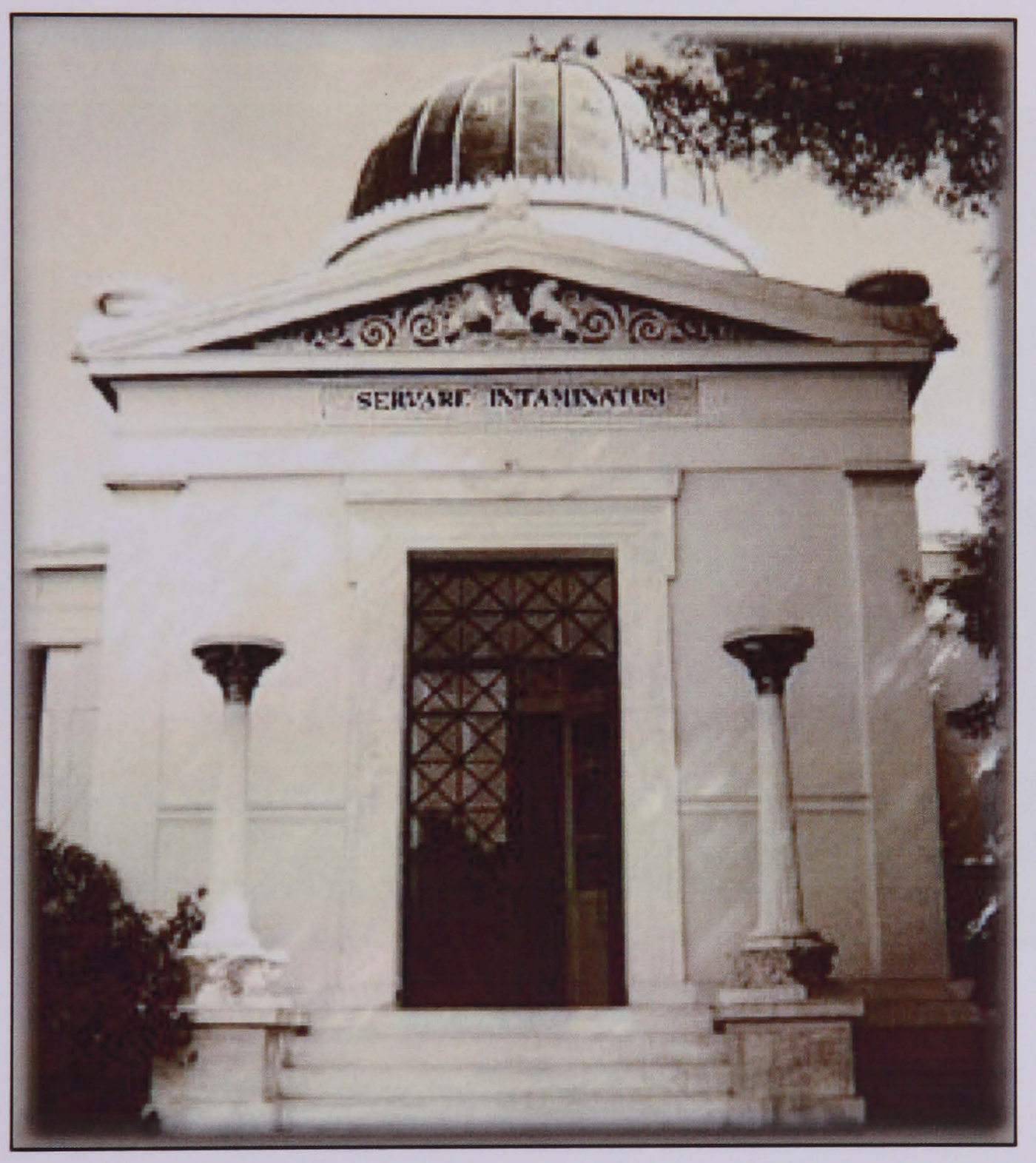

Figure 4.9 - National Observatory of Athens (NOA)

Name	Location	Installation Date
NOAIG	37.97N – 23.72E	22/05/2004

Table 4.2 - Prototype VHF EMV central station information

The central station comprises of (a) an EMV Data Collector Server, (b) a Serial Device Server and (c) an Uninterrupted Power Supply unit. The following sections describe these devices in detail.

4.5.1 EMV Data Collector Server

In the central station a Windows XP 32-bit based server is responsible for the EMV data collection from each field station. Under this situation, dedicated software has been developed (see section 3.5). This software adopts a polling technique for sequential data collection. It is responsible for incoming data validation using backward error correction (BEC) and for monitoring the health status of each field station. Figure 4.10 illustrates the EMV Data Collector Server.

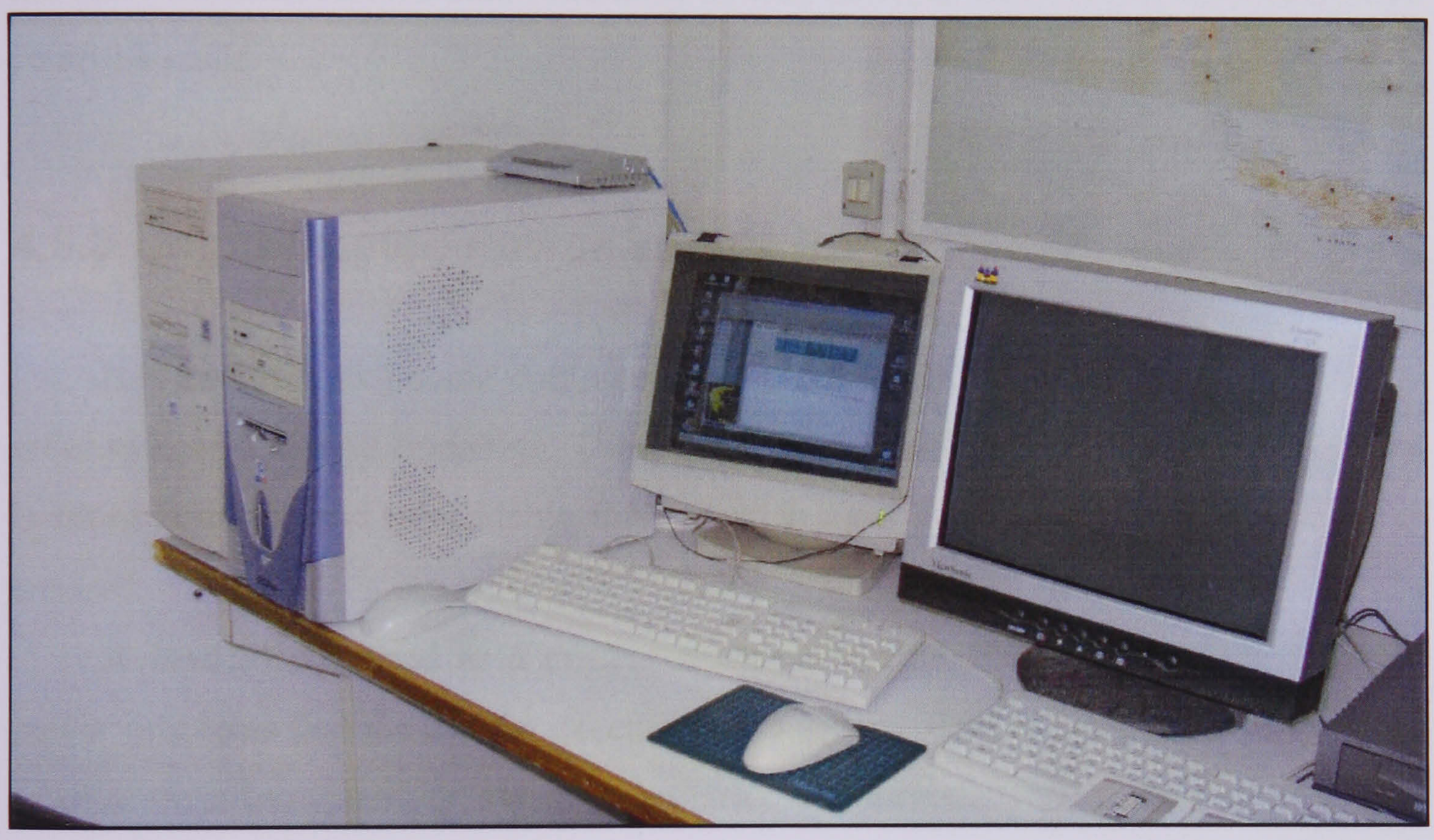

Figure 4.10 - EMV Data Collector Server

4.5.2 Serial Device Server

The central station incorporates a Serial Device Server (SDS) manufactured by MOXA Technologies Inc. (Figure 4.11). NPort 5600 series Serial Device Server provides a transparent way to establish an Ethernet connection and ensures future network expandability. In particular, the model NPort 5610-16 can transparently exchange data bi-directionally between the serial and Ethernet interfaces. This device provides sixteen (16) serial ports and a single 10/100Mbit Ethernet interface.

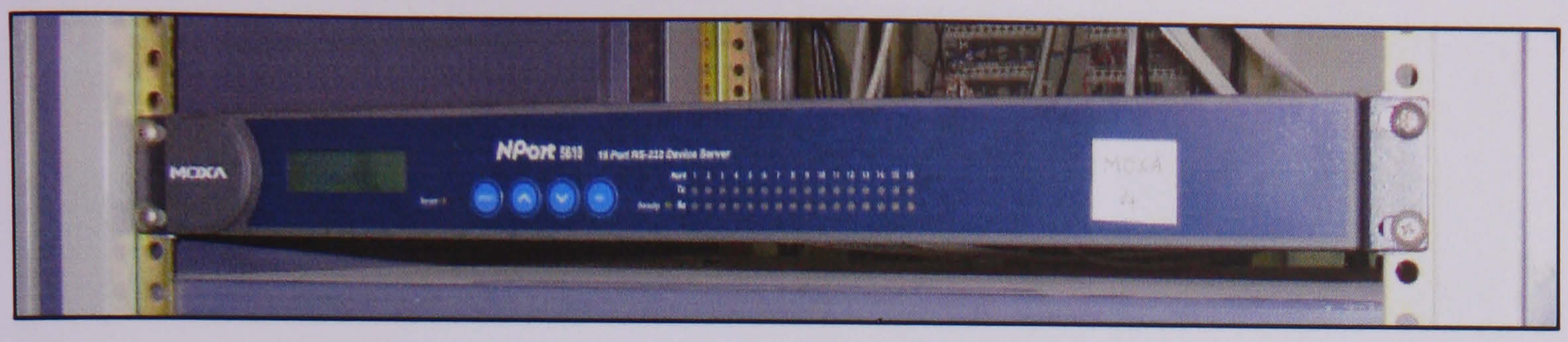

Figure 4.11 - Serial Device Server (NPort 5610-16)

After installing the Real COM/TTY driver that comes with this device, the serial ports on NPort 5610-16 are recognized as Real COM ports by the Windows Operating System, or Real TTY ports by Linux environments. NPort provides both the basic transmit/receive data functions, as well as RTS, CTS, DTR, DSR and DCD control signals.

4.5.3 Uninterrupted Power Supply (UPS)

It is essential that some computers and electrical devices run uninterruptedly in order to keep a system operating. These "electrical loads" require a power source that is more constant and dependable than most to certify that continuous operation is ensured.

A load that is used in a critical situation can be affected by many different power problems that disturb the execution of a service. The biggest problem attached to all of these interferences is their irregularity and unpredictability. As a result of this randomness, any action taken to protect vital equipment has to be in operation continuously when the load is being used. There are many types of main power failure and many problems to consider, including spikes, electrical noise, power surges, sags, harmonics, blackouts, brownouts and much more. This can influence the operation of most electrical equipment and commercial computer systems.

In this project, it is essential for the EMV Data Collector service to run continuously on the central server. Under this situation, the need of an Uninterrupted Power Supply (UPS) was obvious. Figure 4.12 illustrates this device.

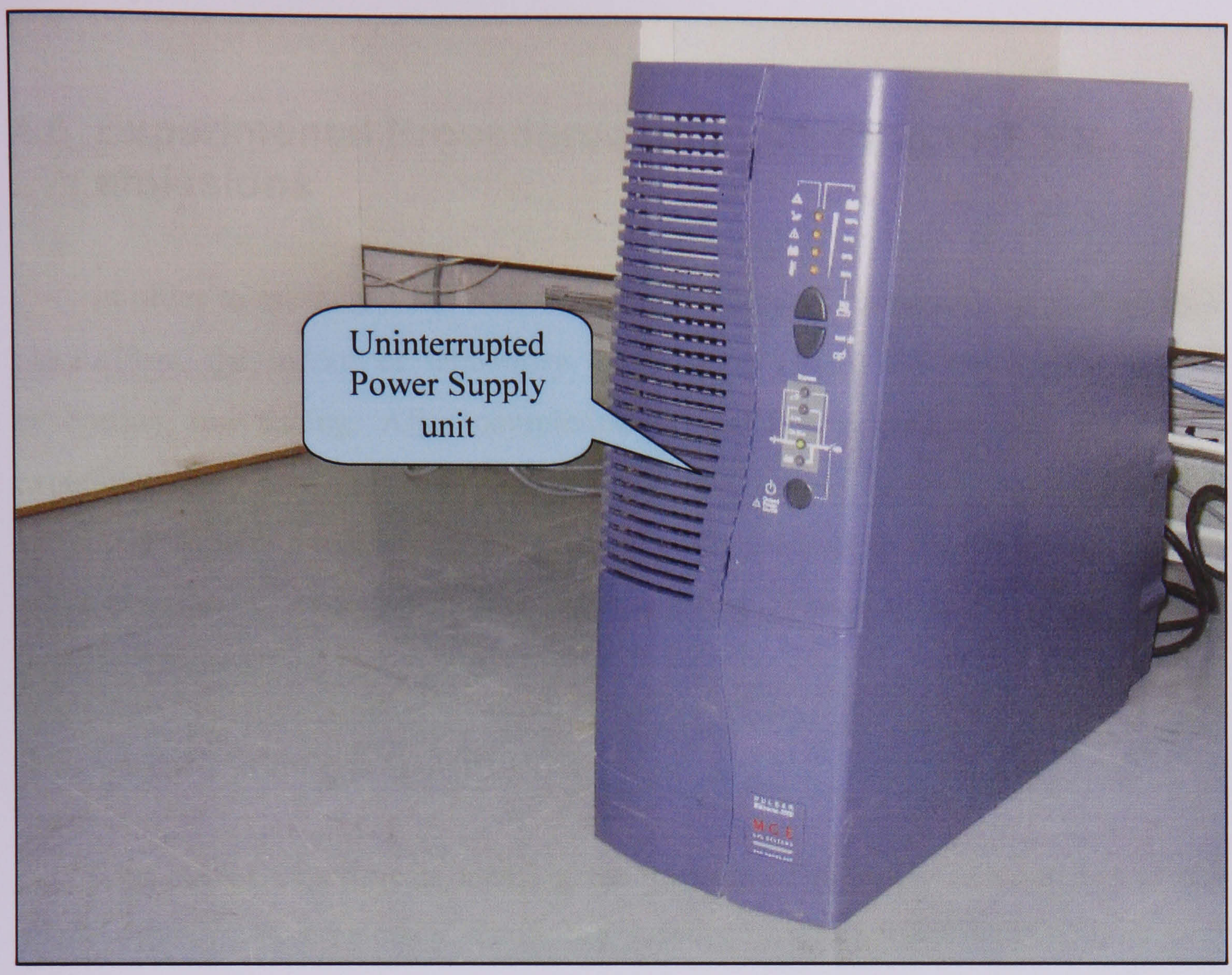

Figure 4.12 - Central station - UPS

4.6 Experimental Procedures for measuring VHF EM emissions

In order to measure VHF electromagnetic emissions, a two-fold procedure took place. First, the indoor or laboratory experiments ensure the appropriate devices calibration and testing. After completion of the first procedure, the main field experiments are ready to take place. Finally, the outdoor or field experiments play extremely important role in capturing trustworthily measurements. These experiments are responsible for avoiding conflicts from any type of radio emissions of local video or audio broadcasting.

4.6.1 Laboratory Experiments

The indoor experiments attach great importance to stable functionality of the whole system. As previously mentioned (section 2.5.2.2), dedicated software and hardware designed and implemented in order to accurately, test and calibrate the constructed VHF receivers. The VHF testing software is able to plot the sensitivity curves of the receivers, as well as the frequency response of them. In this stage of testing it was necessary the use of the RF programmable synthesizer (HAMEG HM-8134-2).

Sensitivity curves for the receiver after calibration are shown in Figure 2.15. Each colour represents the sensitivity of the VHF tuner in different frequencies. The VHF receiver has good linearity over most of the range and there is little inter-receiver variability, eliminating the need for individual calibration once gain levels were set up. Performance at levels below -110dBm is likely dominated by noise rather than departure from linearity. Sensitivity is about 23.2mV/dBm and is linear up to -50dBm. Maximum input is -44dBm before saturation, but linearity is not maintained between -50dBm and -44dBm. The tuner's Intermediate Frequency (IF) is 37.3MHz, while the bandwidth of the receiver is about 180 KHz. This is wide enough to detect EM emissions and narrow enough to reduce the possibility of co-channel interference.

After completing the indoor testing and calibration procedure, the main outdoor experimental procedure is ready to start.

4.6.2 Field Experiments

Outdoor experiments are essential in order to capture reliable electromagnetic emissions in VHF band and extinguish any kind of artificial noise. An in depth spectrum scanning took place in order to avoid conflicts from any type of radio emissions of local video or audio broadcasting.

Frequencies from 70MHz to 130MHz have not been included in order to avoid conflicts from radio emissions of local radio stations and amateurs. The appropriate region selection is very important in order to achieve isolation from culture noise. In other words, field stations should be installed in the countryside isolated from man-made, artificial noise. In order to exclude these frequencies from being monitored, a commercial RF receiver with scanning capability was used for creating a site emission survey. The result of this task was the generation of a list with frequencies that will be excluded from monitoring. The selected monitoring frequencies were 142MHz, 178MHz, 230MHz, 320MHz, 390MHz and 415MHz.

Concluding, the outdoor or field experiments play extremely important role in capturing reliable measurements.

4.7 Overall System Evaluation

4.7.1 DAS Specifications

The dedicated design of this DAS offers advantages in aspects of sensor measurement, direct communications, external devices control and data storage in removable, non-volatile storage medium using circular buffer technique in order to increase the life of the Compact Flash™ card.

This experimental acquisition device can simultaneously measure up to sixteen (16) analogue signals, up to eight (8) temperatures and finally one (1) relative humidity value. Furthermore, for covering the needs of an experiment, the DAS can acquire up to six (6) different VHF frequencies through the external VHF signal measuring device (See section 2.5.2). Regarding the communication interface, the

DAS contains a RS-232 interface for establishing communication link in data rates from 300 bps to 115.200 Kbps.

A battery-backed Real-Time Clock (RTC) assures accurate timekeeping. The whole device is power failure tolerant, containing a 1.2Ah backup battery that ensures uninterrupted operation for up to 12 hours after a possible complete primary power loss.

Input Device	Channel	Caption	Unit	Multiplier	Range
ADC 10bit	1	-	-	-	-
ADC 10bit	2	-	-	-	-
ADC 10bit	3	-	-	-	-
ADC 10bit	4	-	-	-	-
ADC 10bit	5	-	-	-	-
ADC 10bit	6	-	-	-	-
ADC 10bit	7	-	-	-	-
ADC 10bit	8	-	-	-	-
ADC 12bit	1	3KHz EW	mV	1,221	0..5000
ADC 12bit	2	3KHz NS	mV	1,221	0..5000
ADC 12bit	3	10KHz EW	mV	1,221	0..5000
ADC 12bit	4	10KHz NS	mV	1,221	0..5000
ADC 12bit	5	41MHz	mV	1,221	0..5000
ADC 12bit	6	46MHz	mV	1,221	0..5000
ADC 12bit	7	Battery	mV	4,884	0..20000
ADC 12bit	8	Tuner	mV	1,221	0..5000
VHF Tuner	1	142MHz	mV	1,221	0..5000
VHF Tuner	2	178MHz	mV	1,221	0..5000
VHF Tuner	3	230MHz	mV	1,221	0..5000
VHF Tuner	4	320MHz	mV	1,221	0..5000
VHF Tuner	5	390MHz	mV	1,221	0..5000
VHF Tuner	6	415MHz	mV	1,221	0..5000
VHF Tuner	7	-	-	-	-
VHF Tuner	8	-	-	-	-
Thermometer	1	Indoor Temp	°C	1,000	-55..+125
Thermometer	2	Outdoor Temp	°C	1,000	-55..+125
Thermometer	3	-	-	-	-
Thermometer	4	-	-	-	-
Thermometer	5	-	-	-	-
Thermometer	6	-	-	-	-
Thermometer	7	-	-	-	-
Thermometer	8	-	-	-	-
Relative Humidity	1	-	-	-	-

Table 4.3 - Configuration of Data Acquisition System

The DAS provides a comprehensive set of processing and control functions through a sophisticated and well designed operating system that simultaneously supports real-time measurement and communication operations. Moreover, DAS is

fully customizable through a dedicated MS-Windows compatible GUI application that will be used for configuring or administrating the device later on.

As mentioned before, the DAS must meet the requirements of the existing telemetry system, as well as provides some new operations and measurements. All measurements that must be performed are outlined in the Table 4.3.

Where "Unit" is the measuring unit of the applied signal, "Multiplier" is the coefficient that the stored measurement should be multiplied with and "Range" is the input range of the current channel.

The full detailed DAS specifications are described in APPENDIX B' (Specifications - Schematics - PCBs)

4.7.2 DAS Configuration Procedure

Configuration of the DAS is achieved through entry of the information contained in the Table 4.3, by using the accompanied programmer software. The programming operation requires an active communication link to be established through a standard RS-232 port and the accompanied programming software to be executed on a PC-based machine running any Windows 32-bit Operating System (OS). The communication link must be negotiated and the programming session must be established within 4 minutes. If the programming session fail to reconfigure the DAS and the old but valid configuration exists, the DAS will reboot in order to run acquisition services. Otherwise the DAS is waiting the programming session to be established.

After connecting the DAS to the host PC-based system using an RS-232 cable and the DAS is powered-up, the programmer application in the host PC-based station is executed and the main form of the program appears as shown in Figure 4.13.

In order to establish a communication link with the DAS, the appropriate serial port number and data link rate have to be set, and then the user should press the "Connect" button. After a couple of seconds the application gathers information from the attached DAS. The software displays information including time and date settings, as well as the existing configuration of the DAS.

The next step of this procedure is the configuration of the DAS. In this step, the channels, the date and time settings, as well as the preferred sampling period should be configured.

By using the information of the Table 4.3, each corresponding channel was enabled and the supplemental parameters of the measurement signal were entered. After that, the RTC of the DAS was synchronized and the sampling period was set to one (1) second. If the "Upload" button of the programmer is pressed, the configuration parameters will be transferred from the host PC-based system to the DAS. Finishing the configuration procedure, the DAS reboots and after 4 minutes of waiting for potential firmware upgrade, it is fully operational.

Figure 4.13 - DAS Configuration Software

4.7.3 DAS Evaluation Procedure

In order to evaluate the previous programming procedure and ensure the right operation of the DAS a series of tests should be performed. These tests include acquisition and data transfer evaluation procedures. The first test ensures that all channels are acquired and stored without problems, while the second one ensures that the stored data are correctly transferred to the host PC-based station.

4.7.3.1 Acquisition Laboratory Experiments

For testing the acquiring functions, the usage of the following devices was necessary:

(1) RF programmable synthesizer (HAMEG HM-8134-2),
(2) An adjustable hot-air rework station and
(3) A USB Compact Flash™ reader.

After applying analogue signals to the inputs, as well as to the attached thermometers, the measurements were displayed on the external LCD display of the DAS. After a ten minute operation of the device, the attached flash card was removed and inserted in the USB flash reader. Using a commercial Hex Editor software, as shown in Figure 4.14, the flash memory was edited in hex mode and the integrity, as well as the correctness of the stored data were checked by comparing the stored data with the input signals that were previously applied.

After successfully completing the first test regarding the correctness of the stored data the second test took place.

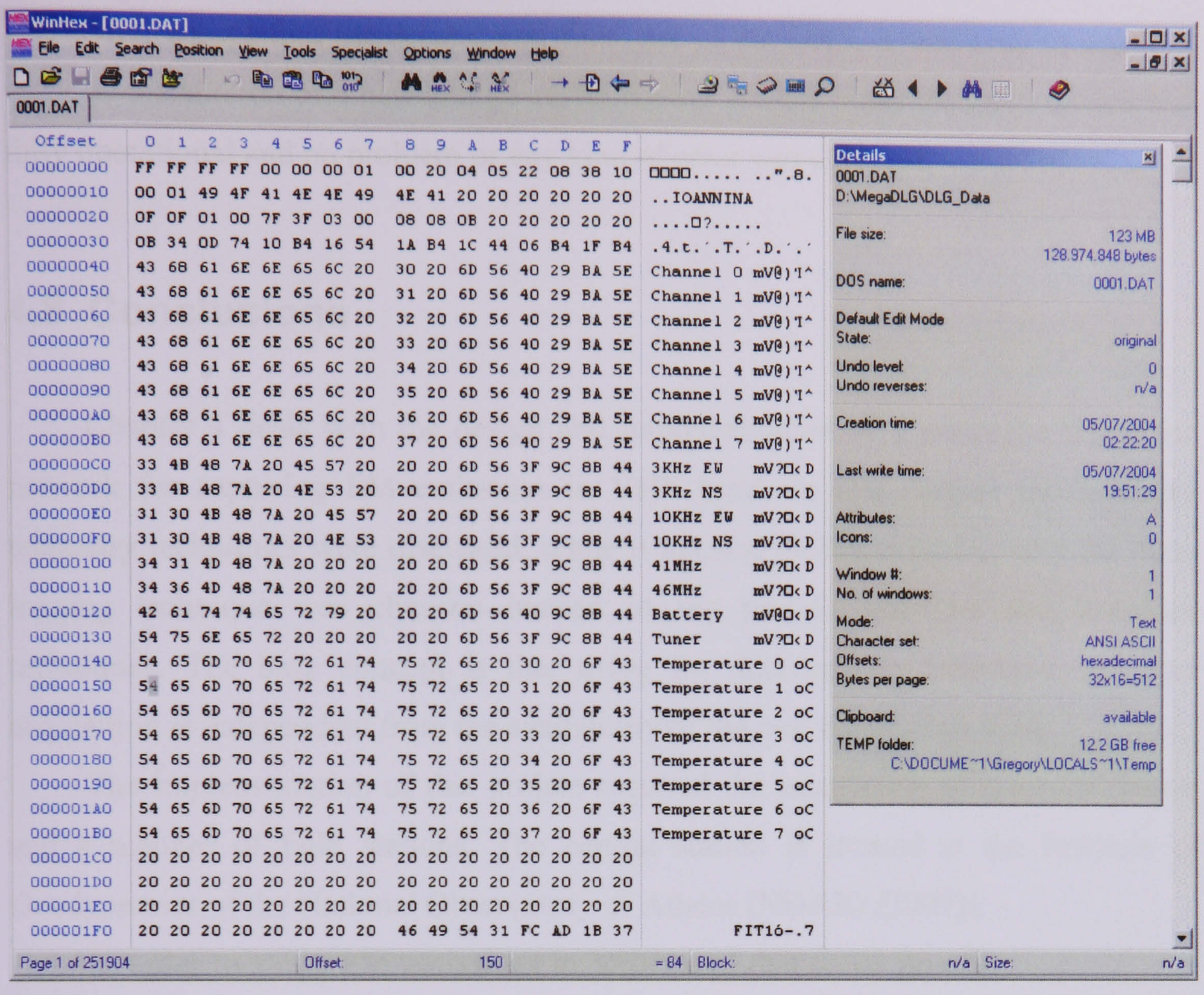

Figure 4.14 - Hex Editor

4.7.3.2 Communication Laboratory Experiments

The final and most important test deals with the integrity of the transferred data. In this test the accompanied application called "MEGADLG" was used, in "Collector" mode. Section 3.5 describes in full detail the operation of this software.

Collector software is running unremittingly on the central station and is responsible for the creation and the continuous update of a binary file, which is the exact copy (image) of the CF™ removable medium of the DAS. After a ten minute operation of the DAS device, the "Collector" software was executed and a new file (0001.dat) was created in the predefined directory of the host PC-based system. After completing successfully the first step, the second one took place. The attached CF™ card was removed, inserted in the USB CF™ reader and the downloaded binary file was compared to the data contained in the CF™ memory using the previously mentioned commercial Hex Editor.

After completing the second and final test of the DAS, it was time to continue with the installation of a new and powerful central station, since the DAS device was fully operational and no problem or any kind of error was detected.

4.8 Conclusions

Chapter 4 deals with the design and implementation of a prototype telemetric network for capturing EM emissions in VHF band. In this chapter the available telemetry techniques were discussed, while it became clear the reason why the data-logging technique was choosen instead of the pseudo real-time and analogue techniques. The base concept is that using the data-logging technique, the data acquisition is independent from the availability of the communication links.

The implementation of this project required the installation of a central server and a number of field stations. The central station is located at the Institute of Geodynamics of the National Observatory of Athens [NOAIG (2007)].

In order to study EM emissions in VHF band that could possibly occur due to strong earthquakes, an area with a permanent high level of seismicity had to been selected. The field stations have to be installed to cover such an area. In this case the highest seismic activity in Europe occurs currently in the region of the Western Hellenic subduction zone which includes the Ionian Islands. This criterion led our team to study this geographic region and four (4) prototype field stations were installed on the Western Greece.

Indoor and outdoor experimental tests were performed in order to ensure reliable capturing of electromagnetic emissions in VHF band. For the completion of this project it was necessary an overall system evaluation procedure to be included, in order the system to be estimated. After the final tests were completed, overall network was fully operational without detecting any problems or any kind of errors.

5 Evaluation of EM emissions from field stations installed parallel to Hellenic Arc

5.1 Introduction

Some researchers in the field of seismology are trying to correlate EM recordings, also called seismo-electromagnetic emissions, with seismic events. The previously described DAS covers the need of reliable, long time and continuous time-series recordings of such phenomena, able to cover a wide range of frequencies.

The design and implementation of a prototype EMV telemetric network in VHF band have already been covered in chapter 4. This telemetric network was launched on 06/2004 and is operating up to now (06/2006).

The current chapter focuses on the data acquired from DAS during this period, the attempt to correlate it with seismic events and the results derived from this attempt in order to contribute in the field of seismology.

It is noted that the EM data captured could originate from other sources of EM emission like solar activity.

5.2 Literature Review on EM emissions

The purpose of this literature review is to present the background for the application of the DAS to seismic prediction. It focuses on previous observations of electromagnetic phenomena, which have been associated with earthquake activity.

5.2.1 Observations of EM phenomena

Seismo-electromagnetic phenomena in the lithosphere, atmosphere and ionosphere have been observed during the last three decades [e.g. Gokhberg M. B. et al. (1982a), (1982b), Varotsos and Alexopoulos (1984a), (1984b), Hayakawa and

Fujinawa (1994), Hayakawa and Molchanov (2000), Tzanis et al. (2000), Kopytenko et al. (2001)]. Some researchers in the field believe that seismo-electromagnetic phenomena are accompanied by crack generation in the Earth's crust [Molchanov and Hayakawa (1995), (1998a), (1998b)]. Some published works are going to be presented.

Correlations of geo-magnetic disturbances before an earthquake event have been conceived in Japan (1855), when a strong earthquake affected Edo (Tokyo). At the earthquake that affected Nobi in 1891, intensive geomagnetic disturbances were detected by Rikitake et al. (1997). Warwick et al. (1982) re-examined the observations of American radio-telescopes and observed a significant EM disturbance at 18MHz six days before the earthquake of May 22nd 1960 in Chile with magnitude 8.1 Richter. These EM emissions were observed from six different stations in the Northern Hemisphere. In the light of these data and the statistical correlation, the assumption was made that these phenomena were related to the earthquake event. The work also showed that EM emission could propagate long distances when trapped in the natural waveguide of the Earth-ionosphere.

The time of occurrence of a precursor has been seen to vary widely. There are not systematic reported studies of emissions or theories to explain it sufficiently. Bernardi A. et al. (1991) in the same work reported that emissions are observed between three hours to as long as one month before seismic events. Maki and Ogawa (1983) reported a reduction in such components, as a precursor to seismic events when the epicentre was located on land, but report no change when the epicentre was at sea. Hayakawa and Sato (1994) and Gokhberg et al. (1995) summarized the data of EM emissions before earthquakes and concluded that:

a) EM emissions are a pre-seismic phenomenon,
b) The mechanisms of genesis and propagation of pre-seismic EM emissions are not clearly understood,
c) Precursors do not give a reliable estimate of place, size and time of an earthquake.

It is probable that EM emissions have been observed over a wide range of frequencies and thus several studies have been conducted.

5.2.1.1 EM emissions in ULF/ELF/VLF/LF band

Gokhberg, et al. (1982a), (1982b) were the first to publish recordings of EM emissions at 81KHz possibly related to seismic activity that had been detected by a receiver (narrow bandwidth loop antenna), installed in a station in Japan (Sugadaira, 36°31'N, 138°19'E). The disturbance was a smooth increase of intensity, and was observed one hour before the seismic event. This growth was interrupted at the moment of the earthquake with a quick fall at the quiescent level. They also claim the existence of a 1.63MHz precursor detected 30 minutes prior to the arrival of the earthquake event.

Litho-ionospheric coupling has been seen recently as a possible pre-seismic EM disturbance. EM emissions in Very Low Frequencies (VLF) band (from 500 up to 3600Hz) have been studied along with the behaviour of ionosphere. Parrot and Lefeuvre (1985), observed such abnormalities before the earthquake swarms of the Kerguelen Islands from 24 to 25 of April 1980. It is noted that they associated the recordings of pre-seismic disturbances with a concurrent disturbance of the ionosphere. EM emissions recordings analysis, in the same spectrum region, by Ralchovsky and Komarov (1988), showed similar results.

Adams (1990) mentions the detection of EM emission in the region of 1 KHz possibly related to Loma Prieta earthquake (October 17th, 1989). In contrast Bernardi A. et al. (1991) did not detect any abnormalities at Extremely Low Frequencies (ELF) or Very Low Frequencies (VLF). Instead of that they reported emissions at Ultra Low Frequencies (ULF) band (0.01-0.5Hz).

Electromagnetic emission in the VLF and LF band, associated to shallow earthquakes, has been credited to small scale cracks opened in the focal zone. These emissions have also been compared to EM emissions due to lightning. Such measurements have been performed by Oike and Yamada et al. (1994) by using the AGC of radio receivers as sensor for EM emission reception. They studied the band of frequencies from 100Hz to 15 KHz and found that strong earthquakes had intense EM emissions.

5.2.1.2 EM emissions in HF/VHF band

More recently, research has turned to even higher frequencies. This includes the HF band (3-60MHz) where EM emission was recorded as a precursor to earthquake events [Nomicos and Vallianatos (1997), (1998), Vallianatos and Nomicos (1998), Ruzhin et al. (1998), Eftaxias et al. (2000), (2001), (2002), (2003), Kapiris et al. (2002)].

For example, Nomicos and Vallianatos (1997), while studying shallow and intermediate earthquakes that took place in the south Aegean area, demonstrated a strong correlation between electric field variations (41MHz and 54MHz) and earthquake events. Results were also consistent with previous observations suggesting that the delay between the electric signal and the ensuing earthquake event varied between 7 hours and 11 days.

Eftaxias et al. (2002) claimed that HF components have greater lead times than LF components. They also present an example of a single earthquake event for which, regardless of the magnitude, no HF emission was recorded.

Another study of EM emissions at 41MHz and 53MHz, were associated with shallow and intermediate depth earthquakes located in the vicinity of Crete Island (South Aegean - Greece) with magnitude greater than 5 Richter [Nomicos and Vallianatos (1998)]. For one particular earthquake event with Ms=6 Richter, focal depth of 70km and epicentre at Crete island region, Greece (35.90 ^{o} N, 22.50 ^{o} E), they reported that at high frequencies, the EM emissions started two days prior to the event and lasted almost 12 hours, with slight variations that continued during the following day. In a second earthquake event with Ms=6 Richter, focal depth of 66km and epicentre at Crete island region, Greece (35.48^{o} N, 24.70^{o} E), the HF electromagnetic emission was detected one day before the main shock. The field stations were located near the hypocentre of both events.

Since Crete is a highly seismogenic region, several studies have taken place in this area. HF and LF EM emissions have been studied in parallel and it was concluded that they appear to follow the time pattern LF variations, HF variations, earthquake [Nomicos et al. (1997)]. In a further study for measuring telluric and EM emissions (LF and HF), along Crete Island, EM emissions were observed on August 15th of 1993

at several field stations although a field station close to the epicentre did not record any HF variation.

Eftaxias et al. (2000) detected electromagnetic earthquake precursory signals in HF band for Kozani - Grevena earthquake (Ms=6.7 Richter, 1995). The frequency band of the detected EM emissions was considered to be quite wide, since these signals were detected in the frequency range from DC up to HF.

Some studies have attempted to localize the source of the EM. Ruzhin et al. (1998) using a series of observation stations, measuring EM emissions at 40MHz and 50MHz, concluded the source to be in the atmosphere, with the position not dependant on time of day. The result was obtained for earthquakes with epicentre beneath the sea. In these cases the epicentre was over the radio-horizon and signals were found to propagate in excess of 350km with source being between 0.1-10km above the surface.

Telluric and VHF EM emissions have different generation mechanisms; they also have different initiation times before earthquakes. The above makes their study in parallel more complexes. Vallianatos and Nomicos (1998), studied the appearance of telluric and EM emissions in nineteen earthquake events with Ms≥ 5.0 Richter which occurred in the vicinity of Crete. Radio-emission was recorded in several cases at 41MHz and 53MHz. It was concluded that seismogenic radio-emission appeared several days prior to strong or moderate, shallow or intermediate depth earthquakes.

In the case of a specific shallow earthquake (Kozani – Grevena), observable surface fault traces of 8-12 km in length were observed [Meyer et al. (1998)], consequently it was expected that the MHz signal was released from the hypocenter area without significant degradation of its spectral characteristics. Kapiris et al. (2002), while investigating this earthquake event, managed to recorded EM anomalies at Zakynthos field station at 41MHz and 54MHz respectively, with increasing EM emission rate (Figure 2a of their work) a few tens of hours prior to the earthquake event. These emissions ceased approximately one hour before the earthquake occurrence. They draw the attention to the almost simultaneous cessation of these EM anomalies at MHz frequency bands although they had very different onset times. After analysing the signals using wavelet transform they concluded that the wavelet spectra of the anomalies at 41MHz and 54MHz were morphologically very similar during their whole recording time [Eftaxias et al. (2001)]. The anomalies ceased

almost one hour before the earthquake, i.e. very close to a possible critical point. The results of this analysis led to the suggestion that the recorded EM is probably emitted from the focal area during micro-fracturing process [Eftaxias et al. (2003)]. In summary, they found that the spectrum of the precursory VHF EM, during the last few tens of hours before the Kozani-Grevena earthquake, exhibited time intervals of the power law $S(f) = a \cdot f^{-\beta}$ with the following unique (in contrast to the background noise) characteristics: Stable spectral exponent β, close to 1.5. The number of the time intervals meeting the above scaling progressively increases approaching the moment of the earthquake; at the tail of the pre-seismic time-series the spectral parameters exhibited continuously the values $\beta = 1.5 \pm 0.2$. Moreover, the detected EM emission appeared as a systematic, nearly exponentially, increasing amplification α, accelerating electromagnetic energy release, during the last few tens of hours before the earthquake. Finally, the detected sequence of electromagnetic signals yielded a frequency shift from MHz to KHz at the end of the detected sequence of EM anomalies. All these findings were used to support their hypothesis that the evolution of the Earth's crust toward the critical point may take place not only in the ULF electromagnetic sense, but also in the VHF electromagnetic sense.

The absence of VHF precursors in several cases of earthquake events has been explained in several ways. It is possible for signals to be attenuated in the crust, if the source point is located at the hypocenter, thus, in the case that the crust ruptures up to the top, VHF precursors are allowed to exit and in the case that the hypocenter area is not connected with any way to the top of the crust, the VHF signals are attenuated in such a way that they are not detectable. A representative case of VHF precursor existence and absence was studied by Eftaxias et al. (2002), who focused on two earthquake events. According to their work, at the Kozani-Grevena area (Ms=6.7 Richter, 1995), electromagnetic field anomalies were detected at the magnetic antennas at both 3 and 10 KHz and at the electric antennas at both 41 and 54MHz located at Zakynthos field station. In a similar seismic event in the Athens area (Ms=5.9 Richter, 1999) no EM anomalies were detected in the VHF band. This difference may be explained from the difference in the nature of earthquakes based on information obtained by radar interferometry (ERS-2 satellite). The absence of VHF signals, noted by Kontoes et al. (2000), may be due to "the upper part of the crust did not rupture during the earthquake", the high frequency component of EM emissions

emanating from the source region being strongly absorbed by the crust. Finally, according to Meyer et al. (1998) in the Kozani-Grevena and Egion-Eratini earthquakes, surface ruptures were observed which permitted the recording of VHF signals [Eftaxias et al. (2000)].

5.2.2 Solar flares and EM emissions

Whilst a number of correlations between EM emissions and seismic events have been observed; an alternative source of EM radiation occurs naturally is solar flares which are able to been detected by our DAS network.

A solar flare is an explosion on the Sun surface that happens when energy stored in certain fields (usually above sunspots) is suddenly released. Flares produce a burst of radiation across the electromagnetic spectrum, from radio waves to x-rays and gamma-rays.

A flare is defined as a sudden, rapid and intense variation in brightness. A solar flare occurs when magnetic energy that has built up in the solar atmosphere is suddenly released. Radiation is emitted across virtually the entire electromagnetic spectrum, from radio waves at the long wavelength end, through optical emission to x-rays and gamma rays at the short wavelength end. The amount of energy released is the equivalent of millions of 100-megaton hydrogen bombs exploding at the same time! The first solar flare recorded in astronomical literature was on September 1, 1859. Two researchers, Richard C. Carrington and Richard Hodgson, were independently observing sunspots at the time, when they viewed a large flare in white light.

There are typically three stages to a solar flare. First is the precursor stage, where the release of magnetic energy is triggered. Soft x-ray emission is detected in this stage. In the second or impulsive stage, protons and electrons are accelerated to energies exceeding 1 MeV. During the impulsive stage, radio waves, hard x-rays, and gamma rays are emitted. The gradual build up and decay of soft x-rays can be detected in the third, decay stage. The duration of these stages can be as short as a few seconds or as long as an hour.

Solar flares extend out to the layer of the Sun called the corona. The corona is the outermost atmosphere of the Sun, consisting of highly rarefied gas. This gas normally has a temperature of a few million degrees Kelvin. Inside a flare, the

temperature typically reaches 10 or 20 million degrees Kelvin, and can be as high as 100 million degrees Kelvin. The corona is visible in soft x-rays, as shown in Figure 5.1, an image from Yohkoh Soft X-Ray Telescope.

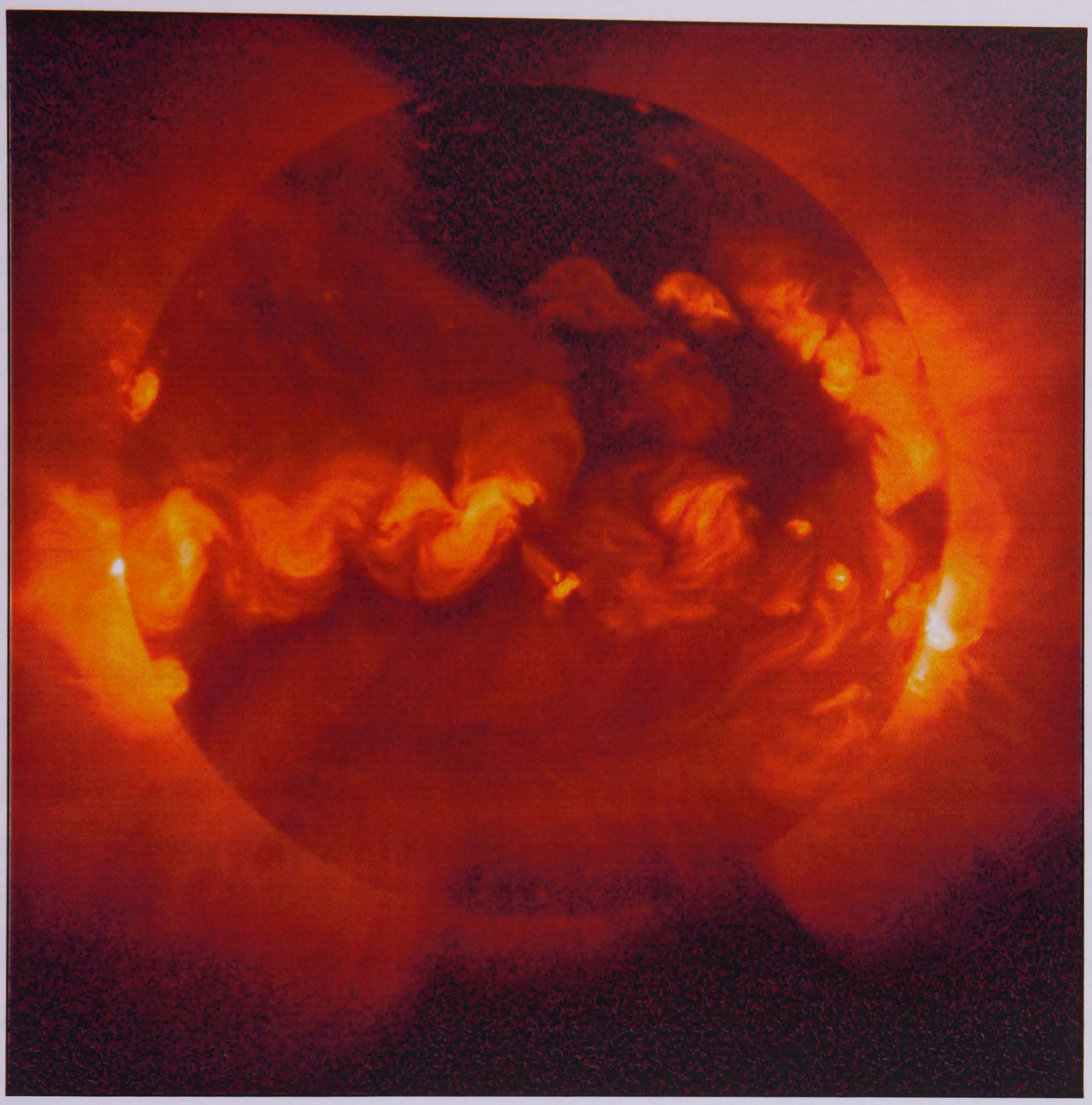

Figure 5.1 - Sun in soft X-Rays (Yohkoh Soft X-Ray Telescope)

Notice that the corona is not uniformly bright, but is concentrated around the solar equator in loop-shaped features. These bright loops are located within and connect areas of strong magnetic field called active regions. Sunspots are located within these active regions.

Solar flares occur in active regions. A recent event, "Martin Luther King Storm" happened during the period from 10/01/05 to 23/01/05. Solar active region 0720 rotated onto the east limb on January 10th and put on a pyrotechnic display characteristic for this phase of the solar cycle before disappearing beyond the west limb on January 23rd. On January 15th and 17th this region released the two of five X-class solar flares. These flares were associated with extraordinary ion storms whose

effect reached Earth's surface (National Geophysical Data Center (NGDC) - NOAA Satellite and Information Service).

Scientists classify solar flares according to their x-ray brightness in the wavelength range 1 to 8 Angstroms. There are 3 categories: (a) X-class flares are strong; they are major events that can trigger planet-wide radio blackouts and long-lasting radiation storms. (b) M-class flares are medium-sized; they can cause brief radio blackouts that affect Earth's Polar Regions. (c) Minor radiation storms sometimes follow an M-class flare. Compared to X- and M-class events, C-class flares are small with few noticeable consequences here on Earth.

Many scientists observed radio signal fading events caused by ionospheric absorption. Usually fading events are associated with solar flares, which are characterized by sudden increase in the solar X-ray flux that causes an increase in the ionization in the lower ionosphere. The abrupt increase of ionization causes the absorption of radio waves propagating in the Earth–ionosphere wave-guide and is reported as radio signal fading events. Contreira B. D. et al. (2005) proposed an experiment to study solar flare effects on radio-communication signals. The experiment based on the collection of the daily variation of the received signal strength of Amplitude Modulated (AM) radio signals in HF range. X-ray solar flux data from the GOES-8 satellite were used to identify X-ray solar bursts associated with solar flares. That system was able to measure the daily variation of the lower ionosphere ionization, as well as being able to identify fading events caused by X-ray solar flares. The same scientists observed 69 days with fading events during 2001, of which 75% were well correlated with X-ray solar flare bursts. This experiment is a typical example that shows these space weather effects.

X-ray emission has been observed from many objects throughout the solar system including Sun, Moon, Earth, Jupiter and comets. Cravens E. T. (2000) gives a brief review of these observations and some of the emission mechanisms suggested explaining the observed X-rays. X-ray emission from Jupiter's auroral region was first observed by the Einstein X-ray observatory [Metzger et al. (1983)]. Additional auroral X-ray observations were subsequently made by the ROSAT observatory [Waite et al. (1994)]. Supplementary, cometary X-ray emissions were also observed. In March 1996, X-ray and extreme ultraviolet emission was observed from comet Hyakutake by the HRI and WFC instruments, respectively, on the ROSAT satellite [Lisse et al.

(1996)] and by the EUVE satellite [Mumma et al. (1997)]. The launch of NASA's Chandra X-ray observatory, which is able to make high spectral resolution observations, gave further impetus to this field.

Comet McNaught–Hartley was observed by Krasnopolsky V. A. et al. (2002) for five days in January 2001 using the Chandra X-ray Observatory (CXO/ACIS). This observation made it possible to study the spatial distribution of X-rays, their temporal variability and correlation with the solar-wind properties, and its spectrum.

5.3 The Experiment

Over the past two years we have developed a prototype EMV telemetric network in VHF band for the study of naturally occurring EM emissions. Our goal is to find evidence that they are related (or not) to strong earthquake events. This network consists of four prototype ground-base monitors.

In order to get more reliable results, we need to study as more events as possible, so, the selection of the appropriate geographic region is of high importance. The region of the Western Hellenic subduction zone which includes the Ionian Islands has the highest seismic activity in Europe [Clément C. et al. (2000), Laigle M. et al. (2002)]. For these reasons, the four prototype ground-base monitors were installed in this region.

This prototype EMV telemetric network was launched on 06/2004 and is working up to now (06/2006). Three sub-sections are going to be summarized (a) the seismic events that occurred within the predefined area, (b) the recorded naturally occurred EM emissions in VHF band and (c) the X-Ray emissions from the Sun during the experiment's period.

5.3.1 Earthquake Events

According to the determinations of Institute of Geodynamics of the National Observatory of Athens [NOAIG (2007)], European-Mediterranean Seismological Centre [EMSC (2007)] and United States Geological Survey [USGS (2007)] the following earthquake events occurred during the experiment's period (06/2004 – 06/2006).

As shown in Table 5.1 and Figure 5.2, during that period eight strong earthquake events happened with magnitude over 5.2 Richter (Mw) at the focused area. On November 23rd 2004, 02:26 UTC, a 5.5 Richter (Mw) earthquake event "EQ1" took place at the northeast Hellenic Arc. On January 31st 2005, 01:05 UTC, an additional 5.7 Richter (Mw) earthquake event "EQ2" occurred at the focused area of Ionian Sea with its epicentre a few kilometres off the western coast of Zakynthos (37.41N,

20.11E). Five more earthquake events happened near island Zakynthos with the same epicentre (37.60N, 20.90E). On 18th October 2005 "EQ3" was the first of them. During the period from 4 to 12 April 2006 "EQ5", "EQ6", "EQ7" and "EQ8" took place. Finally, the most considerable earthquake event "EQ4" occurred on January 8th 2006. It was an intermediate depth earthquake event with the significant magnitude of 6.7 Richter (Mw).

EQ event	Date of Occurrence	Time of Occurrence	Magnitude (Richter)	LAT (N)	LONG (E)	Depth (km)
EQ1	23 Nov 2004	02:26 UTC	5.5 Mw	40.35	20.60	11
EQ2	31 Jan 2005	01:05 UTC	5.7 Mw	37.41	20.11	16
EQ3	18 Oct 2005	15:26 UTC	5.6 Mw	37.58	20.86	22
EQ4	08 Jan 2006	11:34 UTC	6.7 Mw	36.21	23.41	69
EQ5	04 Apr 2006	22:05 UTC	5.5 Mw	37.58	20.93	18
EQ6	11 Apr 2006	00:02 UTC	5.4 Mw	37.64	20.92	18
EQ7	11 Apr 2006	17:29 UTC	5.6 Mw	37.68	20.91	18
EQ8	12 Apr 2006	16:52 UTC	5.6 Mw	37.61	20.95	19

Table 5.1 - Earthquake Events during experiment period

Figure 5.2 - Map of earthquake events

5.3.2 VHF Data Recordings

Four prototype electromagnetic variation (EMV) field stations have already been installed in Western Greece, at the locations: Corfu, Ioannina, Ithomi and Kefallonia. This telemetric network was launched on 06/2004 and is working up to now (06/2006).

The selected monitoring frequencies in VHF band are known to be free from artificial interference. Levels of EM activity in VHF band were recorded for this period. The most significant EM events revealed by initial data analysis. For strong EM events a simple threshold of the signal level proved reliable enough. Although for minor events more powerful algorithms were developed in order to be identified. Among these Standard Deviation level and STA/LTA algorithm proved more accurate (see Section 3.8).

As a result, a number of events during network's working period are achieved. Table 5.2 displays the most significant EM VHF events.

EM VHF event	Date of Occurrence	Time of Occurrence	Duration (in minutes)
EM A	15 Jan 2005	06:40 UTC	~60
EM B	17 Jan 2005	09:50 UTC	~60

Table 5.2 - Most significant EM VHF events

During this period there were eight strong earthquakes with magnitude over 5.2 Richter (Mw) in the wider area of Western Greece (Table 5.1). The second event, EQ2, occurred on 31st Jan 2005. Prior to EQ2 event, two clear EM emissions were recorded simultaneously from all field stations concerning all monitoring frequencies, on 15th and 17th of January 2005. The following three figures illustrate some of these monitoring frequencies. The first one shows a typical day of VHF data recordings (Figure 5.3). The other two figures show EMV recordings on 15th January 2005 «event EM A» (Figure 5.4) and 17th January 2005 «event EM B» (Figure 5.5).

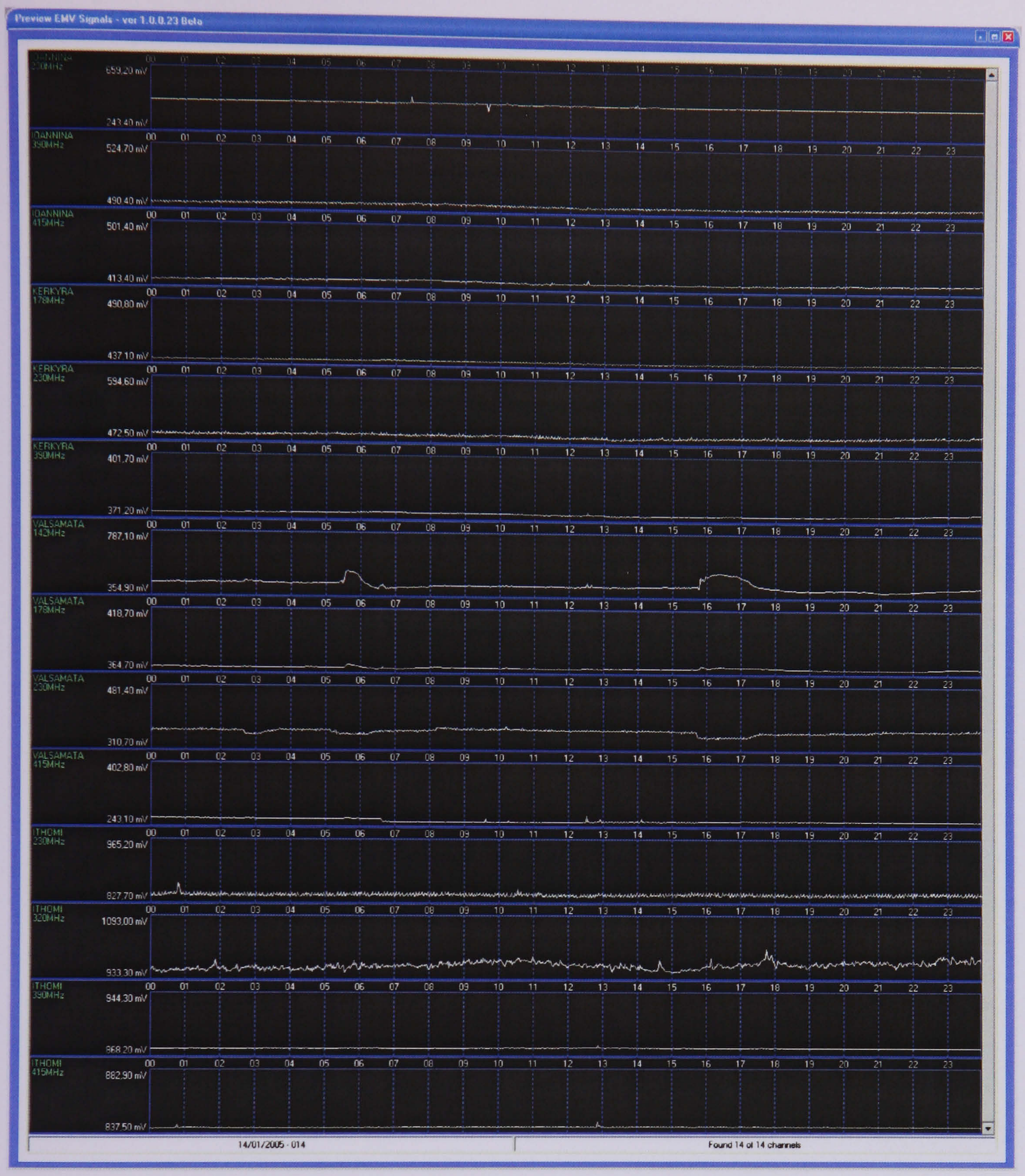

Figure 5.3 - VHF data on 14-01-2005 (Typical day)

Figure 5.4 - VHF data on 15-01-2005 (Event day)

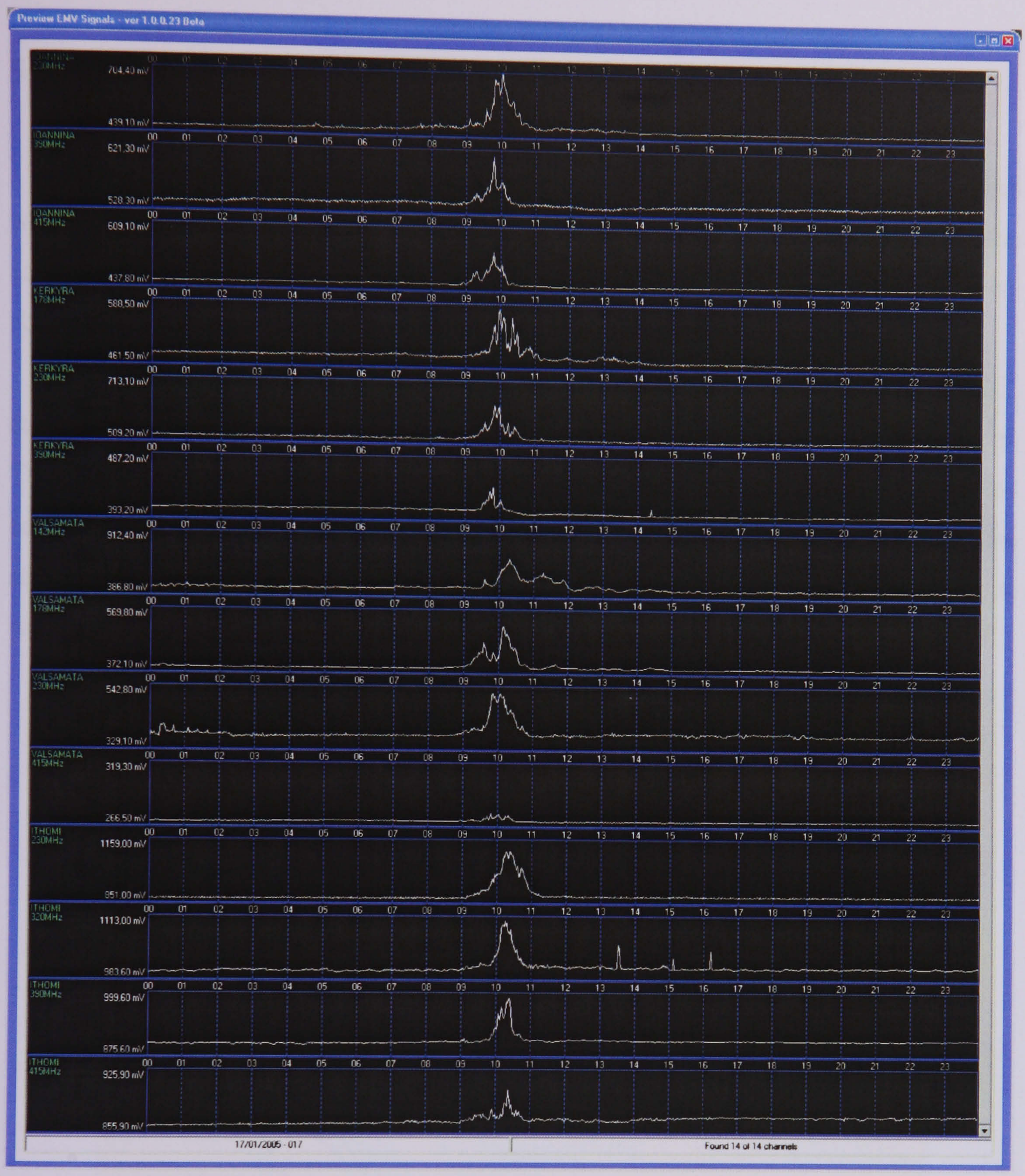

Figure 5.5 - VHF data on 17-01-2005 (Event day)

The fact that a Gaussian distribution has been observed along to all monitoring frequencies implies the assumption that it might be white noise. An initial analysis of these VHF signals is discussed in this thesis, in order to explore the possibility that these signals are somehow related to the EQ2 strong earthquake. Regarding the other events, there was absence of electromagnetic signal recordings.

5.3.3 X-Ray Data Recordings

Having identified events in the EM spectrum but being unable to correlate them with earthquake events, it was decided to explore other events, which might be the source of these signals. The following section refers to X-ray survey carried out by NASA.

The Geostationary Operational Environmental Satellites (GOES-1, GOES-2, etc.) carry on board the Space Environment Monitor (SEM) instrument subsystem. The SEM has provided magnetometer, energetic particle, and soft X-ray data continuously since July 1974. So, the GOES satellites provide information about the strength of x-ray emissions from the Sun. The Sun is constantly producing x-rays, so we are looking for significant increases in the intensity of x-ray above a background.

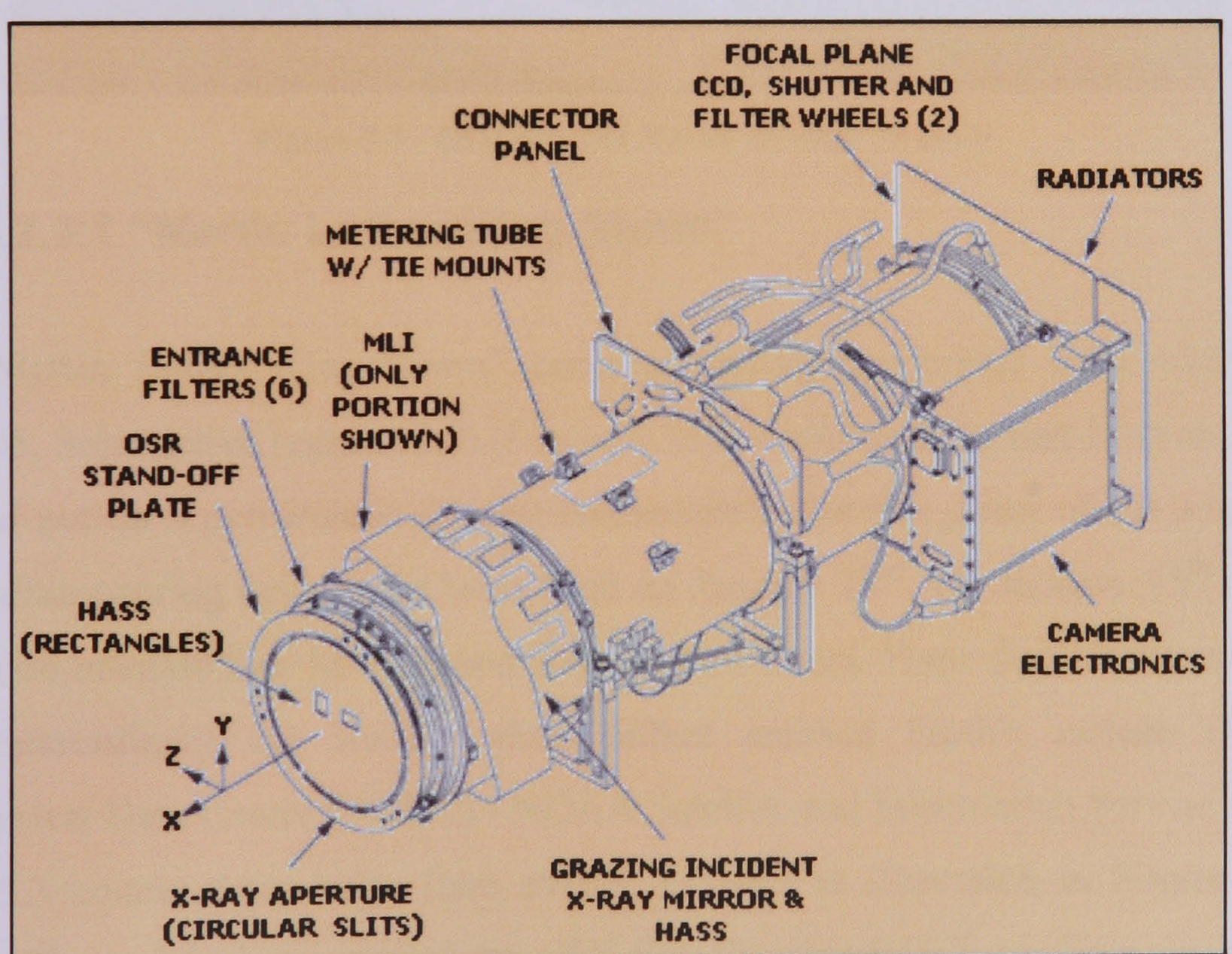

Figure 5.6 - GOESN SXI NASA satellite schematic

Scientists have developed a simple rating system for solar x-ray activity. They have created five levels; A, B, C, M, and X. The GOES x-ray scale is logarithmic. The A level extends from $1.0 \times 10^{-8} W/m^2$ to $9.9 \times 10^{-8} W/m^2$, the B level is $10^{-7} W/m^2$

range, C is $10^{-6}W/m^2$, and so on. Therefore, a B7.9 flare produces $7.9x10^{-7}W/m^2$ [National Geophysical Data Center (NGDC) - NOAA Satellite and Information Service (2007)].

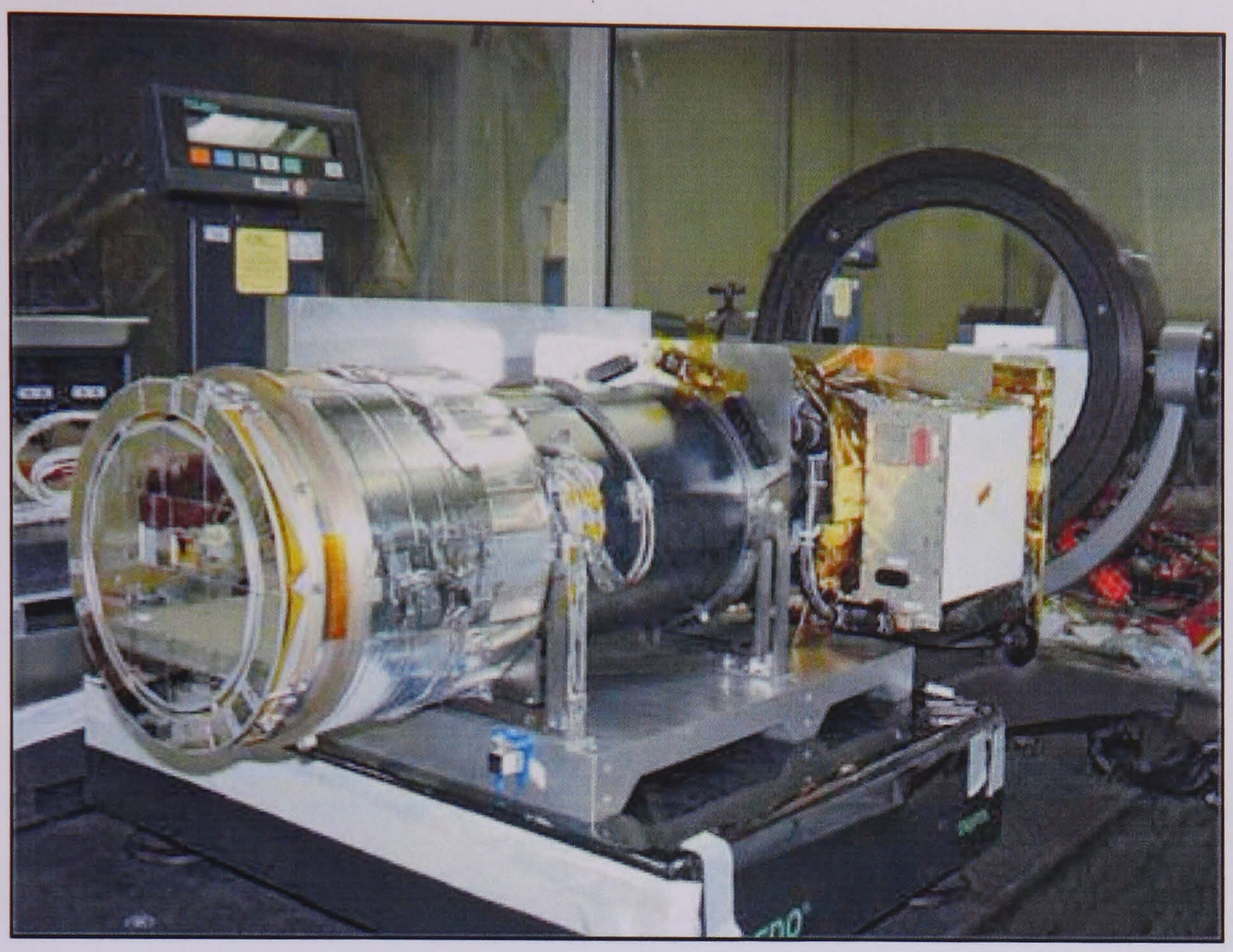

Figure 5.7 - GOESN SXI NASA satellite on table

5.3.3.1 "Martin Luther King Storm"

"Martin Luther King Storm" occurred during the period from 10/01/05 to 23/01/05. Solar active region 0720 (Figure 5.10) rotated onto the east limb on January 10th and put on a pyrotechnic display characteristic for this phase of the solar cycle before disappearing beyond the west limb on January 23rd. On January 15th and 17th this region released four M-class and X-class solar flares. These flares were associated with extraordinary ion storms whose effect reached Earth's surface [National Geophysical Data Center (NGDC) - NOAA Satellite and Information Service (2007)]. Table 5.3 counts these solar flare events, as well as illustrated in Figure 5.9. In contrast Figure 5.8 plots a typical day of X-Ray flux that GOES satellites measures.

X-Ray Event	Date of Occurrence	GOES peak time	GOES X-ray Class	Active region NOAA no.
A	15 Jan 2005	00:43 UTC	X1.2	0720
B	15 Jan 2005	06:38 UTC	M8.6	0720
C	15 Jan 2005	23:02 UTC	X2.6	0720
D	17 Jan 2005	09:52 UTC	X3.8	0720

Table 5.3 - Solar flare events

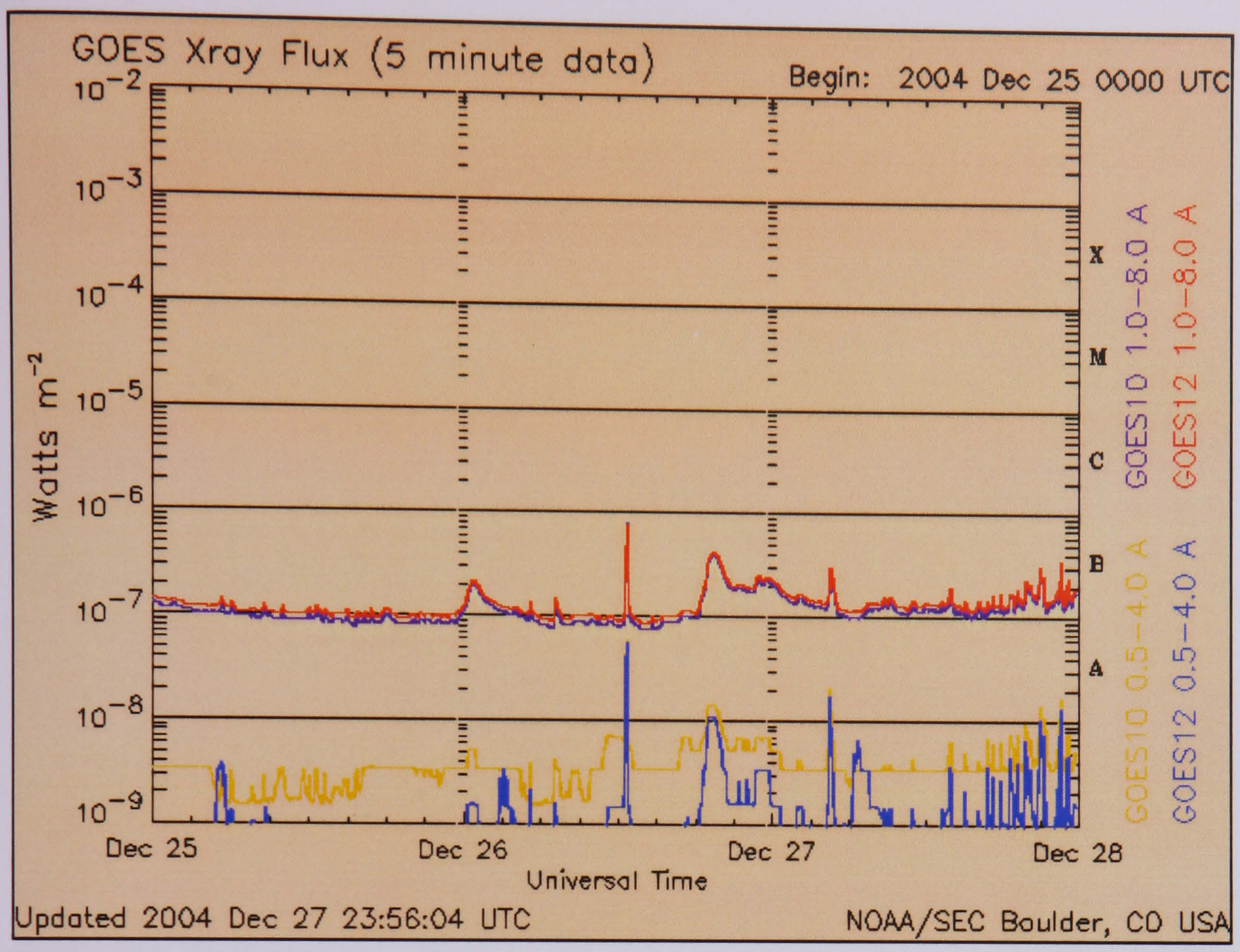

Figure 5.8 - X-Ray flux (Typical day)

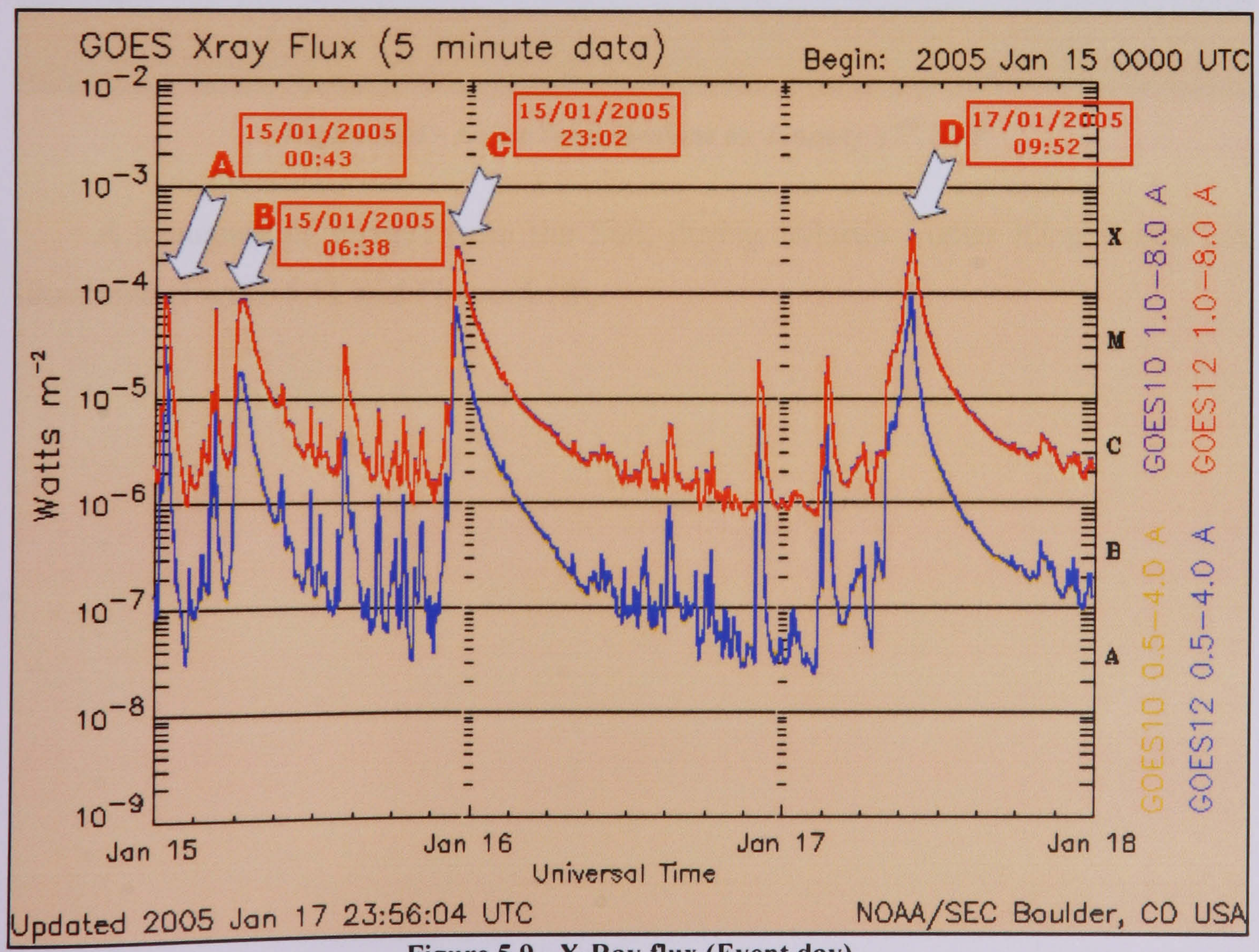

Figure 5.9 - X-Ray flux (Event day)

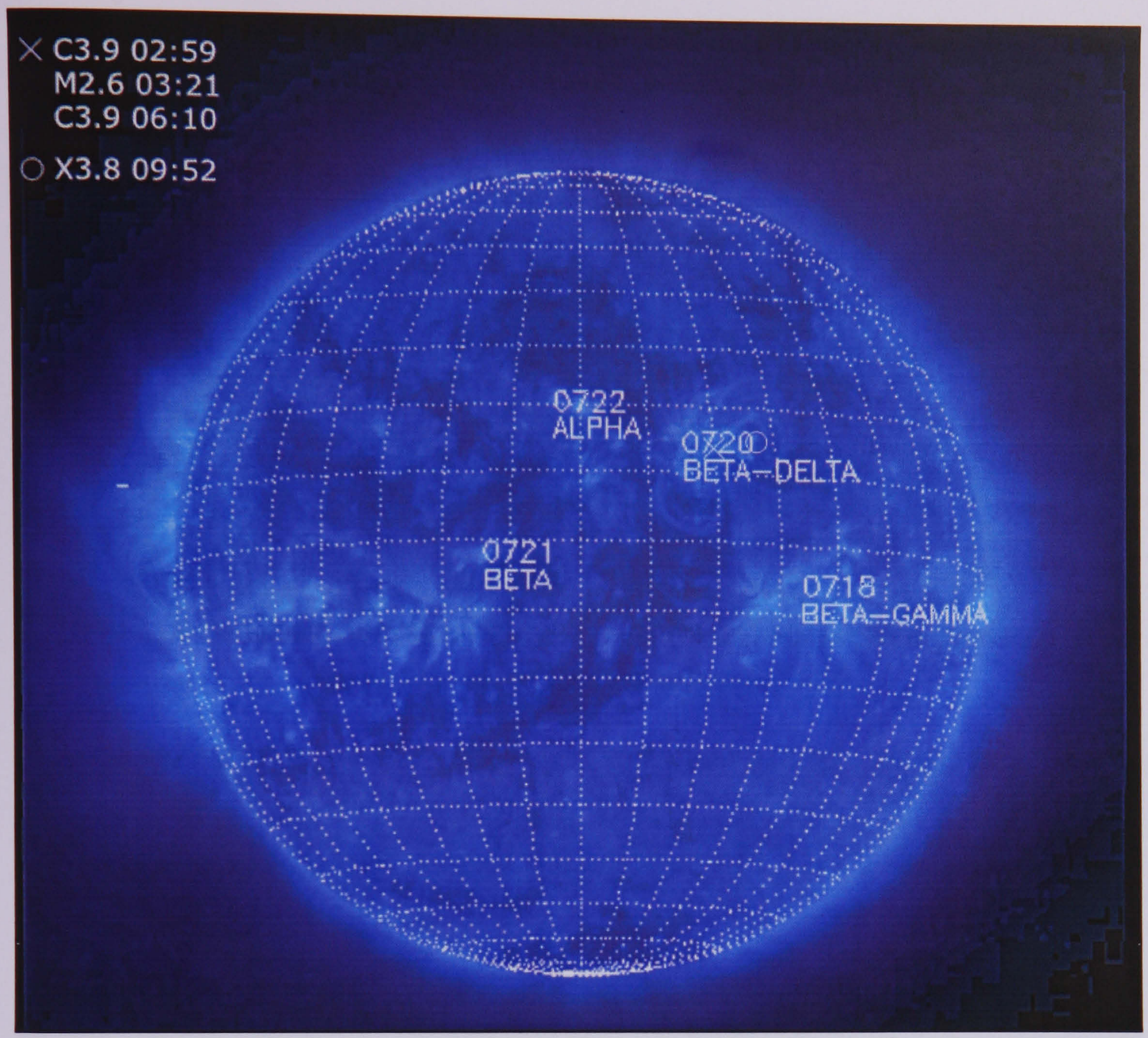

Figure 5.10 - Active Solar Regions on January 17th 2005

A sequence of images from the Sun, during "Martin Luther King Storm", is illustrated (Figure 5.11 and Figure 5.12).

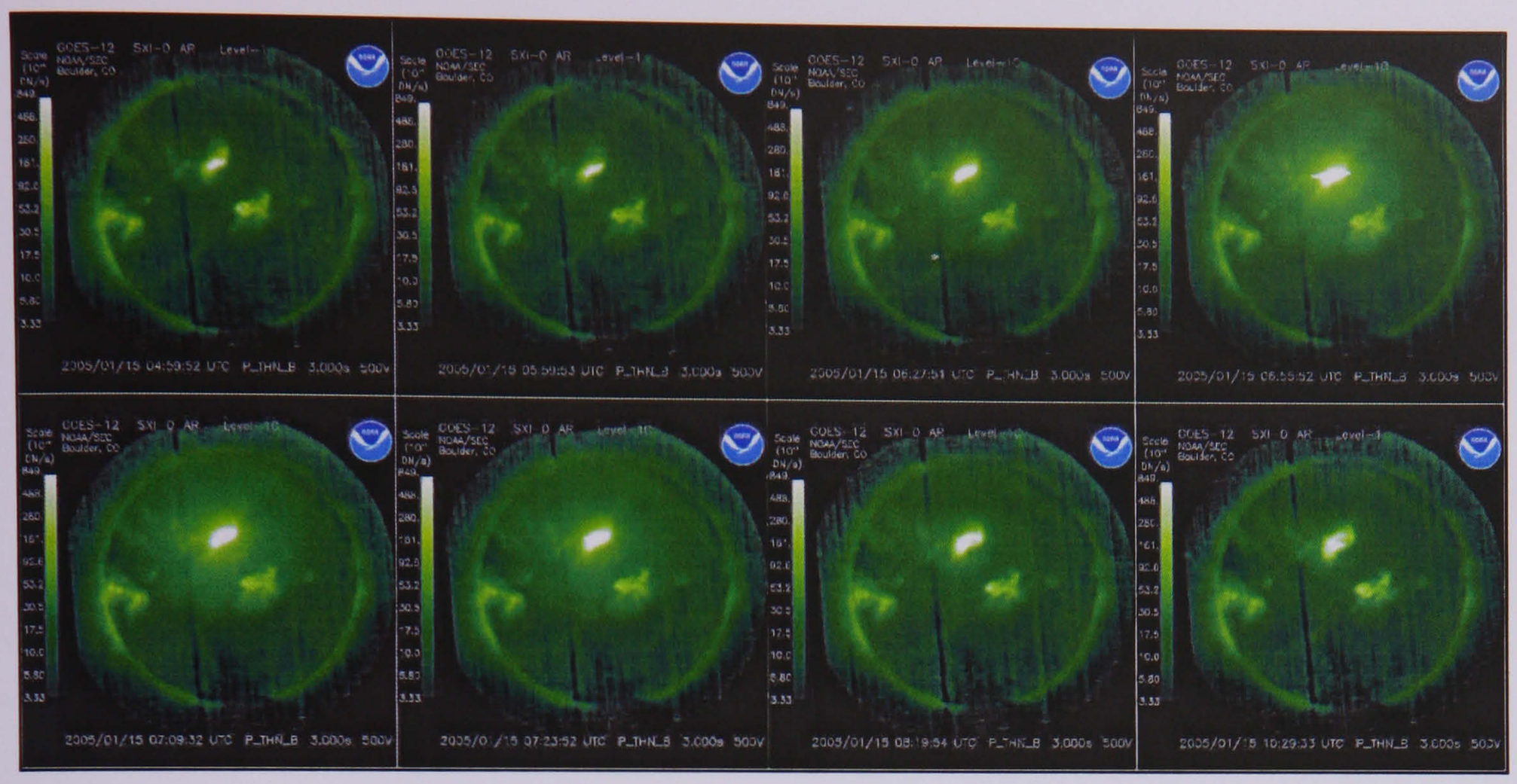

Figure 5.11 - Solar flares on January 15th 2005

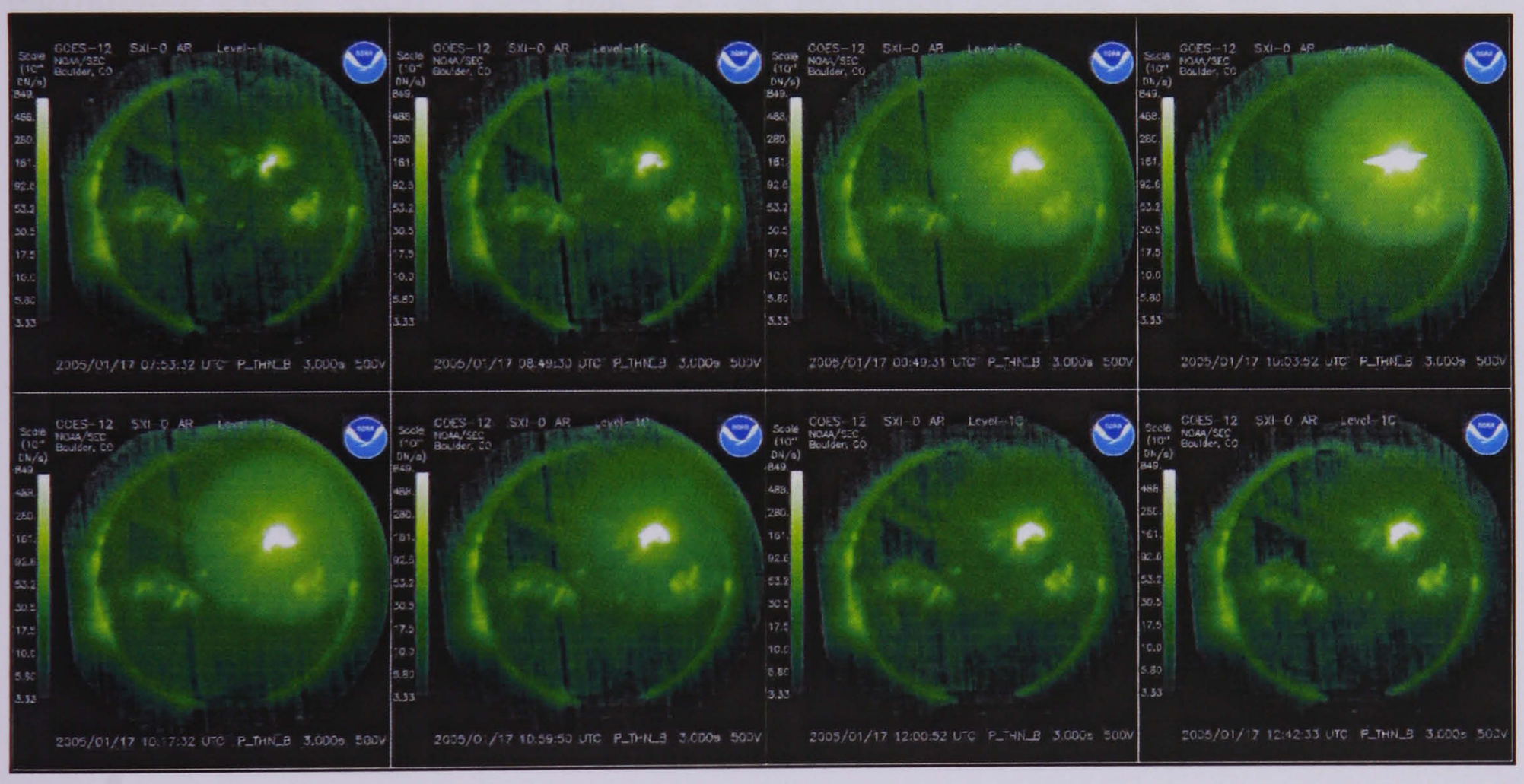

Figure 5.12 - Solar flares on January 17th 2005

5.4 Results of the Experiment

This telemetric network was launched on 06/2004 and is working up to now (06/2006). As shown in Table 5.1 and Figure 5.2, during that period eight strong earthquake events happened with a magnitude of over 5.2 Richter (Mw) in the wider area of Western Greece. The application of DAS gave us the opportunity to acquire the levels of EM activity in VHF band during the same period, at the area of interest. The most significant EM events were revealed by initial data analysis. Table 5.2 displays the most significant EM VHF events. In this subsection is discussed the possibility these significant EM emissions are somehow related to seismic events.

Summarizing, on November 23rd 2004, 02:26 UTC, a 5.5 Richter (Mw) earthquake event "EQ1" took place at the northeast Hellenic Arc. On January 31st 2005, 01:05 UTC, an additional 5.7 Richter (Mw) earthquake event "EQ2" occurred at the focused area of Ionian Sea with its epicentre a few kilometres off the western coast of Zakynthos (37.41N, 20.11E). Five more earthquake events occurred near the island of Zakynthos with the same epicentre (37.60N, 20.90E). On 18th October 2005 "EQ3" was the first of them. During the period from 4 to 12 April 2006 "EQ5", "EQ6", "EQ7" and "EQ8" took place. Finally, the most considerable earthquake event "EQ4" occurred on January 8th 2006. It was an intermediate depth earthquake event with the significant magnitude of 6.7 Richter (Mw).

An initial analysis of acquired EM events in VHF band took place, in order to explore the possibility these EM events are somehow related to the seismic events. Two significant EM emissions detected two weeks prior the second seismic event "EQ2". Regarding the other seismic events, there was absence of EM emissions prior to their occurrence.

On the other hand, the Sun was intensely active from the 10th to the 23rd of January 2005. A series of M-class and X-class solar flares occurred in single extensive active region 0720, as shown in Figure 5.10. During this period, four among this series of flares were those occurring on January 15th and 17th.

As shown in Table 5.3, solar flare event A occurred at 00:43 UTC on January 15th and event C occurred at 23:02 UTC on January 15th, as well. The geographic

region of these four prototype VHF field stations, ground base monitors, was on the night side of the Earth at the time of these events.

Supplementary, solar flare event B occurred at 06:38 UTC on January 15th and event D occurred at 09:52 UTC on January 17th, as well. The last mentioned events (B and D) occurred when ground-base monitors, were on the day side of the Earth. Electromagnetic radio emissions in VHF band were observed by all four ground-base electromagnetic variation monitors, located at Corfu, Ioannina, Kefallonia and Ithomi respectively.

In these flares, intense emissions of hard X-rays and γ-rays have been observed by the satellites. It seems that production of hard X-rays of these solar flares coincided with the production of the hard VHF electromagnetic radiations.

5.5 Conclusions

Chapter 5 focuses on the application of DAS to EM emissions in VHF band. Over the past two years a prototype EMV telemetric network in VHF band has been developed for the study of naturally occurring EM emissions. The goal is to find evidence that they are related (or not) to strong earthquake events. This network consists of four prototype ground-base monitors and is described in chapter 4.

In order to get more reliable results, we needed to study the most events possible, so the selection of the appropriate geographic region is of high importance. The region of the Western Hellenic subduction zone, which includes the Ionian Islands, has the highest seismic activity in Europe [Clément C. et al. (2000), Laigle M. et al. (2002)]. The four prototype ground-base monitors were installed there.

This prototype EMV telemetric network was launched on 06/2004 and is operational up to now (06/2006). During this period eight strong seismic events have occurred within the predefined area with magnitude over 5.2 Richter (Mw) in the wider area of Western Greece. The system worked as expected and acquired the levels of EM activity in VHF band during these two years at the focused area.

An extensive study of acquired EM events took place in order to examine the possibility these EM events are somehow related to the seismic events and whether, in conclusion, they can be considered as precursors. Two significant EM emissions were detected two weeks prior to the second strong seismic event, "EQ2" (see Table 5.1). Regarding the other seismic events, there was absence of EM emissions in VHF band.

Concerning the "EQ2" seismic event, the data gathered seemed promising but it was found out later that these EM emissions were not correlated with the earthquake. The actual source of these signals was the Sun. The Sun was intensely active from the 10th to the 23rd of January 2005. A series of M-class and X-class solar flares occurred in single extensive active region 0720. During this period, four of this series of flares were those occurring on January 15th and 17th.

Solar flare event A occurred at 00:43 UTC on January 15th and event C occurred at 23:02 UTC on January 15th. The geographic region of these four prototype VHF field stations - ground base monitors - was on the night side of the Earth when these events occurred and that was the reason the telemetric system could not gather EM emissions due to Sun at that time. Supplementary, solar flare event B occurred at 06:38 UTC on January 15th and event D occurred at 09:52 UTC on January 17th, as well. The last mentioned events (B and D) occurred when ground-base monitors were on the day side of the Earth. These naturally occurred EM emissions in VHF band were observed by all four ground-base electromagnetic variation monitors, located at Corfu, Ioannina, Kefallonia and Ithomi respectively.

In these flares, intense emissions of hard X-rays and γ-rays have been observed by satellites. It seems that the production of hard X-rays of these solar flares coincided with the production of the hard VHF electromagnetic radiations. Hence, these signals were strong enough to influence our VHF recordings and proved that there was no correlation with any seismic event.

6 Conclusions - Future Work

6.1 Conclusions

This thesis has focused on the definition, design and implementation of a versatile embedded Compact Flash™ based Data Acquisition System (DAS), as a part of the VHF telemetric network which is responsible for capturing reliable electromagnetic emissions in VHF band. This has enabled a long time (two years) study of naturally occurring EM emissions through the deployment of a network of DAS's' throughout the Hellenic arc. This network consists of a number of prototype VHF field stations, a central station and dedicated software, which is responsible for the appropriate data collection and processing. The entire implemented system is described analytically in Chapter 2, 3 and 4. Chapter 5 deals with the application of DAS to EM emissions in VHF band and its potential contribution to the earthquake research is discussed.

Since this device is mainly designed for outdoor experimental purposes, it had to face all the problems derived from rugged environments and also ensuring long term availability, high reliability, high robustness, rich set of certifications in life cycle management and longevity. The innovation of the proposed DAS is the Data Storage System (DSS) that it incorporates. The DSS is an efficient memory-management scheme that increases CF™ lifetime. This memory-management scheme is suitable for large capacity DAS's. In addition, the Acquisition Interface Unit (AIU) is a custom designed sub-unit for capturing EM emissions in VHF band, which is described analytically in Chapter 2.

In order to acquire reliable electromagnetic variation measurements, field stations were installed in the countryside, isolated from man-made, artificial noise. In such types of regions the use of alternative energy sources, like solar cells, is almost always necessary. Hence, the system's total power consumption is of great importance. The common problem in data acquisition systems that are operating in the countryside is to combine the high capacity, non-volatile memory, with the low power

system consumption. Some other problems are the remote data collection, as well as the remote device configuration and the remote application firmware upgrades.

Since this is a large and complex project to maintain, the need of special software exists. This software should be responsible for real time monitoring, configuration, management, data collection, alarm notification operations, data conversion in a universal format e.g. CSV, and a graphical tool to make the results visible to the eye. The survey verified that most of the requirements were not available from those programs, thus incompatibilities with the proposed DAS and problems with the control of the whole telemetry system could occur. After that consideration, the decision to create a dedicated and fully functional software packet for the system that would meet the requirements set was made.

In this thesis, the implemented embedded Compact Flash™ based DAS ensures reliable electromagnetic variation measurements, efficient memory-management scheme that increases CF™ lifetime, uninterrupted operation and low power consumption.

This telemetric network was launched on 06/2004 and is operational up to now (06/2006). During this period eight strong earthquake events happened with magnitude over 5.2 Richter (Mw) in the wider area of Western Greece. The system worked as expected and acquired the levels of EM activity in VHF band during the same period, at the focused area.

The development and deployment of the network has enabled initial analysis of acquired EM events, in order to explore the possibility that these EM events are somehow related to the seismic events and whether, in conclusion, they can be considered as precursors. Two significant EM emissions were detected two weeks prior the second seismic event, “EQ2” (see section 5.3.1). Regarding the other seismic events, there was absence of EM emissions in the investigating band.

Concerning the "EQ2" seismic event, the data gathered seemed promising but it was found out later that this data was not correlated with the earthquake. The actual source of these signals was the Sun. The Sun was intensely active from the 10th to the 23rd of January 2005. A series of M-class and X-class solar flares occurred in single extensive active region 0720. During this period, four of this series of flares were those occurring on January 15th and 17th.

In these flares, intense emissions of hard X-rays and γ-rays have been observed by the satellites. It seems that production of hard X-rays of these solar flares coincided with the production of the hard VHF electromagnetic radiations. Two solar flare events occurred when ground-base monitors were on the day side of the Earth. These naturally occurred EM radio emissions in VHF band were observed by all four ground-base electromagnetic variation monitors, located at Corfu, Ioannina, Kefallonia and Ithomi respectively. In contrast, the geographic region of these four prototype VHF field stations was on the night side of the Earth when two other events occurred and that was the reason why the system was not able to gather EM emissions at that time.

The gathered data, during the experimental period, proved that the DAS in issue succeeded in acquiring EM emissions that are correlated with naturally occurring phenomena. It is known that EM emissions do occur from highly compressed rocks and are therefore present as precursors to earthquakes. A significant finding from the application of the DAS network is that these signals are at very low strength and are effectively hidden in the background noise. The contribution of this thesis is therefore the design and deployment of a novel data network system. Its deployment has informed the seismic community that the detected EM emissions in the selected frequency range of this project can not be clearly correlated with seismic activity.

6.2 Future Work

The purpose of this thesis was to investigate if there is any kind of correlation between EM emissions generated from rock compression and upcoming earthquakes.

A detailed design and deployment of a novel DAS network took place for this purpose. Experimental DAS's were developed in order to meet the requirements of uninterrupted data collection and continuous processing of detected EM emissions.

The main operations of this project including analysis, design, development, data collection and evaluation lasted approximately four years. The results derived from the evaluation phase lead us to some conclusions regarding the eligibility of the developed data network system, as well as the possibility that EM emissions can be treated as earthquake precursors or they are totally irrelevant to seismic activity.

In order to minimise the possibility of error and increase the reliability of the system, further work should be performed in three major sections, namely hardware modification, terrestrial coverage and data analysis.

Regarding the first section of future work, the supplemental peripheral devices should be developed in order to acquire EM emissions in a wider frequency range as well as deliver simultaneously multi frequency monitoring. This promises the implementation of a new sub-unit for the DAS that will be responsible for covering UHF band.

In the second section of concentration, which is the coverage of the telemetry network, some more field stations should be installed across Hellenic Arc. By increasing the number of the installed stations, more reliable results will be collected and demonstrated.

Finally the last section in which we can work, concerns new algorithms to be developed that will offer a more accurate and error free technique for data analysis and representation.

Due to the versatility derived from the cutting edge technology used, as well as the sophisticated design of the DAS, this scientific instrument can be used in a great variety of applications in either experimental or commercial sectors. Furthermore, the device is fully compatible with all analogue sensors and most of the existing digital ones, which are compliant to I^2C and EIA232E interfaces. Another major advantage of this device is that it is fully operational in either standalone or telemetric mode, depending on the requirements and the infrastructure of each project and occasion.

Hence, DAS can ideally be used for a wide range of experimental purposes such as meteorology, climatology, seismology, observation and generally provides an effective way for automated measurement logging. On the other hand, DAS can also be used for commercial purposes such as vehicle tracking/fleet management, temperature sensing/adjustment and in other projects that remote sensing, auditing and control is an essential issue.

References

Alfred Leick (2004) - "GPS Satellite Surveying", Third Edition, ISBN: 0-471-05930-7.

Adams M.H. (1990) - "Some observations of electromagnetic signals prior to California earthquakes", J. Sci. Explor., Volume 4, pp. 137-152

Alfred Leick (Editors), (2004) - "GPS Satellite Surveying", John Wiley and Sons, 3rd Edition, pp. 464, ISBN: 978-0471059301

American National Standards for Information technology (1996) - "AT Attachment with Packet Interface-2 (ATA/ATAPI-2)", ANSIX3.279

American National Standards for Information technology (1997) - "AT Attachment with Packet Interface-3 (ATA/ATAPI-3)", ANSIX3.298

American National Standards for Information technology (1998) - "AT Attachment with Packet Interface-4 (ATA/ATAPI-4)", ANSINCITS.317

American National Standards for Information technology (2000) - "AT Attachment with Packet Interface-5 (ATA/ATAPI-5)", ANSINCITS.340

American National Standards for Information technology (2002) - "AT Attachment with Packet Interface-6 (ATA/ATAPI-6)", ANSIINCITS.361

Asada T., Baba H., Kawazoe M. and Sugiura M. (2001) - "An attempt to delineate very low frequency electromagnetic signals associated with earthquakes", Earth Planets Space, Volume 53, pp. 55-62

ATMEL Corporation (2003) - "ATmega128, 8-bit AVR Microcontroller with 128K Bytes In-System Programmable Flash", Rev. 2467H, AVR

Austerlitz H. (Editors), (2002) - "Data Acquisition Techniques Using PCs", Academic Press, 2nd Edition, pp. 416, ISBN: 978-0120683772

Bernardi A., Fraser-Smith A. C., McGill P. R. and Villard O. G. (1991) - "ULF magnetic field measurements near the epicenter of the Ms 7.1 Loma Prieta earthquake", Physics of The Earth and Planetary Interiors, Volume 68, Issues 1-2, pp. 45-63

Biagi P. F., Piccolo R., Ermini A., Martellucci S., Bellecci C., Hayakawa M., Capozzi V. and Kingsley S. P. (2001) - "Possible earthquake precursors revealed by LF radio signals", Natural Hazards and Earth System Sciences, Volume 1, pp. 99-104

Campbell Scientific (2007) - "Manufacturer Company of Professional Data Acquisition Systems" [Online]
Available: http://www.campbellsci.com/index.cfm

Cantu M. (Editors), (2003) - "Mastering Delphi 7", Sybex Inc, 1st Edition, pp. 992, ISBN: 978-0782142013

Chang L. P. and Kuo T. W. (2002) - "An adaptive striping architecture for flash memory storage systems of embedded systems", in Proc. 8th IEEE Real-Time and Embedded Technology and Applications Symposium (RTAS 2002), IEEE Computer Society, San Jose, California, pp. 187-196, ISBN: 978-0769517391

Chang L. P. and Kuo T. W. (2001) - "A dynamic-voltage-adjustment mechanism in reducing the power consumption of flash memory for portable devices", in Proc. IEEE Conference on Consumer Electronics (ICCE 2001), LA, CA, USA, pp. 218-219, ISBN: 978-0780366220

Chang L. P. and Kuo T. W. (2004) - "An efficient management scheme for large-scale flash-memory storage systems", in Proceedings of the 2004 ACM Symposium on Applied Computing (SAC), Nicosia, Cyprus, pp. 862-868, ISBN:1-58113-812-1

Chang L. P., Kuo T. W. and Lo S. W. (2004) - "Real-time garbage collection for flash-memory storage systems of real-time embedded systems", ACM Transactions and Embedded Computing Systems (TECS), Volume 3, Issue 4, pp. 837-863, ISSN: 1539-9087

Chiang M. L. and Chang R. C. (1999) - "Cleaning policies in mobile computers using flash memory", Journal of Systems and Software, Volume 48, Issue 3, pp. 213-231, ISSN: 0164-1212

Clément C., Hirn A., Charvis P., Sachpazi M. and Marnelisd F. (2000) - "Seismic structure and the active Hellenic subduction in the Ionian islands", Tectonophysics, Volume 329, Issues 1-4, pp. 141-156

Compact Flash™ Association (2004) - "Compact Flash™ 2.1 Specification"

Contreira D.B., Rodrigues F.S., Makita K., Brum C.G.M., Gonzalez W.,Trivedi N.B., da Silva M.R., Schuch N.J. (2005) - "An experiment to study solar flare effects on radio-communication signals", Advances in Space Research, Volume 36, Issue 12, pp. 2455-2459

Cravens T.E. (2000) - "X-ray emission from comets and planets", Advances In Space Research, Volume 26, Issue 10, pp. 1443-1451

DALLAS Semiconductors - MAXIM (2002) - "DS1631, High–Precision Digital Thermometer and Thermostat", Rev. 25/09/2002

DeRemer F. and Kron H. (1975) - "Programming-in-the large versus programming-in-the-small", in Proceedings of the international conference on Reliable software, Los Angeles, California, Volume 10, Issue 6, pp. 114-121

Douglis F., Caceres R., Kaashoek F., Li K., Marsh B. and Tauber J. A. (1994) - "Storage alternatives for mobile computers", in Proc. USENIX Operating Systems Design and Implementation Conf., Monterey, CA, pp. 25-37

Eftaxias K., Kapiris P., Dologlou E., Kopanas J., Bogris N., Antonopoulos G., Peratzakis A. and Hadjicontis V. (2002) - "EM Anomalies before the Kozani earthquake: A study of their behavior through laboratory experiments", Geophysical Research Letters, Volume 29, Issue 8, pp. 69.1-69.4

Eftaxias K., Kapiris P., Polygiannakis J., Bogris N., Kopanas J., Antonopoulos G., Peratzakis A. and Hadjicontis V. (2001) - "Signature of pending earthquake from electromagnetic anomalies", Geophysical Research Letters, Volume 28, Issue 17, pp. 3321-3324

Eftaxias K., Kapiris P., Polygiannakis J., Peratzakis A., Kopanas J., Antonopoulos G. and Rigas D. (2003) - "Experience of short term earthquake precursors with VLF–VHF electromagnetic emissions", Proc. Japan Acad., Volume 3, pp. 217-228

Eftaxias K., Kopanas J., Bogris N., Kapiris P., Antonopoulos G. and Varotsos P. (2000) - "Detection of electromagnetic earthquake precursory signals in Greece", Proc. Japan Acad., Volume 76, Issue 4, pp. 45-50, ISSN: 0386-2208

Embedded PC Modules - PC/104™ (2007) - "PC/104™ Consortium" [Online] Available: http://www.pc104.org

European-Mediterranean Seismological Centre (EMSC) (2007) - "Real Time Seismicity" [Online] Available: http://www.emsc-csem.org/index.php?page=current&sub=list

Forsberg C. (1988) - "XMODEM/YMODEM protocol", Ed., Omen Technology, Inc., Portland, OR [Online] Available: http://www.techfest.com/hardware/modem/xymodem.htm

Fraser-Smith A.C., Bernardi A., McGill P.R., Ladd M.E., Helliwell R.A. and Villard O.G., Jr. (1990) - "Low-frequency magnetic field near the epicenter of the M=7.1 Loma Prieta Earthquake", Geophysical Research Letters, Volume 17, No 19, pp. 1465-1468

Gokhberg M.B., Morgounov V.A. and Pokhotelov O.A. (Editors), (1995) - "Earthquake Prediction: Seismo-electromagnetic Phenomena", Gordon and Breach Publishers, 1st Edition, pp. 193, ISBN: 978-2881249211

Gokhberg M.B., Morgounov V.A., Yoshino T. and Ogawa T. (1982b) - "The results of operative precursor in Japan", Izv. AN SSSR, Fiz Zhemli, Volume 2, pp. 85-87

Gokhberg M.B., Morgounov V.A., Yoshino T. and Tomizawa I. (1982a) - "Experimental measurements of electromagnetic emissions possibly related to earthquakes in Japan", J. Geophys. Res., Volume 87, pp. 7824-7828

Hayakawa M. and Fujinawa Y. (Editors), (1994) - "Electromagnetic phenomena related to earthquake prediction", Terra Scientific Publishing Co., Tokyo, pp. 677, ISBN: 978-4887041134

Hayakawa M. and Molchanov O.A. (2000) - "Effect of earthquakes on lower ionosphere as found by sub-ionospheric VLF propagation", Advances in Space Research, Volume 26, No 8, pp. 1273-1276

Hayakawa M. and Sato H. (Editors), (1994) - "Ionospheric perturbations associated with Earthquakes, as detected by subionospheric VLF propagation, (Electromagnetic Phenomena Related to Earthquake Prediction, Edited by Hayakawa M. and Fujinawa Y.)", Terra Scientific Publishing Co., Tokyo, pp. 391-397, ISBN: 978-4887041134

Hayakawa M., Molchanov O.A., Ondoh T. and Kawai E. (1996) - "Anomalies in the sub-ionospheric VLF signals for the 1995 Hyogo-ken earthquake", J. Phys. Earth, Volume 44, pp. 413-418

Intel Corporation (1995a) - "FLS File Manager Software: LFM"

Intel Corporation (1995b) - "FTL logger exchanging data with FTL systems"

Intel Corporation (1995c) - "Software concerns of implementing a resident flash disk"

Intel Corporation (1998a) - "Flash File System Selection Guide"

Intel Corporation (1998b) - "Understanding the Flash Translation Layer (FTL) Specification"

Intel Corporation (1998c) - "Flash Data Integrator (FDI) User's Guide"

IOcomp Software Incorporated (2003) - "IOcomp Products" [Online] Available: http://www.iocomp.com

Kapiris P., Polygiannakis J., Peratzakis A., Nomicos K. and Eftaxias K. (2002) - "VHF-electromagnetic evidence of the underlying pre-seismic critical stage", Earth Planets Space, Volume 54, pp. 1237-1246

Kapiris P.G., Eftaxias K.A., Nomicos K.D., Polygiannakis J., Dologlou E., Balasis G.T., Bogris N.G., Peratzakis A.S. and Hadjicontis V.E. (2003) - "Evolving towards a critical point: A possible electromagnetic way in which the critical regime is reached as the rupture approaches", Nonlinear Processes in Geoph., Volume 10, pp. 511-524

Kawaguchi A., Nishioka S. and Motoda H. (1995) - "A flash-memory based file system", in Proceedings USENIX Tech. Conf., pp. 155-164

Khoshafian S. and Abnous R. (Editors), (1995) - "Object Orientation: Concepts, Analysis & Design, Languages, Databases, Graphical User Interfaces, Standards", John Wiley & Sons, 2nd Edition, pp. 528, ISBN: 978-0471078340

Kontoes C., Elias P., Sykioti O., Briole P., Remy D., Sachpazi M., Veis G., and Kotsis I. (2000) - "Displacement field and fault model for the September 7, 1999 Athens Earthquake inferred from ERS2 satellite radar interferometry", Geophysical Research Letters, Volume 27, Issue 24, pp. 3989-3992

Kopytenko Y., Ismagilov V., Hayakawa M., Smirnova N., Troyan V. and Peterson T. (2001) - "Investigation of the ULF electromagnetic phenomena related to earthquakes: Contemporary achievements and perspectives", Annali di Geofisica, Volume 44, Issue 2, pp. 325-334

Krasnopolsky A.V., Christian J. D., Kharchenko V., Dalgarno A. and Wolk J. S., Lisse M. C., Stern A. S. (2002) - "X-Ray Emission from Comet McNaught-Hartley (C/1999 T1)", Icarus, Volume 160, Issue 2, pp. 437-447

Laigle M., Hirn A., Sachpazi M. and Clément C. (2002) - "Seismic coupling and structure of the Hellenic subduction zone in the Ionian Islands region", Earth and Planetary Science Letters, Volume 200, Issues 3-4, pp. 243-253

Lantronix Corporation (2005) - "XPort™, Embedded Ethernet Device Server", Rev. 19/10/2005

Lantronix Corporation (2006) - "WiPort™, Embedded Wireless Networking Device Server", Rev. 1.0, 03/2006

Lee H. G. and Chang N. (2003) - "Energy-aware memory allocation in heterogeneous non-volatile memory systems,", in Proceedings of the International Symposium Low Power Electronics and Design (ISLPED 2003), Seoul, Korea, pp. 420- 423, ISBN: 1-58113-682-X

Lekas S. (1996) - "Searching the right Data Acquisition Software, in Evaluation Engineering" [Online]
Available: http://www.iotech.com/eedec96.html

Lisse C., Dennerl K., Englhauser J., Harden M., Marshall F. E., Mumrna M. J., Petre R., Pye J. P., Ricketts M. J., Schmitt J., Truemper J. and West R. G. (1996) - "Discovery of X-ray and extreme ultraviolet emission from comet C/Hyakutake 1996 B2", Science, Volume 274, Issue 5285, pp. 205-209

Maki K. and Ogawa T. (1983) - "ELF emission associated with earthquakes", Res. Let. Atmos. Electr., Volume 3, pp. 41-44

Makropoulos K. and Burton P.W. (1985) - "Seismic hazard in Greece. I. Magnitude recurrence", Tectonophysics, Volume 107, Issues 3-4, pp. 205-257

MAXIM Corporation (1999) - "MAX1270, Multi-range, +5V, 8-Channel Serial 12–Bit ADCs", 19-4782, Rev 1

Merzer M. and Klemperer S.L. (1997) - "Modelling Low-frequency Magnetic-field Precursors to the Loma Prieta Earthquake with a Precursory Increase in Fault-zone Conductivity", Pure and Applied Geophysics, Volume 150, pp. 217–248

Metzger A.E., Gilman D.A., Luthey J.L., Hurley K.C., Schnopper H.W., Seward F.D. and Sullivan J.D. (1983) - "The detection of X-rays from Jupiter", J. Geophys. Res, Volume 88, pp. 7731

Meyer B., Armijo R., Massonet D., De Chabalier J.B., Delacourt C., Ruegg J.C., Achache J. and Papanastasiou N. (1998) - "Results from combining tectonic observations and SAR interferometry for the 1995 Grevena earthquake.: A summary", J. Geodynamics, Volume 26, Issue 2-4, pp. 255-259

Molchanov O.A. and Hayakawa M. (1995) - "Generation of ULF electromagnetic emissions by microfracturing", Geophysical Research Letters, Volume 22, Issue 22, pp. 3091-3094

Molchanov O.A. and Hayakawa M. (1998a) - "Sub-ionospheric VLF signal perturbations possibly related to earthquakes", Journal of Geophysical Research, Volume 103, Issue A8, pp. 17489-17504

Molchanov O.A. and Hayakawa M. (1998b) - "On the generation mechanism of ULF seismogenic electromagnetic emissions", Physics of the Earth and Planetary Interiors, Volume 105, pp. 201-210

Morris A. S. (Editors), (2001) - "Measurement and Instrumentation Principles", Butterworth - Heinemann, 3rd Edition, pp. 475, ISBN: 978-0750650816

Mumma M. J., Krasnopolski V. A. and Abbott M. J. (1997) - "Soft X-rays from four comets observed with EUVE", The Astrophysical Journal, Volume 491, pp. L125-L128

National Aeronautics and Space Administration (NASA) (2007) - "Radio Waves" [Online]
Available: http://sxi.ngdc.noaa.gov/sxi_greatest.html

National Geophysical Data Center (NGDC) (2007) - "NOAA Satellite and Information Service" [Online]
Available: http://son.nasa.gov/tass/radiowaves/sat_goes5_e.htm

National Observatory of Athens (NOA) (2007) - "Institute of Geodynamics (NOAIG)" [Online]
Available: http://www.gein.noa.gr/index-en.htm

Nomicos C. and Giakoumakis G. (1985) - "A frequency division multiplexing system designed on the basis of an abrupt filter", IEEE Circuits and Devices, Volume 1, Issue 4, pp. 14

Nomicos C. (Editors), (1995) - "Telemetry", Technological Education Institute, 1st Edition, ISBN: 9607097499

Nomicos C. and Vallianatos F. (1998) - "Electromagnetic variations associated with the seismicity of the frontal Hellenic Arc", Geologica Carpathica, Volume 49, Issue 1, pp. 57–60

Nomicos C. and Vallianatos F. (1997) - "Transient electric variations associated with large intermediate-depth earthquakes in South Aegean", Tectonophysics, Volume 269, pp. 171-177

Nomicos C., Vallianatos F., Kaliakatsos I., Sideris E. and Bakatsakis M. (1997) - "The latest aspects of telluric and electromagnetic variations associated with shallow and intermediate depth earthquakes in the South Aegean", Annali di Geofisica, Volume XL, Issue 2, pp. 361-374

Oike K. and Yanada T. (Editors), (1994) - "Relationship between shallow earthquakes and electromagnetic noises in the LF and VLF ranges, (Electromagnetic Phenomena Related to Earthquake Prediction, Edited by Havakawa M. and Fujinawa Y.)", Terra Scientific Publishing Co., Tokyo, pp. 115-130, ISBN: 978-4887041134

Papazachos B. and Papazachou C. (Editors), (1997) - "The Earthquakes of Greece", P. Ziti and Co., Thessaloniki, pp. 304

Parrot M., Lefeuvre F., Corcuff. Y. and Godefroy P. (1985) - "Observation of VLF emission at the time of earthquakes in Kerguelen Islands", Annales. Geophys., Volume 3, pp. 731-736

Pham V.N., Boyer D., Chouliaras G., Savvaidis A., Stavrakakis G. and Le Mouel J.L. (2002) - "Sources of anomalous transient electric signals (ATESs) in the ULF band in the Lamia region (central Greece): electrochemical mechanisms for their generation", Phys. of the Earth and Plan. Inter., Volume 130, pp. 209-233

PHILIPS Semiconductors (1996) - "TSA5520, 1.3 GHz universal bus controller TV synthesizer", 9397-750-01353, Rev. 10/1996

PHILIPS Semiconductors (1997) - "SA605, High Performance Low Power Mixed FM IF System", Rev. 07/11/1997

PHILIPS Semiconductors (2000) - "The I^2C-bus Specification", ver 2.1

Qian S., Yian J., Cao H., Shi S., Lu Z., Li J. and Ren K. (Editors), (1994) - "Results of observations on seismoelectromagnetic waves at two earthquake experimental areas in China", Electromagnetic Phenomena Related to Earthquake Prediction, Edited by M.Hayakawa and Y. Fujinawa, TERRAPUB, Tokyo, pp.205-211

Ralchovsky T.M. and Komarov L. (1988) - "On electromagnetic precursors of the I'ranch 30 August 1986 earthquake", fa. ANSSSR. Fiz. Zhemli, Volume 11, pp. 72-77

Rikitake T. (1987) - "Magnetic and Electric Signals precursory to an earthquake: A Historical Review in Japan", Proceedings of International Workshop on SeismoElectromagnetics, Chofu , Tokyo, Volume 39, Issue 1, pp. 47-61

Ruzhin Y., Larkina V. and Depueva A. (1998) - "Earthquake precursors in Magnetically conjugated ionosphere regions", Adv. Space Res, Volume 21, Issue 3, pp. 525-528

SENSIRION Company (2003) - "SHT11, Humidity & Temperature Sensor", Rev. 2003

Sourceforge.Net (2003) - "ComPort Library" [Online]
Available: http://sourceforge.net/projects/comport

Surkov V.V., Molchanov O.A. and Hayakawa M. (2003) - "Pre-earthquake ULF electromagnetic perturbations as a result of inductive seismo-magnetic phenomena during micro-fracturing", Journal of Atmospheric and Solar-Terrestrial Physics, Volume 65, Issue 1, pp. 31-46

Szyperski C. (Editors), (2002) - "Component Software: Beyond Object-Oriented Programming", Addison-Wesley Professional, 2nd Edition, pp. 624, ISBN: 978-0201745726

Telit Communications (2004) - "GM862-GPRS, Cellular phone module with GPRS support", Rev. 10/ 2004

Texas Instruments Incorporated (2001) - "TLC279, LinCMOS™ Precision Quad Operation Amplifiers, SLOS092D", Rev. 03/2001

Tzanis A., Vallianatos F. and Gruszow S. (2000) - "Identification and discrimination of transient electrical earthquake precursors: Fact, fiction and some possibilities", Physics of the Earth and Planetary Interiors, Volume 121, pp. 223-248

U.S. Geological Survey (USGS) (2007) - "Earthquake Hazards Program"

Vallianatos F. and Nomicos K. (1998) - "Seismogenic radio-emissions as precursors to earthquakes in Greece", Phys. Chem. Earth, Volume 23, Issues 9-10, pp. 953-957

Varotsos P. and Alexopoulos K. (1984a) - "Physical properties of the variations of the electric field of the earth preceding earthquakes I.", Tectonophysics, Volume 110, pp. 73-98

Varotsos P. and Alexopoulos K. (1984b) - "Physical properties of the variations of the electric field of the earth preceding earthquakes. II Detection of epicentre and magnitude", Tectonophysics, Volume 110, pp. 99-125

Waite J. H. Jr., Bagenal F., Seward F., Na C., Gladstone G. R., Cravens T. E., Hurley K. C., Clarke J. T., Elsner R. and Stern S. A. (1994) - "ROSAT observations of the Jupiter aurora", J. Geophys. Res., Volume 99, Issue A8, pp. 14799-14809

Warwick J.W., Stoker C. and Meyer T.R. (1982) - "Radio emission associated with rock fracture: possible application for the Great Chilean Earthquake of 22 May 1960", J. Geophys. Res., Volume 87, pp. 2851–2859

Weber E., Ford N. and Weber C. (Editors), (1995) - "Developing With Delphi: Object-Oriented Techniques", Prentice Hall, 1st Edition, pp. 418, ISBN: 978-0133781182

Wu C. H., Chang L. P. and Kuo T. W. (2003) - "An efficient R-Tree implementation over flash-memory Storage Systems", ACM-GIS 2003, Proceedings of the Eleventh ACM International Symposium on Advances in Geographic Information Systems, New Orleans, Louisiana, USA, pp. 17-24, ISBN: 1-58113-730-3

Wu M. and Zwaenepoel W. (1994) - "eNVy: A non-volatile, main memory storage system", in Proc. ASPLOS VI, San Jose, CA, pp. 86-97

APPENDIX A' (Publications derived from Ph.D.)

Koulouras G., Kontakos K., Stavrakas I., Stonham J. and Nomicos C. (08/2005) - "Embedded Compact Flash™ – A new data storage system designed for a data acquisition system", IEEE Circuits and Devices Magazine, Volume 21, Issue 4, pp. 27-34, ISSN: 8755-3996

Stavrakas I., Clarke M., **Koulouras G.**, Stavrakakis G. and Nomicos C. (02/2007) - "Study of directivity effect on Electromagnetic emissions in the HF band as earthquake precursors: Preliminary results on field observations", Tectonophysics, Volume 431, Issue 1-4, pp. 263-271

Koulouras G., Kiourktsidis I., Nannos E., Kontakos K., Stonham J. and Nomicos C. - "Solar activity and Electromagnetic emissions in VHF band acquired from ground base monitors during «Martin Luther King Storm» happened on January 15th and 17th 2005", Tectonophysics, Submitted on 08/2007.

Koulouras G., Kontakos K., Minadakis G., Stavrakas I., Stonham J. and Nomicos C. (07/2005) - "A Data Acquisition System using Compact Flash™ memory", 2005 WSEAS 2nd International Conference on ENGINEERING EDUCATION, Vouliagmeni – Athens – Greece, pp. 519-524, ISBN: 960-8457-28-9

Pelegris P., Petropoulos F., Klimopoulos A., **Koulouras G.**, Kontakos K., Chatzidiakos P., Nassiopoulos A. and Nomicos C. (07/2005) - "A telemetric system based on GPRS technology", 2005 WSEAS 2nd International Conference on ENGINEERING EDUCATION, Vouliagmeni – Athens – Greece, pp. 528-531, ISBN: 960-8457-28-9

Georgiadis P., Piliouras N., Sidiropoulos K., **Koulouras G.**, Minadakis G., Cavouras D. and Nomicos C. (07/2005) - "Smartphone–based system for monitoring electromagnetic signals", 2006 WSEAS 2nd International Conference on ENGINEERING EDUCATION, Vouliagmeni – Athens – Greece, pp. 525-527, ISBN: 960-8457-28-9

Tsiriggakis V., Efthimiatos K., **Koulouras G.**, Stavrakas I., Kapiris P., Ninos K., Katsimaglis G., Voudouris K., Banitsas K., Eftaxias K., Koulopoulos A., Panagiotopoulos L. and Nomicos C. (07/2005) - "A versatile telemetric system based on mixed Internet and wireless transmission", 2007 WSEAS 2nd International Conference on ENGINEERING EDUCATION, Vouliagmeni – Athens – Greece, pp. 532-536, ISBN: 960-8457-28-9

Piliouras N., Kalatzis I., Georgiadis P., Ninos D., **Koulouras G.**, Minadakis G., Cavouras D. and Nomikos C. (09/2004) - "Electromagnetic seismic signal analysis employing pattern recognition methods", 1st International Conference "From Scientific Computing to Computational Engineering" – Athens – Greece, ISBN: 960-8457-28-9

Kapiris P., Nomikos K., Kopanas J., Antonopoulos G., **Koulouras G.**, Skountzos P., Zissos A., Mylonas S. and Eftaxias K. (09/2004) - "Lessons from the Athens earthquake", 4th International Workshop on magnetic, electric and electromagnetic methods in seismology and volcanology, La Londe les Maures – France

Stavrakas I., **Koulouras G.**, Nomicos C., Melis N. and Stavrakakis G. (11/2003) - "Algorithmic analysis of Electromagnetic variations possibly related to earthquake events", 1st International Conference on Earthquake Prediction, Athens – Greece

Koulouras G., Kontakos K., Avgoustis G., Stonham J., Ruzhin Y., Stavrakakis G., Eftaxias C. and Nomicos C. (04/2007) - "Electromagnetic emissions in the 142 to 415 MHZ band", European Geosciences Union 2007, Geophysical Research Abstracts, Vienna - Austria, Volume 9, SRef-ID: EGU2007-A-04778

Ruzhin Yu., Nomicos C., Afraimovich E., Bershadskaya I., **Koulouras G.** and Fomichev V. (04/2007) - "On possibility of seismic VHF network calibration by simultaneous observations of solar flare radio emission at spaced sites", European Geosciences Union 2007, Geophysical Research Abstracts, Vienna - Austria, Volume 9, SRef-ID: EGU2007-J-04801

Stavrakas I., Clarke M., **Koulouras G.**, Stavrakakis G. and Nomicos C. (04/2006) - "Study of Electromagnetic emissions in the HF band earthquake precursors", European Geosciences Union 2006, Geophysical Research Abstracts, Vienna - Austria, Volume 8, SRef-ID: EGU06-A-07568

Koulouras G., Kontakos K., Minadakis G., Stonham J., Stavrakakis G., Nomicos C. (04/2006) - "Capturing Electromagnetic Emissions in the VHF Band possibly related to Earthquake Activity", European Geosciences Union 2006, Geophysical Research Abstracts, Vienna - Austria, Volume 8, SRef-ID: EGU06-A-10156

APPENDIX B' (Specifications - Schematics - PCBs)

SPECIFICATION OF DATA ACQUISITION SYSTEM

Physical Characteristics	
Dimensions	With Mounting Plate: 10.5cm L x 20.5cm W x 6cm H
Weight	Approximately ~1.2 kg (battery pack included)
Peripherals (Communications)	
Peripheral RS-232 Port	9pin connector, 300bps to 115.2Kbps data rate with Autobaud(default 38400)
Analog Inputs	Up to 8 Input channels 10bit(0 .. 2500mV DC / 1MΩ Impedance) Up to 8 Input channels 12bit(0 .. 5000mV DC / 1MΩ Impedance)
VHF Scanner	Up to 8 Monitoring Frequencies (Range: 70MHz to 470MHz) (ADC Resolution: 12bit)
Temperature Inputs	Up to 8 temperature inputs via I/O expander (12bit, -55 ... +125°C, ±0.5°C accuracy)
LCD Display	2 lines x 20 characters LCD with backlight
Informative LEDs	1 power led 1 reset led 1 CF access led
Buttons	1 reset button 1 informative mode selection button
System Characteristics	
CPU	Atmel Mega AVR 128 (128KB Flash, 4KB SRAM, 4KB EEPROM)
Operating System	Custom made Operating System implementing all necessary functions/drivers
Storage	Embedded Compact Flash Card socket (reads/writes CF type I & II cards 32MB to 8GB)
Data File System	Efficient Data File System that increases CF lifetime. (DSS ver 1.0)
Real Time Clock	Battery Backup Real Time clock with leap year compensation up to 2100.
Input Voltage	9-36 V DC
Battery Backup	1.2Ah backup battery. Provides 12 hours of operation after complete loss of primary power
Environmental Characteristics	
Operating Temperature	Typically -20 .. +55°C (Depends on the independent characteristics of the components used)
Storage Temperature	-30 .. +80°C
General Characteristics	
Firmware Update	Remote Firmware Update Capability
Communication Options	RS232, RS485, Ethernet, WiFi, GPRS
Multi-slave connection	Up to 65K devices. Each device has its own ID.
Installation	Easy Installation

DATA ACQUISITION SCHEMATIC DIAGRAM

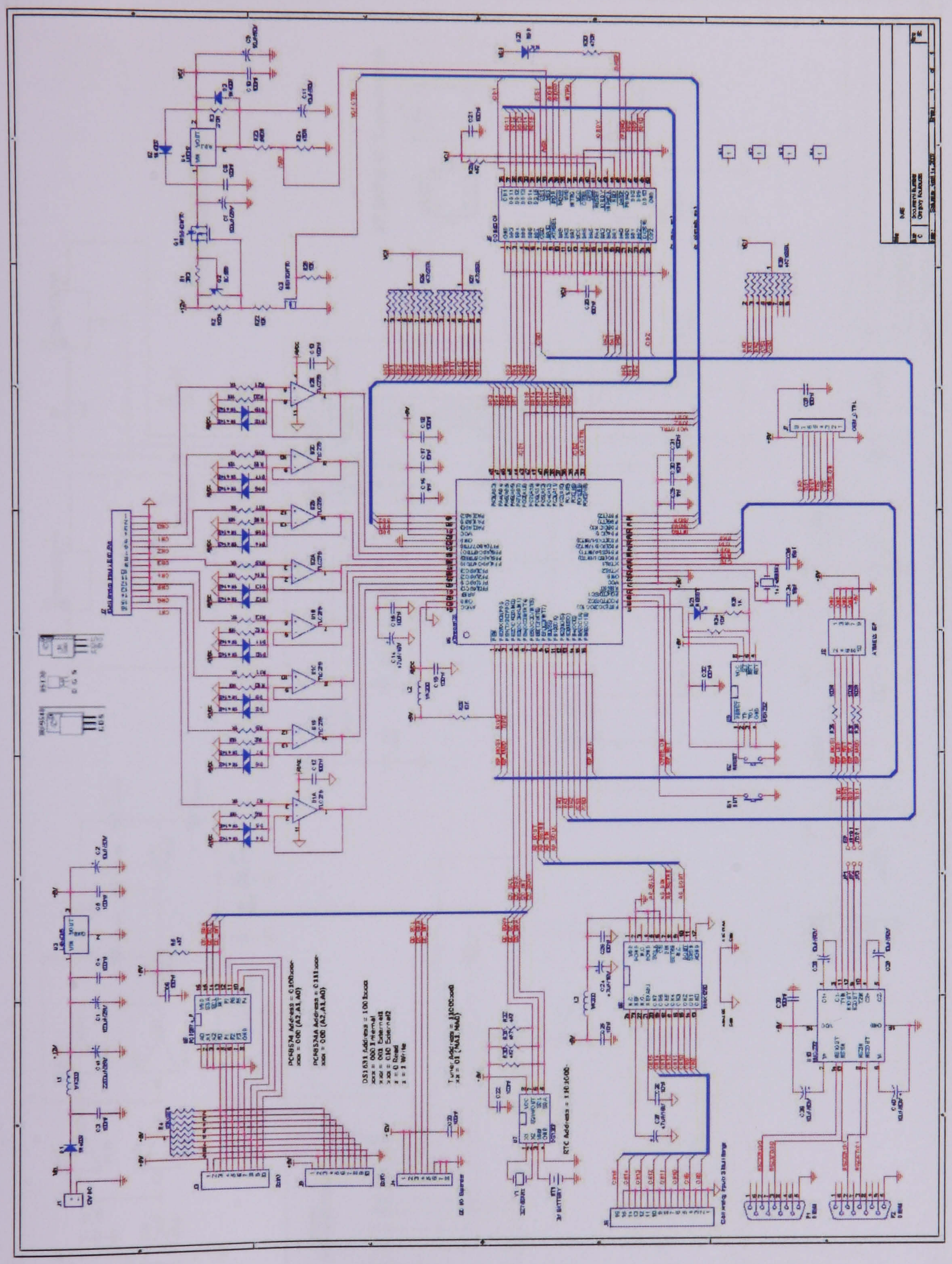

DAS VHF RECEIVER SCHEMATIC DIAGRAM

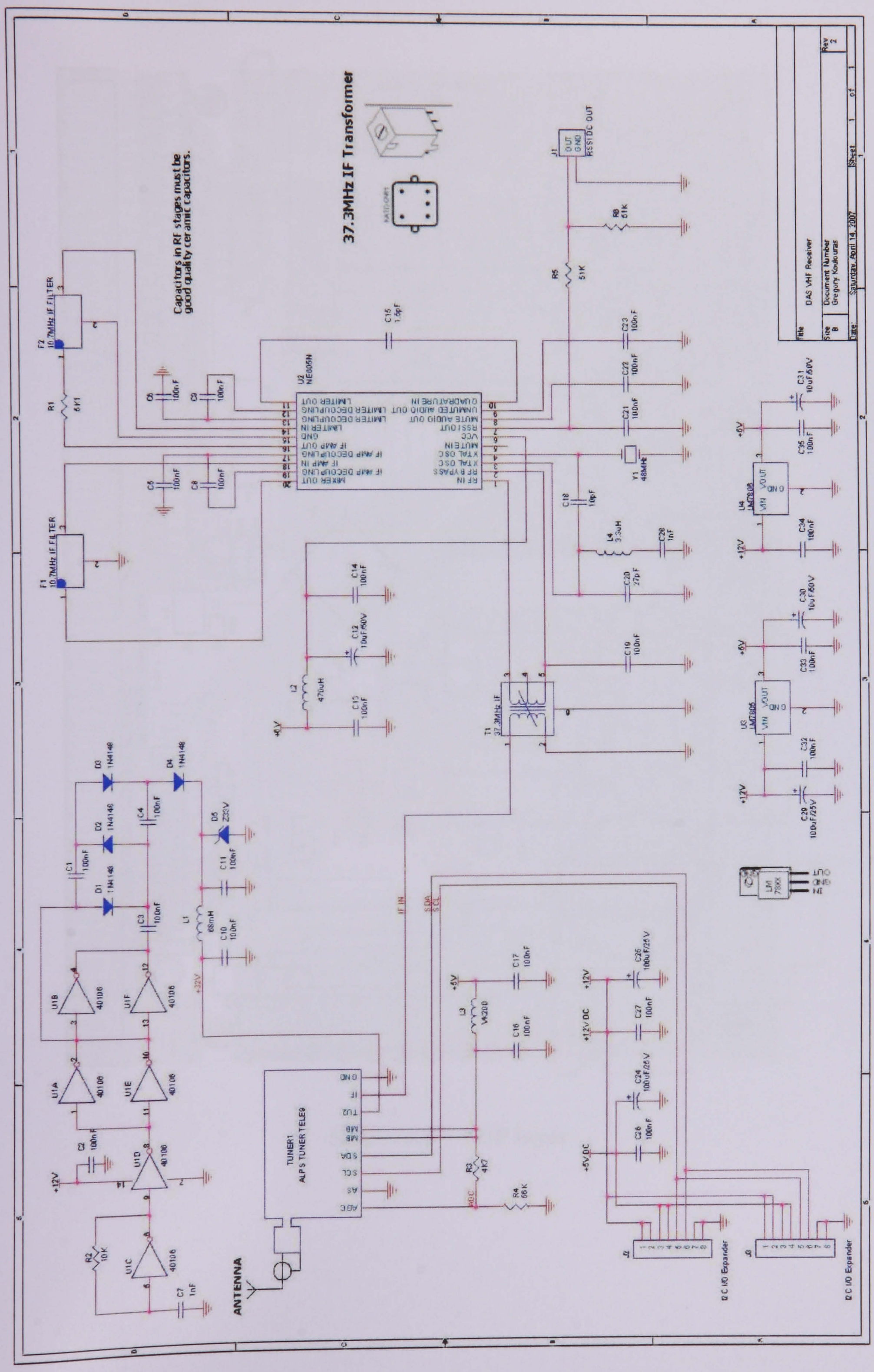

DATA ACQUISITION PRINTED CIRCUIT BOARD

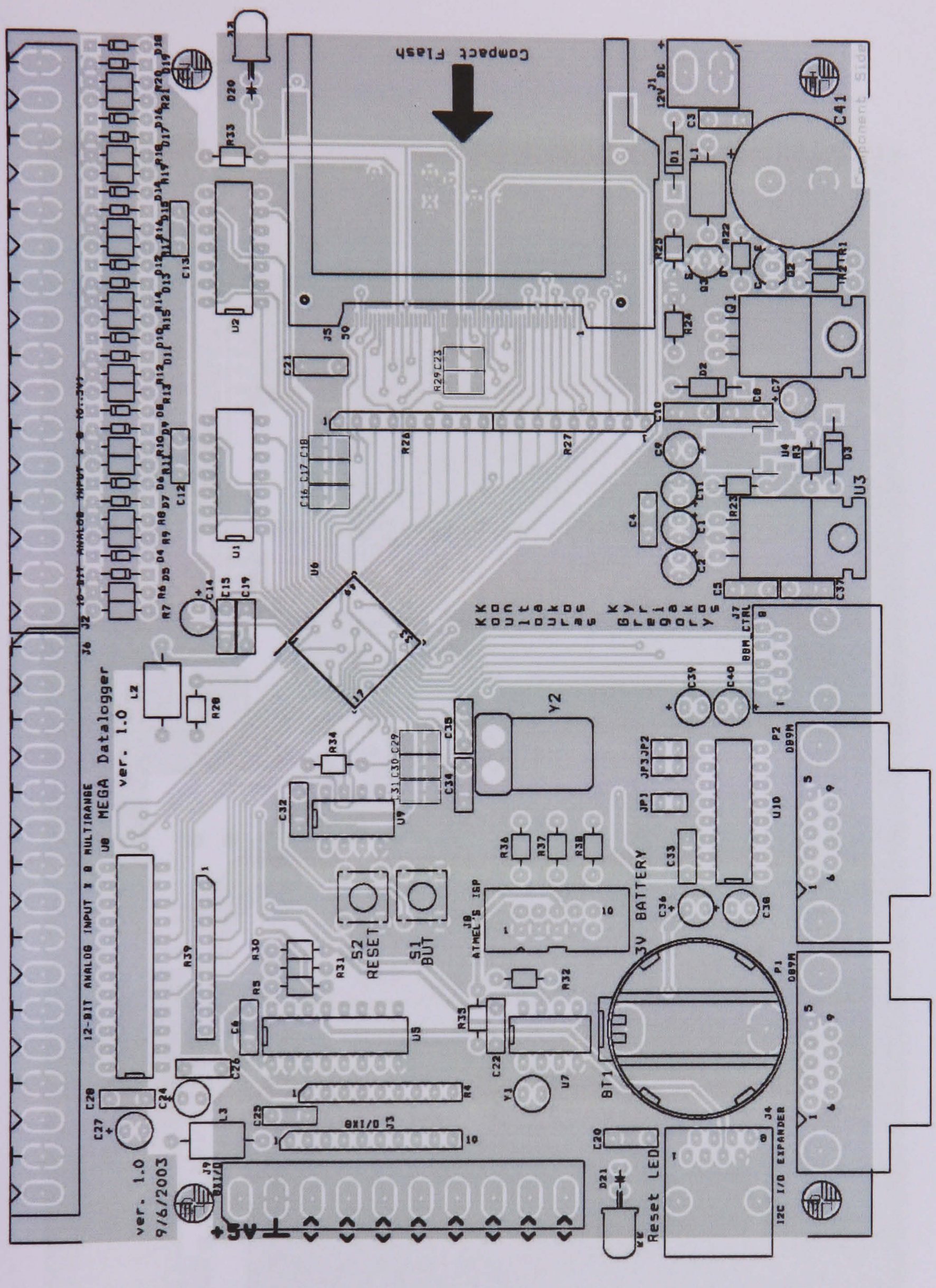

Silkscreen - TOP layer

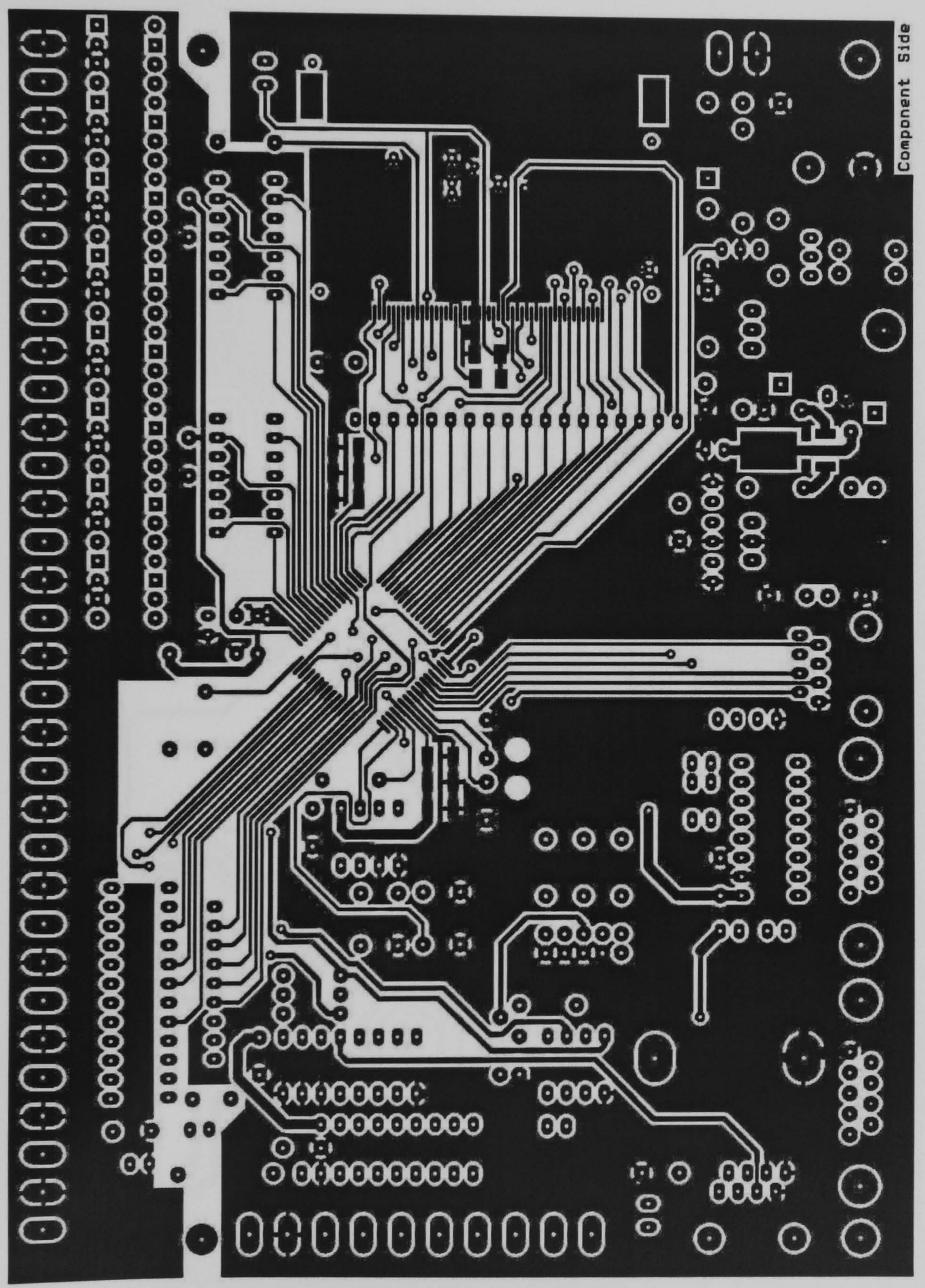

Copper - TOP layer

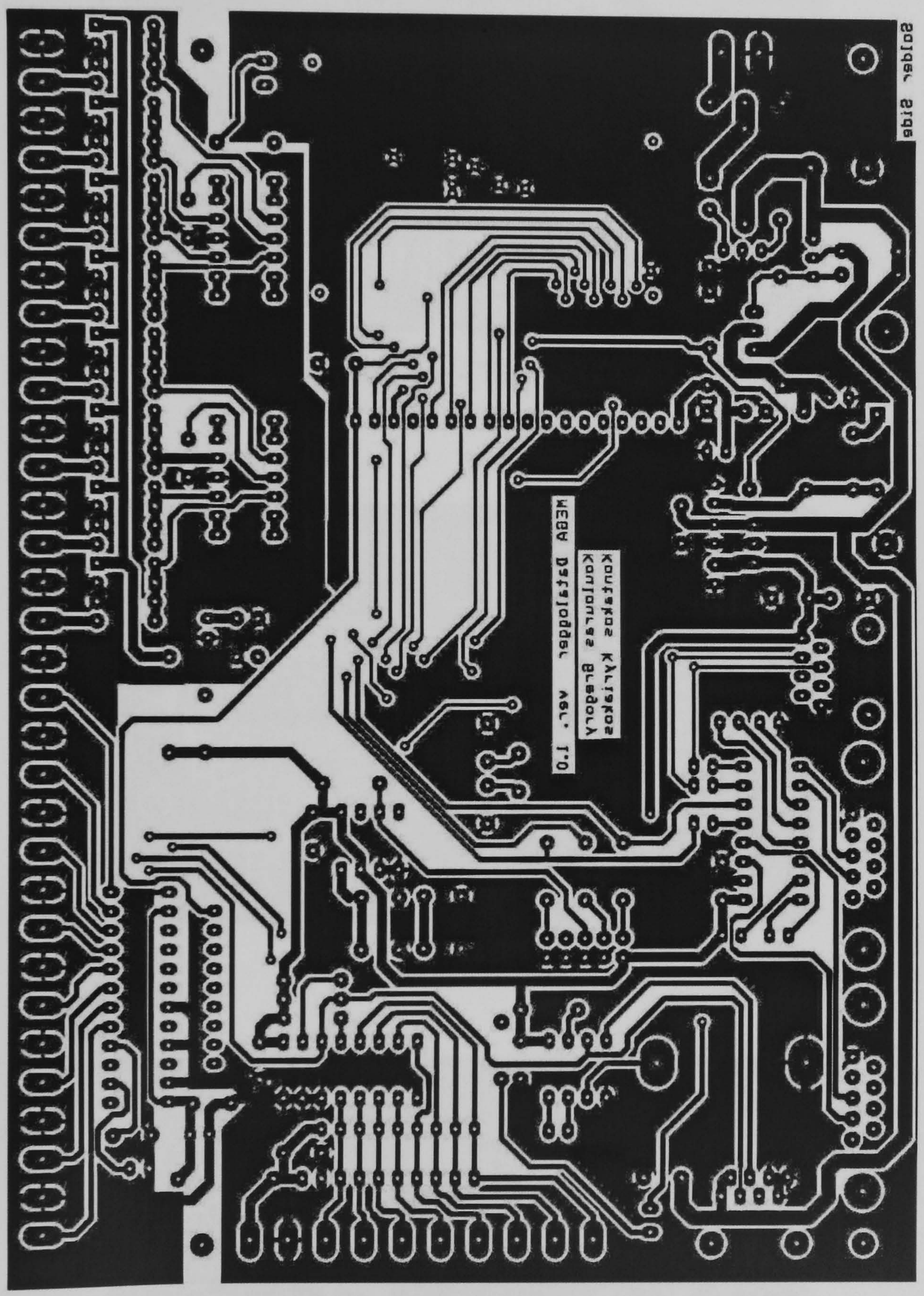

Copper - BOTTOM layer

VHF TUNER PRINTED CIRCUIT BOARD

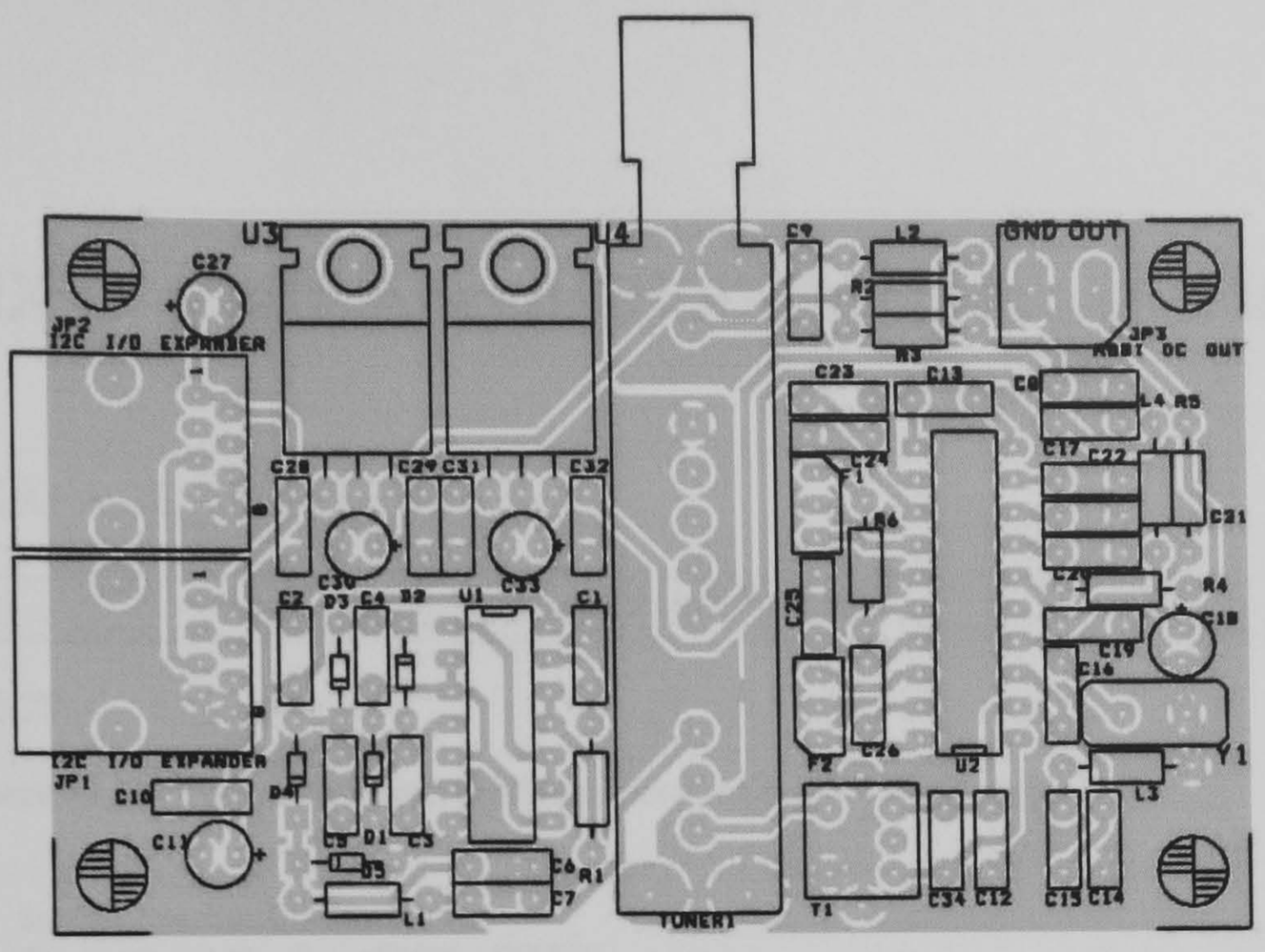

Silkscreen - TOP layer

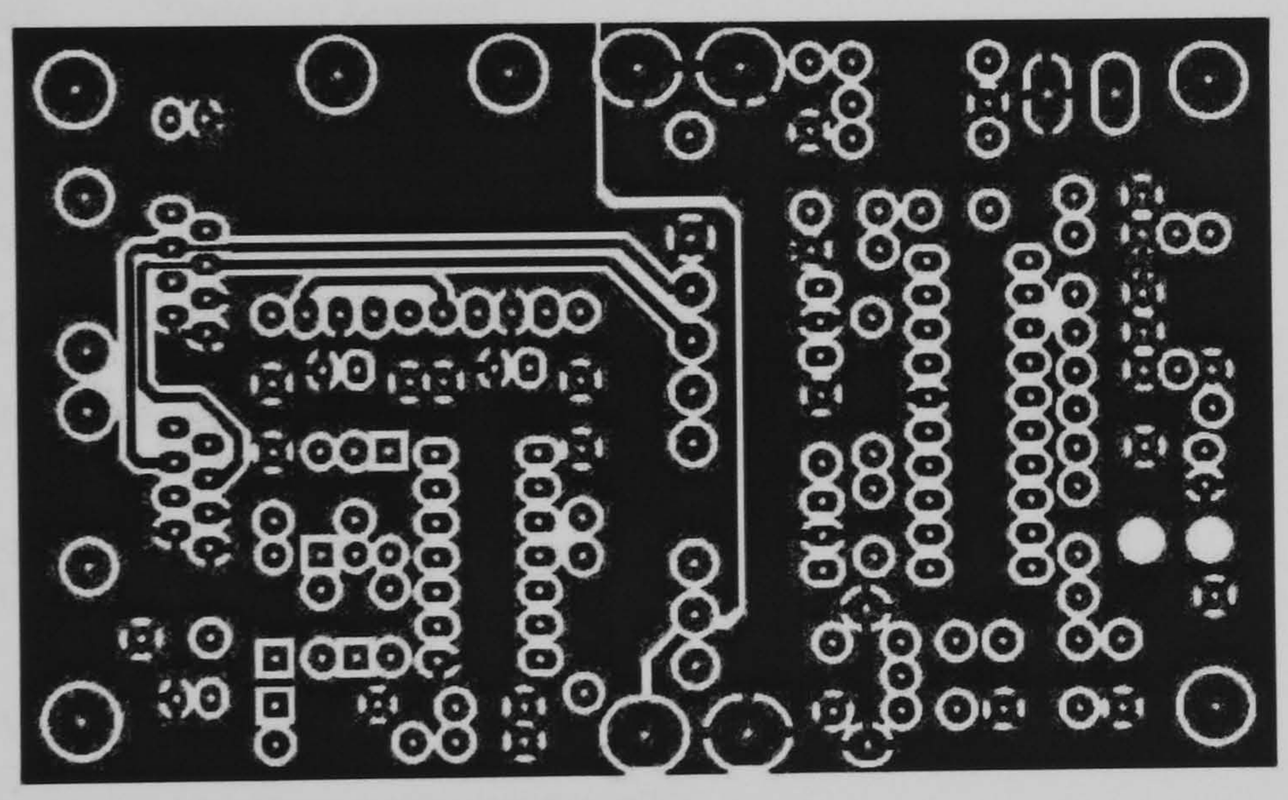

Copper - TOP layer

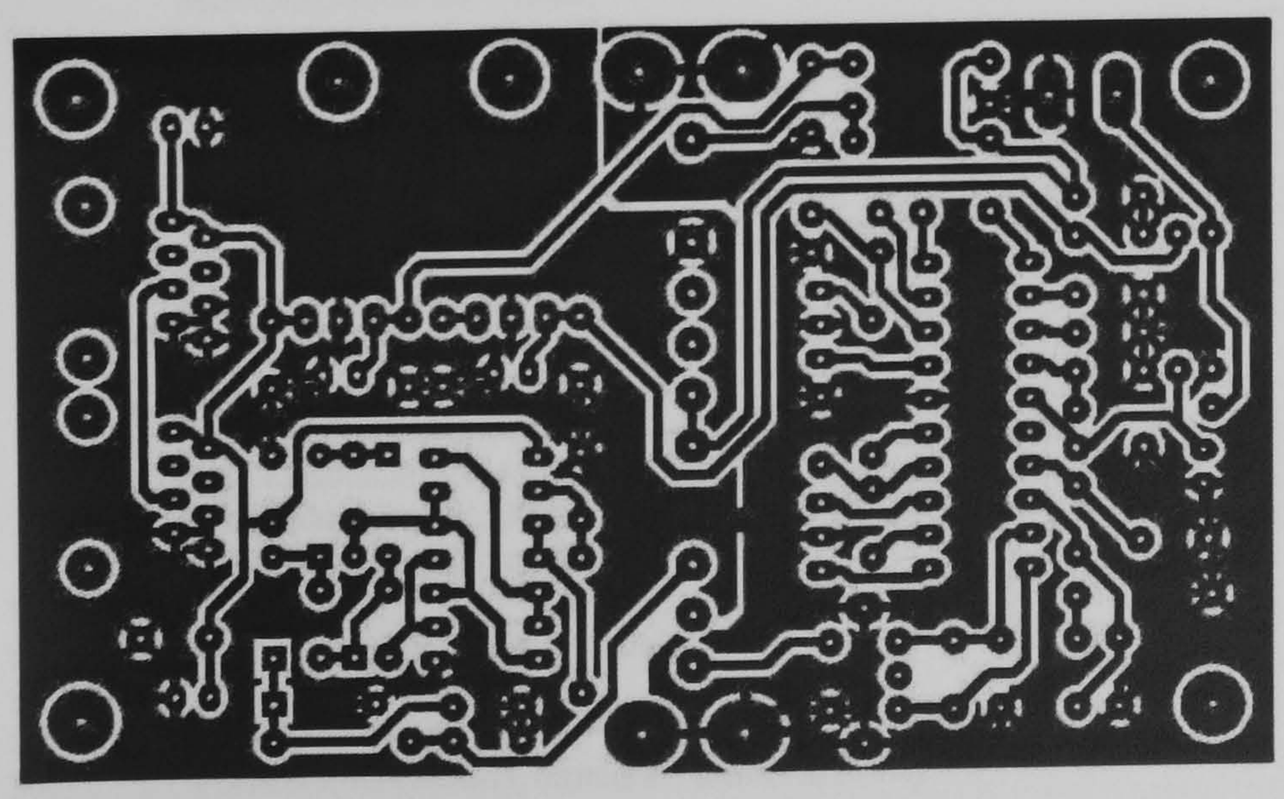

Copper - BOTTOM layer

APPENDIX C' (Data Acquisition System - API interface)

API FUNCTIONS

SERIAL INTERFACE LIBRARIES

GENERAL FUNCTIONS

DEVICE CONNECT

function DeviceConnect(var ComPort: TComPort; SerialNum:Word; var Retries: Byte): Byte;

INPUT:
ComPort: Serial Com Port Component
Serial: Device Serial Number {$0000...$FFFF)
Retries: Number of retries {$00...$FF)

OUTPUT:
Retries: Number of retries left
DeviceConnect: Result Byte
$00: ' Password Accepted!'
$01: 'ComPort is Closed!'
$02: 'Device is not Alive!'
$03: ' Wrong Password '
$04: 'CRC Error Detected'
$05: 'Unknown Error'

HARDWARE & SOFTWARE VERSION INFORMATION

function CommandVER(var ComPort: TComPort; Serial:Word; var VersionInfo:TDTL_VersionInfo):Byte;

INPUT:
ComPort: Serial Com Port Component
Serial: Device Serial Number {$0000...$FFFF)

OUTPUT:
VersionInfo: Version Informarion Record (Main – BackUp – BooTLoader)
MainSoftwareVersion: String[13];
MainHardwareVersion: String[7];
MainDeviceName: String[16];
MainDeviceDescription: String[31];
MainDeviceIdentifier: String[7];
MainDateModified: TDate;
BackUpSoftwareVersion: String[13];
BackUpHardwareVersion: String[7];
BackUpDeviceName: String[16];
BackUpDeviceDescription: String[31];
BackUpDeviceIdentifier: String[7];
BackUpDateModified: TDate;
BooTLoaderSoftwareVersion: String[13];
BooTLoaderHardwareVersion: String[7];
BooTLoaderDeviceName: String[16];
BooTLoaderDeviceDescription: String[31];
BooTLoaderDeviceIdentifier: String[7];
BooTLoaderDateModified: TDate;
BooTLoaderSerialNumber: Word;
CommandVER: Result Byte
$00: 'Version Information is Availiable'
$01: 'ComPort is Closed!'
$02: 'Device is not Alive!'
$03: 'Version Information Command Needs Authority'
$04: 'CRC Error Detected'
$05: 'Unknown Error'

RESET FUNCTIONS

SOFTWARE RESET – MAIN PROGRAM IS RUNNING

function CommandRUN(var ComPort: TComPort; Serial:Word): Byte;

INPUT:
ComPort: Serial Com Port Component
Serial: Device Serial Number {$0000...$FFFF)

OUTPUT:
CommandRUN: Result Byte
$00: 'Software Reset. Main program is Running...'
$01: 'ComPort is Closed!'
$02: 'Device is not Alive!'
$03: 'RUN Command Needs Authority'
$04: 'CRC Error Detected'
$05: 'Unknown Error'

SOFTWARE RESET – BOOTLOADER PROGRAM IS RUNNING

function CommandSRS(var ComPort: TComPort; Serial:Word): Byte;

INPUT:
ComPort: Serial Com Port Component
Serial: Device Serial Number {$0000...$FFFF)

OUTPUT:
CommandSRS: Result Byte
$00: 'Software Reset. BooTLoader is Running...'
$01: 'ComPort is Closed!'
$02: 'Device is not Alive!'
$03: 'Software Reset Command Needs Authority'
$04: 'CRC Error Detected'
$05: 'Unknown Error'

HARDWARE RESET – BOOTLOADER PROGRAM IS RUNNING

function CommandHRS(var ComPort: TComPort; Serial:Word): Byte;

INPUT:
ComPort: Serial Com Port Component
Serial: Device Serial Number {$0000...$FFFF)

OUTPUT:
CommandHRS: Result Byte
$00: 'Hardware Reset. BooTLoader is Running...'
$01: 'ComPort is Closed!'
$02: 'Device is not Alive!'
$03: 'Hardware Reset Command Needs Authority'
$04: 'CRC Error Detected'
$05: 'Unknown Error'

DATE – TIME FUNCTIONS

READ "DATE – TIME"

function CommandRTD(var ComPort: TComPort; Serial:Word; var DateTime:TDateTime):Byte;

INPUT:
ComPort: Serial Com Port Component
Serial: Device Serial Number {$0000...$FFFF)

OUTPUT:
DateTime: Date Time Output Value
CommandRTD: Result Byte
$00: 'DateTime is Availiable!'
$01: 'ComPort is Closed!'
$02: 'Device is not Alive!'
$03: 'Read TimeDate Command Needs Authority'
$04: 'CRC Error Detected'
$05: 'Unknown Error'

WRITE "DATE – TIME"

function CommandWTD(var ComPort: TComPort; Serial:Word; DateTime:TDateTime; RTCEnable:Boolean):Byte;

INPUT:
ComPort: Serial Com Port Component
Serial: Device Serial Number {$0000...$FFFF)
DateTime: Date Time Input Value
RTCEnable: Enable or Disable RTC (Real Time Clock)

OUTPUT:
CommandRTD: Result Byte
$00: ' RTC updated successfully!'
$01: 'ComPort is Closed!'
$02: 'Device is not Alive!'
$03: ' Write TimeDate Command Needs Authority'
$04: 'CRC Error Detected'
$05: 'Unknown Error'

COMPACT FLASH FUNCTIONS

READ "CURRENT LBA" FROM COMPACT FLASH

function CommandRCF(var ComPort: TComPort; Serial:Word; LBAAddress:DWord; var ReceivedData : Array of Byte): Byte;

INPUT:
ComPort: Serial Com Port Component
Serial: Device Serial Number {$0000...$FFFF)
LBAAddress: LBA Address {$00000000...Size Of Compact Flash}

OUTPUT:
ReceivedData: Array of 512 Byte
CommandRCF: Result Byte
$00: 'LBA Readed Successfully'
$01: 'ComPort is Closed!'
$02: 'Device is not Alive!'
$03: 'Read LBA Command Needs Authority'
$04: 'CRC Error Detected'
$05: 'Unknown Error'

ERASE "CURRENT LBA" FROM COMPACT FLASH

function CommandECF(var ComPort: TComPort; Serial:Word; LBAAddress:DWord): Byte;

INPUT:
ComPort: Serial Com Port Component
Serial: Device Serial Number {$0000...$FFFF)
LBAAddress: LBA Address {$00000000...Size Of Compact Flash}

OUTPUT:
CommandECF: Result Byte
$00: 'LBA Erased Successfully'
$01: 'ComPort is Closed!'
$02: 'Device is not Alive!'
$03: 'Erase LBA Command Needs Authority'
$04: 'CRC Error Detected'
$05: 'Unknown Error'

WRITE "CURRENT LBA" TO COMPACT FLASH

function CommandWCF(var ComPort: TComPort; Serial:Word; LBAAddress:DWord; TransmitedData: Array of Byte): Byte;

INPUT:
ComPort: Serial Com Port Component
Serial: Device Serial Number {$0000...$FFFF)
LBAAddress: LBA Address {$00000000...Size Of Compact Flash}
TransmitedData: Array of 512 Byte

OUTPUT:
CommandWCF: Result Byte
$00: 'LBA Writted Successfully'
$01: 'ComPort is Closed!'
$02: 'Device is not Alive!'
$03: 'Write LBA Command Needs Authority'
$04: 'CRC Error Detected'
$05: 'Unknown Error'

READ "COMPACT FLASH STATUS"

function CommandSCF(var ComPort: TComPort; Serial:Word; var CF_Status:TCF_Status):Byte;

INPUT:
ComPort: Serial Com Port Component
Serial: Device Serial Number {$0000...$FFFF)

OUTPUT:
CF_Status: Compact Flash Status Record
DataReg: Word;
ErrorReg: Byte;
FeaturesReg: Byte;
SectorCountReg: Byte;
LBAReg: DWord;
StatusReg: Byte;
CommandReg: Byte;
AlternateReg: Byte;
DeviceControlReg: Byte;
DriveAddressReg: Byte;
CF_Size: DWord;

CommandSCF: Result Byte
$00: 'Compact Flash Status is Availiable'
$01: 'ComPort is Closed!'
$02: 'Device is not Alive!'
$03: 'Compact Flash Status Command Needs Authority'
$04: 'CRC Error Detected'
$05: 'Unknown Error'

READ "COMPACT FLASH IDENTITY"

function CommandICF(var ComPort: TComPort; Serial:Word; var CF_Identity: TCF_Identity):Byte;

INPUT:
ComPort: Serial Com Port Component
Serial: Device Serial Number {$0000...$FFFF)

OUTPUT:
CF_Identity: Compact Flash Identity Record
GeneralConfigurationInformation: Word;
NumberOfCylinders: Word;
NumberOfHeads: Word;
NumberOfUnformattedBytesPerTrack: Word;
NumberOfUnformattedBytesPerSector: Word;
NumberOfSectorsPerTrack: Word;
NumberOfSectorsPerCard: DWord;
VendorUnique: Word;
SerialNumber: String[20];
BufferType: Word;
BufferSize: Word;
ECCLength: Word;
FirmwareVersion: String[8];
ModelNumber: String[40];
MaximumBlockCount: Word;
DWordIOSupport: Word;
Capabilities: Word;
PIOTimingMode: Word;
DMATransferTimingMode: Word;
TranslationParameters: Word;
NumberOfCurrentCylinders: Word;
NumberOfCurrentHeads: Word;
NumberOfCurrentSectorsPerTrack: Word;
CurrentCapacityInSectors: DWord;
CurrentSettingForBlockCount: Word;
TotalNumberOfAddressableLBAMode: DWord;
SecurityStatus: Word;
PowerRequirementDescription: Word;
CommandICF: Result Byte
$00: 'Compact Flash Identify Information is Availiable'
$01: 'ComPort is Closed!'
$02: 'Device is not Alive!'
$03: 'Compact Flash Identify Information Command Needs Authority'
$04: 'CRC Error Detected'
$05: 'Unknown Error'

READ "COMPACT FLASH WRITE POINTER"

function CommandPCF(var ComPort: TComPort; Serial:Word; var WritePointer: TCF_Pointer):Byte;

INPUT:
ComPort: Serial Com Port Component
Serial: Device Serial Number {$0000...$FFFF)

OUTPUT:
WritePointer: Compact Flash Write Pointer Record
PacketNumber: DWord;
NextLBA: DWord;
ReadCounter: Byte;

CommandPCF: Result Byte
$00: 'Compact Flash Write Pointer is Availiable'
$01: 'ComPort is Closed!'
$02: 'Device is not Alive!'
$03: 'Read "Write Pointer" Command Needs Authority'
$04: 'CRC Error Detected'
$05: 'Unknown Error'

WRITE "COMPACT FLASH READ POINTER"

function CommandLCF(ComPort: TComPort; Serial:Word; ReadPointer: TCF_ReadPointer):Byte;

INPUT:
ComPort: Serial Com Port Component
Serial: Device Serial Number {$0000...$FFFF)
ReadPointer: Compact Flash Write Pointer Record
LastReadLBA: DWord;

OUTPUT:

CommandLCF: Result Byte
$00: 'Compact Flash Read Pointer is Availiable'
$01: 'ComPort is Closed!'
$02: 'Device is not Alive!'
$03: 'Write "Read Pointer" Command Needs Authority'
$04: 'CRC Error Detected'
$05: 'Unknown Error'

MEASURE NOW FUNCTIONS

READ "LCD" REMOTELY

function ReadSRAMLCDInfo(var ComPort: TComPort; Serial: Word; var LCDInfo: TDLG_LCDInfo):Byte;

INPUT:
ComPort: Serial Com Port Component
Serial: Device Serial Number {$0000...$FFFF)

OUTPUT:

LCDInfo: LCD Information Record
Line1: String[40];
Line2: String[40];
Line3: String[40];
Line4: String[40];
ReadSRAMLCDInfo: Result Byte
$00: 'LCD information is Availiable'
$01: 'ComPort is Closed!'
$02: 'Device is not Alive!'
$03: 'Read LCD remotely Command Needs Authority'
$04: 'CRC Error Detected'
$05: 'Unknown Error'

READ "INTERNAL ADC 10BIT" REMOTELY

function ReadSRAMIntADC(var ComPort: TComPort; Serial: Word; Settings: TCF_LBASettings; var AllMeasurements: TDTL_AllMeasurements): Byte;

INPUT:
ComPort: Serial Com Port Component
Serial: Device Serial Number {$0000...$FFFF)
Settings: Device Settings Record
Header: TCF_LBAHeader;
Info: TCF_LBAInfo;
CRC16: DWord;
ErrorCheck: Byte;

OUTPUT:
AllMeasurements: Real Time Measurements Record
IntADC_Value: Array[0..7] of Real;
ExtADC_Value: Array[0..7] of Real;
Temperature_Value: Array[0..7] of Real;
Tuner_Value: Array[0..7] of Real;
GPS_Value: String[80];
ReadSRAMIntADC: Result Byte
$00: 'Internal ADC Values are Availiable'
$01: 'ComPort is Closed!'
$02: 'Device is not Alive!'
$03: 'Internal ADC Values Command Needs Authority'
$04: 'CRC Error Detected'
$05: 'Unknown Error'

READ "EXTERNAL ADC 12BIT" REMOTELY

function ReadSRAMExtADC(var ComPort: TComPort; Serial: Word; Settings: TCF_LBASettings; var AllMeasurements: TDTL_AllMeasurements): Byte;

INPUT:
ComPort: Serial Com Port Component
Serial: Device Serial Number {$0000...$FFFF)
Settings: Device Settings Record
Header: TCF_LBAHeader;
Info: TCF_LBAInfo;
CRC16: DWord;
ErrorCheck: Byte;

OUTPUT:
AllMeasurements: Real Time Measurements Record
IntADC_Value: Array[0..7] of Real;
ExtADC_Value: Array[0..7] of Real;
Temperature_Value: Array[0..7] of Real;
Tuner_Value: Array[0..7] of Real;
GPS_Value: String[80];
ReadSRAMExtADC: Result Byte
$00: 'External ADC Values are Availiable'
$01: 'ComPort is Closed!'
$02: 'Device is not Alive!'
$03: 'External ADC Values Command Needs Authority'
$04: 'CRC Error Detected'
$05: 'Unknown Error'

READ "TEMPERATURES" REMOTELY

function ReadSRAMTemperature(var ComPort: TComPort; Serial: Word; Settings: TCF_LBASettings; var AllMeasurements: TDTL_AllMeasurements): Byte;

INPUT:
ComPort: Serial Com Port Component
Serial: Device Serial Number {$0000...$FFFF)
Settings: Device Settings Record
Header: TCF_LBAHeader;
Info: TCF_LBAInfo;
CRC16: DWord;
ErrorCheck: Byte;

OUTPUT:
AllMeasurements: Real Time Measurements Record
IntADC_Value: Array[0..7] of Real;
ExtADC_Value: Array[0..7] of Real;
Temperature_Value: Array[0..7] of Real;
Tuner_Value: Array[0..7] of Real;
GPS_Value: String[80];
ReadSRAMTemperature:
Result Byte
$00: 'Temperature Values are Availiable'
$01: 'ComPort is Closed!'
$02: 'Device is not Alive!'
$03: 'Temperature Values Command Needs Authority'
$04: 'CRC Error Detected'
$05: 'Unknown Error'

READ "TUNER FREQUENCIES" REMOTELY

function ReadSRAMTuner(var ComPort: TComPort; Serial: Word; Settings: TCF_LBASettings; var AllMeasurements: TDTL_AllMeasurements): Byte;

INPUT:
ComPort: Serial Com Port Component
Serial: Device Serial Number {$0000...$FFFF)
Settings: Device Settings Record
Header: TCF_LBAHeader;
Info: TCF_LBAInfo;
CRC16: DWord;
ErrorCheck: Byte;

OUTPUT:
AllMeasurements: Real Time Measurements Record
IntADC_Value: Array[0..7] of Real;
ExtADC_Value: Array[0..7] of Real;
Temperature_Value: Array[0..7] of Real;
Tuner_Value: Array[0..7] of Real;
GPS_Value: String[80];

ReadSRAMTemperature:
Result Byte
$00: 'Tuner Values are Availiable'
$01: 'ComPort is Closed!'
$02: 'Device is not Alive!'
$03: 'Tuner Values Command Needs Authority'
$04: 'CRC Error Detected'
$05: 'Unknown Error'

INFORMATION FUNCTIONS

READ "FORMAT SETTINGS" FROM COMPACT FLASH

function ReadCFFormatSettings(var ComPort: TComPort; Serial: Word; var CFSettings: Array of Byte):Byte;

INPUT:
ComPort: Serial Com Port Component
Serial: Device Serial Number {$0000...$FFFF)

OUTPUT:
CFSettings: Device Settings Array of 512 Bytes

ReadCFFormatSettings:
Result Byte
$00: 'Compact Flash Format Settings are Availiable'
$01: 'ComPort is Closed!'
$02: 'Device is not Alive!'
$03: 'Read Compact Flash Format Settings Command Needs Authority'
$04: 'CRC Error Detected'
$05: 'Unknown Error'

READ "FORMAT SETTINGS" FROM EEPROM

function ReadEEFormatSettings(var ComPort: TComPort; Serial: Word; var EESettings: Array of Byte):Byte;

INPUT:
ComPort: Serial Com Port Component
Serial: Device Serial Number {$0000...$FFFF)

OUTPUT:
EESettings: Device Settings Array of 512 Bytes

ReadEEFormatSettings:
Result Byte
$00: 'EEPROM Format Settings are Availiable'
$01: 'ComPort is Closed!'
$02: 'Device is not Alive!'
$03: 'Read EEPROM Format Settings Command Needs Authority'
$04: 'CRC Error Detected'
$05: 'Unknown Error'

WRITE "FORMAT SETTINGS" TO EEPROM

function WriteEEFormatSettings(var ComPort: TComPort; Serial: Word; EESettings: Array of Byte):Byte;

INPUT:
ComPort: Serial Com Port Component
Serial: Device Serial Number {$0000...$FFFF)
EESettings: Device Settings Array of 512 Bytes

OUTPUT:

WriteEEFormatSettings:
Result Byte
$00: 'EEPROM Format Settings updated successfully'
$01: 'ComPort is Closed!'
$02: 'Device is not Alive!'
$03: 'Update EEPROM Format Settings Command Needs Authority'
$04: 'CRC Error Detected'
$05: 'Unknown Error'

READ "BOOT INFORMATION" FROM EEPROM

function ReadEEBootInfo(var ComPort: TComPort; Serial: Word; var BTLBootInfo, MainBootInfo: TDTL_TimeStampInfo):Byte;

INPUT:
ComPort: Serial Com Port Component
Serial: Device Serial Number {$0000...$FFFF)

OUTPUT:
BTLBootInfo: BooTLoader Information Reset Counter
ValidA: Boolean;
CounterA: Word;
TimeA: TDateTime;
ValidB: Boolean;
CounterB: Word;
TimeB: TDateTime;
MainBootInfo: Main Program Information Reset Counter
ValidA: Boolean;
CounterA: Word;
TimeA: TDateTime;
ValidB: Boolean;
CounterB: Word;
TimeB: TDateTime;
ReadEEBootInfo:
Result Byte
$00: 'Read EEPROM Reset Information successfully'
$01: 'ComPort is Closed!'
$02: 'Device is not Alive!'
$03: 'Read EEPROM Reset Information Command Needs Authority'
$04: 'CRC Error Detected'
$05: 'Unknown Error'

READ "UPGRADE INFORMATION" FROM EEPROM

function ReadEEWrFlashInfo(var ComPort: TComPort; Serial: Word; var BackUpWrFlashInfo, MainWrFlashInfo: TDTL_TimeStampInfo):Byte;

INPUT:
ComPort: Serial Com Port Component
Serial: Device Serial Number {$0000...$FFFF)

OUTPUT:
BackUpWrFlashInfo: Upgrade Information BackUp Program
ValidA: Boolean;
CounterA: Word;
TimeA: TDateTime;
ValidB: Boolean;
CounterB: Word;
TimeB: TDateTime;
MainWrFlashInfo: Upgrade Information Main Program
ValidA: Boolean;
CounterA: Word;
TimeA: TDateTime;
ValidB: Boolean;
CounterB: Word;
TimeB: TDateTime;
ReadEEWrFlashInfo:
Result Byte
$00: 'Read EEPROM Upgrade Information successfully'
$01: 'ComPort is Closed!'
$02: 'Device is not Alive!'
$03: 'Read EEPROM Upgrade Information Command Needs Authority'
$04: 'CRC Error Detected'
$05: 'Unknown Error'

READ "LOAD COMPACT FLASH DISK INFORMATION" FROM EEPROM

function ReadEETotalLoadDiscInfo(var ComPort: TComPort; Serial: Word; var EETotalLoadDiscInfo: Array of TCF_LoadDiscInfo):Byte;

INPUT:
ComPort: Serial Com Port Component
Serial: Device Serial Number {$0000...$FFFF)

OUTPUT:
EETotalLoadDiscInfo:
Array of CF_LoadDiskInfo (Compact Flash Load Disk Information)
Valid: Boolean;
Index: Byte;
SerialNumber: String[20];
Size: DWord;
InsertDateTime: TDateTime;
EjectDateTime: TDateTime;

ReadEETotalLoadDiscInfo:
Result Byte
$00: 'Read Total Load Disk Information successfully'
$01: 'ComPort is Closed!'
$02: 'Device is not Alive!'
$03: 'Read Total Load Disk Information Command Needs Authority'
$04: 'CRC Error Detected'
$05: 'Unknown Error'